Adaptive Designs for Dose-Finding Trials

Temple, Jane

Award date:
2012

Awarding institution:
University of Bath

Adaptive Designs for Dose-Finding Trials

submitted by

Jane Ruth Temple

for the degree of Doctor of Philosophy

of the

University of Bath

Department of Mathematical Sciences

August 2012

Summary

The pharmaceutical industry is currently facing an industry wide problem of high attrition rates for new compounds and rising development costs. As a result of this, there is an emphasis on making the development process more efficient. By learning more about new compounds in the early stages of development, the aim is to stop ineffective compounds earlier and improve dose selection for compounds that progress to phase III. One approach to this is to use *adaptive designs*. The focus of this thesis is on response adaptive designs within phase IIb dose-finding studies. We explore adapting the subject allocations based on accrued data, with the intention of focusing the allocation on the interesting parts of the curve and/or the best dose for phase III.

In this thesis we have used simulation studies to assess the operational characteristics of a number of response adaptive designs. We found that there were consistent gains to be made by adapting when we were relatively cautious in our method of adaptation. That is, the adaptive method has the opportunity to alter the subject allocation when there is a clear signal in the data, but maintains roughly equal allocation when there is a lot of variability in the data. When we used adaptive designs that were geared to randomising subjects to a few doses, the results were more varied. In some cases the adaptation led to gains in efficacy whilst in others it was detrimental.

One of the key aims of a phase IIb dose-finding study is to identify a dose to take forward into phase III. In the final chapter, we show that the way in which we choose the dose for phase III affects the expected gain, and so begin to consider how we can optimise the decision making process.

Acknowledgements

First and foremost, I would like to thank my supervisor Prof. Chris Jennison for all his patience and support throughout the last four years. I am in no doubt that I would still be writing this thesis if it were not for his continued guidance. I would also like to thank Dr Simon Kirby for his input and advice over the years; including the discussion that initially led me to undertake this project. I am also grateful to both the EPRSC and Pfizer for the case award which funded my research.

Next I would like to thank all the people in the Maths department who have made my PhD so enjoyable. Thanks to my officemates in 1W4.17; Caz, Chris, James and Phil for making the transition back to student life so easy and for the endless distractions. I think moving office was the best thing I did for my thesis, and so thanks also to my officemates in 4W2.19 for allowing me to get some work done! A big thanks also goes to the girls, Andrea, Marion, Melina and Tania; for the Sunday coffees, lengthy chats and enduring friendship. To the 'Drinks in the Parade' crowd, thanks for all the laughs and, of course, all the advice on how to survive my PhD.

Finally, I would like to thank my parents for instilling in me a love of maths from a young age, for always being there for me and for pushing me to be the best that I can be. This thesis is dedicated to you.

Contents

List of Figures

List of Tables

Chapter 1

Introduction

1.1 Background

In the pharmaceutical industry the process of getting a new drug to market is time-consuming and expensive. In order to prove to regulators that a new drug should be made available for the treatment of patients, evidence is collected on the properties of the drug through clinical trials. The ideology is that the early phase clinical trials, phases I and II, are used to *learn* about the effectiveness and toxicity of the drug, while in phase III we aim to *confirm* the drug is both efficacious and safe (Hung et al., 2006). A phase I trial is the first time a new compound is tested in humans, and usually consists of a small number of healthy male volunteers. The aims of phase I trials are to gain crude toxicology data and determine the maximum tolerated dose. The aim of phase II is to construct hypotheses about the compound and learn about the dose range in subjects. Often phase II is separated into two parts; phase IIa proof of concept studies and phase IIb dose-finding studies. Phase IIa proof of concept studies are used to verify that the new compound is efficacious for the disease area it is aimed at. Phase IIb dose-finding studies are used to characterise the dose response relationship and where possible identify a dose with a clinically meaningful effect and acceptable safety profile. If an appropriate dose can be identified in the phase IIb study, then development of the compound is continued into phase III, which generally consists of two large confirmatory studies. The combination of efficacy and safety data collected in phases I to III are then used to convince the regulators that the new drug should be released onto the market.

The focus of this thesis is on phase IIb dose-finding studies. Phase IIb studies often

include multiple doses of the new compound and a control arm, with the aim of characterising the dose response relationship. The dose response relationship is then used to identify the smallest dose with a clinically meaningful, statistically significant difference from control, also known as the minimally effective dose (MED). Providing there are no safety concerns, this would then be the dose that is taken into phase III. However, 'identifying the correct dose is one of the most important and difficult goals in drug development' (Pinheiro et al., 2006). If the dose chosen is too high it may not be tolerable, and if the dose is too low it may not have required efficacy needed for approval.

A review of studies carried out by ten of the biggest pharmaceutical companies from the United States and Europe over a ten year period from 1991-2000, found that the vast majority of attrition occurs in phases IIb and III, with approximately 45% of all compounds that enter phase III failing to make it further in the development process (Kola & Landis, 2004). Another review of phase III studies reported between 1990-2002 (Gordian et al., 2006), found that approximately 42% of the 656 compounds being tested in phase III failed. For 73 of these failed studies, sufficient data were available to determine the cause of failure: 50% of the trials failed to show significant difference from placebo, 31% failed due to safety concerns compared to placebo, and 19% failed to show a differentiation from an active comparator either in terms of efficacy or safety. This suggests that for these studies either the dose chosen for phase III was too low or too high, or the new compounds were ineffective and so halting the development process at an earlier stage would have been beneficial.

It is estimated that only 1 compound in 9 makes it through the full development process (Kola & Landis, 2004) with an associated cost of between $800 million and $2 billion for each drug that makes it to market (DiMasi et al., 2003; Adams & Brantner, 2006; Orloff et al., 2009). One of the main factors attributing to the high development costs has been identified as the 'late-stage failure and the rising costs of phase II and III trials' (Orloff et al., 2009). In 2002 the average development time for a new compound, from registration to market, was 12 years and 10 months (Kola & Landis, 2004). As the standard patent on a new compound is 20 years, this gives a limited time for a company to make a return on their investment. Improving the efficiency of the clinical trial process can therefore reduce development times, allowing a company to maintain exclusivity of a marketed drug for longer.

It is this high rate of attrition in phase III and rising development costs which are

motivating the industry to look at how it can make the clinical trial process more efficient; either by stopping ineffective compounds sooner, therefore saving time and resources, or by increasing the precision with which the dose for phase III is identified. One approach is to use *adaptive designs*, where an adaptive design is defined as 'a multi-stage study design that uses accumulating data to decide how to modify aspects of the study without undermining the validity and integrity of the trial' (Dragalin, 2006). The validity and integrity of the trial are maintained through protecting the family-wise type I error, pre-planning analyses where possible, and ensuring the interim analysis results are blinded. By comparison, we consider traditional non-adaptive designs to be a design where the randomisation schedule and analysis of the trial are specified in advance without possibility for modification during the course of the trial.

1.2 Types of adaptive designs

There are a number of types of adaptive designs which have been explored in literature and in practice. Dragalin (2006) identifies four areas of possible adaptation in a clinical trial. We mention briefly each of these areas here:

- ***the allocation rule***: The ratio with which subjects are allocated to doses is modified during the trial, based on the observed data. This type of adaptive design is generally applied to phase IIb studies, where there are multiple doses of a compound being studied. The aim of the adaptation could be to focus the subject allocation on the dose which has the highest probability of being taken into phase III or alternatively, to drop doses which appear inefficient. This is often referred to as *response adaptive allocation* and is the focus of this thesis.

- ***the sampling rule***: After each interim analysis, the sample size of the next cohort of subjects to enter the trial is modified to take into account estimates of the accrued data. This type of adaptation is generally used in phase III, to account for unexpected variability in the patient population or, potentially, the estimate of the treatment effect itself. Using the treatment effect is more controversial as the adaptation can be used to make inferences about the progress of the trial, and so can introduce potential biases. Hence, when using the treatment effect extra care needs to be taken to maintain the blind of the interim analysis results. Modifying the sampling rule is often referred to as sample size re-estimation (SSR). For a review of sample size re-estimation approaches see Friede & Kieser (2001, 2006).

- ***the stopping rule***: Based on the observed data at an interim analysis, a decision is taken as to whether the trial should be stopped for either efficacy or futility. This type of adaptation is generally used in phase II or phase III. The decision as to whether to stop a trial is often made using boundary crossing methodologies. That is, a test statistic is calculated and, if this test statistic crosses the pre-defined boundary then the trial is stopped. Group sequential methods are the most commonly used of these methods, where the boundaries are constructed to maintain the type I error. For more details on group sequential designs see Jennison & Turnbull (2000). Other approaches to stopping early include using frequentist conditional power (Lachin, 2005) or Bayesian posterior probabilities (Snapinn et al., 2006).

- ***the decision rule***: This is any form of adaptation applied at either an interim analysis or final analysis, not covered by the previous three rules. This covers a wide range of methods which we do not intend to cover here. Examples of a decision rule adaptations are to change the primary endpoint at an interim analysis or to alter the order in which hierarchical testing is carried out. One method for combining p-values from two-stage designs was proposed by Bauer & Kohne (1994) to give a global test of significance.

Although in theory adaptive designs can be used in all phases of the clinical trial process, adapting the sampling size and stopping early are considered as 'well understood adaptations' by the Food and Drug Administration (2010) and so are more suitable for use in confirmatory trials than adapting the allocation and the decision rule, which are considered as 'less well understood adaptations'. Adapting the allocation and the decision rule are more appropriate for phases I and II, where the aim is to learn about potential endpoints and dose response relationships.

1.3 Response adaptive designs

Response adaptive designs are designs where the adaptation is dependent on the accrued responses of the subjects in the trial. The flexibility in the randomisation schedule allows the subject allocation to focus on those doses with the highest probability of success (Dragalin, 2006). In 2005, the Pharmaceutical Research and Manufacturers of America (PhRMA) set up a working group to 'evaluate and develop' types of response adaptive dose-finding designs (Bornkamp et al., 2007). One of the key conclusions of this paper was that 'adaptive dose-ranging designs and methods clearly

lead to gains in power to detect dose response and in precision to select target dose(s) and to estimate the dose response.'

We explore response adaptive designs within phase II dose-finding studies, using three approaches:

Decision theory

Decision theory is focused on optimising the decision making process by quantifying the cost or reward of each decision, based on our beliefs about the current state. Commonly referenced materials on decision theory are Schlaifer & Raiffa (1961) and Berger (1985).

We use decision theory in a response adaptive design to identify the optimal dose for the next subject entering the trial, based on the observed responses. We find the optimal dose by setting up a utility function and choosing the dose that maximises the expected utility. One innovative study which used Bayesian decision theory and paved the way for a new wave of response-adaptive designs was the ASTIN study (Grieve & Krams, 2005; Krams et al., 2003). Here, the optimal dose for the next subject to enter the trial was the dose that minimised the posterior variance of the response at the dose with 95% of the maximal response, commonly referred to as the ED_{95}. More recently, Bornkamp et al. (2007) explored a generalised version of the allocation method used in the ASTIN study, referred to as General Adaptive Dose Allocation (GADA).

Using the posterior probabilities to drop doses

In Bayesian analysis we make inferences about the dose response using the posterior probabilities. In a response adaptive design, we can use the posterior distributions at an interim analysis to make decisions about which doses we should continue to study. If at an interim analysis the posterior probability of a dose having a clinically meaningful difference from placebo is low, then we can drop this dose for futility and focus the subject allocation on the remaining non-futile doses. As we are interested in identifying the minimally effective dose, we also considering dropping doses with high posterior probabilities of having a clinically meaningful difference from placebo, so that we can focus the dose allocation on lower effective doses.

Optimal design theory

In optimal design theory we are concerned with optimising information about some function of the dose response curve. We focus on D-optimality which allocates subjects to maximise a measure of the combined information about all the model parameters. When the dose response is non-linear, the optimal allocation depends on the value of the unknown model parameters. In order to learn about the unknown model parameters, a response adaptive approach is used. The first cohort of subjects are allocated in some arbitrary manner, then at an interim analysis the model parameters are estimated. The parameter estimates are then used to find the optimal allocation for the next cohort of subjects to enter the trial.

1.4 Logistical and technical considerations

The potential drawbacks of response adaptive designs include the extra logistical and technical considerations that need to be taken into account. A survey of adaptive designs used in 13 large and medium sized pharmaceutical companies was carried out by the PhRMA working group (Quinlan et al., 2010). They identified three main areas which presented barriers to implementation of adaptive designs. These were:

- ***technical concerns:*** In general, longer planning time is needed before running an adaptive design in order to assess the operational characteristics of the adaptation through simulation studies. Quinlan et al. (2010) suggest incorporating an additional three months into the project management time lines to account for this. The company infrastructure also needs to be such that the randomisation systems and drug supply can manage the changing randomisation schedule of a response adaptive design. For response adaptive designs it is important that data capture and cleaning can be done in a timely manner, so that maximum number of subjects data are available when determining the next subject allocations.
- ***regulatory risk:*** The Food and Drug Administration (2010) has released guidelines on adaptive designs, categorising adaptations into 'well understood' and 'less well understood' adaptations. Response adaptive designs fall under the category of less well understood and so require additional care to ensure that the validity and rigour of the trial are not compromised.
- ***challenges with team buy-in:*** From the survey presented in Quinlan et al. (2010), one of the main barriers preventing the use of adaptive designs was due to

the study team having a greater comfort level with the traditional non-adaptive designs. Therefore, better understanding of the potential benefits of adaptive designs are needed alongside the ability to communicate the complexity of the designs to all levels of the organisation.

When using adaptive designs it is therefore important not only to consider the purpose of the adaptation, but also the implementation of such designs. The benefits of using an adaptive design need to be weighed against the increased complexity in translating the results and also the increased cost and preparation time. Gallo et al. (2009) provide a detailed overview on good practices to be considered when planning an adaptive design.

1.5 Thesis organisation

The aim of this thesis is to look specifically at how to optimise subject allocations in phase IIb dose-finding studies. We explore how adaptive designs can be used to obtain more information about the interesting parts of the dose response curves and so choose the most appropriate dose to take into phase III. We use simulation studies to compare the operational characteristics of adaptation methods, and compare these with non-adaptive designs. By comparing adaptive and non-adaptive designs, we are able to better understand the potential benefits of the adaptation.

In Chapter 2 we set up our general notation as well as the simulation scenarios and metrics which we use to compare the operational characteristics between methods. In later chapters we are interested in making inferences about the non-linear model using the posterior distribution and so, in Chapter 3 we develop a method which allows us to directly generate samples from the posterior distribution more efficiently than standard methods.

In Chapters 4 to 6, we explore different response adaptive allocation methods. In Chapter 4 we apply Bayesian decision theory and generate results using the General Adaptive Dose Allocation (GADA) approach as used by Bornkamp et al. (2007). In Chapter 5, we simplify the allocation to using cohorts and drop doses based on the posterior probability of a clinically meaningful difference. In Chapter 6 we investigate the use of parametric methods, applying optimal design theory to non-linear models in both frequentist and Bayesian settings.

In Chapter 7 we use the datasets generated from the different response adaptive

approaches in Chapters 4 to 6, and examine how they perform in terms of the expected monetary gain from successfully getting a drug to market when incorporating an element for safety. We can then compare the methods, not just in terms of phase II success but in terms of overall phase III success. Finally, we end with Chapter 8 which is a discussion on response adaptive designs and thoughts on future work that could be carried out on this topic.

Chapter 2

Notation and Simulation scenarios

Across the chapters of this thesis we use the same notation and carry out multiple simulations studies. To avoid repetition, the key notation and settings for the simulation studies are outlined in this chapter. The metrics for measuring the performance of the adaptive and non-adaptive methods are also covered.

2.1 Notation

In the following chapters we are interested in phase II dose response studies where there is a placebo dose, z_0, as well as J active doses, denoted $z_1, \ldots, z_J$. The column vector of doses is denoted

$$z = (z_0, \ldots, z_J)^T.$$

We denote the number of subjects allocated to dose z_j at a given time point as n_j. The column vector for the number of subjects allocated to each dose is denoted

$$n = (n_0, \ldots, n_J)^T.$$

The total number of subjects to be randomised during a simulated clinical trial is denoted as N.

For both parametric and non-parametric models, we denote the expected response of subjects on dose z_j by $\eta(z_j, \theta)$. For the parametric models, θ is the vector of model parameters, and for the non-parametric models $\theta = (\theta_0, \ldots, \theta_J)^T$, where θ_j

is the expected response at dose z_j. An example of a parametric model that is used repeatedly throughout this thesis is the four parameter sigmoid emax model. For this model $\theta = (\theta_1, \theta_2, \theta_3, \theta_4)^T$ and

$$\eta(z_j, \theta) = \theta_1 + (\theta_2 - \theta_1)\frac{z_j^{\theta_4}}{\theta_3^{\theta_4} + z_j^{\theta_4}}. \tag{2.1}$$

The parameters in this model represent aspects of a dose response curve. The response at the placebo dose is given by θ_1, the maximum response by θ_2, the dose with half the treatment effect (commonly known as the ED_{50}) by θ_3, and the slope parameter by θ_4. We can simplify this model by setting the slope parameter $\theta_4 = 1$. The dose response model is then written as

$$\eta(z_j, \theta) = \theta_1 + (\theta_2 - \theta_1)\frac{z_j}{\theta_3 + z_j}.$$

This is known as a three parameter emax model.

In this thesis we consider both frequentist and Bayesian approaches. For the frequentist approaches we denote the estimates of θ as $\hat{\theta}$. The fitted dose response model based on these estimate is then written $\eta(z_j, \hat{\theta})$.

Within the Bayesian framework we place a prior distribution on θ and use Bayes theorem to make inferences based on the posterior distribution for $\theta|Y = y$, where Y is the observed data. For example; when modelling the data using a parametric model in a Bayesian framework, we could make inferences based on the posterior mean response

$$E[\eta(z_j, \theta)|Y = y].$$

The data

When modelling the data we assume normal errors, such that the response of the i^{th} subject ($i = 1, \ldots, n_j$) allocated to dose z_j is

$$\text{frequentist: } Y_{ij} \sim N(\eta(z_j, \theta), \sigma^2) \tag{2.2}$$

$$\text{Bayesian: } Y_{ij}|\theta \sim N(\eta(z_j, \theta), \sigma^2), \tag{2.3}$$

where σ^2 is the between subject variation. In the frequentist setting, the responses of subjects are assumed to be independent, and within the Bayesian setting they are

assumed to be conditionally independent given θ. We denote the entire dataset of responses from subjects allocated to doses $z_0, \ldots, z_J$ as a column vector

$$Y = (Y_{10}, \ldots, Y_{n_0 0}, Y_{11}, \ldots, Y_{n_1 1}, \ldots, Y_{1J}, \ldots, Y_{n_j J})^T.$$

We denote the average response on dose z_j as

$$\bar{Y}_j = \frac{1}{n_j} \sum_{i=1}^{n_j} Y_{ij}$$

thus from (2.2) the likelihood of $\bar{Y}_j$ for a given θ can be expressed as

$$\bar{Y}_j \sim N(\eta(z_j, \theta), \sigma^2/n_j).$$

We denote the column vector of mean responses as

$$\bar{Y} = (\bar{Y}_0, \ldots, \bar{Y}_J)^T.$$

The distribution for the mean responses can then be written as a multivariate normal distribution

$$\bar{Y} \sim N(\eta(z, \theta), \mathbf{\Sigma}),$$

where $\eta(z, \theta) = (\eta(z_0, \theta), \ldots, \eta(z_J, \theta))^T$ is the vector of expected responses and $\mathbf{\Sigma}$ is the diagonal variance-covariance matrix with

$$\Sigma_{jj} = \sigma^2/n_j. \tag{2.4}$$

As $\bar{Y}$ is a sufficient statistic for Y, we note here that when σ^2 is known, the probability density $p(y|\theta)$ for Y is proportional to the probability density $p(\bar{y}|\theta)$ for $\bar{Y}$.

2.2 Simulation setting

The example we use as the background to our simulation studies is that used in the PhRMA working group paper (Bornkamp et al., 2007) and is based around neuropathic pain studies. Neuropathic pain may have been chosen as a suitable example as, these studies are relatively short with a common endpoint being the change from baseline after 6 weeks of treatment. This short treatment period allows subject data to be available relatively quickly, and so adaptation can take place based on as much complete data as possible.

Neuropathic pain is typically collected using a visual analogue scale (VAS) ranging from 0 to 10, where 0 reflects no pain and a score of 10 represents the worst pain imaginable. Subjects are asked to mark where on the scale they feel their pain falls. In order to keep the dose response positive we are interested in a change in the baseline minus week 6 scores. A response is then a decrease in the pain scores from baseline. The primary endpoint in our neuropathic pain example is the change from baseline in the VAS (Gallagher et al., 2001), which is assumed to be normally distributed with variance $\sigma^2 = 4.5$. In practice, the clinically meaningful difference (CMD) would be predetermined during the design stage of the trial, and is based on what is considered to be clinically relevant for that indication in the therapeutic area being studied. Within this therapeutic area we consider a response of 1.3 over placebo to be a clinically relevant difference.

All simulation studies carried out in this thesis follow this neuropathic pain example. Although we would expect the same conclusions to hold for any parallel group dose-finding study with normally distributed efficacy endpoints.

2.3 Simulation scenarios

For the simulation studies we use similar scenarios to those described in the PhRMA working group paper. In this paper, Bornkamp et al. (2007) explored 36 scenarios (2 total samples sizes, 3 dosing schemes and 6 dose response profiles), while a follow up paper (Dragalin et al., 2010) looked at only 14 scenarios (1 total sample size, 2 dosing schemes and 7 dose response profiles). In order to ensure the simulation studies are as comparable as possible with both papers, we use the following scenarios.

Dosing scheme: Nine equally spaced doses 0,...,8mg. In terms of our notation, this relates to z_0=0mg,...,z_8=8mgs.

Total sample size: N=250

We generate response data from nine true dose response profiles. We denote the expected response at dose z_j for each of the true dose response profiles as ν_j and the vector of responses as $\nu = (\nu_0, \ldots, \nu_J)^T$.

Nine dose response profiles: The following profiles are each defined for $j = 0, \ldots, 8$.

- Flat: $\nu_j = 0$
- Linear: $\nu_j = (1.65/8)z_j$
- Emax: $\nu_j = 1.81z_j/(0.79 + z_j)$
- Emax Low: $\nu_j = 1.14z_j/(0.79 + z_j)$
- Sigmoid Low: $\nu_j = 1.65z_j^5/(2^5 + z_j^5)$
- Sigmoid Emax: $\nu_j = 1.70z_j^5/(4^5 + z_j^5)$
- Sigmoid High: $\nu_j = 2.04z_j^5/(6^5 + z_j^5)$
- Logistic: $\nu_j = 1.73/(1 + \exp[1.2(4 - z_j)]) - 0.015$
- Umbrella: $\nu_j = (1.65/3)z_j - (1.65/36)z_j^2$
- Explicit: $\{\nu_0, \ldots, \nu_8\} = \{0, 1.29, 1.35, 1.42, 1.5, 1.6, 1.63, 1.65, 1.65\}$.

For each of the dose response profiles listed above we generate response data for the i^{th} $(i = 1, \ldots, n_j)$ subject on dose z_j using

$$Y_{ij} \sim N(\nu_j, \sigma^2).$$

The dose response profiles are presented in Figure 2-1. The Flat dose response profile represents an inactive compound. For each of the active dose response profiles, except the Emax Low and Logistic, the maximum response, $\max_j\{\nu_j\}$, is set to 1.65. For the Emax Low and Logistic profiles the maximum responses are 1.14 and 1.7 respectively. When the clinically meaningful difference is set to 1.3, all these dose response profiles except the Flat and Emax Low, have at least one clinically relevant dose. The Emax Low profile represents a dose response curve for a drug that has a dose response but does not meet the clinically relevant criteria. Although it appears we have limited ourselves to the case where there is no placebo response, as we are interested in the change from placebo, any placebo effect would be cancelled out when making comparisons.

Throughout this thesis all the simulation studies have been carried out using R version 2.8.1 (Team, 2008). Examples of the functions used to generate and analyse the data for the main simulation studies are included as additional material in the attached CD.

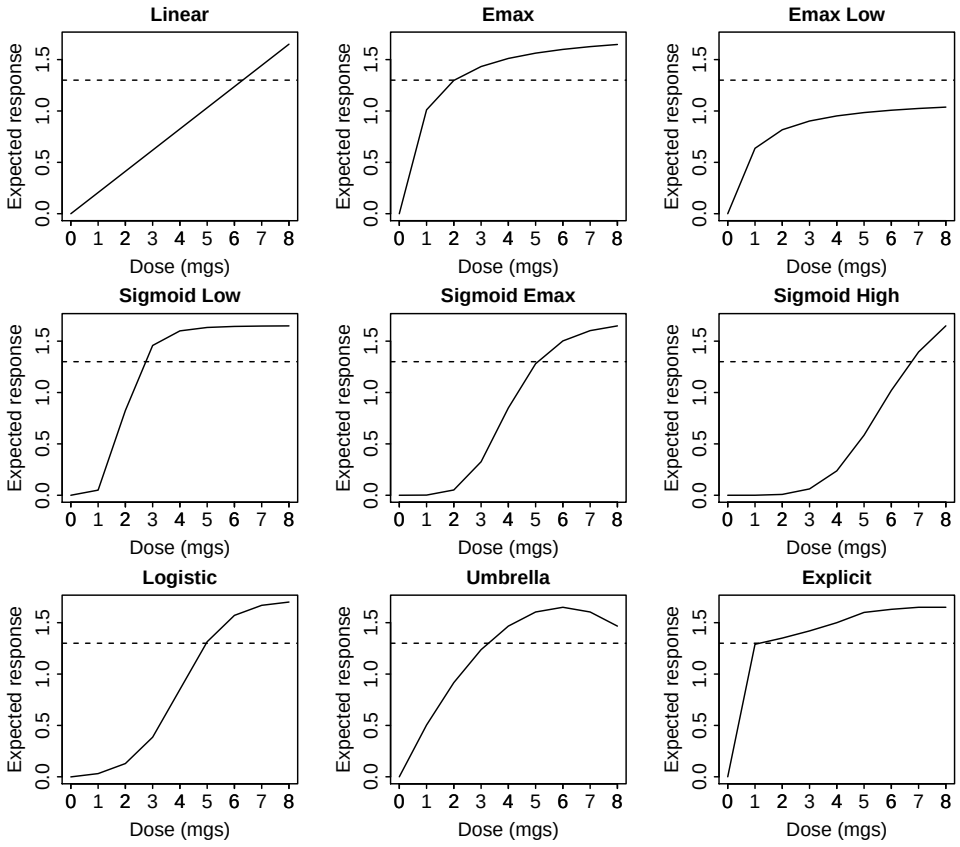

Figure 2-1: Dose response profiles. Reference line at clinically meaningful difference of 1.3 from placebo.

2.3.1 Assumptions

When generating data as part of our simulation studies we make a number of assumptions. The first is that there are no missing data, and that all subjects complete their allocated treatment. Secondly, we assume that complete subject data are available immediately, which can then be used as the basis for any adaptations. Assuming we have complete subject data available at an interim analysis is advantageous to the adaptation process, as it reduces the variability in the data at the interim analysis. When the assumption of complete data is not possible, longitudinal modelling can be employed to predict the final responses for subjects with partial data, as carried out in the ASTIN study (Grieve & Krams, 2005). This allows for the inclusion of partial data in the interim analysis and so maximises the amount of information available. Finally, we assume that there are no serious safety concerns within the dose range we are studying.

2.3.2 Coupling of the simulations

Where possible, the datasets for the simulation studies have been coupled to reduce the simulation error for comparison between different methods. Let us assume we have two methods for allocating subjects that result in n_j and m_j subjects being allocated to dose z_j. For the k^{th} dataset $(k = 1, \ldots, K)$ for each $i = 1, \ldots, \min(n_j, m_j)$, we generate the data so that the response of subject i on dose z_j is the same for both datasets. To ensure the responses are coupled across different methods, we set the random seed for the k^{th} simulation and generate a dataset containing enough subject responses for each dose to cope with all possible allocation methods. We then allocate the subject responses to doses, in order, as required. When we are comparing two methods with non-adaptive equal allocation designs, the datasets for both methods are the same. When we are using an adaptive allocation, the datasets are coupled for the subjects that are common to both methods. To demonstrate the coupling, we generate two datasets with subjects randomly allocated to doses. These datasets are intended to represent two possible subject allocations, from two adaptive methods, for the k^{th} simulation. Figure 2-2 illustrates the subject responses that are coupled for the two adaptive methods. In this figure the grey columns represent those subjects whose data are coupled. The white sections of the columns represent uncoupled subject responses.

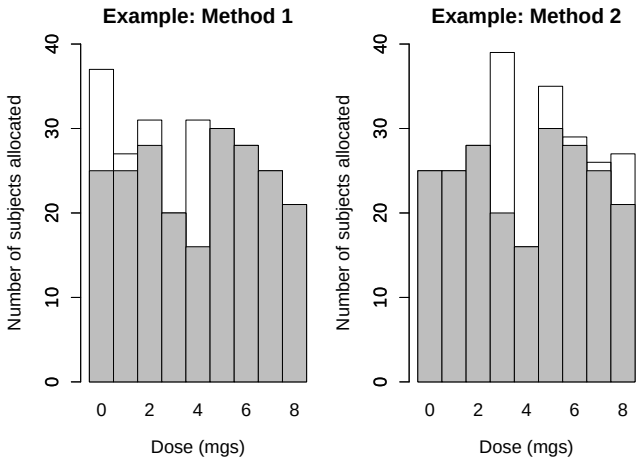

Figure 2-2: Example of coupling subject responses. Grey columns represent coupled responses and white sections of columns represent uncoupled responses.

2.3.3 Target dose

One of the main objectives of a phase II dose-finding study is to identify a dose to take forward into phase III. Often, the aim is to identify the lowest dose that has the

required efficacy. This is referred to as the minimally effective dose (MED). We define our target dose to be the minimum dose with an effect greater than or equal to the clinically meaningful difference (CMD).

since the shape of our true dose response profiles are known, we can identify the target dose for each of the profiles. For all the dose response profiles except the Flat and Emax Low, a target dose can be identified. As the exact target dose based on the dose response profiles is continuous, this is rounded to the nearest available dose. For some of the profiles this results in a target dose with a response less than 1.3. An interval is specified for the target dose, such that doses (rounded to the nearest appropriate dose) that provide ±10% of efficacy of the clinically meaningful difference are deemed acceptable. Exceptions to the rule of rounding to the nearest integer are made for the Emax, Sigmoid Low and Sigmoid High profiles, as rounding down would result in a response that is well below the tolerated boundary. Instead, for these dose response profiles we round up to the nearest dose. The target dose and the corresponding ±10% interval for each of the dose response profiles are given in Table 2.1.

Dose response profile	Target dose		Target dose interval		Response at target dose interval
	Exact	Rounded	Exact	Rounded	
Linear	6.30	6	(5.67, 6.93)	{6,7}	{1.24,1.44}
Emax	2.00	2	(1.44, 2.95)	{2,3}	{1.30,1.43}
Sigmoid Low	2.60	3	(2.40, 2.91)	{3}	{1.46}
Sigmoid Emax	5.06	5	(4.68, 5.58)	{5,6}	{1.28, 1.50}
Sigmoid High	6.69	7	(6.35, 7.09)	{7}	{1.39}
Logistic	4.96	5	(4.65, 5.35)	{5}	{1.30}
Umbrella	3.24	3	(2.76, 3.81)	{3,4}	{1.24, 1.47}
Explicit	1	1	NA	{1,2,3}	{1.29, 1.42}

Table 2.1: Target dose and target dose intervals for the active dose response profiles.

2.4 Measuring the performance of the methods

In order to assess the performance of the methods, we define metrics to measure the operational characteristics. The operating characteristics for each of the methods can then be compared and contrasted. These operating characteristics are intended to give a fair description of a method's performance in terms of detecting a dose response, identifying a clinical relevant response, selecting a dose in the target interval and estimating the dose response curve. The metrics assume the dose response is modelled using the function $\eta(z_j, \theta)$, and that we are interested in the difference from placebo,

$\eta(z_j, \theta) - \eta(z_0, \theta)$.

Dose response: After all subjects have completed the study, we conclude there is evidence of a dose response if there is at least one dose that has a statistically significant improvement over placebo. In order to allow fair comparison between methods, we maintain the family wise one-sided type I error for the Flat dose response profile at the 5% level for the frequentist and Bayesian approaches. In order to maintain a one-sided type I error the confidence or credible intervals are calibrated under the Flat dose response profile.

The dose response for the frequentist approach is established as

- For each z_j, we claim a dose response if the lower bound of the $(1-\gamma) \times 100\%$ one-sided confidence interval for $\eta(z_j, \theta) - \eta(z_0, \theta)$ is > 0.
- We calibrated the value of γ so that the family wise type I error rate α=5% if $\nu_j = 0 \ \forall j$.

The Bayesian approach is similar, except we are interested in the credible intervals rather than the confidence intervals. For the Bayesian methods, a dose response is established if $\Pr(\eta(z_j, \theta) - \eta(z_0, \theta) > 0 | Y = y) > \gamma$. The type I error is calibrated for each method separately, thus each method results in a different value of γ being used to maintain the type I error. We measure the percentage of simulated datasets where a dose response is detected.

Clinical response: A clinical response is concluded if, a dose which has established a dose response also has a clinically meaningful difference (CMD) from placebo. For frequentist methods a dose z_j is considered to have a clinical response if it has a dose response and

$$\eta(z_j, \hat{\theta}) - \eta(z_0, \hat{\theta}) \geq \text{CMD}.$$

That is, if the difference from placebo in the expected response of the fitted dose response curve at dose z_j, is greater than or equal to the clinically meaningful difference.

For Bayesian methods we conclude there is a clinical response based on the posterior distribution for $\theta | Y = y$. A dose z_j is considered to have a clinically relevant response if

$$\Pr(\eta(z_j, \theta) - \eta(z_0, \theta) \geq \text{CMD} | Y = y) > 0.5.$$

We use a probability of being greater than the clinically meaningful difference of 0.5, to ensure the results are as comparable as possible with the frequentist methods, however other decision rules could be applied. We measure the percentage of simulated datasets where a clinical response is established.

Correct dose: If a clinical response can be established, we then select a dose in phase II to be taken forward to phase III. We select the minimum dose with a clinically meaningful difference from placebo. For frequentist methods, the dose we select is

$$\min_j\{z_j : \eta(z_j, \hat{\theta}) - \eta(z_0, \hat{\theta}) \geq CMD\},$$

and for Bayesian methods the dose we select is

$$\min_j\{z_j : \Pr(\eta(z_j, \theta) - \eta(z_0, \theta) \geq CMD | Y = y) > 0.5\}.$$

Where no dose has a clinical response, we do not proceed into phase III therefore no dose is selected. For graphical purposes, these datasets are represented as choosing the placebo dose. We measure the ability to correctly identify the target dose by calculating the percentage of simulated datasets where the selected dose is within the target interval given in Table 2.1.

Estimating the Dose Response: To assess how accurate a method is at predicting the whole of the dose response curve we calculate the prediction error where a clinical response has been established. The prediction error is calculated as the expected difference between the fitted and the true dose response curve across the simulated datasets. For frequentist methods, let $\hat{\theta}(y)$ be the estimate of θ for a dataset $Y = y$. The prediction error at dose z_j is

$$PE_j(y) = \eta(z_j, \hat{\theta}(y)) - \eta(z_0, \hat{\theta}(y)) - (\nu_j - \nu_0)$$

For Bayesian methods the prediction error for a dataset $Y = y$ is

$$PE_j(y) = E[\eta(z_j, \theta) - \eta(z_0, \theta) | Y = y] - (\nu_j - \nu_0).$$

The average absolute prediction error at dose z_j for the frequentist and Bayesian methods is then

$$PE_j = E[|PE_j(y)|].$$

The percent absolute prediction error relative to the clinically meaningful difference is then calculated as

$$pAPE = 100 \times \frac{1}{8} \frac{\sum_{j=1}^{8} |PE_j|}{\text{CMD}}.$$

When plotting the prediction error, we present the median, 5^{th}, 25^{th}, 75^{th} and 95^{th} quantiles of $PE_j(Y)$ at each dose.

2.5 Control for the results: ANOVA approach

When comparing between adaptive and non-adaptive methods we include the 'ANOVA' method as a common comparison. The ANOVA method is considered to be a traditional design for analysing phase II data, and is the same procedure that was used by Bornkamp et al. (2007) as the control method for their results. The ANOVA approach uses pairwise comparisons between the active doses and placebo to test for the presence of a dose response, whilst adjusting for multiple comparisons using an 'allowance' factor as suggested by Dunnett (1955).

In terms of our earlier notation, this could be considered as a non-parametric model where the expected response at each dose is

$$E[Y_{ij}] = \eta(z_j, \theta) = \theta_j,$$

which we estimate by the observed mean,

$$\hat{\theta}_j = \frac{\sum_{i=1}^{n_j} y_{ij}}{n_j}.$$

Dose response is assessed using the Dunnett multiple comparison procedure, which inflates the confidence interval for each dose using an allowance factor to ensure the overall family wise type I error rate is maintained at a prespecified level. The lower bound for the confidence interval is calculated for each $j = 1, \ldots, J$ as

$$LB_j = \hat{\theta}_j - \hat{\theta}_0 - t\sqrt{s^2}\sqrt{\frac{1}{n_j} + \frac{1}{n_0}},$$

where s^2 is the pooled estimate of the variance across all the doses and t is the critical value used to adjust for multiple testing. For one-sided 95% confidence intervals with 8 active doses and a placebo dose a value of $t = 2.38$ is used. Contrast tests are carried out between each of the active doses and placebo, and a dose response is considered

present if one or more of the lower bounds of the adjusted confidence intervals are greater than 0, i.e. if any $LB_j > 0$. Once a dose response has been established, the other metrics listed in Section 2.4 are then applied.

As this method is less computationally intensive than some of the adaptive methods explored, we generate 10,000 simulated datasets for each of the dose response profiles outlined in Section 2.3.

2.6 Known distributions

Throughout this thesis we refer to a number of well known distributions. The densities, $p(x)$, for these distributions are stated below.

Univariate normal distribution ($\mu \in \mathbb{R},\ \sigma^2 > 0$)

$$X \sim N(\mu, \sigma^2)\ ;\ p(x) = \frac{1}{\sqrt{2\pi\sigma^2}} \exp\{-\frac{(x-\mu)^2}{2\sigma^2}\},\ x \in \mathbb{R}.$$

Multivariate normal distribution with k-dimensions ($\mu \in \mathbb{R}^k,\ \mathbf{\Sigma} \in \mathbb{R}^{kk}$)

$$X \sim N(\mu, \mathbf{\Sigma})\ ;\ p(x) = \frac{1}{\sqrt{2\pi}^{k/2}|\mathbf{\Sigma}|^{1/2}} \exp\{-\frac{1}{2}(x-\mu)^T\mathbf{\Sigma}^{-1}(x-\mu)\},\ x \in \mathbb{R}^k.$$

Log normal distribution ($\mu \in \mathbb{R},\ \sigma^2 > 0$)

$$X \sim \ell N(\mu, \sigma^2)\ ;\ p(x) = \frac{1}{x\sqrt{2\pi\sigma^2}} \exp\{-\frac{(\ln(x)-\mu)^2}{2\sigma^2}\}, x > 0.$$

Gamma distribution ($\alpha > 0, \beta > 0$)

$$X \sim G(\alpha, \beta)\ ;\ p(x) = \frac{\beta^\alpha}{\Gamma(\alpha)} x^{\alpha-1} \exp\{-\beta x\}, x \geq 0.$$

Uniform (continuous) distribution ($-\infty < a < b < \infty <$)

$$X \sim U(a, b)\ ;\ p(x) = \begin{cases} \frac{1}{b-a} & \text{if} \quad a \leq x \leq b \\ 0 & \text{otherwise} \end{cases}$$

Chapter 3

Bayesian Sampling for Non-linear Dose Response Models

3.1 Introduction

In this chapter we are interested in generating samples from the posterior distribution of a non-linear dose response model. An example of a non-linear dose response model which is commonly used in the pharmaceutical industry, is the four parameter sigmoid emax model which can be written as

$$\eta(z_j, \theta) = \theta_1 + (\theta_2 - \theta_1)\frac{z_j^{\theta_4}}{\theta_3^{\theta_4} + z_j^{\theta_4}}. \tag{3.1}$$

We assume that the subject responses are normally distributed,

$$Y_{ij} \sim N(\eta(z_j, \theta), \sigma^2),$$

with between subject variance σ^2. We then place prior distributions on the model parameters θ and make inferences based on some function of the posterior distribution, $g(\theta)$. We focus on applying the sampling methods to the posterior distribution of the four parameter sigmoid emax model (3.1), although there are wider applications for the methods proposed.

For simple Bayesian models it is often possible to sample directly from the posterior distribution (Gelman et al., 2004, p. 283). This is especially true when conjugate prior distributions are used and so the posterior takes the form of a well known distribution.

The distribution from which we wish to draw samples is referred to as the target distribution, which has a density known as the target density.

For more complex models with multiple unknown parameters, the computation of the target density becomes intractable and so direct sampling is rarely possible. Popular methods for generating samples from a target distribution, without having to directly calculate the target density are Markov Chain Monte Carlo (MCMC) methods. MCMC methods use Markov chain techniques, where samples are drawn sequentially, conditional on the previous sample. With each additional sample the approximation is improved and so the samples converge to the target distribution (Gelman et al., 2004, p. 286). This creates a sequence of samples where each sample is correlated to the previous samples.

There are a number of ways to sample using MCMC methods. For a detailed description of these methods see Gelman et al. (2004). Availability of software such as WinBUGS (Lunn et al., 2000) and OpenBUGS (Thomas et al., 2006) which are designed to deal with complex hierarchical Bayes models allows for MCMC sampling to be easily carried out.

The advantage of using MCMC methods is that no matter the complexity of the target density it is always possible to generate samples (Geyer, 1992). However there are two disadvantages to using MCMC methods. Firstly, the generated samples are correlated which can cause inefficiencies, as the 'inference from correlated samples is generally less precise than from the same number of independent samples' (Gelman et al., 2004, p. 294). Secondly, the methods rely on the convergence of the sample sequence to the target distribution. If the sequence has not converged, then the samples will not be representative of the target distribution.

When using MCMC sampling there are some commonly implemented techniques to minimise the correlation between samples and ensure convergence. Firstly a 'burn-in' period is us used to generate initial samples which are later discarded. These samples are discarded as they depend on the distribution of the starting point for the iterations, rather than the target distribution. The aim of the burn-in period is also to achieve convergence. Secondly, samples can be thinned so that only one in every so many samples are kept, reducing the correlation between samples. The result of this is that, in order to protect against non-convergence and high correlation, many more MCMC samples need to be generated than are actually useful.

In this chapter we shall explore generating independent samples directly from the posterior distribution for non-linear dose response models such as (3.1). To do this we compartmentalise the non-linear model into linear and non-linear components. We show that if we can sample from the target distribution for the non-linear parameters then it is relatively simple to sample the linear parameters. We present a sampling method which is a hybrid of acceptance-rejection and importance sampling, as a practical solution when the target density is unknown. The method we develop is related to proposals of Liu et al. (1998) and Liu (2001) for sampling data in dynamical systems and a simpler scheme defined by Chen (2005). By combining the hybrid acceptance-rejection importance sampling and reducing the dimensionality of the non-linear model, we have a method which allows us to efficiently generate sample from a posterior distribution. This method offers benefits in reducing the time needed to generate samples, whilst also eliminating the need to check the convergence of the sampler, as may need to be done when using MCMC methods.

We focus on using the four parameter sigmoid emax model (3.1) which is widely used in the pharmaceutical industry, as it captures many essential aspects of dose response curves (Dutta et al., 1996). We show that the time needed to generate independent samples is less than when generating the same number of correlated samples using MCMC methods, and therefore using this direct sampling method is a more efficient than using MCMC sampling for these models.

We discuss in a motivating example why we feel making inferences about the posterior distribution via sampling is more appropriate than using numerical integration for the scenarios we are interested in.

3.1.1 Motivating example

We consider the four parameter sigmoid emax model in (3.1). We are interested in making inferences about the posterior distribution, such as the probability a dose has a clinically meaningful difference from placebo or using a utility function to optimise the placement of the next subject allocated. Katz et al. (1982) separate a non-linear model into linear and non-linear terms, and suggest numerical integration to approximate the posterior density. If we are interested in making inferences about some function of the parameters $g(\theta)$ and we know the posterior density $\pi(\theta|y)$ given a dataset $Y = y$, we

can use numerical integration to estimate the expectation of $g(\theta)$ as

$$E[g(\theta)|Y = y] = \int g(\theta)\pi(\theta|y)\ d\theta.$$

Alternatively, if we can generate a random sample from the posterior density, we are able to estimate the integrals using the sample average

$$E[g(\theta)|Y = y] \approx \frac{1}{T}\sum_{t=1}^{T} g(\theta^t),$$

where θ^t $(t = 1, \ldots, T)$ are i.i.d. samples generated from the density $\pi(\theta|y)$. This is known as *Monte Carlo Integration*.

The success of numerical methods depends on being able to show the results are reliable, through bounding the error of the approximation and showing the error converges as the number of distinct points tends to infinity. The error bounds for conventional numerical methods depend upon the differentiability of the function within the integral domain. If the function $g(\theta)$ has any singularities, the upper bound of the error function is not well-defined, and so it is harder to maintain the accuracy of the method. In contrast, due to asymptotic theory the error of the Monte Carlo integration decreases with order $O(1/\sqrt{T})$ regardless of the dimensionality (Ripley, 1987, p. 120). Therefore provided the number of samples T is sufficiently large we can be confident about the accuracy of the results.

Let us assume we have a placebo dose, z_0, and J active doses denoted z_j $(j = 1, \ldots, J)$. We model the dose response as $\eta(z_j, \theta)$, where θ are the model parameters. We are interested in observing a clinically meaningful difference (CMD) of δ from placebo for a dataset $Y = y$. Some examples of when we are interested in functions of the dose response curve which results in singularities are:

- Probability of being an effective dose: An effective dose is a dose with a difference of δ from placebo. The probability of being an effective dose could be used to decide which dose to take forward into phase III or whether a dose should be dropped for futility at an interim analysis. In this case $g(\theta) = g(z_j, \theta)$ is an indicator variable,

$$g(z_j, \theta) = I_\delta(z_j, \theta) = \begin{cases} 1 & \text{if} \quad \eta(z_j, \theta) - \eta(z_0, \theta) \geq \delta \\ 0 & \text{if} \quad \eta(z_j, \theta) - \eta(z_0, \theta) < \delta. \end{cases}$$

Hence, the integral $\int g(z_j, \theta)\pi(\theta|y)d\theta$ is discontinuous in θ and not differentiable at all points.

- Utility function: In Bayesian decision theory we use a utility function $u(\theta)$ to determine the trial design or to randomise subjects in an adaptive manner. The expected Utility is
$$E[U] = \int u(\theta)\pi(\theta|y)d\theta.$$
An example of a discontinuous utility function is the response at the minimum dose with a difference of δ from placebo,
$$u(\theta) = \{\eta(z_j, \theta) : z_j = \underset{z_k \in \{z_1,\ldots,z_J\}}{\operatorname{argmin}} (\eta(z_k, \theta) - \eta(z_0, \theta) \geq \delta)\},$$
which is discontinuous in θ. The discontinuities arises between the doses, as each dose becomes the smallest dose with a difference of δ from placebo. We look at an adaptive design that uses this utility function as part of the randomisation process in Chapter 4.

3.2 Sampling from a four parameter non-linear model

We wish to sample from the posterior distribution of the four parameter non-linear sigmoid emax model given a dataset $Y = y$. The expected response at a dose z_j $(j = 0, \ldots, J)$ for the sigmoid emax model is
$$\eta(z_j, \theta) = \theta_1 + (\theta_2 - \theta_1)\frac{z_j^{\theta_4}}{\theta_3^{\theta_4} + z_j^{\theta_4}},$$
where $\theta = (\theta_1, \theta_2, \theta_3, \theta_4)^T$ are the model parameters and $\theta_3, \theta_4 > 0$.

By letting $\alpha = (\alpha_1, \alpha_2)^T = (\theta_1, \theta_2)^T$ and $\beta = (\beta_1, \beta_2)^T = (\theta_3, \theta_4)^T$ we can re-parametrise this model so that it is linear in terms of α
$$\eta(z_j, \alpha, \beta) = \alpha_1 + (\alpha_2 - \alpha_1)a(z_j, \beta), \tag{3.2}$$
where $a(z_j, \beta) = \frac{z_j^{\beta_2}}{\beta_1^{\beta_2} + z_j^{\beta_2}}$. In this model, α describes the asymptotes of the model and a is a function of the non-linear parameters β. This compartmentalisation of the non-linear model has been suggested by Katz et al. (1982) for pharmacokinetic applications. We generalise the approach here.

We assume independent prior distributions for α and β. We assume that the asymptotes α are normally distributed with mean $\mu = (\mu_1, \mu_2)^T$ and variance-covariance matrix Δ, $\alpha \sim N(\mu, \mathbf{\Delta})$ which has density $\pi(\alpha)$. We place proper prior distributions on the β parameters which reflect our prior beliefs about the non-linear parameters, we denote the prior density $\pi(\beta)$.

Let us assume the expected subject responses $\bar{Y}$ are normally distributed,

$$\bar{Y}|\alpha, \beta \sim N(X_\beta \alpha, \mathbf{\Sigma}),$$

where X_β is the design matrix for a given β. The variance matrix $\mathbf{\Sigma}$ is a diagonal matrix with $\Sigma_{jj} = \frac{\sigma^2}{n_j}$ $(j = 0, \ldots, J)$ and n_j is the number of subjects allocated to dose z_j. For now we assume that the between subject variation σ^2 is fixed and known.

Using Bayes' Theorem, the joint posterior distribution for α and β is,

$$\pi(\alpha, \beta|y) \propto p(y|\alpha, \beta)\pi(\alpha)\pi(\beta).$$

As the density $p(y|\alpha, \beta)$ for Y is proportional to the density $p(\bar{y}|\alpha, \beta)$ for $\bar{Y}$, the joint posterior distribution can be written as

$$\begin{aligned}
\pi(\alpha, \beta|y) &\propto (2\pi)^{-\frac{J+1}{2}} |\mathbf{\Sigma}|^{-\frac{1}{2}} e^{-\frac{1}{2}(\bar{y}-X_\beta\alpha)^T \mathbf{\Sigma}^{-1}(\bar{y}-X_\beta\alpha)} \\
&\quad \times (2\pi)^{-1} |\mathbf{\Delta}|^{-\frac{1}{2}} e^{-\frac{1}{2}(\alpha-\mu)^T \mathbf{\Delta}^{-1}(\alpha-\mu)} \pi(\beta) \\
&\propto e^{-\frac{1}{2}(\alpha^T (X_\beta^T \mathbf{\Sigma}^{-1} X_\beta + \mathbf{\Delta}^{-1})\alpha - 2\alpha^T (X_\beta^T \mathbf{\Sigma}^{-1} \bar{y} + \mathbf{\Delta}^{-1}\mu))} \\
&\quad \times e^{-\frac{1}{2}(\bar{y}^T \mathbf{\Sigma}^{-1} \bar{y} + \mu^T \mathbf{\Delta}^{-1}\mu)} \pi(\beta).
\end{aligned}$$

Let $\xi_\beta = X_\beta^T \mathbf{\Sigma}^{-1} \bar{y} + \mathbf{\Delta}^{-1}\mu$ and $\mathbf{\Lambda}_\beta = (X_\beta^T \mathbf{\Sigma}^{-1} X_\beta + \mathbf{\Delta}^{-1})^{-1}$, we can complete the square to get a normal distribution for α in terms of β and y, which has density $\pi(\alpha|y, \beta)$. Keeping only the terms depending on α and β, this can be simplified to

$$\begin{aligned}
\pi(\alpha, \beta|y) &\propto e^{-\frac{1}{2}(\alpha-\mathbf{\Lambda}_\beta\xi_\beta)^T \mathbf{\Lambda}_\beta^{-1}(\alpha-\mathbf{\Lambda}_\beta\xi_\beta)} e^{\frac{1}{2}\xi_\beta^T \mathbf{\Lambda}_\beta \xi_\beta} \pi(\beta) \\
&\propto \pi(\alpha|y, \beta)|\mathbf{\Lambda}_\beta|^{\frac{1}{2}} e^{\frac{1}{2}\xi_\beta^T \mathbf{\Lambda}_\beta \xi_\beta} \pi(\beta), \qquad (3.3)
\end{aligned}$$

which is a product of a multivariate normal distribution and a function in terms of the non-linear parameters β. Hence,

$$\alpha|y, \beta \sim N(\mathbf{\Lambda}_\beta \xi_\beta, \mathbf{\Lambda}_\beta) \qquad (3.4)$$

and the conditional density of β given y is proportional to

$$f(\beta|y) = |\mathbf{\Lambda}_\beta|^{\frac{1}{2}} e^{\frac{1}{2}\xi_\beta^T \mathbf{\Lambda}_\beta \xi_\beta} \pi(\beta). \tag{3.5}$$

We write the conditional density of β given $Y = y$ as

$$\pi(\beta|y) = \lambda\, f(\beta|y),$$

where $\lambda = \frac{1}{\int f(\beta|y)d\beta}$ is the normalising constant. The joint posterior distribution can now be written as

$$\pi(\alpha, \beta|y) = \frac{\pi(\alpha|\beta, y) f(\beta|y)}{\int f(\beta|y)d\beta}. \tag{3.6}$$

Suppose we wish to know the expectation of a function of the curve, $g(\theta) = g(\alpha, \beta)$,

$$E[g(\alpha, \beta)|Y = y] = \int g(\alpha, \beta)\pi(\alpha, \beta|y)d(\alpha, \beta).$$

Substituting in (3.6) we have

$$E[g(\alpha, \beta)|Y = y] = \frac{\int g(\alpha, \beta)\pi(\alpha|\beta, y) f(\beta|y)d(\alpha, \beta)}{\int f(\beta|y)d\beta}. \tag{3.7}$$

If we can sample β^t $(t = 1, \ldots, T)$ directly from the target distribution with density $f(\beta|y)$ given in (3.5), then we can easily generate a sample α^t from the conditional distribution of α given β^t and y, which is the multivariate normal distribution given in (3.4). The expectation (3.7) can then be approximated using the weighted average

$$E[g(\alpha, \beta)|Y = y] = \frac{1}{T}\sum_{t=1}^{T} g(\alpha^t, \beta^t). \tag{3.8}$$

3.3 Sampling methods

In the following sections we consider sampling from a one-dimensional distribution with density $f(x)$ which is proportional to $\pi(x)$, i.e. $\pi(x) = \lambda\, f(x)$, where λ is the normalising constant. As we see later this can be extended to higher dimension.

3.3.1 Acceptance-rejection sampling

In acceptance-rejection (AR) sampling we want to generate samples from the target density $f(x)$ but cannot do this directly and so we generate samples from a similar density $h(x)$, known as the *enveloping* density. We then either accept or reject each sample, based on the ratio of the target density to the enveloping density. For a given sample, if the enveloping density is a good approximation to the target density there is a high probability of accepting the sample as being from the target distribution. In this way the method is 'self-monitoring', in that if the choice of enveloping density is poor, few samples will be accepted (Gelman et al., 2004, p. 285).

Let $\lambda f(x)$ be the target density from which we want to draw samples. We follow the key points of the proof for acceptance-rejection sampling from Morgan (1984, p. 98).

- We can simulate random variables X from any density $\lambda f(x)$ as long as we have a method for uniformly and randomly sampling points under $\lambda f(x)$ or equivalently under $f(x)$.
- We identify an enveloping density, $h(x)$ which is relatively easy to simulate from and which has a similar shape to $f(x)$.
- It is simple to obtain a uniform scatter of points under $h(x)$, by taking the coordinates (X, Y) such that X has density $h(x)$, while the conditional density of $Y|X = x \sim U(0, h(x))$.
- In order to completely envelop $f(x)$ we choose a stretching factor c ($c \geq 1$) so that $f(x) \leq c\,h(x)$ for all x. It then follows, that $Y|X = x \sim U(0, c\,h(x))$.
- Generate a uniform sample x with density $h(x)$ and a sample y with distribution $U(0, c\,h(x))$, then accept x if and only if $y \leq f(x)$.

Hence for a suitable $h(x)$ and c, we have the following algorithm for accepting samples from $\lambda f(x)$:

1. Simulate an $X = x$ from $h(x)$.
2. Accept x as a realisation of a random variable with density $\lambda f(x)$ with probability

$$\Pr(\text{accept}) = \frac{f(x)}{c\,h(x)}.$$

It is important for the efficiency of the method that c is as small as possible but still large enough to bound the acceptance probability at 1. The probability of acceptance is

$$\frac{\int f(x)dx}{\int ch(x)dx} = \frac{1}{c\,\lambda}.$$

Therefore, the expected number of samples needed for a single sample to be accepted is $(c\,\lambda)^{-1}$, and so the acceptance-rejection method is optimised (Chib & Greenberg, 1995) by setting

$$c = \max\left(\sup_x \frac{f(x)}{h(x)}, 1\right).$$

3.3.2 Importance sampling

In importance sampling we wish to find the expectation of a function $g(x)$,

$$E[g(X)] = \int g(x)\lambda f(x)dx = \frac{g(x)f(x)dx}{\int f(x)dx}, \tag{3.9}$$

where x has density $\lambda f(x)$ which cannot be sampled from directly. We use a *proposal density* $h(x)$ which is similar to a multiple of $f(x)$ and relatively easy to sample from. We then re-weight the samples based on the likelihood of observing the samples from the target density $\lambda f(x)$. We use the explanation of importance sampling as discussed by Gelman et al. (2004, p. 342). The expectation in (3.9) can be re-written as

$$E[g(X)] = \frac{\int g(x)\frac{f(x)}{h(x)}h(x)dx}{\int \frac{f(x)}{h(x)}h(x)dx}.$$

We generate T samples from $h(x)$ denoted x^t $(t = 1, \ldots, T)$ and estimate the integrals using the sample average

$$\begin{aligned} E[g(X)] &\approx \frac{\sum_{t=1}^{T} g(x_t)\frac{f(x^t)}{h(x^t)}}{\sum_{t=1}^{T}\frac{f(x^t)}{h(x^t)}} \\ &= \frac{\sum_{t=1}^{T} g(x^t)w^t}{\sum_{t=1}^{T} w^t}, \end{aligned}$$

where $w^t = \frac{f(x^t)}{h(x^t)}$ are known as the *importance ratios* or *importance weights*. We use the same samples for the numerator and denominator as it reduces the sampling error of the estimate.

In importance sampling the variance of the estimator is minimised when $h(x) \propto |g(x)\, f(x)|$ (Ripley, 1987, p. 122). This is often not practical and so instead we aim chose $h(x)$ so that $\frac{f(x)\, g(x)}{h(x)}$ are roughly constant. Poor estimates occur when we have a few large weights and a large number of small weights, as the large weights influence our estimator. To avoid this, the density $h(x)$ should 'cover all the important regions of the target distribution' (Gelman et al., 2004, p. 343). In the next section we look at how the variance of the weights impacts the variance of the estimator.

3.3.3 Variance of the estimator

When generating samples, we want to be efficient in terms of the computer time needed to generate samples and the variance of the estimator. For AR sampling the target density $f(x)$ must be completely enveloped by $c\, h(x)$. If our enveloping density is too large then this results in a high rejection rate and a need to generate large numbers of samples in order to accept the required T samples. This method is then expensive in terms of the computational time needed per accepted subject. In contrast, when using importance sampling only T samples need to be generated, however as we show below, the variability of the weights is reflected in the variance of the estimator. Therefore, if the same number of samples are generated with importance weights as are accepted using AR sampling, the variance of the estimator tends to be greater. To reduce the variance of the estimator when using importance sampling, we would need to generate more samples, increasing the computational cost. We show below how the variance of the estimator is dependent on the variance in the weights.

We are interested in

$$\bar{g} = E[g(X)] = \frac{\int g(x) f(x) dx}{\int f(x) dx},$$

which we estimate using the sample approximation

$$\hat{g} = \sum_{t=1}^{T} g(x^t) w(x^t),$$

where $x^1, \ldots, x^T$ are T are i.i.d. samples. These samples represent accepted samples using acceptance-rejection sampling or the equivalent number of samples generated for importance sampling. For the acceptance-rejection and importance sampling schemes these samples are generated from an enveloping and proposal density $h(x)$ respectively. We assume here that for acceptance-rejection sampling $c\, h(x)$ completely envelops $f(x)$. For acceptance-rejection sampling all the samples have equal weights and so

$w(x^t) = 1/T$. For importance sampling we use $w(x^t) = \frac{f(x^t)/h(x^t)}{\sum_{t=1}^{T} f(x^t)/h(x^t)}$.

Let us assume that the densities $g(x)$ and $w(x)$ are independent. This is a strong assumption that may not apply to many cases. Under this assumption, the variance of the estimator is

$$\begin{aligned}
\mathrm{Var}(\hat{g}) &= \sum_{t=1}^{T} \mathrm{Var}(w(X)g(X)) \\
&= T\{E[w(X)^2]E[g(X)^2] - E[w(X)]^2 E[g(X)]^2\} \\
&= T\{\mathrm{Var}(w(X))\mathrm{Var}(g(X)) + (E[w(X)])^2\mathrm{Var}(g(X)) \\
&\quad +(E[g(X)])^2\mathrm{Var}(w(X))\}
\end{aligned}$$

In the case of acceptance-rejection sampling $E[w(X)] = 1/T$ and $\mathrm{Var}(w(X)) = 0$, hence the variance of the estimator for acceptance-rejection sampling is

$$\mathrm{Var}_{\mathrm{AR}}(\hat{g}) = \frac{1}{T}\mathrm{Var}(g(X)), \tag{3.10}$$

which is the sample variance.

For importance sampling $E[w(X)] = 1/T$ but $\mathrm{Var}(w(X)) > 0$ and so the variance of the estimator using importance sampling is

$$\begin{aligned}
\mathrm{Var}_{\mathrm{IS}}(\hat{g}) &= \frac{1}{T}\mathrm{Var}(g(X)) + T\{\mathrm{Var}(w(X))\mathrm{Var}(g(X)) \\
&\quad +(E[g(X)])^2\mathrm{Var}(w(X))\} \\
&= \mathrm{Var}_{\mathrm{AR}}(g(X)) + T\{\mathrm{Var}(w(X))\mathrm{Var}(g(X)) \\
&\quad +(E[g(X)])^2\mathrm{Var}(w(X))\},
\end{aligned} \tag{3.11}$$

which is greater than the variance of the estimator using acceptance-rejection sampling.

For an efficient method, we therefore want a compromise between using an acceptance-rejection sampling method with a high rejection rate and using importance sampling where the weights are highly variable. In the next section we explore a method that aims to make this compromise.

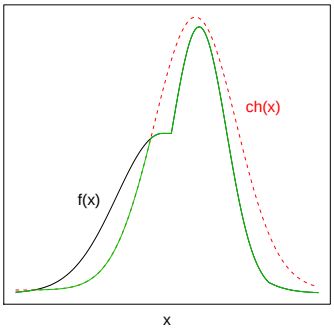

Figure 3-1: Example of a target density $f(x)$ which is not completely enveloped by $ch(x)$. The density $q(x)$ is proportional to the green curve.

3.3.4 Hybrid acceptance-rejection importance sampling (HARIS)

Combining importance and acceptance-rejection sampling was first proposed by Liu et al. (1998) and Liu (2001) for use in simulating dynamical systems. They show that by rejecting streams of samples with low weights and re-sampling new streams, where the streams are re-weighted accordingly, the trial distribution approaches the target distribution more quickly. This method was then simplified by Chen (2005) to the case with only one time point. The proposed method is a practical approach when the target distribution is not known and we have an enveloping density that does not meet the criteria that $f(x) \leq c\,h(x)\ \forall x$. In reality the failure of the enveloping density may not be discovered until the sampling process begins. The proposed method is pragmatic as it allows us to use the generate samples, and so avoids the need to start the sampling again with a new enveloping density.

Suppose we wish to sample from a distribution with density $\lambda\, f(x)$ where λ is unknown. Let $h(x)$ be the density of a distribution that we can sample from and suppose c is chosen so it is likely that $c\,h(x) \geq f(x)$ when x is a random sample from $h(x)$. We define the density $q(x)$ by

$$\begin{aligned} q(x) &= \begin{cases} k\, f(x) & \text{if} \quad f(x) \leq c\, h(x) \\ k\, c\, h(x) & \text{if} \quad f(x) > c\, h(x) \end{cases} \\ &= k \min(f(x), c\, h(x)). \end{aligned}$$

Here k is the normalising constant for $q(x)$. Figure 3-1 illustrates an example where $c\,h(x)$ does not completely envelop $f(x)$; the density $q(x)$ is proportional to the green curve in this plot.

Recall that $q(x) = k \min(f(x), c\,h(x))$, we can sample x from $h(x)$ to obtain samples from the density $q(x)$ using acceptance-rejection sampling with a stretching factor k. We accept x with probability

$$\begin{aligned} \Pr(\text{accept}) = \frac{q(x)}{k\,c\,h(x)} &= \frac{k \min(f(x), c\,h(x))}{k\,c\,h(x)} \\ &= \min\left(\frac{f(x)}{c\,h(x)}, 1\right), \end{aligned}$$

which is bounded by 1 as required. Although the normalising constant k is unknown, we are able to use it in the stretching factor since it cancels in the expression for the acceptance probability.

We now have a method for generating samples from $q(x)$, but we wish to estimate expected values under the density $\lambda\, f(x)$. We achieve this by importance sampling. To estimate the expectation of $g(X)$ when X has density $\lambda\, f(x)$, we write

$$\begin{aligned} E[g(X)] &= \int g(x)\lambda f(x)dx \\ &= \frac{\int g(x)f(x)dx}{\int f(x)dx} \\ &= \frac{\int g(x)\frac{f(x)}{q(x)}q(x)dx}{\int \frac{f(x)}{q(x)}q(x)dx} \\ &\approx \frac{\sum_{t=1}^{T} g(x^t)\frac{k\,f(x^t)}{q(x^t)}}{\sum_{t=1}^{T}\frac{k\,f(x^t)}{q(x^t)}}, \end{aligned}$$

where $x^1, \ldots, x^t$ are values sampled from the density $q(x)$. Let

$$w^t = \frac{k\,f(x^t)}{q(x^t)} = \max\left(1, \frac{f(x^t)}{ch(x^t)}\right),$$

then

$$E[g(X)] \approx \frac{\sum_{t=1}^{T} g(x^t)w^t}{\sum_{t=1}^{T} w^t}. \tag{3.12}$$

The above derivation justifies (3.12) as an estimate of $E[g(X)]$. The density $q(x)$ plays an important role in this derivation but does not appear explicitly in the final formula. We can summarise the implementation of this method as

1. Generate x from $h(x)$.

2. Accept the sample with probability

$$\Pr(\text{accept}) = \min\left(\frac{f(x)}{ch(x)}, 1\right).$$

3. If accepted, assign weight $w = \max\left(\frac{f(x)}{ch(x)}, 1\right)$ to the sample.

4. Repeat until T samples are obtained.

5. Estimate

$$E[g(X)] \approx \frac{\sum_{t=1}^{T} g(x^t)w^t}{\sum_{t=1}^{T} w^t}.$$

We refer to this method as the hybrid acceptance-rejection importance sampling (HARIS) method. This method still relies on the density $c\,h(x)$ enveloping the majority of the curve $f(x)$ in order to keep the importance weights equal to or close to 1, and so we still need to identify a reasonable value for c. We describe in the Section 3.4 how we construct the approximating density $h(x)$ using a grid of points and then in Section 3.4.1 our choice of c.

3.3.5 Markov chain Monte Carlo (MCMC) methods

The final sampling method we consider, is Markov chain Monte Carlo (MCMC) sampling. To generate the MCMC samples we use the OpenBUGS or WinBUGS software. We use the R Team (2008) version 2.13.0 to call both OpenBUGS and WinBUGS using the packages R2OpenBUGS and R2WinBUGS (Sturtz et al., 2005), respectively. When using these packages we use the default sampler to generate samples. Although we acknowledge that other samplers can be specified, we have approached both these packages as many project statisticians may approach them, with a basic understanding of the packages capabilities.

Although the BUGS in OpenBUGS and WinBUGS originally was an acronym for Bayesian inference using Gibbs sampling, since its creation the software has been extended so that the sampler now attempts to 'utilise the most appropriate sampling scheme for each stochastic node' (Lunn et al., 2000). Both the WinBUGS and OpenBUGs software use 'three families of MCMC algorithms: Gibbs, Metropolis Hasting and slice sampling' (online OpenBUGS manual). The Gibbs sampler (Geman & Geman, 1984) is the simplest of the Markov chain algorithms and generates samples for each parameter in succession conditional on the previous samples. The Gibbs sampler is the 'first choice for conditionally conjugate models, where we can directly

sample from each conditional posterior distribution' (Gelman et al., 2004, p. 292). For conditional densities where sampling is not straight forward, the Gibbs sampler may not be feasible as custom algorithms are needed (Neal, 1997). For each iteration a new parameter value is generated.

The Metropolis-Hastings (M-H) (Metropolis et al., 1953; Hastings, 1970) algorithm uses a proposal density to generate conditional samples followed by an acceptance-rejection rule. Due to the acceptance rejection rule, if the next step in the random walk is rejected, the parameter value remains the same and so each iteration does not necessarily result in a new value being generated. The speed of convergence of the M-H algorithm depends on the choice of proposal density, if the choice is poor then the rejection rate will be high resulting in slow convergence. In order to avoid problems with the proposal density, adaptive M-H algorithms have been suggested, where the proposal density is 'tuned' by monitoring the acceptance rate (Haario et al., 2001).

Slice sampling (Neal, 1997, 2003) constructs a Markov chain by 'alternating uniform sampling in the vertical direction with uniform sampling from the horizontal 'slice' defined by the current vertical position.' For each iteration a new parameter value is generated.

One way of assessing the amount of correlation between the samples is to calculate the effective sample size (ESS). The ESS is the number of independent samples that the correlated samples equate to, taking into account the correlation. If the Markov chain has π as the equilibrium distribution and we are drawing samples from $\zeta(x)$, such that $\bar{\zeta}_N = E_\pi[\zeta(x)]$ is the empirical average from N samples and $\tilde{\sigma}^2$ is the asymptotic variance under ζ, then

$$\text{ESS} = \frac{\tilde{\sigma}^2}{\text{var}(\bar{\zeta}_N)}. \tag{3.13}$$

The $\text{var}(\bar{\zeta}_N)$ is estimated using the spectral density at frequency 0, for more details see Ripley (1987, p. 142-146).

3.4 Constructing an approximating density

In the previous section, we have examined methods for generating samples from a distribution with density $\lambda f(x)$, where $f(x)$ is known and λ is the unknown normalising constant. For each of the direct sampling methods, we define an approximating density $h(x)$. So far we have discussed sampling in one-dimension, however as we intend to

apply these methods to the conditional posterior density for the non-linear parameters of the sigmoid emax model (3.5), we now consider constructing our approximate density in two-dimensions. The application of these methods can be extended to higher dimensions if computation power allows.

We construct our approximating density $h(x)$ using a grid for $x = (x_1, x_2)$. We define our grid to have $n \times m$ cells and $(n+1)\times(m+1)$ grid points. We denote the coordinates of each of the grid points as $(x_1(i), x_2(j))$ $(i = 1, \ldots, n+1;\ j = 1, \ldots, m+1)$. Let the grid cell c_{ij} be the cell with corner points $(x_1(i), x_2(j))$, $(x_1(i+1), x_2(j))$, $(x_1(i), x_2(j+1))$ and $(x_1(i+1), x_2(j+1))$.

Our approximating density is then constructed using the following steps.

1. We evaluate $f(x_1(i), x_2(j))$ at each of the grid points $i = 1, \ldots, n+1;\ j = 1, \ldots, m+1$.

2. We define our approximating density for the cell c_{ij} for $x = (x_1, x_2)$ to be the maximum of the four corner points,

$$\begin{aligned} h_{ij}(x) \quad = \quad & \max\{f(x_1(i), x_2(j)),\ f(x_1(i+1), x_2(j)), \\ & \qquad f(x_1(i), x_2(j+1)),\ f(x_1(i+1), x_2(j+1))\}, \end{aligned}$$

   for $x_1(i) \le x_1 \le x_1(i+1)$, $x_2(j) \le x_2 \le x_2(j+1)$.

3. The probability of sampling cell c_{ij} is then

$$p_{ij} \propto (x_1(i+1) - x_1(i))(x_1(j+1) - x_1(j))h_{ij}(x) \tag{3.14}$$

   where $\sum_{i=1}^{n} \sum_{j=1}^{m} p_{ij} = 1$.

The efficiency of the sampling methods depends on how similar our approximating density is to the target density and therefore the placing of the grid. To ensure our grid placement captures the shape of the target density we carry out the following process.

1. Choose an initial grid placement based on where we believe the mass of the target distribution lies. This could be based on the prior beliefs or biological reasoning.

2. Assume the marginal densities $f(X_1)$ and $f(X_2)$ are approximately normally

distributed. Estimate

$$E[X_1] \approx \sum_{i=1}^{n}\sum_{j=1}^{m} p_{ij}\frac{x_1(i+1)-x_1(i)}{2},$$

similarly for $E[X_2]$, $E[X_1^2]$ and $E[X_2^2]$.

3. Using the normal approximation for X_1, we place grid points at our estimate for the mean $E[X_1]$ and $\pm 2, \ldots, \pm 5$ standard deviations from the mean, unless these points are beyond the pre-specified bounds of the grid. The remaining grid points are then evenly spread between the mean and ± 2 standard deviation.

4. To ensure that our grid covers the mass of the target distribution, we calculate the ratio of the density at the edge of the grid versus the maximum density. If this is greater than 0.01 and we are within the pre-specified bounds of the grid, then we update the marginal normal approximations and extend the grid further. This is repeated until we are satisfied that the majority of the target distribution is covered by our grid.

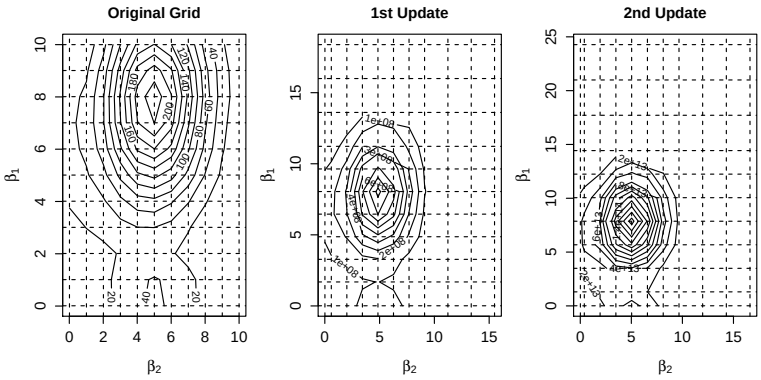

Figure 3-2: Example grid placement for an unknown target density.

Figure 3-2 gives an example of the grid layout based on the contour plot for the target density $f(x)$. As we see, the initial grid was not large enough and so the grid was extended. After the 1^{st} normal approximation a portion of the distribution is still at the edge of the grid and so a 2^{nd} normal approximation was carried out and the grid updated again.

In order to generate samples using the HARIS method (Section 3.3.4), as well as an approximating density $h(x)$ we also need to choose a stretching factor c, with the aim

that $c\,h(x) \geq f(x)$ for all x. If we could chose c to be

$$c = \sup_x \frac{f(x)}{h(x)},$$

for $x = (x_1, x_2)$ as proposed by Chib & Greenberg (1995), then we would ensure the probability of accepting samples is bounded by 1 and so could use AR sampling. However, the search over x for the supremum of the ratio of $f(x)/h(x)$ is costly in terms of computation time. Instead we assume the target distribution is approximately normal. If this assumption is correct, then $h(x) \leq f(x)$ only at the peak of the target density. We then choose our stretching factor c to be the ratio at the maximum of the target density multiplied by some inflation factor (IF). We use an inflation factor to increase the probability that we can generate samples using acceptance-rejection sampling and to protect against observing large importance weights.

The value of c is found as follows.

1. Identify the cells where the maximum of $h(x)$ lies. Due to the way $h(x)$ is constructed, we assume that the maximum of $f(x)$ lies within these cells.
2. Iteratively maximise the conditional density within these cells. For example, for an initial value of x_1 the value of x_2 which maximises $f(x_2|x_1)$ is found. Using this value for x_2 the value of x_1 that maximises $f(x_1|x_2)$ is found. This process is continued until the values for x_1 and x_2 converge.
3. The co-ordinates for $x = (x_1, x_2)^T$ which maximises $f(x)$ are denoted $x_{\max}$.
4. The stretching factor c is calculated as,

$$c = \frac{f(x_{\max})}{h(x_{\max})} \times IF. \tag{3.15}$$

Although for many cases the ratio at the maximum will be close to 1, the iterative search is over a small area and so relatively cheap to do.

Despite our best intentions we still can not ensure $c\,h(x)$ completely envelops $f(x)$, as there may be ridges in the target density with ratios of $f(x)/c\,h(x) \geq 1$. If the ridges are in the tails of the distribution the ratio of the target to the approximate density could be large. In the next section we use this stretching factor c and the grid for $h(x)$ to sample directly from $f(x)$ using the HARIS method described in Section

3.3.4. This method is appropriate as within the grid cells there may be points which we have not observed, where the density of $f(x)$ is greater than $ch(x)$.

3.4.1 Putting the sampling method into practice

We use the following steps to generate a sample $x = (x_1, x_2)$ using the HARIS method (Section 3.3.4).

1. Sample a grid cell c_{ij} with probability p_{ij} (3.14).
2. Generate a value of x from within the grid cell c_{ij}.
3. Accept x probability
$$\Pr(\text{accept}) = \frac{f(x)}{c\,h(x)}. \tag{3.16}$$
4. Assign an importance weight $w = \max\left(1, \frac{f(x)}{c\,h(x)}\right)$.

This method is then repeated until we have the accepted the required T samples. Let us denote the accepted samples as $x^1, \ldots, x^T$ which have corresponding weights $w^1, \ldots, w^T$. If all $w^t = 1$ then this is equivalent to using acceptance-rejection sampling.

3.5 Assessing the method

We perform a simulation study to compare the direct sampling method with established MCMC sampling methods. As part of the simulation study, we assess what effect the initial and updated grids have on the performance of the direct sampling. The efficiency of the method in terms of the number of samples and time needed to accept 1000 independent samples are presented. This is compared with the time needed to generate 1000 correlated samples using the MCMC methods.

The simulation study is based on making inferences about the posterior distribution for the four parameter sigmoid emax model,

$$\eta(z_j, \theta) = \theta_1 + (\theta_2 - \theta_1)\frac{z_j^{\theta_4}}{\theta_3^{\theta_4} + z_j^{\theta_4}}.$$

In order to use the direct sampling method, we let $\alpha = (\alpha_1, \alpha_2)^T = (\theta_1, \theta_2)^T$ and $\beta = (\beta_1, \beta_2)^T = (\theta_3, \theta_4)^T$ and re-write the sigmoid emax model as a linear model in

terms of α,

$$\eta(z_j, \alpha, \beta) = \alpha_1 + (\alpha_2 - \alpha_1)a(z_j, \beta)$$

where $a(z_j, \beta) = \frac{z_j^{\beta_2}}{\beta_1^{\beta_2} + z_j^{\beta_2}}$.

For the simulation study we use 2 sets of prior distributions for α_1, α_2, β_1 and β_2, which we name Prior 1 and Prior 2. As β_1 and β_2 parameters represent the dose with 50% of the maximum efficacy and the slope of the dose response curve respectively, for biological reasons these are both set to be strictly positive. We define these sets of prior distributions as follows.

Prior 1:

- $\alpha_1 \sim N(0, 2)$
- $\alpha_2 \sim N(1, 2)$
- $\beta_1 \sim U(0.01, 16)$
- $\beta_2 \sim U(0.01, 16)$

Prior 2:

- $\alpha_1 \sim N(0, 2)$
- $\alpha_2 \sim N(1, 2)$
- $\beta_1 \sim \ell N(1.5, 0.75)$
- $\beta_2 \sim \ell N(0.75, 0.75)$

The bounds for the initial and updated grids for Prior 1 are $\beta_1 \in [0.01, 16]$ and $\beta_2 \in [0.01, 16]$ which coincide with the uniform prior distributions for β_1 and β_2. For Prior 2, the prior distributions for β_1 and β_2 are not bounded above and so we use bounds on our initial and update grids of $\beta_1 \in [0.01, 32]$ and $\beta_2 \in [0.01, 32]$. The dose range we use in our simulations has 8mgs as the maximum dose, and so the upper limit for the β parameters in Prior 1 and Prior 2 are twice and four times the maximum dose, respectively. For the purposes of the simulation study this was felt to be an appropriate limit and is consistent with what is believed to be biologically plausible for the sigmoid emax model. The bounds for the grids for Prior 2 ensure that at least 99.5% of the prior distribution is covered by the grid.

We generated $K = 1000$ datasets of subject responses for each of the prior distributions, with each dataset consisting of 250 subjects randomised equally across 9 doses $(0, 1, \ldots, 8\text{mgs})$. The subject response data were generated using a sigmoid emax model with model parameters α_1, α_2, β_1 and β_2 sampled from the prior distributions. The sample of parameters values from the prior distributions are denoted (α^k, β^k)=$(\alpha_1^k, \alpha_2^k, \beta_1^k, \beta_2^k)$ $(k = 1, \ldots, K)$. The mean response on dose z_j $(j = 0, \ldots, J)$ for the k^{th}

dataset ($k = 1, \ldots, K$) is

$$\begin{aligned} \bar{Y}_j^k &= \eta(z_j, \alpha^k, \beta^k) + \epsilon_j \\ &= \alpha_1^k + (\alpha_2^k - \alpha_1^k)\frac{z_j^{\beta_2^k}}{\beta_1^{k\beta_2^k} + z_j^{\beta_2^k}} + \epsilon_j, \end{aligned} \tag{3.17}$$

where $\epsilon_j \sim N\left(0, \frac{\sigma^2}{n_j}\right)$, $\sigma^2 = 4.5$ and n_j is the number of subjects allocated to dose z_j. Simulated parameter values are used to generate the data, so that posterior distributions and therefore the target densities take a wide variety of forms. In doing so, we test the robustness of the method.

For the direct sampling method the target distribution is the conditional posterior distribution for β given a dataset $Y = y$, which has a density proportional to the target density $f(\beta|y)$ as given in (3.5). For each simulated dataset we use the HARIS method (Section 3.3.4) to sample T=1000 parameter vectors from the posterior distribution for (α,β)=(α_1, α_2, β_1,β_2). We denote each sample vector as (α^t,β^t)=(α_1^t, α_2^t, β_1^t,β_2^t) ($t = 1, \ldots, T$). We can then estimate the fitted dose response curve to be

$$E[\eta(z_j, \alpha, \beta)|Y = y] \approx \frac{\sum_{t=1}^{T} \eta(z_j, \alpha^t, \beta^t) w^t}{\sum_{t=1}^{T} w^t},$$

where w^t are the important weights.

When choosing our stretching factor c (3.15) we use an inflation factor of 1.5. This was chosen arbitrarily to maximise the probability that the sampling method could use acceptance rejection sampling without the need to adjust using importance weights. Larger inflation factors could be used, but this would reduce the efficiency of the method as there would be a higher rejection rate of samples. We explore using the HARIS sampling method with a range of grid sizes. We explore three sizes for the initial grid: 4x4, 8x8 and 16x16, and three sizes for the updated grids: 10x10, 20x20 and 40x40.

For a fair comparison between the direct sampling and MCMC methods, we take the same datasets and generate MCMC samples using the packages described in Section 3.3.5. For the MCMC sampling we use a burn-in of 1000 samples which are discarded before generating the 1000 samples. It would be possible to use a longer burn-in period and thin the samples to reduce the correlation in the samples, however this

would increase the time needed to generate the samples. We calculate and present the effective sample size (3.13) of the MCMC samples.

Figures 3-3 is an example of one of the simulated datasets, using uniform prior distributions (Prior 1) for the β parameters. The top left plot is the contour plot for the target density which we want to sample from. The top right plot is the fitted posterior mean dose response curves from the direct sampling and MCMC methods. The bottom row shows the scatter graphs of the β samples from the direct method and the two MCMC sampling methods. From these figures we can see that direct method and the two MCMC methods appear to be sampling from the target distribution. It can also be seen that the fitted curves are very similar.

The scatter plot of the samples generated using OpenBUGS (Figure 3-3) is notably more sparse than the plots when samples are generated using direct sampling and WinBUGS. This is because the OpenBUGS sampler uses an adaptive M-H algorithm for the β parameters, and so for some iterations the samples remain at the same value as a move away from that point is rejected. In contrast WinBUGS uses a slice sampler and so at each iteration new samples are generated. This results in each iteration providing different samples, and so the scatter plot appears more populated.

Table 3.1 presents the number of samples generated in order to accept the 1000 required samples, and the time in seconds needed to generate these samples. The size of the updated grid has more of an impact on the mean number of samples generated than the size of the initial grid. Although using an updated grid of 40x40, reduces the number of samples generate, the average time needed to generate these samples increases. This tells us that the cost of evaluating the necessary functions at the additional grid points outweighs the cost of generating the additional samples. The purpose of the initial grid is to estimate where the majority of the density lies. Increasing the size of the initial grid, reduces the standard deviation in the number of samples generated. This is because the more refined the initial grid, the better the estimate of the parameters for the normal approximation, which improves the placement of the updated grid.

The best grid options for this example are an initial grid of 8x8 and an updated grid of 20x20. These conclusions are also true for Prior 2 (Table 3.2). The time needed to generate the samples when log normal prior distributions are used for the β parameters is greater than when uniform prior distributions are used. This is because the average number of grid placements is 1.72 instead of the 1.15 when uniform prior distributions

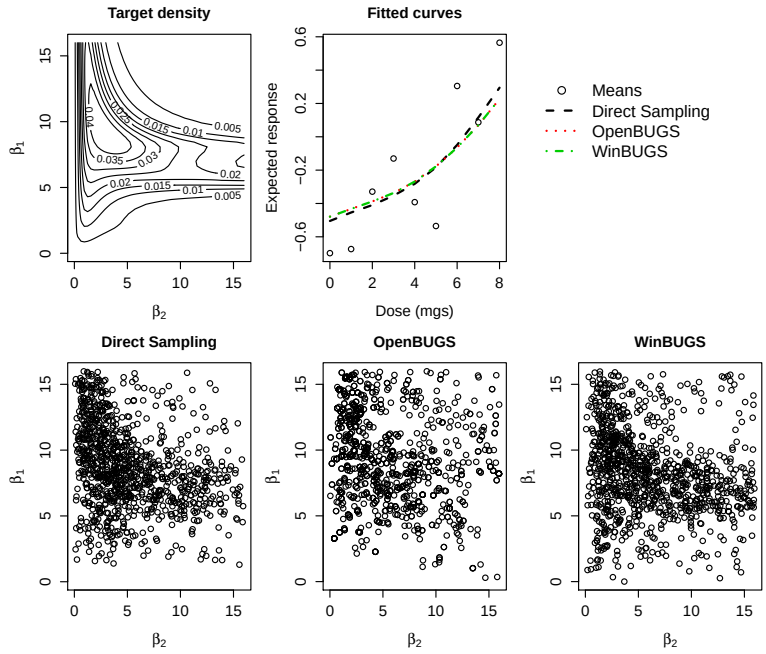

Figure 3-3: Target density, posterior mean fitted dose response curves and samples generated from the target distribution for the non-linear parameters of the four parameter sigmoid emax model (Prior 1).

are used. As the bounds for the log normal prior distributions are larger than for the uniform prior distributions, the grid has more room to roam before settling on a final placement.

Table 3.3 is a summary of how the importance sampling aspect was incorporated when uniform prior distributions were used for the β parameters. When the updated grid is relatively coarse, approximately 25% of the datasets needed to re-weight some of the accepted samples using importance weights. As the updated grid becomes more refined, the frequency with which importance weights are used is reduced from approximately 25% when an updated grid of 10x10 is used, to 1 or 2 % when an updated grid of 40x40 is used.

Figure 3-4 is an example of a dataset when importance weights are used. The initial grid for this example was 4x4 and the updated grid was 10x10. The maximum weight observed for this dataset was 8.32 and 4.7% of samples had a weight greater than 1. This plot shows the samples which had importance weights greater than 1. As we can see, even when importance weights are used the majority of the samples have an importance weight of less than 3. We observe that the samples have an importance

Initial grid size		Updated grid size 10 x 10	20 x 20	40 x 40
4 x 4	Time in secs (sd)	1.14 (0.33)	1.06 (0.21)	1.33 (0.26)
	Samples (sd)	2238 (681)	1876 (416)	1728 (375)
8 x 8	Time in secs (sd)	1.14 (0.25)	1.06 (0.12)	1.32 (0.16)
	Samples (sd)	2203 (517)	1852 (202)	1709 (102)
16 x 16	Time in secs (sd)	1.17 (0.24)	1.10 (0.11)	1.35 (0.14)
	Samples (sd)	2190 (491)	1848 (197)	1706 (96)

Table 3.1: Direct sampling method. Time in seconds and number of samples generated in order to accept 1000 samples from the posterior distribution of the four parameter sigmoid emax model (Prior 1).

Initial grid size		Updated grid size 10 x 10	20 x 20	40 x 40
4 x 4	Time in secs (sd)	1.40 (0.13)	1.14 (0.05)	1.56 (0.09)
	Samples (sd)	2952 (277)	2067 (87)	1798 (50)
8 x 8	Time in secs (sd)	1.39 (0.12)	1.13 (0.06)	1.48 (0.17)
	Samples (sd)	2917 (265)	2064 (80)	1795 (49)
16 x 16	Time in secs (sd)	1.42 (0.12)	1.16 (0.06)	1.47 (0.18)
	Samples (sd)	2910 (263)	2058 (79)	1794 (48)

Table 3.2: Direct sampling method. Time in seconds and number of samples generated in order to accept 1000 samples from the posterior distribution of the four parameter sigmoid emax model (Prior 2).

Initial grid	Updated grid	% of simulations used IS	Mean % of samples with $w > 1$ (where IS used)	Max w
4 x 4	10 x 10	26.5	5.70	16.29
	20 x 20	6.4	1.87	6.59
	40 x 40	2.7	0.85	6.62
8 x 8	10 x 10	25.9	6.00	10.96
	20 x 20	4.8	1.38	2.67
	40 x 40	1.3	0.27	2.38
16 x 16	10 x 10	23.3	5.29	14.89
	20 x 20	4.2	1.29	4.19
	40 x 40	0.4	0.30	2.38

Table 3.3: Summary of importance sampling (IS) weights. Based on 1000 datasets with 1000 samples from the posterior distribution of the four parameter sigmoid emax model (Prior 1).

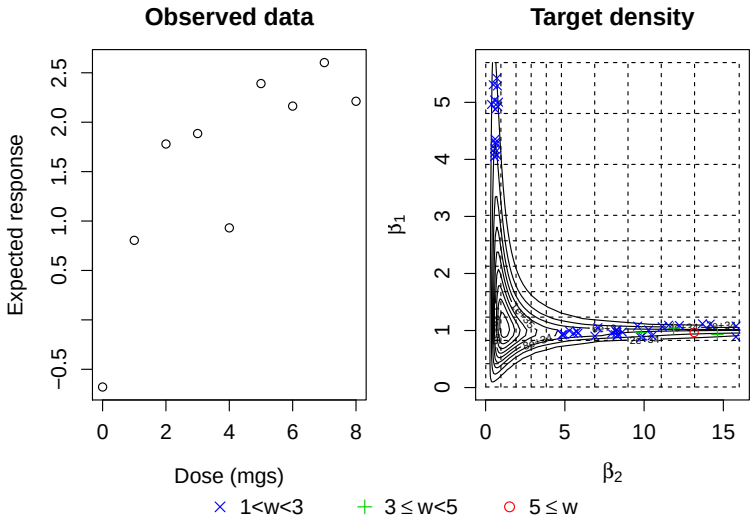

Figure 3-4: Scatter plot of observed means from an example dataset where importance sampling was used when generating samples from the posterior distribution of a four parameter sigmoid emax model. Target density for the non-linear parameters and samples with weight greater than 1 (Prior 1).

weights > 1 when there is a ridge in the target density which occurs within a cell. As the ridge extends into the tails of the target distribution, the ratio of $f(x)/c\,h(x)$ becomes greater and so we see larger importance weights. However, as these large importance weights occur in the tails we sample from these cells relatively rarely. The coarser the updated gird, the more likely we are to sample from the tails and so use importance weights more often.

For the example mentioned above, we calculate the variance of the estimator $g(\alpha, \beta) = \eta(z_j, \alpha, \beta)$ as if the samples had used AR sampling (3.10) and taking into account the importance weights (3.11), under the assumption that $g(\alpha, \beta)$ and the weights are independent. Across the doses z_j (j=0,. . . , 8) the variance of the estimator accounting for the importance weights was between 0.01% and 0.7% greater than if we had been able to use AR sampling. This loss in efficiency is relatively small compared to having to re-run the simulation study with an increased inflation factor.

When using log normal prior distributions for the β parameters, the summary of the importance weights was similar, however the frequency with which importance sampling was needed was reduced. When an updated grid of 40x40 was used, none of the datasets used importance sampling as part of the sample generation.

		Priors 1	Priors 2
OpenBUGS	Time in secs (sd)	2.32 (0.16)	2.41 (0.86)
	Effective sample size (sd)		
	α_1	304 (224)	229 (112)
	α_2	297 (246)	141 (151)
	β_1	67 (39)	39 (23)
	β_2	73 (29)	48 (20)
WinBUGS	Time in secs (sd)	4.14 (0.32)	4.35 (0.22)
	Effective sample size (sd)		
	α_1	533 (274)	524 (200)
	α_2	490 (309)	302 (247)
	β_1	251 (153)	159 (76)
	β_2	422 (182)	254 (77)

Table 3.4: MCMC methods. Time in seconds to generate 1000 samples from the posterior distribution of the four parameter sigmoid emax model and the mean effective sample size for each of the parameters.

Table 3.4 presents a summary of the time needed to generate samples and the effective sample sizes for the two MCMC methods, for Prior 1 and Prior 2. Investigation into the samplers used by OpenBUGS and WinBUGs revealed that for the α parameters both packages used a Gibbs sampler. For the β parameters OpenBUGS used an adaptive M-H block algorithm whereas WinBUGS used a slice sampler. Although the adaptive M-H algorithm is faster, as some moves in the random walk are rejected, the samples of the model parameters remain the same over iterations and so there is a higher auto-correlation resulting in a lower effective sample size. Using the slice sampler in WinBUGS is slower, but results in each iteration generating new values for the model parameters. The effective samples size of the parameters is lower for Prior 2 than Prior 1. This is because the log normal prior distribution and so the posterior distribution is not bounded above, and so there is slower mixing of the MCMC.

Comparing the two sampling approaches, the direct sampling method is faster than the MCMC approaches. For Prior 1, with an initial grid of 8x8 and an updated grid of 20x20, the average time in seconds is 1.06 compared to 2.32 and 4.14 for the OpenBUGS and WinBUGS MCMC approaches respectively. One of the main advantages of the direct sampling method is that it generates independent samples, rather than the correlated samples generated using the MCMC methods. Table 3.4 shows that the effective number of samples from the MCMC methods are substantially lower than the 1000 independent samples generated using the direct sampling method.

If we were wanted to generate enough MCMC samples so that the effective samples size was 1000, then depending on which parameter we were interested in, using OpenBUGS would be between approximately 8 and 50 times slower than direct sampling, and using WinBUGS would be between approximately 8 and 24 times slower.

3.6 The three parameter non-linear case

The three parameter emax model is a special case of the four parameter sigmoid emax model, where the slope parameter θ_4=1. The emax model is written

$$\eta(z_j, \theta) = \theta_1 + (\theta_2 - \theta_1)\frac{z_j}{\theta_3 + z_j},$$

where $\theta = (\theta_1, \theta_2, \theta_3)^T$ are the model parameters.

By letting $\alpha = (\alpha_1, \alpha_2)^T = (\theta_1, \theta_2)^T$ and $\beta = \theta_3$, then as with the four parameter case we can re-parametrise the model so that it is a linear model in terms of α with a non-linear function in terms of β,

$$\eta(z_j, \alpha, \beta) = \alpha_1 + (\alpha_2 - \alpha_1)a(z_j, \beta), \tag{3.18}$$

where $a(z_j, \beta) = \frac{z_j}{\beta + z_j}$. This is the same as the linearised model for the four parameter case in Section 3.2 but with a simpler non-linear function.

We use the same prior distributions for α and β as used in Section 3.2. Following through with the algebra, for a given dataset $Y = y$, we end up with the same form for the joint posterior distribution for α and β given by (3.3). For the three parameter case the β parameter only has one dimension and so the approximating density $h(\beta|y)$ is a one-dimensional grid. Setting up the initial grid and then using a normal approximation to improve the grid placement is carried out in the same way as before but in one dimension. Sampling using the HARIS method follows the same principles as in Section 3.3.4.

3.6.1 Assessing the method

In Section 3.5, a simulation study was performed to compare the direct sampling method against the established MCMC sampling used in OpenBUGS and WinBUGS. We carry out a similar simulation study here for the three parameter case.

For the simulation study we set prior distributions on α_1, α_2, and β. These prior distributions are as follows:

- $\alpha_1 \sim N(0, 2)$
- $\alpha_2 \sim N(1, 2)$
- $\beta \sim U(0.01, 16)$

We define the bounds of our grid to coincide with the prior distribution for β, i.e. $\beta \in [0.01, 16]$. We found that for the four parameter case, using uniform prior distributions for the β parameters produced more awkward target densities than when log normal prior distributions were used. This resulted in importance sampling being utilised more frequently as part of the HARIS method. We therefore use a uniform prior distribution for β here as a worst case scenario, to test the robustness of the method.

As in Section 3.5 we generate K=1000 datasets, with 250 subjects randomised equally across 9 doses $(0, 1, \ldots, 8\text{mgs})$. The subject response data are generated from the sigmoid emax model in (3.17), with parameter values sampled from the prior distribution. To reduce the model to the three parameter emax model we set $\beta_2^k = 1$ $(k = 1, \ldots, K)$.

For the direct sampling method, the target distribution is the conditional posterior distribution for β given a dataset $Y = y$, which has a density proportional to the target density $f(\beta|y)$ as given in (3.5). In the one-dimensional case, the target density is better behaved and so we reduce the inflation factor used to find the stretching factor for the HARIS method to 1.05. For each dataset, we generate 1000 independent samples from the posterior distribution using the HARIS method with a range of grid sizes. The initial number of cells for the one-dimensional grid are; 2, 4 and 10. For the updated grid we use; 10, 20 and 40 cells.

As a comparison, we also generate 1000 MCMC samples using packages described in Section 3.3.5. For the MCMC sampling with use a burn-in of 1000 samples which are discarded before generating the 1000 samples. We compare the time needed to generate the samples for the direct and MCMC methods. We also calculate the effective sample size (3.13) of the MCMC samples.

Initial grid size		Updated grid size 10	20	40
4	Time in secs (sd)	0.53 (0.05)	0.51 (0.02)	0.50 (0.02)
	Samples (sd)	1219 (120)	1154 (48)	1126 (30)
8	Time in secs (sd)	0.53 (0.05)	0.51 (0.02)	0.50 (0.02)
	Samples (sd)	1216 (109)	1153 (43)	1124 (27)
16	Time in secs (sd)	0.53 (0.04)	0.51 (0.02)	0.50 (0.01)
	Samples (sd)	1213 (102)	1152 (41)	1124 (26)

Table 3.5: Direct sampling method. Time in seconds and number of samples generated in order to accept 1000 samples from the posterior distribution of the three parameter emax model.

Initial grid	Updated grid	% of simulations used IS	Mean % of samples with $w > 1$ (where IS used)	Max w
4	10	2.7	8.65	1.10
	20	0.3	3.27	1.01
	40	0.0		1.00
8	10	3.0	7.47	1.09
	20	0.1	1.60	1.01
	40	0.0		1.00
16	10	3.3	9.48	1.08
	20	0.1	1.60	1.01
	40	0.0		1.00

Table 3.6: Summary of importance sampling (IS) weights. Based on 1000 datasets with 1000 samples from the posterior distribution of the three parameter emax model.

With the three parameter model (Table 3.5), the size of the initial and updated grids has little impact on the number of samples and time needed to generate the independent samples. The inflation factor has been reduced to 1.05, compared to 1.5 used in the four parameter case, and so this reduces the average number of samples generated to accept the 1000 required sample. The reduced inflation factor and the fact that we are working in one-dimension, makes the sampling reasonably efficient. Although we have reduced the inflation factor, the frequency with which importance weights are needed (Table 3.6) is relatively low and the maximum importance weights observed are small. This suggests that the approximating density $h(\beta|y)$ is close to the target density $f(\beta|y)$. In this case, we have found using an updated grid with 40 cells results in acceptance-rejection sampling being possible for all the simulated datasets.

Figure 3-5 is and example of a dataset where importance sampling was utilised. The initial grid for this example was 4x4 and the updated grid was 10x10. Due to

the poor placement of the grid, we do not observe the maximum of the target density and so search for the stretching factor c in the tail of the distribution. Therefore, the samples around the maximum of the target distribution have a weight greater than 1. From the 1000 samples generated, 7.8% had a weight greater than 1 and the maximum weight observed was 1.10. As all the importance weights are close to 1, this is of little concern. The variance of the estimator from using importance sampling (3.11) was <0.05% larger than if all the samples had weights of 1 (3.10). As the number of grid points in the updated grid increases, we can identify where the maximum is with more accuracy and so this reduces the frequency with which we need to incorporate importance sampling.

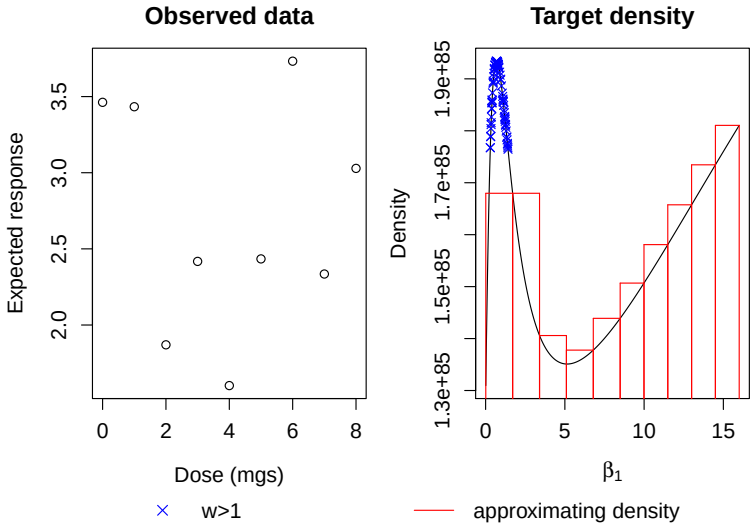

Figure 3-5: Scatter plot of observed means from an example dataset where importance sampling was used when generating samples from the posterior distribution of a three parameter max model. Target density for the non-linear parameter and samples with weight greater than 1.

As the different grid options explored all take a similar time to generate the 1000 samples, this suggests there is a balance between the set up costs of constructing the approximate density and the time needed to generate the samples. The coarser grid options are faster at approximating the density, but need to generate more samples, as there is a higher rejection rate. The finer grids are slow to set up, but have a higher acceptance rate and so need to generate less samples. Therefore if we only wanted to generate a few samples it might be worth using the coarser grid, but for if we wish to generate large number of samples then using an initial grid of 16 and an updated grid

	OpenBUGS	WinBUGS
Time in secs (sd)	1.32 (0.13)	2.03 (0.11)
Effective sample size (sd)		
α_1	73 (23)	757 (305)
α_2	75 (23)	606 (352)
β	72 (20)	318 (162)

Table 3.7: MCMC methods. Time in seconds to generate 1000 samples from the posterior distribution of the three parameter emax model and the mean effective sample size for each of the parameters.

of 40 would be advisable.

Table 3.7 presents a summary of the performance for the two MCMC methods. The effective sample size of the OpenBUGS method is a lot lower than the WinBUGS method. The OpenBUGS program uses a adaptive M-H block algorithm to generate the samples whereas WinBUGS using a Gibbs sampler for the α parameters and a slice sampler for the β parameter. The adaptive M-H algorithm on average had a high rejection rate, which resulted in the small effective sample size. One reason for this could be the co-linearity of the α_2 (maximum response) and β (dose with 50% of the maximum response) parameters. It is known that MCMC methods can be slow to converge 'when parameters are highly correlated in the target distribution' (Gelman et al., 2004, p. 292).

We conclude that for the three parameter emax case, the direct sampling method is faster than the MCMC method. Using an initial grid with 16 cells and an updated grid with 40 cells, the direct sampling method takes 0.5 seconds compared with 1.32 seconds using OpenBUGS and 2.03 seconds using WinBUGS. Taking into account the reduced effective sample size of the MCMC methods, the direct sampling method is between (approximately) 5 and 35 times more efficient than the MCMC methods, depending on which parameter we are most interested in and which MCMC method we use. This conclusion is consistent with the four parameter sigmoid emax case.

3.7 Including a prior on the between subject variance

So far we have assumed that the between subject variance, σ^2 is fixed and known. In this section we put a prior distribution on σ^2 and examine the effect this has on the form of the joint posterior distribution.

The linearisation of the non-linear model remains the same as given in (3.2). As before, we assume that the asymptotes α are normally distributed, $\alpha \sim N(\mu, \Delta)$ which has density $\pi(\alpha)$. We place prior distributions on the β and σ^2 parameters which reflect our prior beliefs, and denote the densities of these prior distributions as $\pi(\beta)$ and $\pi(\sigma^2)$ respectively.

We assume that the expected subject responses $\bar{Y}$ are normally distributed,

$$\bar{Y}|\alpha, \beta, \sigma^2 \sim N(X_\beta \alpha, \sigma^2 \Gamma),$$

where X_β is the design matrix for a given β, Γ is a diagonal matrix with $\Gamma_{jj} = \frac{1}{n_j}$ and n_j is the number of subjects allocated to dose z_j.

Using Bayes' Theorem, this joint posterior distribution can be written as

$$\pi(\alpha, \beta, \sigma^2|y) \propto p(y|\alpha, \beta, \sigma^2)\pi(\alpha)\pi(\beta)\pi(\sigma^2) \tag{3.19}$$

As σ^2 is unknown, it no longer holds that the density $p(y|\alpha, \beta, \sigma^2)$ for Y is proportional to the density $p(\bar{y}|\alpha, \beta, \sigma^2)$ for $\bar{Y}$. Instead, we note then when $n = \sum_{j=0}^{J} n_j$ the density for Y can be written

$$\begin{aligned} p(y|\alpha, \beta, \sigma^2) &= \prod_{j=0}^{J}\prod_{i=1}^{n_j} \frac{1}{\sqrt{2\pi\sigma^2}} e^{-\frac{1}{2\sigma^2}(y_{ij}-\eta(z_j,\alpha,\beta))^2} \\ &= \left(\frac{1}{\sqrt{2\pi\sigma^2}}\right)^n e^{-\frac{1}{2\sigma^2}\sum_{j=0}^{J}\sum_{i=1}^{n_j}(y_{ij}-\eta(z_j,\alpha,\beta))^2} \\ &\propto (\sigma^2)^{-\frac{n}{2}} e^{-\frac{1}{2\sigma^2}\sum_{j=0}^{J}\sum_{i=1}^{n_j}(y_{ij}-\bar{y})^2} e^{-\frac{1}{2\sigma^2}\sum_{j=0}^{J}\sum_{i=1}^{n_j}(\bar{y}-\eta(z_j,\alpha,\beta))^2}. \end{aligned}$$

In the equation above, the second exponential term is proportional to $(\sigma^2)^{\frac{J+1}{2}} p(\bar{y}|\alpha, \beta, \sigma^2)$. Hence when σ^2 is unknown the density of Y is related to the density of $\bar{Y}$ as follows

$$p(y|\alpha, \beta, \sigma^2) \propto (\sigma^2)^{\frac{J+1}{2}} (\sigma^2)^{-\frac{n}{2}} e^{-\frac{1}{2\sigma^2}\sum_{j=0}^{J}\sum_{i=1}^{n_j}(y_{ij}-\bar{y})^2} p(\bar{y}|\alpha, \beta, \sigma^2).$$

The joint posterior distribution for α, β and σ^2 given $Y = y$ is then,

$$\begin{aligned}
\pi(\alpha,\beta,\sigma^2|y) &\propto p(y|\alpha,\beta,\sigma^2)\pi(\alpha)\pi(\beta)\pi(\sigma^2) \\
&\propto (\sigma^2)^{\frac{J+1}{2}}(\sigma^2)^{-\frac{n}{2}}e^{-\frac{1}{2\sigma^2}\sum_{j=0}^{J}\sum_{i=1}^{n_j}(y_{ij}-\bar{y})^2}p(\bar{y}|\alpha,\beta,\sigma^2)\pi(\alpha)\pi(\beta)\pi(\sigma^2) \\
&\propto (\sigma^2)^{\frac{J+1}{2}}(\sigma^2)^{-\frac{n}{2}}e^{-\frac{1}{2\sigma^2}\sum_{j=0}^{J}\sum_{i=1}^{n_j}(y_{ij}-\bar{y})^2} \\
&\quad \times(2\pi)^{-\frac{J+1}{2}}|\sigma^2\mathbf{\Gamma}|^{-\frac{1}{2}}e^{-\frac{1}{2}(\bar{y}-X_\beta\alpha)^T(\sigma^2\mathbf{\Gamma})^{-1}(\bar{y}-X_\beta\alpha)} \\
&\quad \times(2\pi)^{-\frac{1}{2}}|\mathbf{\Delta}|^{-\frac{1}{2}}e^{-\frac{1}{2}(\alpha-\mu)^T\mathbf{\Delta}^{-1}(\alpha-\mu)}\pi(\beta)\pi(\sigma^2) \\
&\propto e^{-\frac{1}{2}(\alpha^T(X_\beta^T(\sigma^2\mathbf{\Gamma})^{-1}X_\beta+\mathbf{\Delta}^{-1})\alpha-2\alpha^T(X_\beta^T(\sigma^2\mathbf{\Gamma})^{-1}\bar{y}+\mathbf{\Delta}^{-1}\mu))} \\
&\quad \times(\sigma^2)^{-\frac{n}{2}}e^{-\frac{1}{2\sigma^2}\sum_{j=0}^{J}\sum_{i=1}^{n_j}(y_{ij}-\bar{y})^2}e^{-\frac{1}{2}(\bar{y}^T(\sigma^2\mathbf{\Gamma})^{-1}\bar{y}+\mu^T\mathbf{\Delta}^{-1}\mu)}\pi(\beta)\pi(\sigma^2).
\end{aligned}$$

Letting $\mathbf{A}_{\beta,\sigma^2} = (X_\beta^T(\sigma^2\mathbf{\Gamma})^{-1}X_\beta + \mathbf{\Delta}^{-1})^{-1}$ and $B_{\beta,\sigma^2} = X_\beta^T(\sigma^2\mathbf{\Gamma})^{-1}\bar{y} + \mathbf{\Delta}^{-1}\mu$, we can complete the square to get a normal distribution $N(\mathbf{A}_{\beta,\sigma^2}B_{\beta,\sigma^2}, \mathbf{A}_{\beta,\sigma^2})$ which has density as $\pi(\alpha|\beta,\sigma^2,y)$. Keeping only the terms which depend on α, β and σ^2, this can be written

$$\begin{aligned}
\pi(\alpha,\beta,\sigma^2|y) &\propto e^{-\frac{1}{2}(\alpha-\mathbf{A}_{\beta,\sigma^2}B_{\beta,\sigma^2})^T\mathbf{A}_{\beta,\sigma^2}^{-1}(\alpha-\mathbf{A}_{\beta,\sigma^2}B_{\beta,\sigma^2})}e^{\frac{1}{2}B_{\beta,\sigma^2}^T\mathbf{A}_{\beta,\sigma^2}B_{\beta,\sigma^2}} \\
&\quad \times(\sigma^2)^{-\frac{n}{2}}e^{-\frac{1}{2\sigma^2}\sum_{j=0}^{J}\sum_{i=1}^{n_j}(y_{ij}-\bar{y})^2}e^{-\frac{1}{2}(\bar{y}^T(\sigma^2\mathbf{\Gamma})^{-1}\bar{y})}\pi(\beta)\pi(\sigma^2) \\
&\propto \pi(\alpha|\beta,\sigma^2,y)|\mathbf{A}_{\beta,\sigma^2}|^{\frac{1}{2}}e^{\frac{1}{2}B_{\beta,\sigma^2}^T\mathbf{A}_{\beta,\sigma^2}B_{\beta,\sigma^2}} \\
&\quad \times(\sigma^2)^{-\frac{n}{2}}e^{-\frac{1}{2\sigma^2}\sum_{j=0}^{J}\sum_{i=1}^{n_j}(y_{ij}-\bar{y})^2}e^{-\frac{1}{2}(\bar{y}^T(\sigma^2\mathbf{\Gamma})^{-1}\bar{y})}\pi(\beta)\pi(\sigma^2). \quad (3.20)
\end{aligned}$$

Hence, the joint posterior distribution in (3.19) is a product of a multivariate normal distribution and a function in terms of only β and σ^2. From (3.20)

$$\alpha|\beta,\sigma^2,y \sim N(\mathbf{A}_{\beta,\sigma^2}B_{\beta,\sigma^2}, \mathbf{A}_{\beta,\sigma^2}),$$

which is the same as in (3.4), when σ^2 was assumed to be fixed. The joint conditional density for β, σ^2 given $Y = y$ is proportional to

$$\begin{aligned}
f(\beta,\sigma^2|y) &= (\sigma^2)^{-\frac{n}{2}}e^{-\frac{1}{2\sigma^2}\sum_{j=0}^{J}\sum_{i=1}^{n_j}(y_{ij}-\bar{y})^2}|\mathbf{A}_{\beta,\sigma^2}|^{1/2}e^{\frac{1}{2}B_{\beta,\sigma^2}^T\mathbf{A}_{\beta,\sigma^2}B_{\beta,\sigma^2}} \\
&\quad \times e^{-\frac{1}{2}(\bar{y}^T(\sigma^2\mathbf{\Gamma})^{-1}\bar{y})}\pi(\beta)\pi(\sigma^2).
\end{aligned}$$

We write the joint conditional density of β, σ^2 given y as

$$\pi(\beta,\sigma^2|y) = \tau\, f(\beta,\sigma^2|y),$$

where $\tau = \frac{1}{\int f(\beta,\sigma^2|y)\, d(\beta,\sigma^2)}$ is the normalising constant. The joint posterior can now be written

$$\begin{aligned} \pi(\alpha,\beta,\sigma^2|y) &= \pi(\alpha|\beta,\sigma^2,y)\,\tau\, f(\beta,\sigma^2|y) \\ &= \frac{\pi(\alpha|\beta,\sigma^2,y) f(\beta,\sigma^2|y)}{\int f(\beta,\sigma^2|y) d(\beta,\sigma^2)}. \end{aligned} \tag{3.21}$$

The target density $f(\beta,\sigma^2|y)$ is a three dimensional density, and so we use a three dimensional array to construct our approximating density. The method for construction the grid follows the same principles as Section 3.4. The initial grid is updated using the marginal normal approximations for the three parameters. We sample from the joint posterior distribution using the HARIS method (Section 3.3.4).

3.7.1 Assessing the method

As in Sections 3.5 and 3.6.1, a simulation study is performed to compare the direct sampling method with the established MCMC sampling methods.

For the simulation study we set prior distributions on α_1, α_2, β_1, β_2 and σ^2. These prior distributions are as follows:

- $\alpha_1 \sim N(0,2)$
- $\alpha_2 \sim N(1,2)$
- $\beta_1 \sim U(0.01,16)$
- $\beta_2 \sim U(0.01,16)$
- $\sigma^2 \sim G(2.25,0.5)$

A gamma distribution is used for the prior of σ^2 to restrict the parameter to positive values. For the bounds of the 3D array we use $\beta_1 \in [0.01,16]$, $\beta_2 \in [0.01,16]$ and $\sigma^2 \in [0.01,10]$.

Like for the previous simulation studies, we generated $K = 1000$ datasets of subject responses, consisting of 250 subjects randomised equally across 9 doses $(0,1,\ldots,8\text{mgs})$. The subject response data were generated using a sigmoid emax model with model parameters α_1, α_2, β_1, β_2 and σ^2 sampled from the prior distributions. The sample of parameters values from the prior distributions are denoted $(\alpha^k,\beta^k)=(\alpha_1^k, \alpha_2^k, \beta_1^k,\beta_2^k)$

Initial grid size		Updated grid size 10 x 10 x 10	15 x 15 x 15	20 x 20 x 20
4 x 4 x 2	Time in secs (sd)	3.35 (0.88)	4.39 (1.40)	7.22 (2.96)
	Samples (sd)	5282 (1542)	3677 (806)	3236 (603)
8 x 8 x 5	Time in secs (sd)	3.37 (0.83)	4.21 (1.38)	6.75 (2.88)
	Samples (sd)	5237 (1490)	3651 (816)	3211 (605)
16 x 16 x10	Time in secs (sd)	3.79 (0.88)	4.47 (1.16)	6.95 (2.40)
	Samples (sd)	5246 (1644)	3613 (612)	3187 (428)

Table 3.8: Direct sampling method. Time in seconds and number of samples generated in order to accept 1000 samples from the posterior distribution of the four parameter sigmoid emax model with a prior distribution on σ^2

and $\sigma^{2(k)}$ $(k = 1, \ldots, K)$. The mean response on dose z_j $(j = 0, \ldots, J)$ for the k^{th} dataset $(k = 1, \ldots, K)$ is

$$\begin{aligned} \bar{Y}_j^k &= \eta(z_j, \alpha^k, \beta^k) + \epsilon_j^k \\ &= \alpha_1^k + (\alpha_2^k - \alpha_1^k)\frac{z_j^{\beta_2^k}}{\beta_1^{k\beta_2^k} + z_j^{\beta_2^k}} + \epsilon_j^k, \end{aligned}$$

where $\epsilon_j^k \sim N\left(0, \frac{\sigma^{2(k)}}{n_j}\right)$ and n_j is the number of subjects allocated to dose z_j.

For each simulated dataset, we sample T=1000 parameter vectors from the posterior distribution for $(\alpha,\ \beta,\ \sigma^2)$=$(\alpha_1,\ \alpha_2,\ \beta_1,\ \beta_2,\ \sigma^2)$, where each sample vector is denoted $(\alpha^t$,$\beta^t,\ \sigma^{2(t)})$=$(\alpha_1^t,\ \alpha_2^t,\ \beta_1^t,\ \beta_2^t,\ \sigma^{2(t)})$ $(t = 1, \ldots, T)$. We can then estimate the fitted dose response curve to be

$$E[\eta(z_j, \alpha, \beta)|Y = y] \approx \frac{\sum_{t=1}^T \eta(z_j, \alpha^t, \beta^t) w^t}{\sum_{t=1}^T w^t},$$

where w^t are the important weights from the HARIS method (Section 3.3.4).

When choosing our stretching factor c (3.15) we use an inflation factor of 1.5. For each dataset, 1000 independent samples were generated from the posterior distribution using the HARIS sampling method with a range of grid sizes. We explore three sizes for the initial three dimensional grid: 4x4x2, 8x8x5 and 16x16x10, and three sizes for the updated grids: 10x10x10, 15x15x15 and 20x20x20.

From Table 3.8 we can see that the size of the updated grids impacts the time needed to generate the samples. As the grid is now in three dimensions, doubling the grid size

Initial grid	Updated grid	% of simulations used IS	Mean % of samples with $w > 1$ (where IS used)	Max w
4x4x2	10x10x10	29.1	4.69	76.3
	15x15x15	8.4	1.20	3.93
	20x20x20	5.3	0.98	6.5
8x8x5	10x10x10	30.3	4.79	21.7
	15x15x15	8.2	1.17	3.2
	20x20x20	3.4	1.13	2.0
16x16x10	10x10x10	27.4	3.9	67.6
	15x15x15	8.3	1.25	5.9
	20x20x20	3.3	0.88	5.4

Table 3.9: Summary of importance sampling (IS) weights. Based on 1000 datasets with 1000 samples from the posterior distribution of the four parameter sigmoid emax model with a prior distribution on σ^2.

results in 8 times as many grid points being evaluated. It is therefore more efficient to use and updated grid of 10x10x10 with a higher rejection rate than to increase the grid to 20x20x20. Increasing the size of the initial grid reduces the standard deviation. As the purpose of the initial grid is to locate where the majority of the density lies, we want this process to be as cheap as possible whilst still providing a reliable estimate. If the grid is too coarse, then the updated grid may be poorly placed which results in either the grid needing to be re-positioned or a higher rejection rate. If the initial grid is too refined, then this is costly in terms of computing time.

Table 3.9 is a summary of how often importance sampling was employed when generating samples. We can see that for the coarsest grid with 4x4x2 cells in the initial grid and 10x10x10 cells in the updated grid, that importance sampling is used to generate samples for 29.1% of the simulated datasets. For this grid option, when importance sampling is used on average 4.69% of the samples have an importance weight greater than 1. This is a relatively small number of the 1000 samples, however the maximum importance weight observed across the simulated datasets was 76.3. This is a large importance weight, which will have undue influence on the estimator. Increasing the updated grid to 15x15x15 is slightly slower than using a 10x10x10 grid, but substantially reduces the maximum importance weight and so is a better option for generating samples.

Compared to the scenarios when σ^2 was assumed to be fixed, the average time (sd) in seconds for the direct sampling has gone from 1.06 (0.12) to 4.21 (1.38). This reflects the extra computational intensity from adding another unknown parameter. Although

	OpenBUGS	WinBUGS
Time in secs (sd)	4.28 (0.39)	4.95 (0.54)
Effective sample size (sd)		
α_1	418 (225)	529 (273)
α_2	420 (279)	463 (306)
β_1	243 (161)	247 (162)
β_2	394 (193)	393 (185)
σ^2	953 (128)	940 (119)

Table 3.10: MCMC methods. Time in seconds to generate 1000 samples from the posterior distribution of the four parameter sigmoid emax model with a prior distribution on σ^2 and the mean effective sample size for each of the parameters.

this method is still relatively efficient, increasing the number of dimensions further would slow the process down, making it less practical.

Table 3.10 presents a summary of the two MCMC methods. Both the OpenBUGS and WinBUGS methods give similar results in terms of the time needed to generate the samples and the effective sample size. To generate the samples both packages used a Gibbs sampler for the α parameters and a slice sampler for the β and σ^2 parameters.

Using a initial grid of 8x8x5 and an updated grid of 15x15x15 the average time of generating 1000 samples using direct sampling was 4.21 compared with 4.28 using OpenBUGS and 4.95 using WinBUGS. On average the direct sampling method is still competitive with the MCMC methods and has the advantage that there are 1000 independent samples being generated. The effective sample size for the α and β parameters are markedly less than 1000 and so to increase the precision on the estimator for the MCMC methods a larger sample would need to be generated which would then slow down the MCMC methods.

It should be noted that it would be also possible to put a prior on σ^2 in the three parameter Emax case. This would then become a 2 parameter problem similar to that of the four parameter sigmoid emax model without a prior on σ^2.

3.8 Discussion

We have seen that sampling directly from the posterior density of the non-linear model using the proposed HARIS method, offers savings in time over the MCMC methods. Sampling directly also provides uncorrelated sample, whereas the MCMC samples

have, in some cases, a high autocorrelation, reducing the effective size of the sample substantially. Our results show that for the four parameter sigmoid emax model, direct sampling can be between 8 and 50 times more efficient than using the MCMC methods.

Although direct sampling may not be possible or ideal in all situations, we have shown that it does offer an alternative to the MCMC methods for the types of models explored in this chapter. The direct sampling method may be especially beneficial when large scale simulation studies are being carried out and the convergence and autocorrelation of each individual simulation can not be checked. We acknowledge that we are not experts in using either the WinBUGS or OpenBUGS packages, and so we have approached these packages in a naive manner using the default settings for the sampling algorithms. Therefore there may be ways of making the MCMC methods more efficient which have not been explored here.

Reilly (1976), comments that a disadvantage of the grid method is the need to use discrete parameter values. We have overcome this problem by sampling within each of the grid cells, allowing continuous parameter values to be generated. One concern that remains with using a grid method, is that the grid only covers a finite region and so situations may arise where the mass of the target distribution is on the edge of or outside the range of the grid. We have attempted to overcome this by allowing the grid to re-position itself as necessary within the prespecified bounds. Provided the bounds of the grid are set to be large enough to cover biologically reasonable values, then situations where the mass of the target distribution are outside the grid should be minimised.

Our sampling method uses a hybrid acceptance rejection and importance sampling (HARIS) approach. This allows us to compromise between having a high rejection rate and high variability in the importance weights. We have shown how this method, which was originally proposed by Liu et al. (1998) for dynamical models, can be applied to this problem. For the examples we have used, the more refined the grid we sample from, the less often the importance sampling element needs to be employed. When the importance sampling is used, provided the grid has enough points, the maximum importance weights observed are relative small.

In this chapter we focus on the sigmoid emax model as it is a common model used in the pharmaceutical industry, and is a model which we are interested in fitting in later chapters. However, the method holds for other non-linear models which can be

re-written as a linear model with a non-linear term, and where the linear parameters are normally distributed. The limiting factor on the generalisability of the method is the number of non-linear parameters. As the number of non-linear parameters increases the computational intensity of the sampling method increases and so with more than three non-linear parameters it may be more efficient to use the MCMC methods. For some models there may be situations where the target density is bi-modal, and so the normal approximation used to update the grid may not result in an effective grid placement. A poor updated grid placement would then lead to a high rejection rate and large importance weights.

The grid placements we have used in our sampling schemes have shown to be efficient for the sigmoid emax model, but we recognise that further development could be carried out to improve the efficiency further. For example, rather than discarding the initial grid these points could be incorporated into the updated grid thereby increasing the overall the number of points. The way in which the grid points are updated could also be an area for improvement. We use a normal approximation to dictate where the updated grid should be placed, but with some exploration this could no doubt be improved upon.

Chapter 4

General Adaptive Dose Allocation Approach (GADA)

4.1 Introduction

One of the motivating papers for this thesis, is the white paper on adaptive designs written by the PhRMA working group (Bornkamp et al., 2007). In the Bornkamp et al. (2007) paper, two response adaptive designs were explored. These designs both adapted the subject allocation based on the observed information. The designs explored are the General Adaptive Dose Allocation (GADA) approach and an adaptive D-optimal design. In this chapter we explore the GADA method and in Chapter 6 the D-optimal approach.

The GADA method uses Bayesian decision theory (Berry et al., 2001) to randomise each subject individually to either the optimal dose or placebo. The optimal dose is defined as the dose that results in the maximum increase in information about some specified aspect of the dose response curve. The methodology implemented in the PhRMA working group paper was a generalisation of the design used in the ASTIN study (Grieve & Krams, 2005; Krams et al., 2003). The ASTIN study was the first study to successfully apply such an adaptive design to a dose-finding study. Although the results of the ASTIN study were negative, the implementation of the adaptive design resulted in the study being stopped early for futility. This saved subjects being exposed to an ineffective treatment, as well as saving the company time and resources.

A review of the literature revealed only one other dose-finding study that had applied

a response adaptive design to randomised subjects individually based on Bayesian decision theory (Shen et al., 2011). Other studies have dropped or added doses based on interim analyses (Berry et al., 2010; Smith et al., 2006). Padmanabhan et al. (2012) present a simulation study where a normal dynamic linear model (NDLM) (West & Harrison, 1997) is used to jointly model safety and efficacy data, with a response adaptive design.

In this chapter we explore the mechanism of randomising subjects individually to ensure that we can identify the optimal dose with a degree of accuracy. We investigate the impact of putting prior distributions on the model parameters and then finally replicate the scenarios used in the Bornkamp et al. (2007) paper. The methods used in this chapter are similar to those used in the ASTIN study and the Bornkamp et al. (2007) paper, however we aim to cover aspects of the design in more detail than has previously been seen.

4.1.1 Background

Figure 4-1 illustrates the study design that was employed in the ASTIN study. The ASTIN study was a response adaptive dose-finding study where subjects were randomised sequentially based on the observed data. Here, a longitudinal model was used to predict the final outcomes for subjects with only partial data available. In the PhRMA working group paper this aspect was disabled and complete data were assumed to be available immediately. The dose response was modelled using an NDLM and a stopping rule was incorporated so the study could be stopped for either futility or efficacy. Constraints were built into the ASTIN study design, such that the study could be stopped at the decision of a Data Monitoring Committee (DMC), only after a prespecified number of subjects had entered the trial, in order to ensure the decision was based on sufficient evidence. The simulation studies carried out in this chapter do not implement any form of stopping rules.

In the ASTIN trial, if the decision was to continue recruitment, then based on Bayesian decision theory, the dose which optimised some specified aspect of the dose response curve was found. The next subject was then randomised to either the placebo or the optimal dose, maintaining a minimum allocation to placebo to protect against a drift in the study population that could potentially bias the results (Grieve & Krams, 2005). As the doses in ASTIN were given intravenously, there was flexibility in the doses used in the study. Once the subject was randomised to a dose this was translated to the

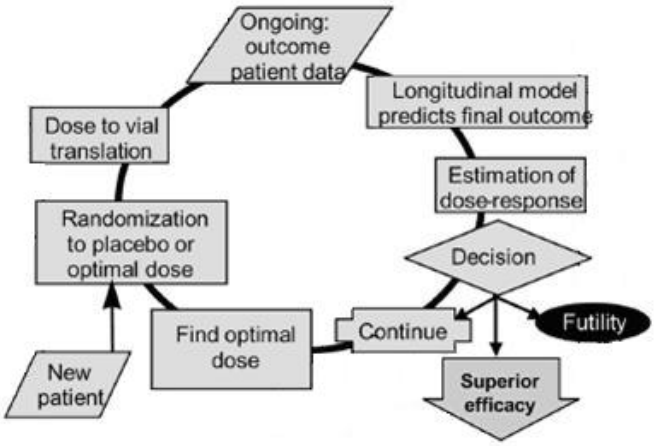

Figure 4-1: GADA method as implemented in the ASTIN study. (Source: Berry et al. (2001))

appropriate vial specifications. This flexibility in doses could also be achieved for other indications using different tablet combinations. For a full account of the methodology used in the ASTIN study see Berry et al. (2001).

4.2 Methodology

4.2.1 The normal dynamic linear model (NDLM)

The GADA method models the dose response using a second order polynomial normal dynamic linear model (NDLM) as outlined by West & Harrison (1997, p. 211). The NDLM allows flexibility as it makes no assumptions about the shape of the dose response curve or that the dose response curve is monotonic.

The system equations of the NDLM are used to construct the prior distribution for θ, which has prior density $\pi(\theta)$. For the prior distribution we assumed that $\theta_0 \sim N(0, W_0)$ and $\delta_0 \sim N(0, W_0)$. The prior distribution for θ_j $(j = 1, \ldots, J)$ is then constructed as

$$\begin{aligned} \delta_j &= \delta_{j-1} + \epsilon_j \qquad \text{where} \qquad \epsilon_j \sim N(0, W_j), \\ \theta_j &= \theta_{j-1} + \delta_{j-1} + \omega_j \qquad \text{where} \qquad \omega_j \sim N(0, W_j). \end{aligned} \tag{4.1}$$

Here, W_j is called the evolution variance at dose z_j. The error sequences ω_j and ϵ_j are independent (West & Harrison, 1997, p. 32). In the NDLM the δ_j can generate a trend between the doses. The $E[\theta_j] = 0$ for all j, and so the prior belief is that on average

there no dose response.

Specifying a suitable evolution variance is not easy. For forecasting models, West & Harrison (1997, p. 51) suggest $W_j = C_{j-1}(1-r)/r$ where C_{j-1} is the posterior variance at time $j-1$ and r is a discount factor typically between 0.8 and 1. Translating this to a dose response model is not straightforward, as we consider the dose response curve as a whole. Instead we use $W_j = W\sigma^2$ as used in the ASTIN trial (Weir et al., 2007). Although this may not be ideal for some of the underlying dose response curves, it seems a fair assumption without prior knowledge about the shape of the dose response curve. In the prior distribution, W acts like a scaling factor for the variation, where larger values of W result in more uncertainty. For now we assume W is fixed and takes values $0 < W \leq 1$.

From the system equations (4.1) we can write the prior distribution for θ as a multivariate normal distribution,

$$\theta \sim N(\mu, W\boldsymbol{\Delta}), \tag{4.2}$$

where μ is a zero vector and $\boldsymbol{\Delta}$ is the evolution variance matrix. The variance of the j^{th} dose can be written as,

$$\text{Var}(\theta_j) = W\boldsymbol{\Delta}_{jj} = W(j+1+\sum_{k=0}^{j} k^2)\sigma^2$$

and the covariance of the i^{th} and j^{th} doses ($i < j$) is,

$$\text{Cov}(\theta_i, \theta_j) = W\boldsymbol{\Delta}_{ij} = W(i+1+\sum_{k=0}^{i} k(k+j-i))\sigma^2.$$

As the variance of θ_j depends on j, doses further away from placebo have more uncertainty associated with them in the prior distribution for θ_j. The construction of the variance covariance matrix assumes that the doses are equally spaced. If we do not have equally spaced doses, we can reflect the additional variability in doses which are further apart by constructing the variance matrix for a larger set of equally spaced doses. We can then construct a new variance matrix using the rows and columns of the original variance matrix for those doses we are interested in, and use this new variance matrix in our NDLM.

Using the notation laid out in Chapter 2, we assume the expected response of subject i on dose z_j is

$$E[Y_{ij}] = \theta_j$$

and so our dose response model

$$\eta(z_j, \theta) = \theta_j.$$

We assumed the expected response at dose z_j is normally distributed,

$$\bar{Y}_j|\theta \sim N(\eta(z_j, \theta), \sigma^2/n_j) \tag{4.3}$$

where n_j is the number of subjects allocated to dose z_j. The vector of expected responses can be written as a multivariate normal distribution,

$$\bar{Y}|\theta \sim N(\eta(z, \theta), \mathbf{\Sigma}),$$

where $\mathbf{\Sigma}$ is the diagonal variance matrix (2.4). We assume that the variance σ^2 is known, and therefore with a fixed value for W in the prior distribution, $W\sigma^2$ is also known. Later, we relax this assumption.

4.2.2 Finding the posterior distribution of θ

As data are accumulated into the trial the posterior distribution $\theta|y$ for a given dataset $Y = y$ is updated using Bayes theorem so that $\pi(\theta|y) \propto \pi(\theta)p(y|\theta)$. For the purposes of notation we note that as $\bar{Y}$ is a sufficient statistic for Y, when σ^2 is known, $p(y|\theta) \propto p(\bar{y}|\theta)$ and so $\pi(\theta|y) \propto \pi(\theta|\bar{y})$. As the prior distribution (4.2) and the likelihood (4.3) are both multivariate normal, the posterior distribution for $\theta|y$ is also multivariate normal and can be written

$$\theta|y \sim N(\mathbf{\Lambda}\xi, \mathbf{\Lambda}) \tag{4.4}$$

where $\xi = (W\mathbf{\Delta})^{-1}\mu + \mathbf{\Sigma}^{-1}\bar{y}$ and $\mathbf{\Lambda} = ((W\mathbf{\Delta})^{-1} + \mathbf{\Sigma}^{-1})^{-1}$ (Evans, 1965). Within the prior distribution, W acts as a scaling factor on the variation. In the posterior distribution W acts a smoothing factor, with smaller values of W resulting in less fluctuation in the fitted NDLM.

It should be noted that the variance matrix of $\bar{Y}$, $\mathbf{\Sigma}$, is only non-singular if there are subjects allocated to every dose. In the case where some doses have no subjects allocated then in the formulas for ξ and $\mathbf{\Lambda}$, the precision matrix should be used in place

of $\boldsymbol{\Sigma}^{-1}$, where the precision matrix is written

$$\begin{bmatrix} \frac{n_0}{\sigma^2} & 0 & \dots & 0 \\ 0 & \frac{n_1}{\sigma^2} & \dots & 0 \\ \vdots & & \ddots & \vdots \\ 0 & \dots & & \frac{n_J}{\sigma^2} \end{bmatrix}.$$

4.2.3 Finding the optimal dose for the next subject

The aim of the adaptive allocation is to learn about some function of the dose response curve. In our case, we are interested in learning about the target dose, where the target dose is defined as the minimum dose with a clinically meaningful difference (CMD) from placebo. We define $g(\theta)$ to be the response at the target dose which is calculated as

- if there exists a θ_j such that $\theta_j - \theta_0 \geq \text{CMD}$ then $g(\theta) = \theta_{j*}$ where

$$z_{j*} = \min_j(z_j : \theta_j - \theta_0 \geq \text{CMD}),$$

- if $\forall\theta$, $\theta_j - \theta_0 < \text{CMD}$ then $g(\theta) = \max_j(\theta_j - \theta_0)$.

The latter definition, is the case where none of the doses reach the threshold for being clinically meaningful. In this case we consider the most interesting dose, to be the dose with the maximum change from placebo.

We learn about the function of interest, $g(\theta)$, through a utility function. The utility function we use, aims to minimise the posterior variance of the response at the target dose. We write this utility function as

$$u[Y] = -\text{Var}(g(\theta)|Y).$$

For the purposes of notation, we define Y to be the available responses of the n subjects currently enrolled in the trial. In a slight abuse of notation, where necessary we assume this also includes information of the dose each subject was allocated to, and the order of the allocation. If we let $Y_{\max}$ denote the responses of the subjects for a completed trial, then we aim to maximise the expected utility

$$U[Y_{\max}] = E[u[Y_{\max}]] = E[-\text{Var}(g(\theta)|Y_{\max})].$$

Theoretically the maximum utility could be solved for all the subjects entering the trial, for example by backwards induction; working from the end of the trial backwards through all possible scenarios in a deterministic approach. However, in this circumstance this would be computationally intractable and so a 'myopic' or 'one-step-ahead' approach is adopted (Berry et al., 2001). Using a myopic approach, the utility is only maximized for the next subject to be randomised. Once this subject has completed the study, his/her response is then incorporated into the accumulated dataset and the method repeated for the subsequent subject to enter the trial. To ensure subject data are available to drive the decision about the optimal dose, we begin the randomisation with a 'run-in' period where subjects are allocated equally doses. After a suitable run-in period, the adaptive allocation is utilized and subjects are sequentially allocated to the optimal dose.

For this one step ahead approach, we let $\tilde{Y}_j$ denote the unknown response of the next subject to enter the trial on dose z_j. The utility function including the response of the next subject to be allocated to dose z_j is written

$$u_j[y, \tilde{y}_j] = -\text{Var}(g(\theta)|Y = y, \tilde{Y}_j = \tilde{y}_j), \tag{4.5}$$

which is the variance of the response at the target dose after observing a response $\tilde{y}_j$ on dose z_j. For a specific value of θ and dataset $Y = y$, the expected utility is computed by averaging over the distribution of the unknown variable $\tilde{Y}_j$

$$U_j[y] = \int u_j[y, \tilde{y}_j]\, p(\tilde{y}_j|y)\, d\tilde{y}_j. \tag{4.6}$$

Key to evaluating (4.6), is being able to re-write the utility function in terms of the posterior density $\pi(\theta|y)$ which we can sample from directly

$$U_j[y] = \int\int u_j[y, \tilde{y}_j]\, p(\tilde{y}_j|\theta)\, \pi(\theta|y)\, d\tilde{y}_j\, d\theta. \tag{4.7}$$

This allows us to estimate the expected utility by simulation. To do this we first generate M i.i.d. samples for θ from the posterior distribution with density $\pi(\theta|y)$, denoted θ^m $(m = 1, \ldots, M)$. For each θ^m a response for the next subject entering the trial on dose z_j is generated from distribution with density $p(\tilde{y}_j|\theta_j^m)$. This simulated response is denoted $\tilde{y}_j^m$. The integral (4.7) is then estimated as

$$\hat{U}_j[y] = \frac{1}{M} \sum_{m=1}^{M} u_j[y, \tilde{y}_j^m]. \tag{4.8}$$

The optimal dose is the minimum dose which maximizes (4.8).

In the literature, there are then two different methods for estimating $u_j[y, \tilde{y}_j^m]$. The first uses direct simulation and is detailed in Berry et al. (2001). This was the method employed in the ASTIN study (Grieve & Krams, 2005; Krams et al., 2003) and is assumed to be the method employed by Bornkamp et al. (2007). The second method for evaluation $u_j[y, \tilde{y}_j^m]$ employs importance sampling and is suggested by Weir et al. (2007) to be a less computationally intensive method.

Direct Simulation

This method relies on using the unbiased estimator for $-\text{Var}(g(\theta)|Y = y, \tilde{Y}_j = \tilde{y}_j^m)$ to estimate $u_j[y, \tilde{y}_j^m]$ for each $\tilde{y}_j^m$. The following steps are used to calculate the unbiased estimator.

1. Calculate the parameter values of the multivariate normal posterior distribution of θ given $Y = y$ and $\tilde{Y}_j = \tilde{y}_j^m$ (4.4).
2. Generate T i.i.d. samples for θ from the posterior distribution with density $\pi(\theta|y, \tilde{y}_j^m)$. These samples are denoted θ^t $(t = 1, \ldots, T)$.
3. Calculated $g(\theta^t)$ for each $t = 1, \ldots, T$.

Hence, the unbiased estimator for $-\text{Var}(g(\theta)|Y = y, \tilde{Y}_j = \tilde{y}_j^m)$ is

$$\hat{u}_j[y, \tilde{y}_j^m] = -\widehat{\text{Var}}(g(\theta)|Y = y, \tilde{Y}_j = \tilde{y}_j^m) = -\frac{1}{T-1}\sum_{t=1}^{T}(g(\theta^t) - \bar{g}(\theta))^2$$

where $\bar{g}(\theta) = \frac{1}{T}\sum_{t=1}^{T} g(\theta^t)$. The expected utility $U_j[y]$ at dose z_j is then estimated using the sample average of the estimates $\hat{u}_j[y, \tilde{y}_j^m]$ (4.8). This method is computationally intensive as it relies on generating T samples for each $\tilde{y}_j^m$.

Importance Sampling

The strategy suggested by Weir et al. (2007) uses importance sampling to estimate the posterior variance of $g(\theta)$.

Firstly, we find $E[g(\theta)|y, \tilde{y}_j^m]$ and $E[g(\theta)^2|y, \tilde{y}_j^m]$ and then use these to calculate

$$-\text{Var}(g(\theta)|Y = y, \tilde{Y}_j = \tilde{y}_j^m) = (E[g(\theta)|y, \tilde{y}_j^m])^2 - E[g^2(\theta)|y, \tilde{y}_j^m]. \tag{4.9}$$

The expectation of $g(\theta)$ is

$$E[g(\theta)|y, \tilde{y}_j^m] = \int g(\theta)\pi(\theta|y, \tilde{y}_j^m)d\theta.$$

We re-write the posterior for θ in terms of the prior and likelihood to get

$$E[g(\theta)|y, \tilde{y}_j^m] = \frac{\int g(\theta)p(\tilde{y}_j^m|\theta)\pi(\theta|y)d\theta}{\int p(\tilde{y}_j^m|\theta)\pi(\theta|y)d\theta}.$$

These integrals can be approximated by sampling directly from the posterior distribution with density $\pi(\theta|y)$ and taking the sample average of $g(\theta)p(\tilde{y}_j^m|\theta)$ for the upper integral and of $p(\tilde{y}_j^m|\theta)$ for the lower integral. As the samples are generated from the posterior distribution of θ given $Y = y$ they do not depend on $\tilde{y}_j^m$, hence we can use the same sample for both the denominator and the numerator, reducing the variance of the estimator. Let θ^t denote i.i.d. samples from then density $\pi(\theta|y)$ $(t = 1, \ldots, T)$, then

$$E[g(\theta)|y, \tilde{y}_j^m] \approx \sum_{t=1}^{T} g(\theta^t) \left(\frac{p(\tilde{y}_j^m|\theta_j^t)}{\sum_{t=1}^{T} p(\tilde{y}_j^m|\theta_j^t)} \right) \tag{4.10}$$

which is a weighted average of $g(\theta^t)$, where the weights are proportional to the likelihood of observations $\tilde{y}_j^m$ given θ^t. We use the same set of samples θ^t for each of the $\tilde{y}_j^m$ $(m = 1, \ldots, M;\ j = 0, \ldots, J)$. This coupling of the samples has a beneficial impact on the differences in the expected utilities between different doses.

The same approach can be used to show

$$E[g(\theta)^2|y, \tilde{y}_j^m] = \sum_{t=1}^{T} g(\theta^t)^2 \left(\frac{p(\tilde{y}_j^m|\theta_j^t)}{\sum_{t=1}^{T} p(\tilde{y}_j^m|\theta_j^t)} \right). \tag{4.11}$$

Using (4.10) and (4.11) for the expectation of $g(\theta)$ and $g(\theta)^2$ respectively, the estimate of the utility function for the simulated response $\tilde{y}_j^m$ is

$$\hat{u}_j[y, \tilde{y}_j^m] = \left(\sum_{t=1}^{T} g(\theta^t) \left(\frac{p(\tilde{y}_j^m|\theta_j^t)}{\sum_{t=1}^{T} p(\tilde{y}_j^m|\theta_j^t)} \right) \right)^2 - \sum_{t=1}^{T} g(\theta^t)^2 \left(\frac{p(\tilde{y}_j^m|\theta_j^t)}{\sum_{t=1}^{T} p(\tilde{y}_j^m|\theta_j^t)} \right).$$

M	T	Direct Sampling	Importance Sampling
50	50	0.46	0.02
100	50	0.96	0.02
200	50	1.94	0.04
500	50	4.84	0.10
50	100	0.82	0.02
100	100	1.64	0.04
200	100	3.32	0.06
500	100	8.22	0.12
50	1000	7.10	0.10
100	1000	14.28	0.16
200	1000	28.48	0.30
500	1000	71.20	0.72

Table 4.1: Time in seconds to randomise one subject using the direct and importance sampling methods.

4.2.4 Choosing a sampling scheme for finding the optimal dose

For the GADA method, the fundamental design element is the adaptation of the randomisation. In order for this method to be effective the algorithm must be able to randomise subjects in a reliable and reproducible manner. This means that the method can identify the optimal dose for the next subject with a degree of certainty. In order to fully explore and understand the operational characteristics of the design it must also be computationally possible to generate a large number of simulated trials within a reasonable time frame.

We implemented the GADA method using both the direct and importance sampling methods, and recorded the time needed to randomise each individual subject using different values of M simulated responses and T samples from the posterior distribution (Table 4.1). We can see from Table 4.1 that the method suggested by Weir et al. (2007) which incorporates importance sampling, is substantially faster than the method that samples directly from the posterior density.

The reproducibility of a sampling scheme is measured against a benchmark sampling scheme which has sufficient samples that we can reasonable sure we have identified the optimal dose. The benchmark sampling scheme for the direct sampling method is M=1000 and T=1000, and for the importance sampling method is M=1000 and T=100000. We have used a larger T for the importance sampling method as this method is faster to run.

To assess how good each scheme is at identifying the same optimal dose as the gold standard, we carried out a small simulation study. We generated 100 datasets, with 100 subjects allocated equally across all the doses. The responses of the subjects in the datasets were generated using the Emax dose response profile (see Section 2.3). For each dataset we find the optimal dose for the 101^{st} subject to enter the trial. We then repeat this 100 times and calculate the percentage of times the sampling scheme identified the same optimal dose as the benchmark sampling scheme. For the simulation study we assume a fixed W of 0.5.

The percentage of times the different sampling schemes identify the same optimal dose as the benchmark across the 100 simulated datasets, when T=100 and M=50, 100, 200 and 500 are presented in Figure 4-2. The importance sampling method identifies the optimal dose with more consistency than the direct sampling method. This is most likely because the importance sampling reuses the samples from the posterior distribution, coupling the utilities across the simulated responses and across the different doses, making it easier to identify the optimal dose. From this we conclude, that not only is the importance sampling method faster but for the number of samples we can afford to generate, it is more reliable than the direct sampling method in terms of identifying the optimal dose. The benchmark sampling schemes for the direct and importance sampling, identified the same optimal dose for 98 out of the 100 datasets.

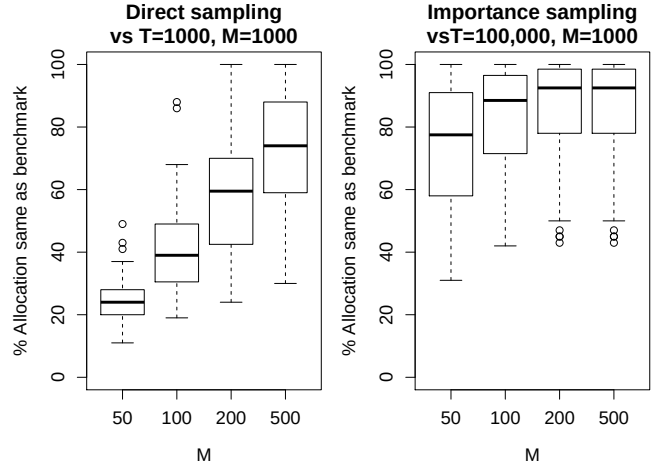

Figure 4-2: Box plots of the percentage of times the same dose is chosen as the benchmark, using direct sampling and importance sampling (T=100).

Having identified that the importance sampling method is more able to identify the

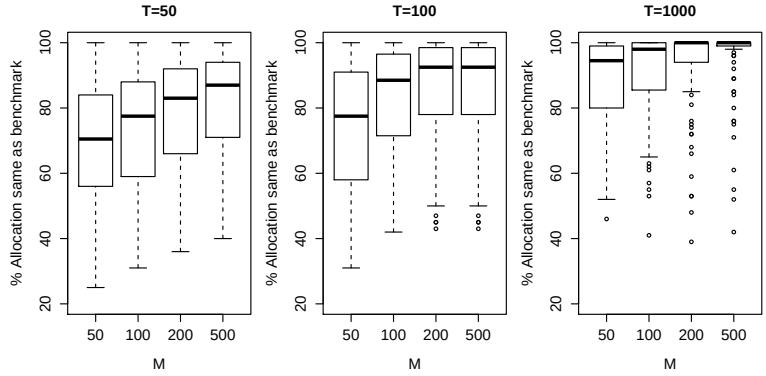

Figure 4-3: Box plot of the percentage of times the same dose is chosen as the benchmark, using importance sampling with varying values of M and T.

optimal dose with fewer samples, we must now decide on which sampling scheme to use for our larger simulation studies. Figure 4-3 shows the percentage of times the importance sampling method agrees with the benchmark for different values of M and T. Increasing both M and T improves the ability of the method to identify the optimal dose.

If we were just interested in randomising the next subject within a trial, then in practice we could use the benchmark sampling scheme. However, for large scale simulation studies this is not practical as it would take too long to explore a wide number of scenarios. With M=500 and T=1000 randomising one subject takes 0.72 seconds (Table 4.1), so to simulate one trial with 250 subjects would take over 2.5 minutes and to simulate 5000 trials would take over 9 days. Therefore we need to make a compromise between a sampling scheme that is cheap to run but also can identify the optimal dose.

We note that the reliability of the sampling scheme to identify the optimal dose may depend on n, and so to ensure the choice of sampling scheme does not have a large impact on the final results, we run a simulation study with 1000 simulated datasets and three dose response profiles from the set of dose response profiles listed in Section 2.3. The expected response ν_j at dose z_j for each of these dose response profiles is as follows (j=0,...,8)

- Flat: $\nu_j = 0$
- Linear: $\nu_j = (1.65/8)z_j$

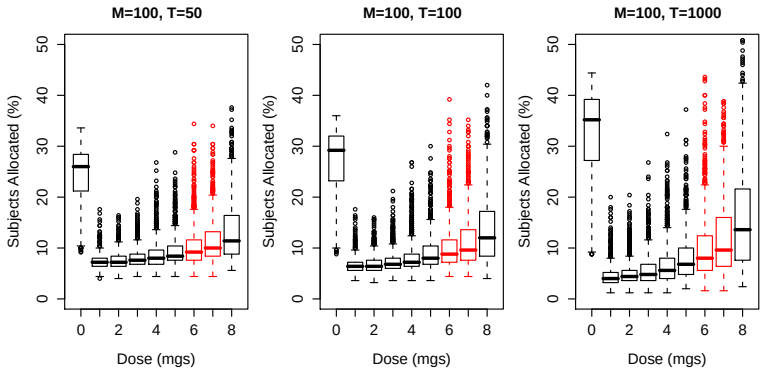

Figure 4-4: Box plot of subject dose allocations for the GADA method with M=100 and increasing values of T. Based on 1000 simulations with data generated from the Linear profile. The target dose interval is given in red.

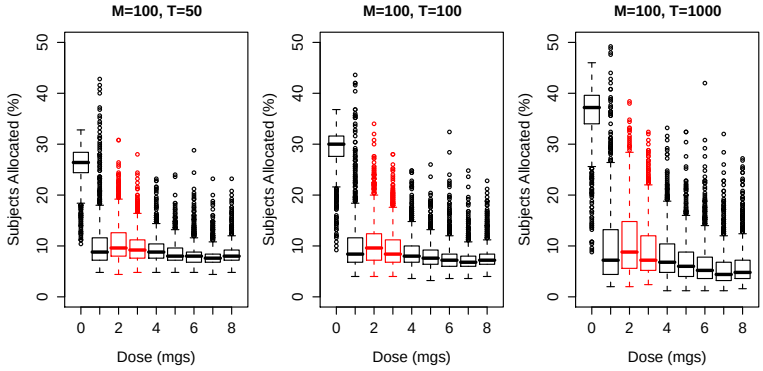

Figure 4-5: Box plot of subject dose allocations for the GADA method with M=100 and increasing values of T. Based on 1000 simulations with data generated from the Emax profile. The target dose interval is given in red.

- Emax: $\nu_j = 1.81 z_j/(0.79 + z_j)$

We find the optimal dose using importance sampling with six sampling schemes; M=100 and 200, T=50, 100 and 1000. Each trial consists of 250 subjects and the adaptive randomisation takes place after allocating 3 subjects to each dose. A fixed W of 0.5 is used.

Figures 4-4 and 4-5 are box plots of the subject allocations across the simulated datasets when M=100 and the dose response profiles follow the Linear and Emax profiles, respectively. We can see from these figures that the general trends of the subject allocations remain the same as T increases. As T increases, the variability in the subject allocations increases, and more subjects are allocated to the placebo dose.

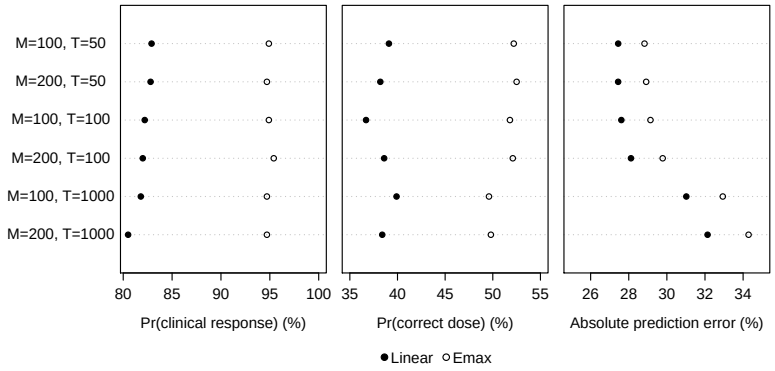

Figure 4-6: Operational characteristics for the GADA method with different M and T used to find the optimal dose: probability of detecting a dose response, a clinical response and selecting a dose in the target interval.

This suggests that for some of the simulated datasets when a large number of samples are used to find the optimal dose, the allocation method can get 'stuck' exploring only a couple of the potential doses.

The aim of the GADA method is to learn about the target dose. In the case of the Linear profile the target dose is z_6 and so the subject allocation is focused around the higher doses. The target dose for the Emax profile is z_2 and so the allocation focuses on the lower doses. As T increases, the allocation criterion is applied more strictly and so there is a concentration of subjects around the target dose intervals. With a lower T, the criterion is still applied, but with more variation in the expected utility and so the choice of optimal doses, the subjects are allocated more equally across doses.

Figure 4-6 presents estimates of the performance metrics when different values of M and T are used in implementing the GADA sampling scheme. For each of the different M and T combinations, the one-sided type I error under the Flat dose response profile was maintained at 5% (see Section 2.4). The different values for M and T have the least impact on the probability of detecting a clinical response. Although the sampling scheme is aimed at minimising the posterior variance at the target dose, it does not appear from Figure 4-6 that increasing the number of samples used to identify the optimal dose, improves the ability of the method to select a dose in the target dose interval. The absolute prediction error increases as the number of samples used to identify the optimal dose increases. This is because, as the allocation focuses on few doses, less subjects are allocated elsewhere, meaning that the prediction error over the whole of the dose range increases.

Based on the results of this simulation study, all further simulations use a sampling scheme of M=100 and T=100. This sampling scheme has been chosen as it balances the computational cost of randomising each individual subject with the operational characteristics from this small simulation study.

4.2.5 Choice of smoothing factor

Within the NDLM model, the choice of W governs the extent of the movements in θ. If W is too small then the posterior variance, $\mathbf{\Lambda}$, is dominated by the prior information and the posterior means tend towards a linear or flat model. If the choice of W is too large, then the posterior means will tend towards the empirical means and so there is little benefit from the dependence structure built into the NDLM. The choice of W is important as the extent of the smoothing impacts the subject allocation and the final inferences.

To illustrate the impact of using different values of W, 1000 datasets were simulated where the subject responses were generated from the Flat, Linear and Emax dose response profiles (as listed in the previous section). The optimal dose for the next subject was found using M=100 simulated responses and T=100 samples from the posterior. The between subject variance was $\sigma^2 = 4.5$ and 250 subjects were randomised for each simulation, with a run-in period of 3 subjects on each dose before the adaptive allocation was implemented. Three smoothing factors were explored; $W = 0.01$, $W = 0.1$ and $W = 0.5$.

The subject allocations using different values of fixed W when the data were generated using the Linear and Emax profiles are presented in Figures 4-7 and 4-8, respectively. With W=0.01 the posterior variances at the low doses are already small so there is less to be learnt from allocating subjects to these doses. Therefore the method allocates subjects to the higher doses, where the potential to reduce the posterior variance is greatest.

To fully understand the impact different values of W have on the fitted NDLM, the datasets generated above were then analysed using each of the three values of W. This was done to assess what the key contributing factor is that influences the final results: the allocation or the analysis. The operational characteristics when the data are generated from the Linear and Emax profiles are presented in Table 4.2. For each

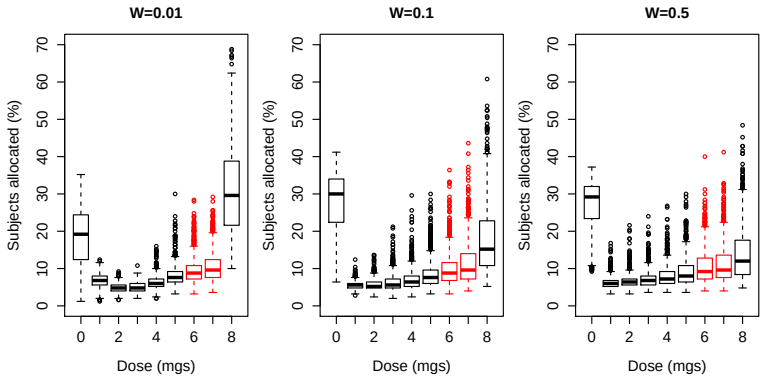

Figure 4-7: Box plot of subject dose allocations for the GADA method with different values of fixed W in the prior distribution. Based on 1000 simulations with data generated from the Linear profile. The target dose interval is given in red.

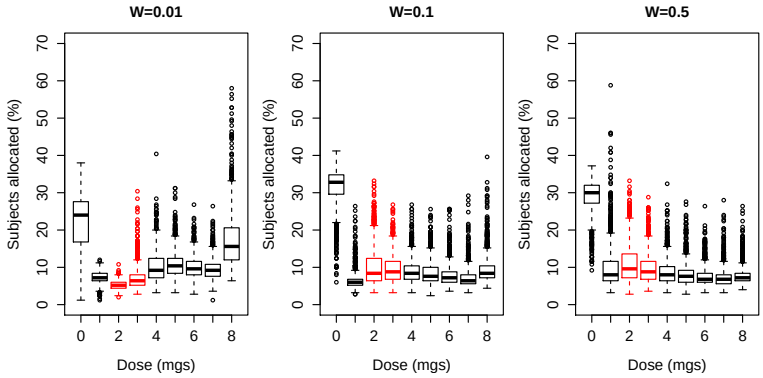

Figure 4-8: Box plot of subject dose allocations for the GADA method with different values of fixed W in the prior distribution. Based on 1000 simulations with data generated from the Emax profile. The target dose interval is given in red.

combination of W used to allocate and analyses the data, the one-sided type I error is maintained at 5% under the Flat dose response profile.

From Table 4.2 we can see that, while the value of W used to randomise subjects and make the final inferences has an impact on the results, it is the choice of W used for the final analysis that has the greatest impact. As predicted, using a small W when the dose response is Linear gives the best operational characteristics, as there is a lot of smoothing in the fitted NDLM and so it tends towards a linear fit. When the data follows the Emax dose response, using a larger W results in better operational characteristics, as the NDLM requires more flexibility to fit the Emax dose response profile. Therefore we can conclude that the choice of W impacts both the randomisation

Linear Model

W Used to Randomise	W used to analyse final data								
	Clinical Response (%)			Correct Target Dose (%)			Absolute Prediction Error (%)		
	0.01	0.1	0.5	0.01	0.1	0.5	0.01	0.1	0.5
0.01	93.5	87.0	85.4	61.8	41.6	34.0	12.2	19.8	25.5
0.1	85.7	81.8	80.3	55.9	40.2	33.8	12.8	19.9	25.1
0.5	82.9	80.6	80.2	55.4	41.5	36.5	12.7	19.7	24.5

Emax Model

W Used to Randomise	W used to analyse final data								
	Clinical Response (%)			Correct Target Dose (%)			Absolute Prediction Error (%)		
randomise	0.01	0.1	0.5	0.01	0.1	0.5	0.01	0.1	0.5
0.01	94.1	91.5	93.2	15.6	52.3	48.3	19.0	19.9	24.4
0.1	92.6	94.6	96.0	23.3	55.1	49.5	19.2	21.1	25.1
0.5	91.8	94.5	95.3	26.1	53.4	52.1	18.6	21.1	25.1

Table 4.2: Operational characteristics using fixed values of W to randomise subjects and analyse the final dataset: probability of a clinical response, selecting a dose in the target interval and the percentage absolute prediction error.

and analysis, and that there is no one value of W that provides the best results for the different dose response profiles. We therefore need to choose the best value of W based on the shape of the underlying dose response profile. In the next section we consider the use of a prior distribution for W.

4.2.6 Giving W a prior distribution

So far we have assumed that a fixed value for W is adequate regardless of the underlying dose response profile. However, it has been shown in the previous section, that this assumption is not valid and different values of W are needed depending on the shape of the underlying model. Putting a prior distribution on W allows the data to influence the amount of smoothing in the posterior.

When there is a prior distribution on W, the GADA method is implemented in the same way, however the posterior distribution is hierarchical as θ now depends on W and Y. The hierarchical nature of the posterior distribution also feeds into the calculation of the utility function, which is used to find the optimal dose for the next subject to enter the trial. In this section we revisit these aspects of the GADA method.

As seen in Section 4.2.1, the prior distribution for the NDLM and the likelihood are both multivariate normal distributions written, $\theta|w \sim N(\mu, w\mathbf{\Delta})$ and $\bar{Y} \sim N(\theta, \mathbf{\Sigma})$, respectively. Let the prior for W have density $\pi(w)$. The joint posterior multivariate density $\pi(\theta, w|y)$ is then a hierarchical Bayes model. Using the fact that as σ^2 is known, the density $p(y|\theta, w)$ for Y is proportional to the density $p(\bar{y}|\theta, w)$, for $\bar{Y}$, we can write the joint posterior density as

$$\begin{aligned}
\pi(\theta, w|y) &\propto p(y|\theta, w)\pi(\theta, w) \\
&\propto p(\bar{y}|\theta, w)\pi(\theta|w)\pi(w) \\
&= (2\pi)^{-\frac{(J+1)}{2}} |\mathbf{\Sigma}|^{-\frac{1}{2}} e^{-\frac{1}{2}(\bar{y}-\theta)^T\mathbf{\Sigma}^{-1}(\bar{y}-\theta)} \\
&\quad \times (2\pi)^{-\frac{(J+1)}{2}} w^{-\frac{(J+1)}{2}} |\mathbf{\Delta}|^{-\frac{1}{2}} e^{-\frac{1}{2}(\theta-\mu)^T(w\mathbf{\Delta})^{-1}(\theta-\mu)}\pi(w) \\
&\propto w^{-\frac{J+1}{2}} e^{-\frac{1}{2}\theta^T((w\mathbf{\Delta})^{-1}+\mathbf{\Sigma}^{-1})\theta+2\theta^T((w\mathbf{\Delta})^{-1}\mu+\mathbf{\Sigma}^{-1}\bar{y})} e^{-\frac{1}{2}(\mu^T(w\mathbf{\Delta})^{-1}\mu)}\pi(w).
\end{aligned}$$

Letting $\xi = (w\mathbf{\Delta})^{-1}\mu + \mathbf{\Sigma}^{-1}\bar{y}$ and $\mathbf{\Lambda} = ((w\mathbf{\Delta})^{-1} + \mathbf{\Sigma}^{-1})^{-1}$, we can complete the square for $\theta|w, y \sim N(\mathbf{\Lambda}\xi, \mathbf{\Lambda})$ to get,

$$\pi(\theta, w|y) \propto \pi(\theta|w, y)\ |\mathbf{\Lambda}|^{\frac{1}{2}}\ w^{-\frac{(J+1)}{2}} e^{-\frac{1}{2}(\mu^T(w\mathbf{\Delta})^{-1}\mu)}\ e^{\frac{1}{2}\xi^T\mathbf{\Lambda}\xi}\ \pi(w). \tag{4.12}$$

As

$$\pi(\theta, w|y) = \pi(\theta|w, y)\ \pi(w|y),$$

the posterior density for W is

$$\pi(w|y) \propto |\mathbf{\Lambda}|^{\frac{1}{2}}\ \ w^{-\frac{(J+1)}{2}}\ \ e^{-\frac{1}{2}(\mu^T(w\mathbf{\Delta})^{-1}\mu)}\ e^{\frac{1}{2}\xi^T\mathbf{\Lambda}\xi}\ \pi(w) \tag{4.13}$$

For the purposes of making inferences, the marginal distribution for θ is found by integrating over W,

$$\pi(\theta|y) = \int \pi(\theta|w, y)\ \pi(w|y)\ dw. \tag{4.14}$$

The prior distribution for W has an impact on the process of allocating the next subject to the optimal dose. The utility function and the method used to calculate the expected utility are essentially the same as those used in Section 4.2.3, when W was assumed to be fixed. However, placing a prior distribution on W means that the expected utility is now averaged over the possible values of W.

Let $Y = y$ denote the responses from the n subjects currently enrolled in the trial. As before, with a slight abuse of notation we assume that Y also contains information on which dose each subject was allocated to, and the order of the allocation. As before,

the utility function is the posterior variance at the target dose,

$$u_j[y] = -Var(g(\theta)|Y = y).$$

We denote the response for the next subject to enter the trial on dose z_j as $\tilde{Y}_j$. To find the expected utility function we average over the posterior distribution for W and the unknown response of the next subject $\tilde{Y}_j = \tilde{y}_j$,

$$U_j[y] \quad = \quad \int\int u_j[y, \tilde{y}_j]\ p(\tilde{y}_j|w, y)\ \pi(w|y)\ d\tilde{y}_j\ dw. \tag{4.15}$$

Re-writing this in terms of $\pi(\theta|w, y)$

$$\begin{aligned} U_j[y] \quad = \quad & \int\int\int u_j[y, \tilde{y}_j]\ p(\tilde{y}_j|\theta)\ \pi(\theta|w, y) \\ & \times\pi(w|y)\ d\tilde{y}_j\ dw\ d\theta. \end{aligned} \tag{4.16}$$

Similarly to when using a fixed value for W, the integral is approximated using the sample average. As the model is hierarchical, the sampling of the M simulated responses is done in a hierarchical manner.

First we generate M i.i.d samples for W from the distribution $W|y$ which has density $\pi(w|y)$. These samples are denoted w^m $(m = 1, \ldots, M)$.

$\downarrow$

Next we generate θ^m from the distribution for $\theta|w^m, y$ which has density $\pi(\theta|w^m, y)$. These samples are denoted θ^m.

$\downarrow$

Finally we generate $\tilde{y}_j^m$ from the distribution for $\tilde{Y}_j|\theta^m, w^m, y$ which has density $p(\tilde{y}_j|\theta^m, w^m, y)$ and denote these samples $\tilde{y}_j^m$.

Equation 4.16 is then replaced by the sample average

$$\hat{U}_j[y] = \frac{1}{M}\sum_{m=1}^{M} u_j[y, \tilde{y}_j^m]. \tag{4.17}$$

For each generated response $\tilde{y}_j^m$ the utility function $u_j[y, \tilde{y}_j^m]$ is evaluated using the method suggested by Weir et al. (2007). The utility function for each new response $\tilde{y}_j^m$ can be written,

$$u_j[y, \tilde{y}_j^m] = -\text{Var}(g(\theta)|Y = y, \tilde{Y}_j^m = \tilde{y}_j^m) = (E[g(\theta)|y, \tilde{y}_j^m])^2 - E[g(\theta)^2|y, \tilde{y}_j^m].$$

The expectation of $g(\theta)$ is

$$E[g(\theta)|y, \tilde{y}_j^m] = \int g(\theta)\pi(\theta|y, \tilde{y}_j^m)d\theta.$$

This can be written

$$E[g(\theta)|y, \tilde{y}_j^m] = \int\int g(\theta)\pi(\theta|w, y, \tilde{y}_j^m)\pi(w|y, \tilde{y}_j^m)dw\ d\theta.$$

Then as before, we re-write the posterior for θ in terms of the prior distribution for $\theta|w, y$ and the likelihood for $\tilde{Y}_j$,

$$E[g(\theta)|y, \tilde{y}_j^m] = \frac{\int\int g(\theta)p(\tilde{y}_j^m|\theta)\ \pi(\theta|w, y)\ \pi(w|y)\ d\theta\ dw}{\int\int p(\tilde{y}_j^m|\theta)\ \pi(\theta|w, y)\ \pi(w|y)\ d\theta\ dw}$$

This is also evaluated by simulation, where the samples are generated in a hierarchical manner.

We generate T samples for W from the distribution $W|y$ which has density $\pi(w|y)$. These samples are denoted w^t $(t = 1, \ldots, T)$.

$\downarrow$

Next we generate a θ from the distribution $\theta|w^t, y$ which has density $\pi(\theta|w^t, y)$ and denote these samples as θ^t.

We estimate the above integrals by

$$\begin{aligned} E[g(\theta)|y, \tilde{y}_j^m] &\approx \frac{\sum_{t=1}^T g(\theta^t)p(\tilde{y}_j^m|\theta_j^t)}{\sum_{t=1}^T p(\tilde{y}_j^m|\theta_j^t)}, \\ &= \sum_{t=1}^T g(\theta^t)\left(\frac{p(\tilde{y}_j^m|\theta_j^t)}{\sum_{t=1}^T p(\tilde{y}_j^m|\theta_j^t)}\right). \end{aligned}$$

As before, we use the same samples of θ for the numerator and the denominator. Placing a prior distribution on W has not substantially increased the work load in finding the optimal dose, as we only generate M and T samples from the posterior distribution of $W|y$ once.

Using the above calculations for $E[g(\theta)|y, \tilde{y}_j^m]$ and using a similar method to calculate $E[g^2(\theta)|y, \tilde{y}_j^m]$, we can estimate the utility function for the simulated response $\tilde{y}_j^m$ as

$$\hat{u}_j[y, \tilde{y}_j^m] \approx -\text{Var}(g(\theta)|Y = y, \tilde{Y}_j = \tilde{y}_j^m) = (E[g(\theta)|y, \tilde{y}_j^m])^2 - E[g^2(\theta)|y, \tilde{y}_j^m].$$

The expected utility can then be estimated by taking the sample average of the M simulated responses, using equation (4.17). The optimal dose for the next subject is then the dose which maximizes the expected utility.

So far in this section we have assumed that the prior distribution on W is continuous. To simplify the computational intensity of the method, later we assume a discrete uniform prior distribution for W. To find the posterior distribution of θ given $Y = y$ we replace the integral in (4.14) with the sum,

$$\pi(\theta|y) = \sum_{i}^{I} \pi(\theta, w_i|y)\ \pi(w_i|y).$$

In finding the optimal dose, the relevant integrals should also be changed to summations. As we are evaluating the integrals using simulation, the use of a discrete prior distribution does not impact the way in which the optimal dose is identified.

4.2.7 The appropriateness of the NDLM model

An NDLM has been used to model the data as it assumes no knowledge about the shape of the underlying dose response profile, making it a flexible model that can adapt to the information accrued. The NDLM builds in a dependence structure between the doses through the evolution matrix which determines the smoothing across the doses. The amount of smoothing between the doses is determined by the posterior distribution of $W|y$ which had density $\pi(w|y)$. As $W|y$ moves towards zero there is less variability and so more smoothing between the doses .

From (4.13) for a continuous prior distribution on W the posterior density for W given $Y = y$ is

$$\pi(w|y) \propto |\mathbf{\Lambda}|^{\frac{1}{2}}\ w^{-\frac{(J+1)}{2}}\ e^{-\frac{1}{2}(\mu^T(w\mathbf{\Delta})^{-1}\mu)}\ e^{\frac{1}{2}\xi^T\mathbf{\Lambda}\xi}\ \pi(w),\ w \in (0,1),$$

where $\xi = (w\mathbf{\Delta})^{-1}\mu + \mathbf{\Sigma}^{-1}\bar{y}$ and $\mathbf{\Lambda} = ((w\mathbf{\Delta})^{-1} + \mathbf{\Sigma}^{-1})^{-1}$. We assign a discrete uniform prior distribution to W, with I points w_i, and now let $\pi(w_i) = \Pr(W = w_i)$ and

$$\pi(w_i|y) \propto |\mathbf{\Lambda}_i|^{\frac{1}{2}}\ w_i^{-\frac{(J+1)}{2}}\ e^{-\frac{1}{2}(\mu^T(w_i\mathbf{\Delta}_i)^{-1}\mu)}\ e^{\frac{1}{2}\xi_i^T\mathbf{\Lambda}_i\xi_i}\ \pi(w_i),\ w_i \in \{w_1, \ldots, w_I\},$$

where $\xi_i = (w_i\mathbf{\Delta})^{-1}\mu + \mathbf{\Sigma}^{-1}\bar{y}$ and $\mathbf{\Lambda}_i = ((w_i\mathbf{\Delta})^{-1} + \mathbf{\Sigma}^{-1})^{-1}$. We used a discrete uniform distribution with $w_i \in \{0.001, 0.011, \ldots, 0.991, 1\}$. In order to assess how appropriate

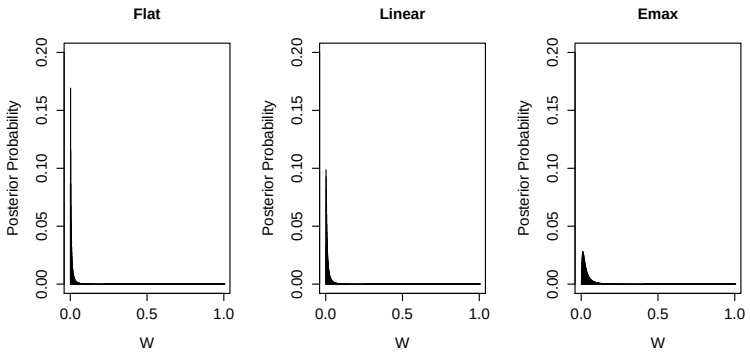

Figure 4-9: Posterior probability of $W|y$.

the NDLM model is, we fit the NDLM to true dose response profiles. To do this, we set the means of the data $\bar{y}$ equal to the dose response for the Flat, Linear and Emax profiles. We set the between subject variance, $\sigma^2 = 4.5$ and use 250 subjects allocated equally across the doses. The posterior density for $W|y$ under the Flat, Linear, and Emax dose response profiles are plotted in Figure 4-9. For all the dose response profiles, the posterior distribution is skewed towards zero, which would result in a lot of smoothing in the posterior distribution for the NDLM.

We then fit the NDLM using this same data with the same discrete uniform prior distribution on W and subject responses equal to the true dose response profiles. The posterior expected responses of $\theta|y$ versus the true dose response profiles are presented in Figure 4-10. For the dose response profiles that are non-linear, the fitted NDLM over smooths the curvature of the true dose response profile. For the Emax dose response profile, for example, this has the effect of underestimating the responses at the early doses. In practice, this would result in the NDLM wrongly selecting higher doses to take forward into phase III. This suggests that the structure of the NDLM used may be more suitable when the dose response profile is more gradually increasing, rather than when there is a steep change in the dose response, especially in the early doses which are anchored by the placebo dose.

4.3 Results

The following results are based on the neuropathic pain example, with scenarios and performance measures as defined in Section 2.3. For each scenario considered, 5000 simulated datasets were generated. Within each dataset 3 subjects were initially

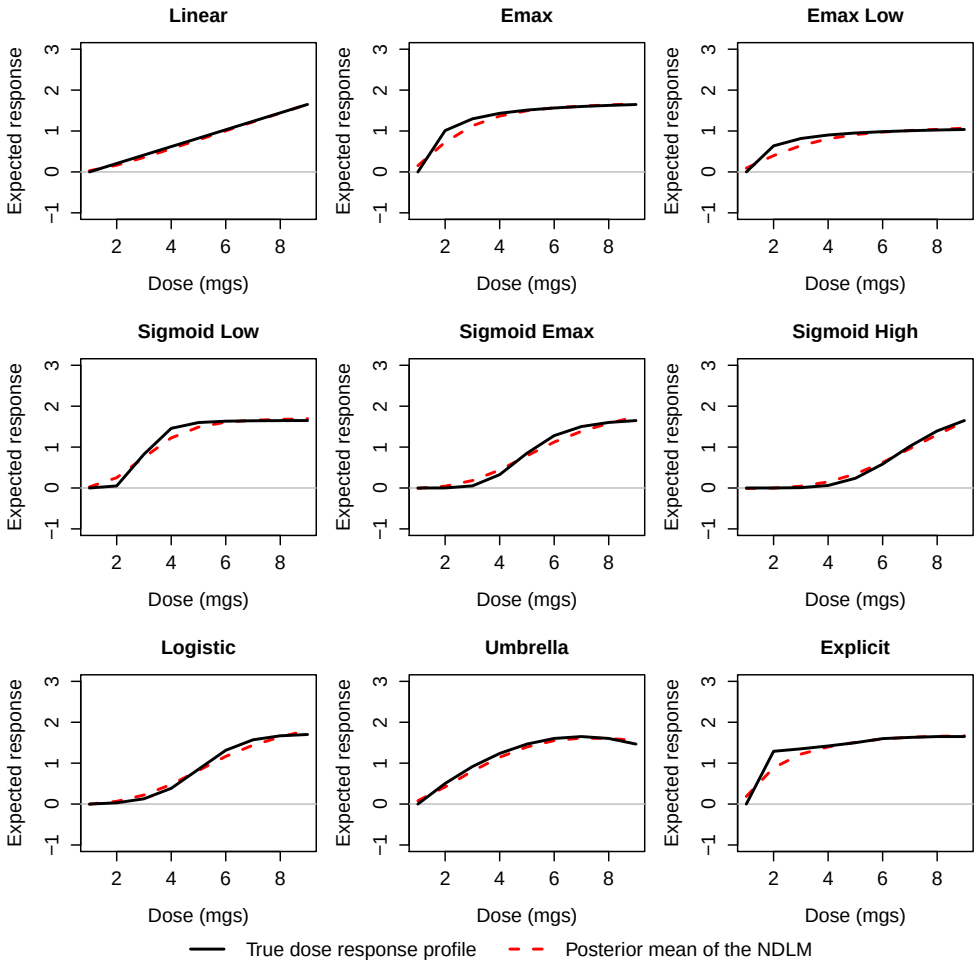

Figure 4-10: Posterior mean of the NDLM versus true dose response profiles.

randomised to each dose as a run-in period before the adaptive allocation approach began. A total sample size of 250 subjects were randomised per dataset. The optimal dose for the next subject to enter the trial was the dose that minimised the posterior variance at the target dose. The optimal dose for the next subjection was found using M=100 simulated responses and T=100 samples from the posterior distribution. For the allocation of subjects, σ^2 was assumed to be known and set to 4.5 and a discrete uniform prior distribution was used for W with $w_i \in \{0.001, 0.011, \ldots, 0.991, 1\}$.

The results of the GADA method are compared with the ANOVA method, described in Section 2.5. For the ANOVA method subjects were randomised equally to all the doses and inferences made using pairwise testing with a Dunnett (1955) adjustment for multiple testing. The metrics for the operational characteristics are as described in

Section 2.4.

Subject allocation

The subject allocations for the active dose response profiles are presented in Figure 4-11. The GADA approach focuses on allocating subjects to minimize the posterior variance of the response at the target dose. It can be seen that for all the active dose response profiles, there are more subjects allocated to the target dose and neighbouring doses with the exception of the top dose, z_8. In the calculation of the utility, when no dose met the target dose criteria, the maximum response was treated as the best dose to investigate. This could explain why dose z_8 often received additional subjects, especially in the case of the Emax Low model where none of the doses met the clinically meaningful threshold. Dose z_8 also has substantially more variance in the prior distribution as it has only one neighbouring dose from which to borrow strength. This means that there is more potential to learn about the utility function by allocating to this dose.

Detecting dose response

For the ANOVA method, under the Flat dose response profile the one-sided type I error rate was controlled at 5% using a Dunnett adjustment of 2.38. For the GADA method, the one-sided type I error under the Flat dose response profile is maintained at 5% (see Section 2.4).

For the active dose response models, a dose response is identified in nearly 100% of the simulated datasets (Figure 4-12). The ANOVA method has a consistently lower probability of a detecting dose response than the GADA method. For the ANOVA method the probability of detecting a dose response is highest for the steeper curves which reach a plateau early in the dose range (i.e the Emax and Sigmoid Low profiles). This is because these profiles have more doses with a clinical response and so the probability of the pairwise testing identifying a dose response is increased.

We have excluded the Emax Low profile from the plots as it tends to have a low probability of detecting a dose response and clinical response and so requires its own axis. The Emax Low model reaches a plateau early in the dose range, but its maximum response is only 1.14 compared with 1.65 for the other active dose response profile, and so the ANOVA method struggles to identify that there is a dose response. The

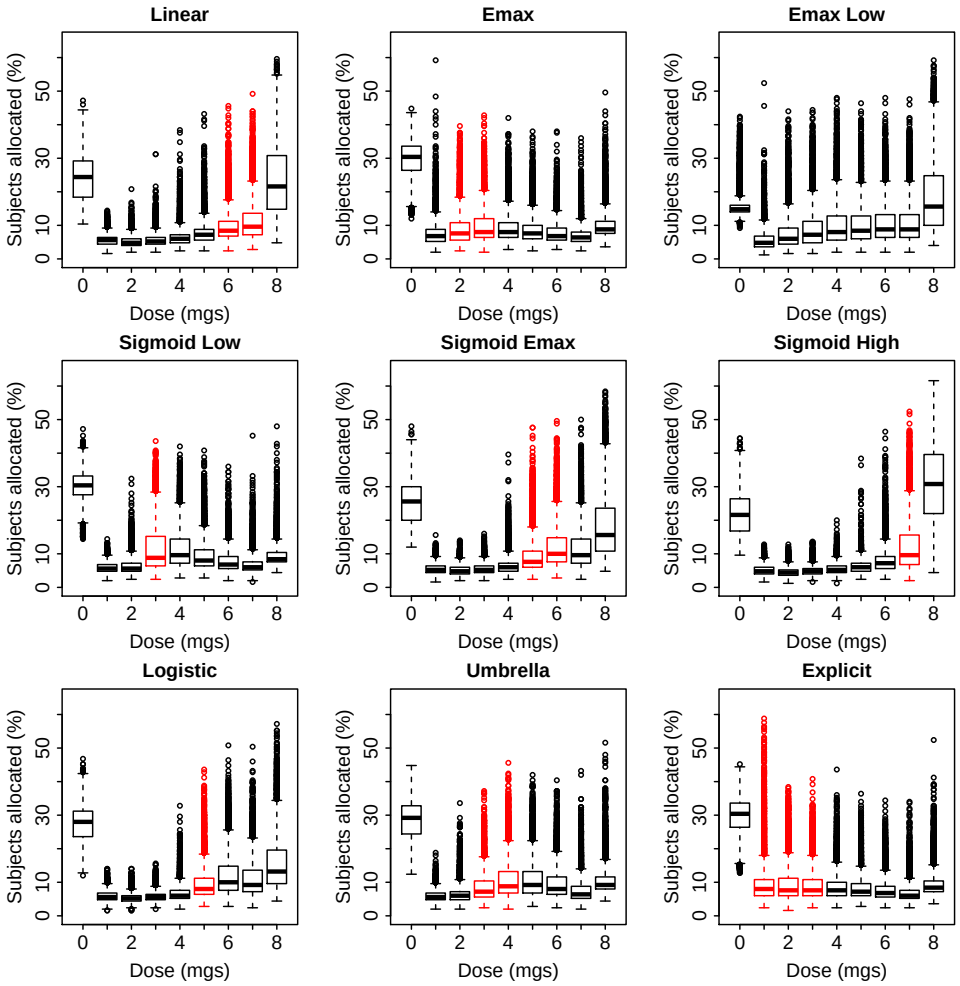

Figure 4-11: Box plot of subject dose allocations for the GADA method. Target dose intervals are given in red.

probability of detecting dose response for the Emax Low model is 0.6 for the ANOVA method compared with 1 for the GADA method.

Detecting a clinical response

For all the active dose response profiles, using the ANOVA method the probability of detecting a clinical response is approximately the same as the probability of detecting a dose response (Figure 4-12). Due to the adjustment for multiple testing used in the ANOVA method, the expected responses have large confidence intervals and so large

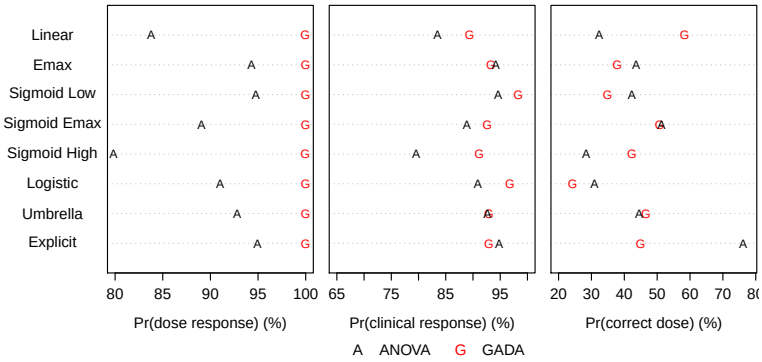

Figure 4-12: Operational characteristics for the GADA versus ANOVA methods: probability of detecting a dose response, a clinical response and selecting a dose in the target interval.

differences from placebo need to be observed to conclude there is a dose response. Therefore the majority of times a dose response is concluded a clinical response is also identified. In comparison, the NDLM is constructed so doses borrow strength from neighbouring doses, reducing the variability in the fitted model. This makes it easier for the NDLM to detect a dose response but not necessarily a clinical response. The Emax Low model, which has a dose response but no doses that meet the criteria for a clinical response, is a good example of how the NDLM can differentiate between dose response and clinical response. With the ANOVA method the probability of detecting a dose response and a clinical response are both approximately 0.63, but with the GADA method the probability of detecting a dose response is close to 1, while the probability of detecting a clinically relevant response is only 0.2. This is not necessarily a characteristic unique to the GADA method, but is one of the advantages of modelling the data.

Correctly selecting a dose in the target dose interval

The target dose is defined as the minimum dose that achieves at least a 1.3 improvement over placebo. The percentage of simulated datasets where the dose selected is within the target dose interval are presented in Figure 4-12. Despite the GADA method being tailored to identify the target dose, this method does not do consistently better than the ANOVA method in terms of correctly identifying a dose in the target dose interval. In fact, it is only for the Linear model that the GADA method does substantially better than the ANOVA method. It should be noted that the percentage of times the dose selected was in the target dose interval for the GADA method is notably less

than that observed in the PhRMA working group paper (Bornkamp et al., 2007). This paper did not give a full description of the construction of the prior distribution for the NDLM, whether stopping rules were used or the decision rule used for selecting a dose. Therefore, it is difficult to compare the results presented here with those from the Bornkamp et al. (2007) paper.

Histograms of the dose identified as the target dose across the simulations for the Linear, Emax and Sigmoid Emax dose response profiles are given in Figure 4-13 for the GADA and ANOVA methods. Based on these histograms the GADA method tends to identify higher doses compared to the ANOVA method. For the Linear profile this is an advantage and results in a higher percentage of simulations selecting a dose in the target dose interval, whilst for the Emax profile this is detrimental.

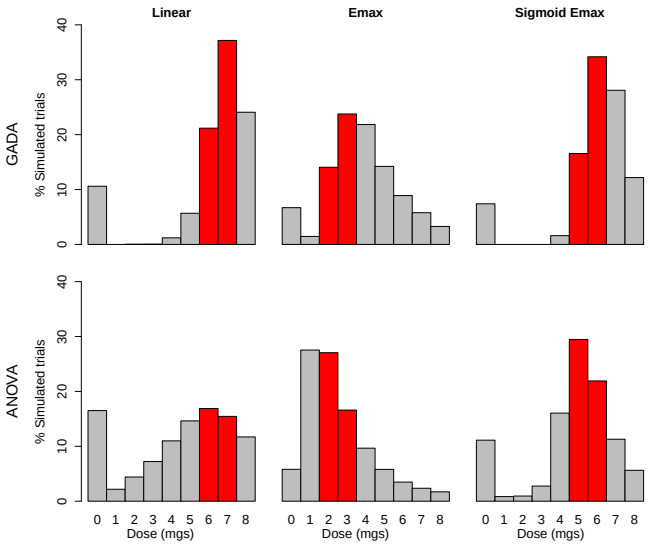

Figure 4-13: Histograms of dose selected for phase III, for the GADA and ANOVA methods. Target dose intervals given in red.

Prediction error

Figure 4-14 presents plots of the median prediction error for the GADA method with the prediction error quantiles. Overall the NDLM best fits the data when the underlying dose response profile is Linear, with the median prediction just slightly underestimating the true model at the lower doses. Using the GADA method, the NDLM substantially underestimates the response at the lower doses, where the target doses for the Emax dose response profile lies. When the underlying dose response is

Sigmoid Emax, the NDLM overestimates the response at the early convex part of the curve, then underestimates the response at the later concave part of the curve. These prediction errors are consistent with the NDLM model fitted in Figure 4-10. We have only included plots of the prediction errors for the GADA method, as the ANOVA approach models the means at each dose independently and so the 50^{th} percentile for the dose response profiles is approximately flat with wide percentiles.

The impact of the NDLM underestimating the dose response curves is reflected in the ability of the method to correctly select a dose in the target dose interval. When the target dose is at the part of the curve which is underestimated, for example, as with the Emax model, then the GADA method will tend to select a higher dose. This is reflected in Figure 4-13.

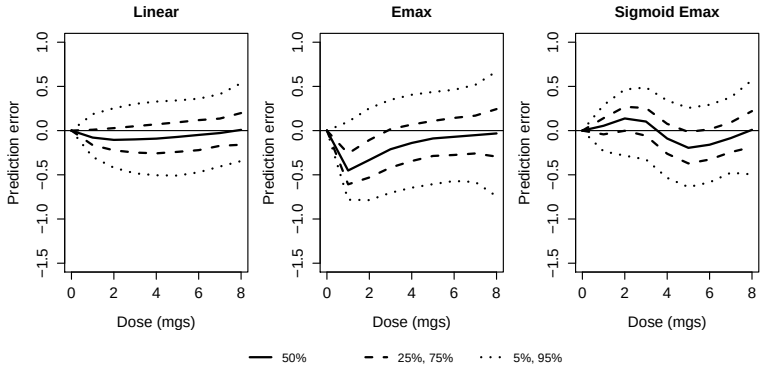

Figure 4-14: Median prediction error and prediction error quantiles for the GADA method.

Simulation error

Although we have generated large numbers of datasets for the GADA and ANOVA methods, there is still simulation error in our results. Let $\hat{p}_G$ and $\hat{p}_A$ be the estimated probabilities of detecting a clinical response in the GADA and ANOVA methods respectively, based on the N_{sim}=5000 simulated datasets the two methods have in common. If the datasets were generated independently we can calculate the standard error of the difference $\hat{p}_G - \hat{p}_A$ as

$$\text{se}(\hat{p}_G - \hat{p}_A) \approx \sqrt{\frac{p_G(1-p_G)}{N_{\text{sim}}} + \frac{p_A(1-p_A)}{N_{\text{sim}}}}. \tag{4.18}$$

Dose response profiles	$\hat{p}_G$	$\hat{p}_A$	$\hat{p}_G - \hat{p}_A$	se$(\hat{p}_G - \hat{p}_A)$	coupled se$(\hat{p}_G - \hat{p}_A)$
Linear	89.4	84.0	5.4	0.7	0.6
Emax	93.3	94.3	-1.0	0.5	0.5
Sigmoid Emax	92.6	89.2	3.4	0.6	0.5

Table 4.3: Simulation error for the difference in probability of detecting a clinical response (%) between the GADA and ANOVA methods.

We estimate the standard error of the difference by substituting in $\hat{p}_G$ and $\hat{p}_A$ for p_G and p_A respectively in (4.18). As subjects across datasets were coupled as far as possible (Section 2.3.2) this reduces the simulation error. To estimate the standard error of the difference when the datasets are coupled, we define a variable for each dataset $k = 1, \ldots, N_{\text{sim}}$,

$$I_k = \begin{cases} -1 \text{ if only the ANOVA method has a clinical response} \\ 0 \text{ if both the GADA and ANOVA methods have a clinical response} \\ 1 \text{ if only the GADA method has a clinical response} \end{cases}.$$

The standard error of the difference taking into account the coupling, is then estimated as the standard error of the set of values $I_1, \ldots, I_{N_{\text{sim}}}$. Table 4.3 presents the simulation errors of the difference in for detecting a clinical response between the GADA and ANOVA methods, for a selection of the true dose response profiles.

From Table 4.3 we can see that even without the coupling of the datasets, because we have generated a large number of simulated datasets, the simulation error of the difference is less than 0.7%. Using the coupling only reduces the standard error of a difference a small amount. In this case the subject allocations of the GADA and ANOVA methods have limited subjects in common. The impact of the coupling is also reduced by the different final analysis of the GADA and ANOVA methods. In future chapters, where methods use the same final analysis, the coupling has more impact in reducing the standard error of the difference. The standard error of the difference in the probability of selecting a dose in the target dose interval without taking account of the coupling is closer to 1%, as the probability of selecting a dose in the target dose interval is closer to 50% for each of the methods. Again, coupling the datasets reduces the simulation error by approximately 0.1%. We have calculated the estimates of the standard error based on the 5000 simulated datasets both methods have in common, in order to assess the impact of the coupling. In reality, the standard error of the differences are even smaller than presented here as we actually generate 10000 datasets

for the ANOVA method.

When we interpret the results, we are interested in seeing differences of a couple of percent or more to conclude that there is differences between methods. As we have shown, with 5000 generated datasets the simulation error of the difference is at most 1% and so we can interpret our results and conclusions as being accurate enough. We do not re-visit the topic of simulation error when comparing methods in future chapters, as these results hold.

Conclusion

The GADA method is a response adaptive method which allocates subjects to doses with the aim of minimizing the posterior variance of the response at the target dose. The results of the simulation study show that the method has been somewhat successful in achieving this. The adaptive allocation tends to lead to more subjects being randomised to the target dose and neighbouring doses than some of the less effective doses. However, there is a large amount of variability in the allocation method and so at times the randomisation can become focused on a few doses, which may not always be the optimal doses.

The rules used to define the operational characteristics were chosen so that the results are comparative across the GADA and ANOVA methods. The results show that the GADA method consistently outperforms the ANOVA method in terms of detecting a dose response and a clinical response. However, although the method is designed to minimize the posterior variance of response at the target dose, the GADA method does not consistently identify a dose within the correct target interval with more success than the ANOVA method. One reason for this, is that the NDLM used to model the data often underestimates the dose response curve at the target dose, leading to higher doses being chosen.

Depending on the primary outcome of the trial and the belief about the underlying dose response model, there may be some advantages to using the GADA approach. However, the benefits are not consistent, especially if choosing the target dose or understanding the whole of the dose response curve is the main aim of the study. One must also take into account the extra complexity and operational intensity it takes to run such an adaptive design when designing their trial.

4.4 Discussion

One of the conclusion of the PhRMA working group paper (Bornkamp et al., 2007) was that 'adaptive dose-ranging designs clearly lead to gains in power to detect dose response and in precision to select the target dose interval and to estimate the dose response.' The results shown here are not consistent with this conclusion, or the results presented in the paper for the GADA method. Due to the large number of methods covered in the paper, there are certain important details about how the GADA method was implemented that are unfortunately lacking. For example; the exact construction of the NDLM used, the parameter of interest, the decision rule used to identify a dose for phase III, and whether a stopping rule was employed.

Although the exact methods used in the PhRMA working group paper cannot be ascertained, there are certain aspects of the results which are similar to those presented here. Their plots of the prediction error for the Logistic dose response profile with N=150 subjects, shows similar overestimation of the responses at the low doses and underestimation at the higher doses. However despite the NDLM having problems with underestimating the dose response at the target dose, the Bornkamp et al. (2007) paper reports higher probabilities of identifying a dose in the correct target interval. If the differences cannot be attributed to the choice of NDLM used to model the data, then potentially the difference could be due to the decision rules used to select the target doses. As Grieve (2007) comments in reference to the Bornkamp et al. (2007) paper, 'there are few clear statements of the decision criteria that are used by the different approaches.' The decision rules used here, were chosen so that the results would be comparable with the results from the ANOVA method.

Using a prior distribution for the between subject variation σ^2 was considered, but was found to have little impact on the operational characteristics. Placing a prior distribution on σ^2 required the optimal dose to be found using MCMC methods in either WinBUGS or OpenBUGS. Using either of these packages, substantially slowed down running of the simulations, and so we decided to use a fixed σ^2 in this simulation study.

The GADA method explored here is very complex in nature, with a number of different components that differentiates it from the traditional methods. It uses a Bayesian framework with a non-parametric model for the prior distribution and an adaptive allocation process with utility function to identify the optimal dose for the next subject

entering the trial. Although the results here are not as conclusive as those presented in the PhRMA working group paper, there is still some potential to the method. In the next chapter we explore simplifying this method to randomise subjects in cohorts rather than individually.

Chapter 5

The Cohort Method - a Simplified Adaptive Approach

5.1 Introduction

In the previous chapter we explored using the General Adaptive Design Allocation (GADA) approach. This approach uses a Bayesian framework and models the data using a normal dynamic linear model (NDLM). Subjects are allocated to doses, based on accrued responses, using a Bayesian utility function. We observed in the previous chapter that allocating subjects using the GADA approach resulted in a large amount of variability in the subject allocations, with the algorithm occasionally getting stuck exploring a few doses. The operational characteristics for the GADA method showed no clear and consistent improvement over the simpler ANOVA method in terms of correctly selecting a dose in the target dose interval. In this chapter we investigate simplifying the adaptation and randomising subjects in cohorts. Where the GADA method allocates subjects to minimise the posterior variance of the response at the target dose, the cohort method aims to drops doses at interim analyses and focus the allocation on the range of doses where the minimally effective dose (MED) is believed to lie.

The cohort method models the data using the same NDLM as the GADA method, and applies a simplification of the adaptation rule. Within the cohort method we randomise groups of subjects to doses based on the posterior probabilities of having a clinically meaningful difference from placebo. At an interim analysis, subjects are randomised to the placebo doses, and a range of doses from the lowest non-futile dose to the lowest

effective dose. This allows us to focus the randomisation on the range of doses that have the most potential to be the minimally effective dose. There are many examples of trials that have explored dropping treatment arms based on futility, either utilising frequentist group sequential methods or Bayesian posterior probabilities. There are limited examples of studies where dropping doses based on posterior probabilities from an NDLM are explored (Smith et al., 2006; Berry et al., 2010; Padmanabhan et al., 2012). Smith et al. (2006) explored dropping up to two futile doses at interim analyses while Berry et al. (2010) used a two stage design, where in the second stage additional doses could be explored based on the posterior probabilities from the first stage. Padmanabhan et al. (2012) altered the randomisation probabilities for the next cohort to allocate subjects to doses that 'decrease the variance of the difference between the response at the optimal safe dose and the placebo response.' All of these papers included the possibility of stopping the trial due to futility.

The methodology in this chapter differs from the papers mentioned above, as we don't consider doses independently of the neighbouring doses, but aim to identify a range of doses where the subject allocation should focus. We also include the ability to re-utilise doses that may have been dropped at early interim analyses, if the posterior probabilities at these doses has changed accordingly.

Previously the GADA method has been compared with the ANOVA method, a frequentist approach which uses a Dunnett (1955) adjustment for multiple testing. The GADA method differs from the ANOVA method in terms of the design and analysis, and so it is hard to isolate whether it is the adaptation or the final inference which most affects the operational characteristics. Comparing the GADA method with an adaptive cohort approach and a non-adaptive equal allocation, both analysed using the same NDLM, allows us to make a fairer comparison and assess what impact the adaptivity has.

We compare the operational characteristics of the cohort method with those generated in the previous chapter. We make the following comparisons between the analysis and design elements:

1. Analysis: frequentist ANOVA versus Bayesian NDLM, both with a non-adaptive equal allocation.

2. Design: GADA method versus adaptive cohort allocation versus non-adaptive equal allocation, all modelled using the same NDLM.

5.2 Methodology

The cohort approach we propose here, randomises groups of subjects at interim analyses, based on the observed data. The aim of the method is to focus the subject allocation on the target dose, where the target dose is the minimum dose with a clinically meaningful difference from placebo. The target dose is also referred to as the minimally effective dose (MED). We focus the subject allocation on the target dose by dropping doses that are deemed futile and those above the target dose. We drop doses above the target dose as we are looking for the lowest dose with a clinically meaningful effect. There may also be potential safety concerns about allocating subjects to higher doses.

The data are modelled using the NDLM described in Section 4.2.6. As in the previous chapter, we assume that there is a placebo dose z_0 and J active doses denoted z_j $(j = 1, \ldots, J)$. We assume that the expected response of the i^{th} subject on dose z_j is normally distributed

$$Y_{ij} \sim N(\eta(z_j, \theta), \sigma^2) = N(\theta_j, \sigma^2),$$

and the mean response on dose z_j is distributed

$$\bar{Y}_j \sim N(\eta(z_j, \theta), \sigma^2/n_j) = N(\theta_j, \sigma^2/n_j),$$

where n_j is the number of subjects allocated to dose z_j. The vector of mean response $\bar{Y}$ then has a multivariate normal distribution,

$$\bar{Y} \sim N(\theta, \mathbf{\Sigma}),$$

where $\mathbf{\Sigma}$ is as defined in (2.4). The prior distribution for θ is constructed using equations (4.1). The prior distribution for θ can be written as a multivariate normal distribution,

$$\theta \sim N(\mu, W\mathbf{\Delta}),$$

where W is a random variable. We place a prior distribution on W such that W has prior density $\pi(w)$. The posterior distribution for $\theta|w, y$ is then also multivariate normal

$$\theta|w, y \sim N(\mathbf{\Lambda}\xi, \mathbf{\Lambda})$$

where $\xi = (w\boldsymbol{\Delta})^{-1}\mu + \boldsymbol{\Sigma}^{-1}\bar{y}$ and $\boldsymbol{\Lambda} = ((w\boldsymbol{\Delta})^{-1} + \boldsymbol{\Sigma}^{-1})^{-1}$. If W is given a continuous prior distribution, the posterior distribution for $W|y$ has density

$$\pi(w|y) \propto |\boldsymbol{\Lambda}|^{\frac{1}{2}} \; w^{-\frac{(J+1)}{2}} \; e^{-\frac{1}{2}(\mu^T(w\boldsymbol{\Delta})^{-1}\mu)} \; e^{\frac{1}{2}\xi^T\boldsymbol{\Lambda}\xi} \; \pi(w), \; w \in (0,1).$$

We assign a discrete uniform prior distribution to W, with I points w_i, and now let $\pi(w_i) = \Pr(W = w_i)$ and

$$\pi(w_i|y) \propto |\boldsymbol{\Lambda}_i|^{\frac{1}{2}} \; w_i^{-\frac{(J+1)}{2}} \; e^{-\frac{1}{2}(\mu^T(w_i\boldsymbol{\Delta}_i)^{-1}\mu)} \; e^{\frac{1}{2}\xi_i^T\boldsymbol{\Lambda}_i\xi_i} \; \pi(w_i), \; w_i \in \{w_1, \ldots, w_I\},$$

where $\xi_i = (w_i\boldsymbol{\Delta})^{-1}\mu + \boldsymbol{\Sigma}^{-1}\bar{y}$ and $\boldsymbol{\Lambda}_i = ((w_i\boldsymbol{\Delta})^{-1} + \boldsymbol{\Sigma}^{-1})^{-1}$. The marginal posterior density $\pi(\theta|y)$ is found by summing over the possible values for W

$$\pi(\theta|y) = \sum_{i=1}^{I} \pi(\theta|y, w_i) \; \pi(w_i|y).$$

Using the posterior distribution of θ_j at dose z_j for a given dataset $Y = y$, we define the target dose as the minimum dose with a clinically meaningful difference (CMD) from placebo, written

$$\min_j(z_j : \Pr(\theta_j - \theta_0 > \text{CMD}|Y = y) > 0.5).$$

The randomisation process is carried out as follows:

1. Subjects in the first cohort are randomised equally to all doses.

2. At the interim analysis, the posterior distribution for $\theta|y$ is calculated using the NDLM. Based on the posterior distribution, the lowest non-futile dose (LND) is defined as

$$\text{LND} = \min_j\{z_j : \Pr(\theta_j - \theta_0 > \text{CMD}|Y = y) > 0.2\}, \tag{5.1}$$

   and the lowest effective dose (LED) as

$$\text{LED} = \min_j\{z_j : \Pr(\theta_j - \theta_0 > \text{CMD}|Y = y) > 0.6\}. \tag{5.2}$$

3. Subjects in the next cohort are allocated equally to the placebo dose and the range of doses from the LND up to and including the LED.

4. At the next interim analysis, the posterior distribution is updated and the allocation for the next cohort found.

5. This process is repeated until all subjects have been randomised.

Doses that have been previously dropped can be re-utilised at a later interim analysis if the accumulated data has changed the probabilities accordingly. As the intention here is not to explore early stopping, if all doses are deemed futile the next cohort is randomised equally across all doses. If there were no safety concerns and doses higher than the target dose were of interest, then this approach could be modified to drop only the futile doses. As the NDLM does not always take a monotonic shape, in order to prevent dropping a non-futile dose between two effective doses, only those doses below the lowest non-futile dose are dropped. This restricts the method to dropping doses at the lower and upper ends of the dose range, and not in the middle of the dose range.

Figure 5-1 illustrates the probability of each dose having a clinically meaningful difference from placebo, based on the fitted NDLM (red dashed line) when the data follow the true dose response profiles (black solid line). Data were set to equal to the true profiles, such that $\bar{y}_j = \nu_j$. We use three values of n to represent the number of subjects enrolled in the trial at the time of the first interim analysis, n=50, 125 and 200. The variation in the likelihood and prior distribution were assumed to be $\sigma^2 = 4.5$. We use a discrete uniform distribution for W, such that $w_i \in \{0.001, 0.011, \ldots, 0.991, 1\}$. Based on the criteria (5.1) and (5.2) for dropping doses (black dashed lines), in addition to the placebo dose, the green columns represent doses we would randomised to if we knew the shape of the true dose response curve, and the red columns are the doses we would drop at the interim analyses. As we can see from Figure 5-1, that when there is less data available, fewer doses are dropped at the interim analysis. When we know the shape of the true underlying dose response profile, the criteria result in us randomising subjects to at least one dose from the target dose interval (Table 2.1).

The criteria chosen to define a non-futile and the effective dose, were chosen such that as n increases there is a reasonable probability of dropping both the futile and high doses, therefore maximising the number of subjects that could be allocated to and around the target dose. We also chose the criteria taking into account other published studies. In Smith et al. (2006) doses were dropped for futility if their posterior probability of being the MED was ≤ 0.2 and so this is consistent with what is used here. Smith et al. (2006) did not allow doses to be dropped or the trial ended early due to efficacy. Shen et al. (2011) allowed their study to stop for efficacy if the posterior probability of a particular dose being the MED was ≥ 0.6, and the posterior probability of the maximum dose being the greater than the MED was ≥ 0.8. We have used a threshold of 0.6 for concluding a dose is effective, as we are not stopping the whole trial but

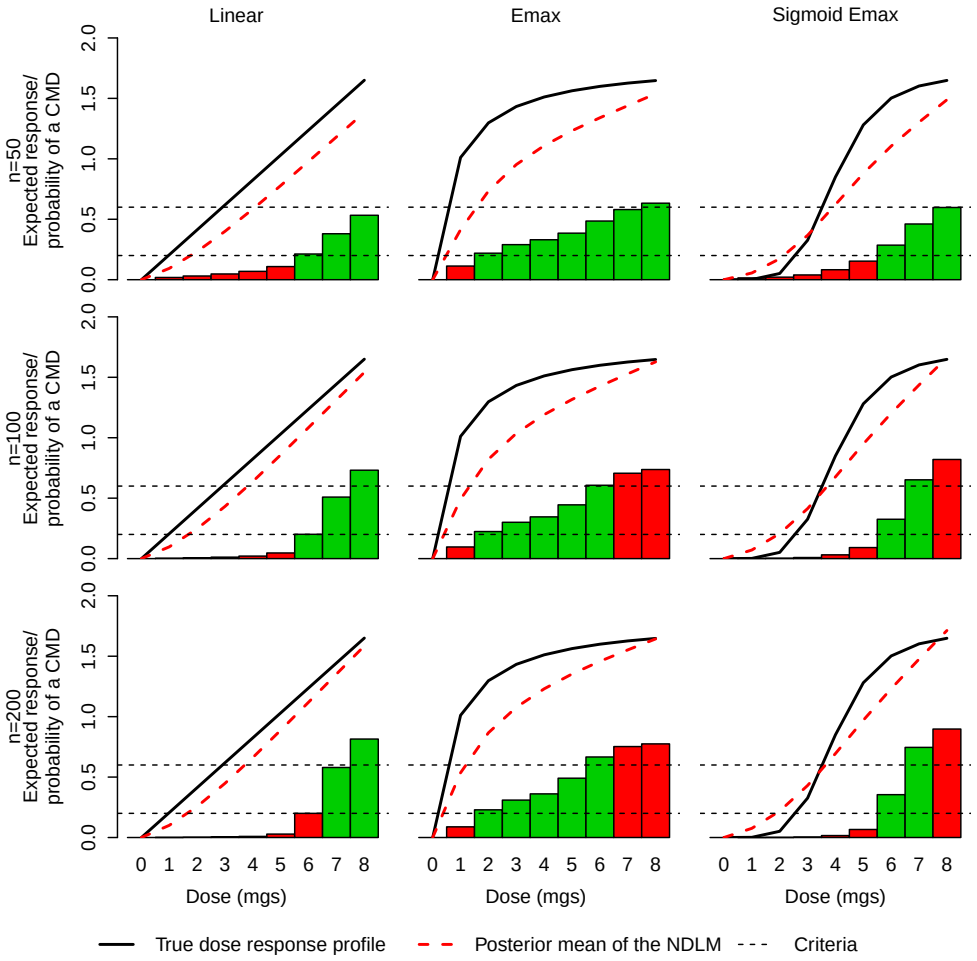

Figure 5-1: Plot of the true dose response profile and the posterior mean of the NDLM for different values of n. Bar plots of the probability of a dose having a clinically meaningful difference (CMD) from placebo based on the posterior distribution of θ. Green columns represent doses we would allocate the next cohort to in addition to the placebo dose, and the red columns represent doses that we would drop at the interim analysis. The criteria for dropping doses are given in (5.1) and (5.2)

only dropping doses which can be resumed later if necessary. Therefore the amount of information about a dose at an interim does not need be as conclusive.

5.3 Results: cohort allocation

The results we now present are based on the neuropathic pain example described in Section 2.2. To evaluate the operation characteristics of the cohort allocation, a simulation study was carried out with 10,000 datasets generated from each of the true underlying dose response profiles specified in Section 2.3. Each simulated dataset consists of a total of 250 subjects across 9 doses $(0, 1, \ldots 8\text{mgs})$. We explore the effect of using 0,1,2,3,4, and 9 equally spaced interim analyses (IAs) (i.e. 1,2,3,4,5 and 10 cohorts). When there is no interim analysis, this is equivalent to using a non-adaptive equal allocation design. The simulation study is the same as that performed in Chapter 4, where the data are modelled using an NDLM with a discrete uniform prior distribution on W, $w_i \in \{0.001, 0.011, \ldots, 0.991, 1\}$ and σ^2=4.5. The metrics for the operational characteristics are as described in Section 2.4.

Subject allocation

The criteria for dropping doses at each of the interim analyses are aimed at focusing the subject allocation on the target dose. It can be seen from the box plots of the subject allocations in Figure 5-2, that this has been achieved to a certain degree. As the method identifies a range of suitable doses to allocate to, a reasonable proportion of subjects are randomised to the target dose interval and the doses around the target dose interval. The target dose intervals for each model are outlined in red in the plots.

We can see from Figure 5-2, that the method is effective in dropping the low, futile doses for the Linear and Sigmoid Emax profiles. There is a decrease in the number of subjects allocated to the top doses, but in general the method finds it harder to identify doses that should be dropped above the target dose. There is some change in the subject allocations as the number of interim analyses increases, however after 2 interim analyses the overall shape of the subjects allocations changes very little. The doses the subject allocations focus on are consistent with the doses we highlighted in green in Figure 5-1.

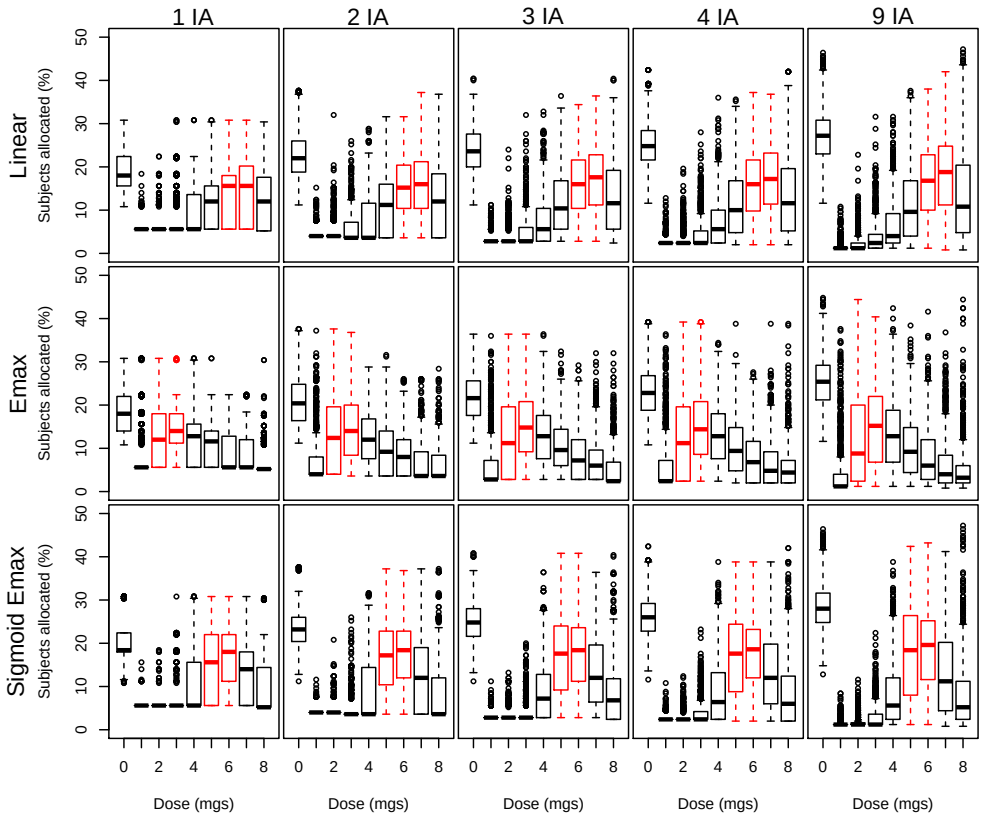

Figure 5-2: Box plot of subject dose allocations for the cohort method with increase numbers of interim analyses. Target dose intervals are given in red.

Detecting a dose response

For each of the number of interim analysis, we maintain one-sided type I error under the Flat dose response profile of 5%. The probability of detecting a dose response for the active profiles is around 100% for all the true underlying curves irrespective of the number of cohorts used in the allocation process.

Detecting a clinical response

The probability of detecting a clinical response based on the number of interim analyses, is presented in the left hand plot of Figure 5-3. In this plot the number indicates the number of interim analyses used in the trial design. In terms of detecting a clinical response, for all the active dose response profiles except the Emax Low, there is some improvement from adapting at the interim analyses compared to the non-adaptive design with 0 interim analyses. Adapting at the interim analyses results in the largest improvement in detecting a clinical response for the Linear and Sigmoid Emax profiles. For some of the profiles, the probability of detecting a clinical response increases with the number of interim analyses, whereas for other profiles there is little to be gained from using more that one interim analysis. In practice, it would be up to the project team to consider if the benefit from additional interim analyses outweighs the extra operational burden.

For the Emax Low dose response profile, we want to be able to identify that there isn't a clinical response. There is no benefit from using the adaptive allocation in achieving this goal, with the probability of detecting a clinical response being approximately 29% regardless of the number of interim analyses. When all the doses are futile we randomise the next cohort of subjects using equal allocation. Therefore for many of the datasets the subject allocation is very similar or the same as using equal allocation from the start. Hence, it is unsurprising that the methods with the opportunity to adapt at the interim analyses give similar results to the non-adaptive design. If we were interested in stopping the trial for futility when no doses show a clinical response, then using interim analyses have shown to be of benefit in terms of saving subjects numbers (Smith et al., 2006).

Correctly selecting a dose in the target dose interval

For all the dose response profiles, there is an increase in the probability of correctly selecting a dose in the target dose interval when 1 interim analysis is used compared to

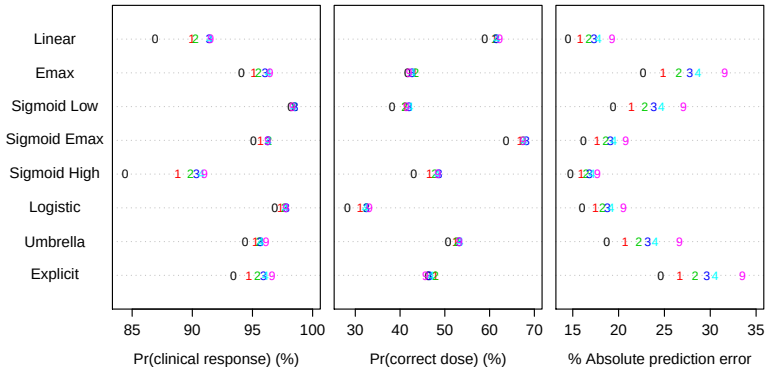

Figure 5-3: Operational characteristics for the cohort method with increasing numbers of interim analyses: probability of detecting a clinical response, selecting a dose in the target interval and the percentage absolute prediction error.

0 interim analyses. The benefit of more than 1 interim analysis is less clear. For some dose response profiles there is a slight benefit from using more interim analyses (e.g. the Linear and Sigmoid High), but for other profiles using more interim analyses results in similar results to using 0 interim analyses (e.g. the Emax and Explicit profiles).

Prediction Error

As the number of interim analyses increases, the subject allocation focuses on fewer doses, and so the absolute prediction error increases (Figure 5-3). This is to be expected as, when we focus the subject allocation on a few doses, the prediction error at the other doses increases, increasing the overall absolute prediction error.

5.4 Results: cohort vs GADA allocation

For all the dose response profiles there is an improvement in the ability to detect a clinical response and identify the target dose when 1 interim analysis is used compared to 0 interim analyses. The advantage of using more than 1 interim analysis is less apparent. Increasing the number of interim analyses could also result in increased operational costs, and so we use 1 interim analysis for our comparison with the GADA method examined in Chapter 4. For continuity we also include the ANOVA method (Section 2.5) which randomises subjects using a non-adaptive equal allocation. As the ANOVA method differs from the GADA and cohort methods in terms of design and analysis, for completeness we include the results from using 0 interim analyses. The case with 0 interim analyses is equivalent to using a non-adaptive equal allocation

design where the data are modelled using the same NDLM as the adaptive cohort and GADA methods.

Comparing the operational characteristics of these four methods allows us to make the following comparisons between the analysis and design elements:

1. Analysis: frequentist ANOVA versus Bayesian NDLM, both with a non-adaptive equal allocation.
2. Design: GADA method versus adaptive cohort allocation versus non-adaptive equal allocation, all modelled using the same NDLM.

Subject Allocation

Box plots of the subject allocations for the GADA and cohort method with 1 interim analysis are presented in Figure 5-4. We see that the GADA method has much more variability in the subject allocation than the cohort method. This is due to the method randomising subjects individually rather than in cohorts. The cohort method is better able to identify and allocate more subjects to the target doses than the GADA method. The median percentage of subjects allocated on the target doses for the cohort method is approximately twice as many as the GADA method. The cohort method also has the ability to drop the higher doses, minimising the number of subjects allocated to theses doses. In comparison, the GADA method tends to randomise more subjects to the top dose. If there were potential safety concerns, then dropping the higher doses would be beneficial.

Detecting a dose response

The type I error under the Flat dose response profile for the GADA, cohort method with 1 interim analysis and equal allocation design are maintained at the 5% level. For the ANOVA method a Dunnett adjustment of 2.38 was used to maintain the type I error at 5%. The left plot in Figure 5-5 displays the probability of detecting a dose response for each of the active dose response curves. We can see that the cohort methods with 1 interim analysis and the equal allocation using an NDLM, give similar results to the GADA method. The ANOVA method struggles to detect a dose response as often as the methods modelled using the NDLM.

For the Emax Low dose response profile, which has a dose response but not a clinical

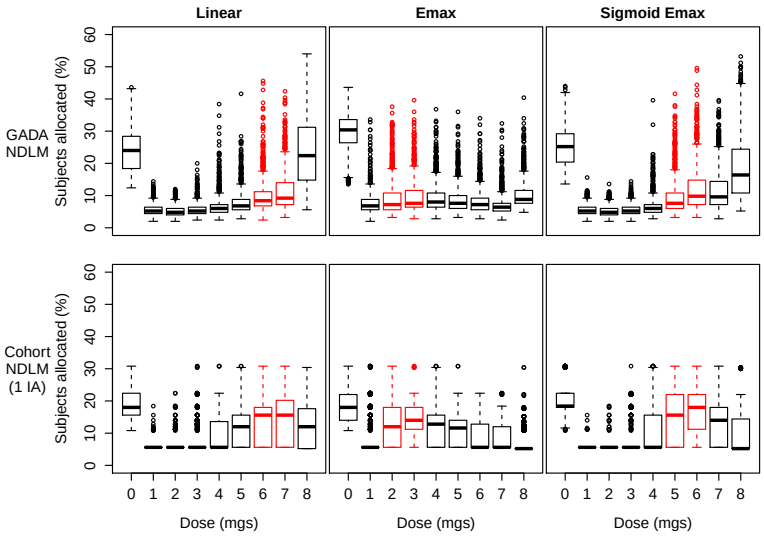

Figure 5-4: Box plot of subject dose allocations for the GADA versus the cohort method with 1 interim analysis. Target dose intervals are given in red.

response, the probability of detecting a dose response is approximately 100% for the allocation methods which model the data using an NDLM, but only around 64% for the ANOVA method.

Detecting a clinical response

All the allocation methods that use a Bayesian framework and model the data using an NDLM, have a higher probability of detecting a clinical response than the ANOVA method for all the active dose response models except the Emax Low model. For the Emax Low profile, the Bayesian methods are better at detecting that there is not a clinical response. The probability of incorrectly claiming a clinical response for the Emax Low profile using the ANOVA method is approximately 64% compared with 30% for the cohort and equal allocation approaches, and 20% for the GADA method.

Comparing the different allocation methods which model the data using an NDLM, using 1 interim analyses tends to have a highest probability of detecting a clinical response with the exception of the Sigmoid High profile, for which the GADA method gives the best results. When the target dose interval is at the upper end of the dose range (e.g. the Linear and Sigmoid High profile), there are more low doses which can be dropped for futility, hence there is more of a benefit from using an adaptive design over equal allocation compared to the profiles where the target dose is at the lower end

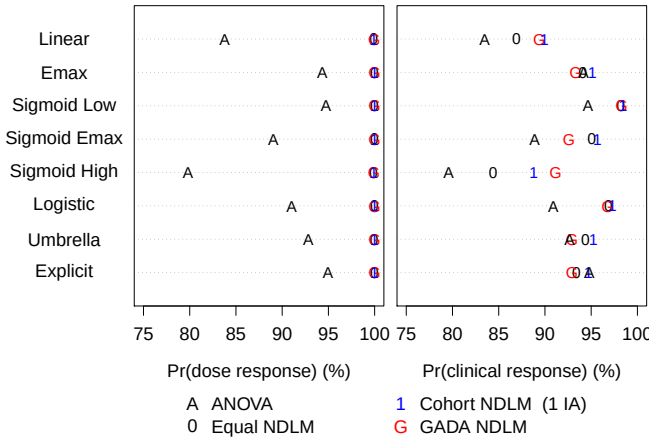

Figure 5-5: Operational characteristics for GADA, cohort and equal allocation modelled using an NDLM, and ANOVA methods: probability of detecting a dose response and a clinical response.

of the dose range (e.g. the Sigmoid Low profile).

Correctly selecting a dose in the target dose interval

No method of analysis consistently outperforms the others in terms of correctly identifying a dose in the target dose interval across all the dose response curves. The ANOVA method does better, when there is a steep incline in the dose response curve at the low doses which the NDLM model is not flexible enough to cope with (see Section 4.2.7).

Comparing the Bayesian methods which model the data using the NDLM, the cohort method does consistently better than the equal allocation and GADA methods. Using the GADA method is detrimental to the probability of selecting a dose in the target dose interval compared with the equal allocation method. Figure 5-7 presents the histograms of the selected dose for each of the methods, for the Linear, Emax and Sigmoid Emax profiles. As we can see, the methods which model the data using an NDLM tend to choose higher doses than the ANOVA method. Within the different allocation methods which model the data using an NDLM, the cohort method tends to select slightly lower doses than the GADA method, which increases the probability of detecting a dose in the target dose interval.

Figure 5-8 is an example of a coupled dataset for the three Bayesian methods when the

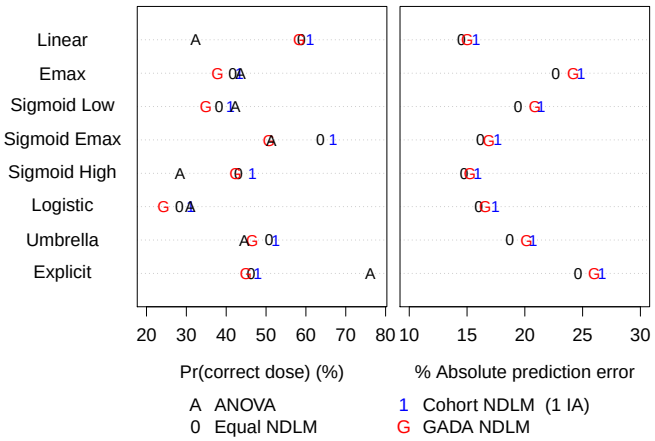

Figure 5-6: Operational characteristics for GADA, cohort and equal allocation modelled using an NDLM, and ANOVA methods: probability of selecting a dose in the target interval and the percentage absolute prediction error.

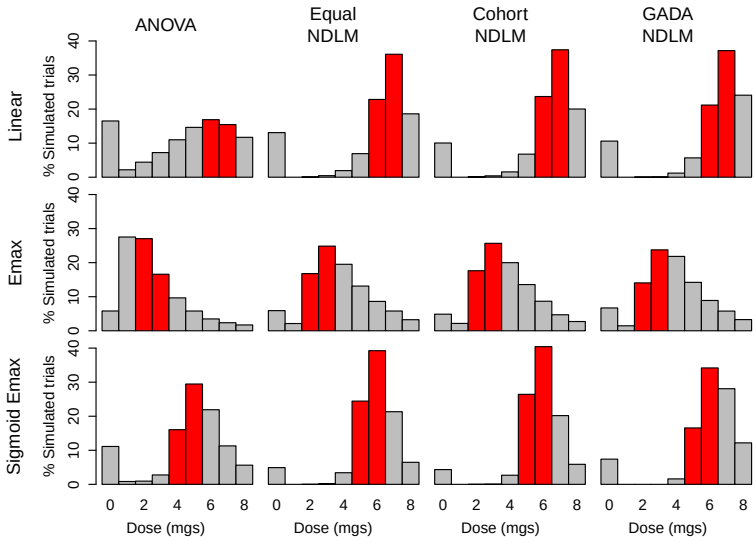

Figure 5-7: Histograms of dose selected for phase III for the GADA, cohort and equal allocation modelled using an NDLM, and ANOVA methods. Target dose intervals given in red.

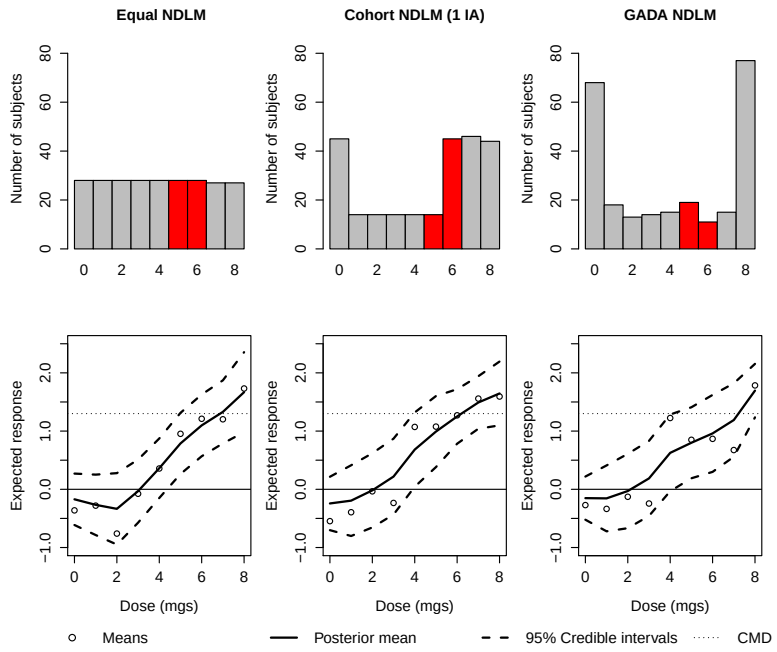

Figure 5-8: Example of coupled datasets for the GADA, cohort and equal allocation methods. Top row is the subject allocations for the three methods and the bottom row is the observed data and the posterior mean of the NDLM with 95% credible intervals.

data are generated from the sigmoid emax model. In this figure, we can see the final subject allocations of each of the methods, the observed means, the posterior means of the NDLM and the 95% credible intervals. The first thing we note is that of the two adaptive allocations, the cohort method tends to allocate to lower doses. This is because it allocates to a range of doses, from the lowest non-futile dose rather than trying to identify the dose which minimises the posterior variance at the target dose. When we allocate more subjects to doses z_6 and z_7 in the cohort methods, we see that the responses are higher than estimated using the GADA method, and so this brings the whole NDLM model up. The result of this is that based on the change from placebo, the cohort method selects dose z_6 which is in the target dose interval, whereas the GADA and equal allocation methods selected dose z_7 which is outside the target dose interval.

Prediction error

The percentage absolute prediction error is lowest when subjects are randomised using equal allocation, followed by the GADA method with the cohort method having the largest absolute prediction error (Figure 5-6). The GADA and cohort methods have

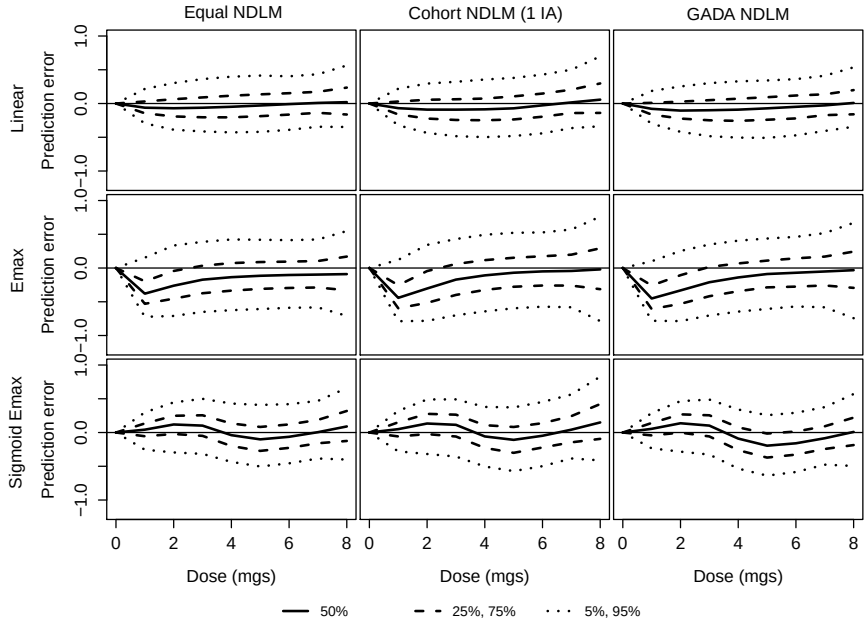

Figure 5-9: Median prediction error and prediction error quantiles for the GADA, cohort and equal allocation modelled using an NDLM.

higher absolute prediction errors than the equal allocation, as they tend to focus the subject allocation on a few doses, increasing the overall prediction error. The GADA method has a smaller absolute prediction error than the cohort method as the prediction error is based on the change from placebo and the GADA method tends to allocate more subjects to placebo,

The prediction error quantiles for the Linear, Emax and Sigmoid Emax profiles are presented in Figure 5-9. The GADA method has a better prediction at the top dose, as it tends to allocate subjects there. The median prediction errors for the doses in the target dose interval are smallest for the cohort method with 1 interim analysis, as this is where the method focuses the subject allocation. The ANOVA method treats each dose independently and so the median absolute prediction error is approximately zero for all the dose response profiles, but with larger prediction error quantiles than the NDLM.

Conclusion

We have found an improvement in the operational characteristics from applying the cohort method with 1 interim analysis over using non-adaptive equal allocation with the

same form analysis. However, we found that there was little to be gained from adapting at more than 1 interim analysis. For a complete comparison we have also compared cohort method with the GADA method and the non-adaptive equal allocation using the same Bayesian analysis, where the data are modelled using an NDLM. This has allowed us to separate out the design and analysis elements of each method when making our conclusions.

Analysis: To examine if it is the method of analysis which impacts the operational characteristics we compare the frequentist ANOVA approach with the Bayesian equal allocation approach, where the data were modelled using an NDLM.

Modelling the data using the NDLM reduces the posterior variance at the doses by borrowing strength from the other doses. This makes it easier to detect a significant difference from placebo than the ANOVA method which treats each dose as independent and then adjusts for multiple testing. Therefore there is a higher probability of detecting a dose response and a clinical response when we model the data. In terms of correctly identifying a dose in the target dose interval, neither the ANOVA or NDLM approach consistently outperforms the other.

The ANOVA method is better at selecting a dose in the target dose interval when the dose response curve is very steep in the early part of the dose range. This is because the NDLM finds it hard to fit a model to the data when the rate of change between the placebo and the first dose is high, and so tends to underestimate the response at the early doses. This results in the NDLM method choosing higher doses for phase III. For the other active dose response profiles, the Bayesian NDLM analysis results are similar or better than those of the ANOVA method in terms correctly identifying a dose in the target dose interval.

Design: To examine if it is the method of adaptation which impacts the operational characteristics we compare the non-adaptive equal allocation with the adaptive cohort and GADA methods, all modelled using the same Bayesian NDLM.

Comparing the equal, cohort and GADA methods, we found that the cohort allocation offer consistent gains over the equal allocation in terms of detecting a clinical response and selecting a dose in the target dose interval. The GADA method led to some gains over the equal allocation in detecting a clinical response, but was detrimental in terms of selecting a dose for phase III. The difference in the operational characteristics

between the cohort and GADA methods can be attributed to the allocation of subjects. Although the GADA method is designed to optimise the subject allocation, there is a large amount of variability in the allocations, and for some realisations the allocation tended to only explore a few non-consecutive doses. As the cohort method identifies a range of doses from the lowest non-futile dose, it tends to allocate subjects to lower doses and so select slightly lower doses for phase III. As the cohort method allocates to a range of doses, there also tends to be more information at and around the estimated target dose, leading to better dose response estimates at these doses.

5.5 Decision rule

So far for the Bayesian methods, once a dose response has been established, we have used the following definitions for determining if there is a clinical response and to identify the target dose;

- clinical response if $\Pr(\theta_j - \theta_0 \geq \text{CMD}|Y = y) \geq 0.5$
- target dose $\min_j\{z_j : \Pr(\theta_j - \theta_0 \geq \text{CMD}|Y = y) \geq 0.5\}$.

These decision criteria were chosen, so the results were as comparable as possible with the frequentist results, which rely on the estimated mean difference from placebo being greater than the clinically meaningful difference (CMD). However, when using Bayesian methods we can be more flexible, and specify thresholds that optimise our operational characteristics. Let us instead define these metrics as

- clinical response if $\Pr(\theta_j - \theta_0 \geq \text{CMD}|Y = y) \geq \gamma$
- target dose $\min_j\{z_j : \Pr(\theta_j - \theta_0 \geq \text{CMD}|Y = y) \geq \gamma\}$,

where $0 < \gamma \leq 1$. All the other metrics are as previously defined. As we rely on establishing a dose response before assessing if there is a clinical response, the type I error for the Flat dose response profile is maintained at a one-sided 5% level. Therefore, as our thresholds for γ changes we still adhere to the frequentist ideal of maintaining the type I error.

Ideally we would choose a value of γ that maximises the probability of detecting a clinical response when there is a clinical response whilst minimising the probability of incorrectly identifying a clinical response for those dose response curves that don't meet

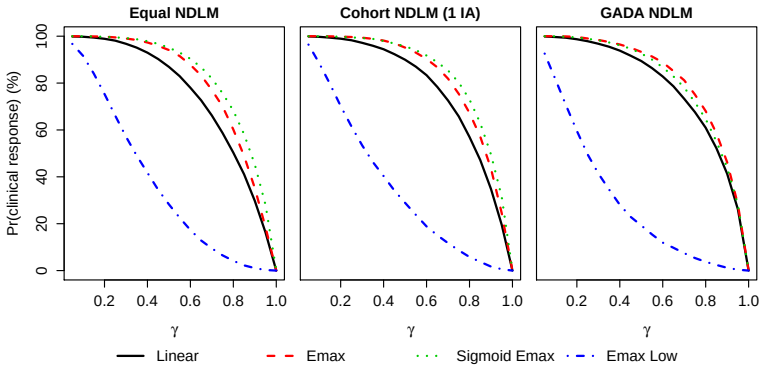

Figure 5-10: Probability of detecting a clinical response for increasing values of γ.

the clinically meaningful threshold. The probability of detecting a clinical response for the Linear, Emax and Sigmoid Emax profiles, and the probability of incorrectly claiming a clinical response for the Emax Low profile for different values of γ are presented in Figure 5-10. When γ is less than 0.8, the rate with which we incorrectly claim a clinical response for the Emax Low profile increases faster than the rate with which we correctly identifying a clinically meaningful difference increases. Therefore for lower values of γ, we lose more in terms of incorrectly continuing to phase III than we gain in power.

Let m_k $(k = 1, \ldots, K)$ denote the underlying dose response profile which have a dose response and a clinical response and $\tilde{m}_l$ $(l = 1, \ldots, L)$ denote the underlying dose response profiles which have a dose response but no clinical response. For a given value of γ, we let $f_\gamma(m_k)$ be the probability of detecting a clinical response in the k^{th} underlying dose response profile with a clinical response, and $f_\gamma(\tilde{m}_l)$ the probability of detecting a clinical response in the l^{th} underlying dose response profile without a clinical response. Then we could aim to maximise

$$\frac{1}{K}\sum_{k=1}^{K} f_\gamma(m_k) - \frac{1}{L}\sum_{l=1}^{L} f_\gamma(\tilde{m}_l). \tag{5.3}$$

If we did this for our set of dose response profiles in Section 2.3 (excluding the Flat dose response), the difference between correctly and incorrectly identifying a clinical response for different values of γ are as shown in Figure 5-11. The difference is maximised when $\gamma = 0.6$ for the GADA method and $\gamma = 0.65$ for the cohort and equal allocations.

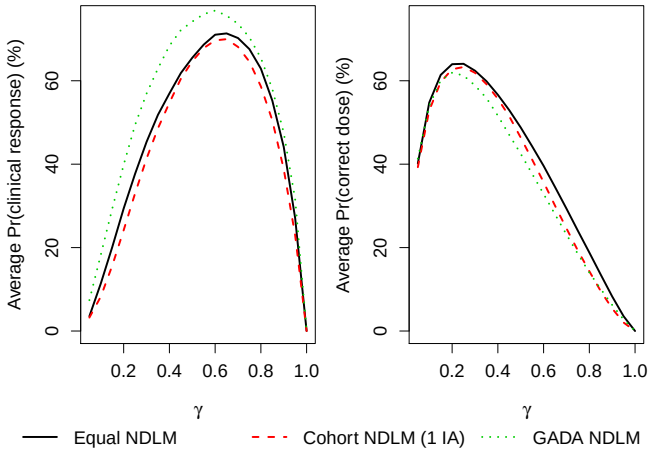

Figure 5-11: Difference between the average probability of correctly and incorrectly detecting a clinical response, and the average probability of correctly identifying a dose in the target dose interval for increasing values of γ.

Based on maximising (5.3), increasing the value of γ we use to determine whether there is a clinical response from 0.5 improves our overall decision making ability, as although we are less likely to observe a clinical response for some of the underlying dose response models, we are also less likely to incorrectly claim a clinical response. Increasing γ also has an impact on identifying a dose in the target dose interval. For higher values of γ more evidence is needed of a clinically meaningful difference, and so higher doses are identified. The right hand plot of Figure 5-11 shows the average probability of correctly identifying a dose in the target dose interval over the active dose response profiles where a clinically meaningful difference exists. Increasing the γ from 0.5 to 0.6 for the GADA method and to 0.65 for the cohort and equal allocations, results in an average reduction in the ability to correctly identify the target dose of between 10 and 15%.

Finding the value of γ which maximises (5.3) assumes that we believe all the dose response profiles are equally likely to occur. This may not be a realistic assumption, and so to reflect our beliefs about which dose response profiles are more likely we could use prior weights. Let, α_k $(k = 1, \ldots, K)$ be the prior weights placed on the profiles with a clinically meaningful difference and $\tilde{\alpha}_l$ $(l = 1, \ldots, L)$ be the prior weights assigned to the profiles that do not meet the clinically meaningful threshold, such that

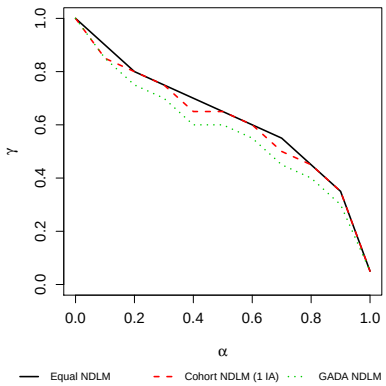

Figure 5-12: Value of γ which maximises decision for increasing values of α.

$\sum_{k=1}^{K} \alpha_k + \sum_{l=1}^{L} \tilde{\alpha}_l = 1$. We can now aim to maximise

$$\sum_{K=1}^{K} \alpha_i f(m_k) - \sum_{l=1}^{L} \tilde{\alpha}_l f(\tilde{m}_l). \tag{5.4}$$

For ease of computation, let us assume that we believe all the dose response profiles with a clinical response are equally likely to occur and all those dose response profiles without a clinical response are also equally likely to occur. Then (5.4) can be re-written as

$$\frac{\alpha}{K} \sum_{i=1}^{K} f(m_k) - \frac{(1-\alpha)}{L} \sum_{l=1}^{L} f(\tilde{m}_l). \tag{5.5}$$

Figure 5-11 shows the value of γ that maximises the probability of detecting a clinical response for different values of α. As α increases we put less weight on the Emax Low profile occurring and so decrease the probability of incorrectly identifying a clinical response. This results in a lower value of γ maximising (5.5). As α decreases, we are less sure we are going to observe a clinical response and so we need to use a larger value of γ to protect against the probability of incorrectly identifying a clinical response.

In this section, we have begun to think about how we can optimise the decision making process when we believe the true underlying dose response profile can take a range of curves. Although we have allowed γ to decrease to 0 realistically there may be regulatory concerns from lowering the bar for concluding a clinical response and so for this reason there may be a minimum value of γ that a company feels is acceptable. Increasing the value of γ can be beneficial in terms of our overall decision making process, if we believe there is a reasonable chance the underlying dose response curve will not meet the clinically meaningful threshold.

In Chapter 7 we formalise the concept of optimising the operational characteristics using Bayesian decision theory. Bayesian decision theory uses a utility function to attributes costs and rewards to the decision making process. Decision theory also allows us to take into account the uncertainty in the parameter estimates, by optimising the utility function over the posterior distribution,

5.6 Discussion

In this chapter we have examined adapting subject allocations at interim analyses based on the posterior probabilities from an NDLM. This method has been compared with the frequentist ANOVA method, a Bayesian equal allocation approach and the GADA method. Comparing the adaptive and non-adaptive allocations modelled using the NDLM, we observed some gains from adaptation in detecting a clinical response. The cohort method performed consistently better than the equal and GADA methods in terms of selecting a dose for phase III. The GADA method was less able to correctly select a dose in the target dose interval when compared to the equal allocation. Previous results by Bornkamp et al. (2007) compared the GADA method and other adaptive methods with the frequentist ANOVA method, but did not compare the results of the adaptive designs with an equal allocation design using the same final analysis. With the opportunity to vary many aspects of a clinical trial design, such as the randomisation, stopping rules and analysis, it is important to determine through simulations studies which elements have the greatest impacts on the results. This could be done by planning a simulation study that uses a factorial design to assess the impact of each design option.

Finally, we consider the decision rule used to conclude a clinical response, and to identify the target dose. Up until now we have used an arbitrary value in order to make the results of the Bayesian analysis as comparable as possible with the frequentist results. By increasing the amount of evidence needed to conclude efficacy we can reduce the probability of incorrectly detecting a clinical response and so overall we improve our decision making process. However, this comes at the cost of the power of detecting a clinical response for some of the dose response profiles and identifying a dose in the target dose interval. With increased evidence of efficacy needed, we also tend to chose higher doses as the target dose, which could result in potential safety concerns. We formalise optimising the decision making process in Chapter 7 using decision theory.

Chapter 6

Optimal Design Theory

6.1 Introduction

In a clinical trial context, optimal design theory is concerned with placing subjects in a way that minimises some pre-defined criterion so 'that the statistical inference about the quantities of interest can be improved' (Chaloner & Verdinelli, 1995). Optimal designs were first explored by Smith (1918) and then became the topic of many papers. Key authors of early work in this area are Kiefer & Wolfowitz (1960) and Kiefer (1974), who focused on the general mathematical theory of optimal designs, while Box & Lucas (1959) were concerned with the application of such designs. Parallel to this in the USSR, Fedorov (1972) also developed methods for optimal designs. For more information on the development of optimal designs see survey papers by Atkinson (1982, 1988) and Ford et al. (1989). There are many different types of optimal designs each focused on optimising some aspect of the experiment. The most researched area of optimal design is D-optimality, and this is also the type of optimal design most often used in clinical trial literature.

The aim of a D-optimal design is to allocate subjects to doses in such a way as to increase the information about the unknown parameters θ in the dose response curve. Specifically this is done estimating the parameters using the maximum likelihood estimator, $\hat{\theta}$, and then maximising the determinant of the information matrix of these parameters. Another commonly used criterion is c-optimality, where the aim is to maximise the information about a linear combination of the parameters. Han & Chaloner (2003) and Dette et al. (2008, 2010) give examples of how to construct optimal designs for non-linear models often used in the pharmaceutical industry.

For linear models, the D-optimal design does not depend on the unknown model parameters, and so can always be found in advance of carrying out the experiment. This is not true with non-linear models, as the optimal design relies on knowledge about the model parameters. A design is known as a 'locally' optimal design (Chernoff, 1953) if it is optimal for a specific $\hat{\theta}$. The limitation of using locally optimal designs for non-linear models, is that they rely on a good estimate of the parameter values. Mis-specification of these parameter estimates can lead to designs that are far from optimal. Meeker (1984) found that non-optimal designs can often be more robust to departures from the assumption about parameter estimates than optimal designs. Dette et al. (2008) showed that c-optimal designs are sensitive to the assumptions about the parameter estimates and the choice of model fitted. The dependence of the design on the assumptions about unknown parameter estimates is one of the main reasons these designs are rarely applied in practice (Ogungbenro et al., 2009).

Adaptation provides a way of overcoming the dependence of locally optimal designs on the initial parameter estimates. By adapting at interim analyses throughout the course of the trial, we are able to learn about the parameter values and so randomise the next cohort of subjects in a near optimal manner. As the number of subjects increases, the parameter estimates tend towards the true values of the parameters, and so the design tends towards the optimal design. Sequential adaptive simulation studies have been carried out by Abdelbasit & Plackett (1983) and Dragalin et al. (2007, 2010). Abdelbasit & Plackett (1983) found that, for binary data, using sequential stages is only beneficial when the initial estimates are poor. Dragalin et al. (2010) showed little or no improvement in the operational characteristics as the number of interim analyses increased.

An alternative method to using a point estimate, is to place a prior distribution on the model parameters, and maximise the expected value of the locally optimality criterion over the prior distribution. This Bayesian approach takes into account the prior uncertainty in the parameter estimates, producing a design which should perform well on average whilst being more robust to parameter mis-specification (Ogungbenro et al., 2009). It is possible to then use adaptive designs with Bayesian D-optimality, such that at later interim analyses the prior distributions have less impact on the Bayesian D-optimal design for the next cohort of subjects. For a detailed review of Bayesian experimental design see Chaloner & Verdinelli (1995).

This chapter is organised as follows. In Section 6.2 we define the notation used throughout this chapter. In Section 6.3 we outline methods for finding the locally optimal design and the general equivalence theorem used for confirming the optimality of a design. In Section 6.3 we describe how our adaptive D-optimal design is constructed and propose a quasi-adaptive method, which only adapts using the locally D-optimal design if the design is relatively robust to parameter mis-specifications. In Section 6.3 we also define how the Bayesian D-optimal design is constructed.

As locally D-optimal designs are known to be sensitive to model mis-specification, in Section 6.4 we explore how sensitive the locally D-optimal designs are to a choice of candidate models. We also explore the sensitivity of the Bayesian D-optimal design to the prior distribution placed on the model parameters. In Section 6.5 we investigate different methods for dealing with non-convergence of the algorithm used to find the parameter estimates. Finally, in Sections 6.6, 6.7 and 6.8 we present the results from using the adaptive D-optimal, quasi-adaptive D-optimal and Bayesian D-optimal designs, respectively.

6.2 Notation

The notation that follows is that of Atkinson & Donev (1992). In order to make the notation relevant to the topic of this thesis, we describe the experimental designs in terms of the numbers of subjects allocated to the available doses. We consider the situation where the expected response of the data at dose z_j is modelled as a function $\eta(z_j, \theta)$, where θ are the model parameters. The response of the i^{th} subject on the j^{th} dose is distributed as

$$Y_{ij} \sim N(\eta(z_j, \theta), \sigma^2),$$

where σ^2 is the between subject variation. For the models we are concerned with, $\eta(z_j, \theta)$ is typically non-linear in θ. An example of a non-linear model which is commonly used in the pharmaceutical industry and throughout this chapter, is the four parameter sigmoid emax model introduced in Chapter 2,

$$\eta(z_j, \theta) = \theta_1 + (\theta_2 - \theta_1)\frac{z_j^{\theta_4}}{\theta_3^{\theta_4} + z_j^{\theta_4}}.$$

Suppose we have a placebo dose z_0 and J active doses of a drug, $z_1, \ldots, z_J$. We denote the set of doses as $\mathscr{Z} = \{z_j : j = 0, \ldots, J\}$. A design is defined as a measure, or probability distribution, on $\mathscr{Z}$. We shall discuss the set of continuous designs, in which

there are exact designs. We denote the set of continuous designs as $\mathscr{H}$. In a continuous design we assign weights w_j to each of the doses such that the design is written as

$$\xi = \begin{Bmatrix} z_0 & z_1 & \dots & z_J \\ w_0 & w_1 & \dots & w_J \end{Bmatrix},$$

where $w_j \geq 0$ for $j = 0, \dots, J$ and $\sum_{j=0}^{J} w_j = 1$. The weight w_j represents the proportion of subjects that are allocated to dose z_j. Within the design ξ, the doses z_j are fixed and the weights are chosen to give a specific design. These weights are chosen to optimise the stated criterion, where the criterion is some function of the variance of the model parameters, $\text{Var}(\hat{\theta})$, for the design ξ. The design which optimises the criterion is denoted ξ^*.

For some realisations of w_j, the total number of subjects, N, multiplied by w_j is not an integer, hence it is not possible to allocate Nw_j of subjects to dose z_j. We refer to designs where the weights are constrained to take values which relate to subject allocations as exact designs. If N is the number of subjects to be allocated then this is known as an N-design and can be written

$$\xi_N = \begin{Bmatrix} z_0 & z_1 & \dots & z_J \\ n_0/N & n_1/N & \dots & n_J/N \end{Bmatrix}, \tag{6.1}$$

where n_j is the number of subjects allocated to dose z_j and $\sum_{j=0}^{J} n_j = N$.

We estimate the variance of the parameter estimates using Fisher's information matrix (Kiefer, 1974; Whittle, 1973; Atkinson & Donev, 1992). Let $\eta(z, \theta) = (\eta(z_0, \theta), \dots, \eta(z_J, \theta))^T$ denote the vector of expected responses for a model with p parameters, $\theta = (\theta_1, \dots, \theta_p)^T$. Let θ denote the true parameter value and $g(z_j, \theta) = \left(\frac{\partial \eta(z_j,\theta)}{\partial \theta_1}, \dots, \frac{\partial \eta(z_j,\theta)}{\partial \theta_p}\right)^T$ $(j = 0, \dots, J)$. The Fisher's information matrix for a single observation on dose z_j is

$$\frac{1}{\sigma^2} g(z_j, \theta) g(z_j, \theta)^T.$$

For an N-design ξ_N with n_j subjects allocated to dose z_j, the normalised Fisher information per subject is

$$M(\xi_N, \theta) = \sum_{j=0}^{J} \frac{1}{\sigma^2} \frac{n_j}{N} g(z_j, \theta) g(z_j, \theta)^T. \tag{6.2}$$

Generalising this to the continuous design ξ with weights $w = (w_0, \ldots, w_j)^T$, the Fisher information is

$$M(\xi, \theta) = \sum_{j=0}^{J} \frac{w_j}{\sigma^2} g(z_j, \theta) g(z_j, \theta)^T. \tag{6.3}$$

For large sample sizes, $N^{-1}M^{-1}(\xi_N, \theta)$ is a good approximation to the variance-covariance matrix of the maximum likelihood estimator (MLE) of the unknown parameters θ (Rao, 1965). Since the matrix $M(\xi_N, \theta)$ is determined by the design ξ_N and the model parameters θ, for a given θ, it is possible to determine the best placement of subjects to maximise a specified function of the information matrix $M(\xi_N, \theta)$ or to minimise a function of the variance $N^{-1}M^{-1}(\xi_N, \theta)$. For ease of notation we shall sometimes refer to $M(\xi_N, \theta)$ as M and to $M^{-1}(\xi_N, \theta)$ as M^{-1}.

We shall denote the design criterion we wish to maximise by as $\Psi\{M(\xi, \theta)\}$. There are a number of different design criteria which can be used to maximise the information about a specific aspects of a dose response model. Some examples of these design criteria are given in Table 6.1.

Criterion	Aim of Criterion	Ψ
A-optimality	Maximise the *average* information of the parameter estimates	$trM(\xi, \theta)$
D-optimality	Maximise the generalised information using the *determinant* of the information matrix	$\log \lvert M(\xi, \theta) \rvert$
c-optimality	Maximise the information for a linear *combination* of the parameters $c^T\theta$	$c^T M(\xi, \theta) c$

Table 6.1: Examples of optimality criterion.

6.3 Finding the optimal design

6.3.1 Construction of continuous optimal designs and the general equivalence theorem

In the scenarios we wish to explore, a continuous design allocates weights w_j to each dose z_j $(j = 0, \ldots, J)$ which is a finite set of doses. The optimal design is the design with weights allocated in such a way to maximise the criterion of interest. In this section we explore the general equivalence theorem which is used to confirm the optimality of a design. We are interested in maximising concave criteria, such as those given in Table 6.1. For any two designs ξ', $\tilde{\xi}$ and for $\alpha \in [0, 1]$, we use the following definition of

concavity,

$$\Psi\{M((1-\alpha)\xi' + \alpha\tilde{\xi}, \theta)\} \geq (1-\alpha)\Psi\{M(\xi', \theta)\} + \alpha\Psi\{M(\tilde{\xi}, \theta)\}.$$

In order to find the optimal design we first define the directional derivative for a given θ as

$$\phi_\theta(\xi', \tilde{\xi}) = \lim_{\alpha \to 0} \frac{1}{\alpha}[\Psi\{(1-\alpha)M(\xi', \theta) + \alpha M(\tilde{\xi}, \theta)\} - \Psi\{M(\xi', \theta)\}]. \tag{6.4}$$

This is the directional derivative of Ψ at ξ' in the direction of $\tilde{\xi}$. Suppose ξ' is a non-optimal design and the optimal design for a given θ is denoted ξ^*. Then because of concavity we note that $\phi_\theta(\xi', \xi^*) \geq 0$, as the derivative in the direction of the optimal design is positive and $\phi_\theta(\xi^*, \xi') \leq 0$, as the derivative in the direction away from the optimal design is negative.

Let us now define the design ξ_j to be a design measure with unit mass at dose z_j. If the design $\tilde{\xi}$ assigns weights w_j to dose z_j $(j = 0, \ldots, J)$ then it is possible to write $\tilde{\xi}$ as a linear combination of ξ_j, i.e. $\tilde{\xi} = w_0\xi_0 + \ldots + w_j\xi_J$. In our application $\phi_\theta(\xi', \tilde{\xi})$ is linear in $\tilde{\xi}$, and so following the general notation of Whittle (1973) we can refer to Ψ as differentiable at ξ' and represent this as

$$\phi_\theta(\xi', \tilde{\xi}) = \int D_\theta(z_j, \xi')\tilde{\xi} dz_j, \tag{6.5}$$

where $D_\theta(z_j, \xi')$ is a perturbation at ξ' in the direction z_j,

$$D_\theta(z_j, \xi') = \phi_\theta(\xi', \xi_j).$$

As we are using a finite set of doses we can re-write (6.5) as a summation,

$$\phi_\theta(\xi', \tilde{\xi}) = \sum_{j=0}^{J} D_\theta(z_j, \xi').$$

As defined by Whittle (1973), the maximum rate of change of Ψ from ξ' to $\tilde{\xi}$ is given by,

$$\bar{D}_\theta(\xi') = \sup_{\tilde{\xi} \in \mathscr{H}} \phi_\theta(\xi', \tilde{\xi}). \tag{6.6}$$

For the differentiable case this is

$$\bar{D}_\theta(\xi') = \max_{z_j} D_\theta(z_j, \xi'). \tag{6.7}$$

The general equivalence theorem forms the criteria for confirming that a design is optimum. This equivalence theorem was originally proved to be true for linear models by Kiefer & Wolfowitz (1960) and then extended by White (1973) to cover non-linear models. Whittle (1973) has proved this for general concave functions in the context of the information matrix. We refer to theorem given by Whittle (1973), and rewrite this in our notation.

Theorem 6.3.1. General equivalence theorem (Whittle, 1973)
a) If Ψ is concave, then an optimal design, ξ^*, can be equivalently characterized by any of the three conditions:

1. *The design ξ^* maximises $\Psi\{M(\xi,\theta)\}$*
2. *The design ξ^* minimises $\bar{D}_\theta(\xi)$*
3. *$\bar{D}_\theta(\xi^*)$=0.*

b) The point (ξ^*,ξ^*) is a saddle point of ϕ_θ in that

$$\phi_\theta(\xi^*,\xi') \leq 0 = \phi_\theta(\xi^*,\xi^*) \leq \phi_\theta(\zeta,\xi^*) \text{ for } \xi',\zeta \in \mathscr{H}.$$

c) If Ψ is also differentiable, then the support of ξ^* is contained in the set of z for which $D(z_j,\xi^*)=0$.

We will not re-prove the theorem here, but note that while parts a) and b) are intuitive, the proof for part c) follows from

$$D_\theta(z_j,\xi^*) = \phi_\theta(\xi^*,\xi_j) \leq 0,$$

$$\sum_{j=0}^{J} D_\theta(z_j,\xi^*) = \phi_\theta(\xi^*,\xi^*) = 0.$$

A support point is a dose z_j that has weight $w_j > 0$. The proof follows that either z_j is a support point in ξ^* and so $D_\theta(z_j,\xi^*)=0$ or z_j is not a support point in ξ^* and so the directional derivative at ξ^* in the direction of z_j is negative.

Using Whittle's theorem, we can find the optimal design iteratively assigning weight to the dose z_j which maximises the rate of change $\phi_\theta(\xi',\xi_j)$. We denote ξ_α to be a linear combination of ξ' and ξ_j,

$$\xi_\alpha = (1-\alpha)\xi' + \alpha\xi_j. \tag{6.8}$$

Hence, when α is chosen correctly in the direction z_j that maximises the change in Ψ, $\Psi(\{M(\xi_\alpha,\theta)\} \geq \Psi\{M(\xi',\theta)\}$. We can then use Theorem 6.3.1 to confirm when the optimal design has been found.

Let the Fisher information matrix $M(\xi',\theta)$ given in (6.3) be a $p \times p$ matrix where p is the length of the vector of unknown model parameters θ. We find the directional derivative (6.4) at ξ' in the direction ξ_j by differentiating $\Psi\{M(\xi_\alpha,\theta)\}$ with respect to α using the chain rule,

$$\begin{aligned}
\left.\frac{d\Psi\{M(\xi_\alpha,\theta)\}}{d\alpha}\right|_{\alpha=0^+} &= \sum_{i=1}^{p}\sum_{k=1}^{p}\left(\frac{d\Psi\{M(\xi_\alpha,\theta)\}}{dM(\xi_\alpha,\theta)}\right)_{ik}\left.\frac{dM(\xi_\alpha,\theta)_{ik}}{d\alpha}\right|_{\alpha=0^+} \\
&= \sum_{i=1}^{p}\sum_{k=1}^{p}\left(\frac{d\Psi\{M(\xi',\theta)\}}{dM(\xi',\theta)}\right)_{ik}(M(\xi_j,\theta)-M(\xi',\theta))_{ik} \\
&= \sum_{i=1}^{p}\sum_{k=1}^{p}(M(\xi_j,\theta)-M(\xi',\theta))_{ki}\left(\frac{d\Psi\{M(\xi',\theta)\}}{dM(\xi',\theta)}\right)_{ik} \\
&= \sum_{k=1}^{p}\left(M(\xi_j,\theta)\frac{d\Psi\{M(\xi',\theta)\}}{dM(\xi',\theta)}\right)_{kk} - \\
&\quad \left(M(\xi',\theta)\frac{d\Psi\{M(\xi',\theta)\}}{dM(\xi',\theta)}\right)_{kk} \\
&= \mathrm{tr}\left(M(\xi_j,\theta)\frac{d\Psi\{M(\xi',\theta)\}}{dM(\xi',\theta)}\right) - \mathrm{tr}\left(M(\xi',\theta)\frac{d\Psi\{M(\xi',\theta)\}}{dM(\xi',\theta)}\right) \\
&= \mathrm{tr}\left(\frac{1}{\sigma^2}g(z_j,\theta)^T\frac{d\Psi\{M(\xi',\theta)\}}{dM(\xi',\theta)}g(z_j,\theta)\right) \\
&\quad -\mathrm{tr}\left(M(\xi',\theta)\frac{d\Psi\{M(\xi',\theta)\}}{dM(\xi',\theta)}\right).
\end{aligned}$$

For ease of notation the derivative is written

$$\phi_\theta(\xi',\xi_j) = \frac{1}{\sigma^2}g(z_j,\theta)^T\frac{d\Psi}{dM}g(z_j,\theta) - \mathrm{tr}M\frac{d\Psi}{dM}. \tag{6.9}$$

For certain types of optimality the second term of this equation is a constant and so we can maximise the directional derivative by maximising the first term. In optimal design theory the first term of (6.9) is known as the ***sensitivity function***

$$d(z_j,\xi,\theta) = \frac{1}{\sigma^2}g(z_j,\theta)^T\frac{d\Psi}{dM}(\xi,\theta)g(z_j,\theta). \tag{6.10}$$

Some optimum designs can be found analytically, although this is 'possible only in the simplest case and requires a special approach in each distinct case ' (Fedorov, 1972,

p. 97). Therefore most designs are found numerically using iterative methods until convergence of $\Psi\{M(\xi,\theta)\}$ to its maximum. To construct an optimal design we use the algorithm suggested by Fedorov (1972, p. 102).

Let ξ^0 be an arbitrary initial design,

$$\xi^0 = \begin{Bmatrix} z_0 & z_1 & \dots & z_J \\ w_0^0 & w_1^0 & \dots & w_J^0 \end{Bmatrix},$$

such that $\sum_{j=0}^{J} w_j^0 = 1$. The first step in the iteration process is to place additional weight to the dose which results in the maximal rate of change of Ψ. Let

$$z^* = \arg \max_{z \in \{z_0,\dots,z_J\}} \{D_\theta(z, \xi^0)\}$$

be the dose with the maximal rate of change of Ψ and ξ_z be the design with unit mass at dose z^*. Then

$$\delta = \phi_\theta(\xi^0, \xi_z)$$

is the size of the change, and

$$\alpha_0 = \frac{\delta}{(\delta + (p-1))p}$$

is the additional weight that is placed on dose z^* to improve the design ξ^0. The design for the next step in the iteration is then

$$\xi^1 = (1-\alpha_0)\xi^0 + \alpha_0 \xi_z.$$

This iterative process is continued such that the design after the k^{th} iteration is

$$\xi^k = (1-\alpha_{k-1})\xi^{k-1} + \alpha_{k-1}\xi_z.$$

As $\Psi\{M(\xi^0,\theta)\} \leq \Psi\{M(\xi^1,\theta)\}$ the iterative process is repeated until the $\lim_{k\to+\infty} \Psi\{M(\xi^k,\theta)\}$ corresponds to the optimal design. The optimality of the design ξ^k can be confirmed using the general equivalence theorem (Theorem 6.3.1).

For the D-optimal design with p parameters, $\Psi(M) = \log|M|$ which is a concave function. For the information matrix M which is a $p \times p$ matrix, we denote M_{ik}^* to be the information matrix with row i and column k removed and use Laplace's formula for the determinant of the M, $|M| = \sum_{i=1}^{p} (-1)^{i+k} M_{ik} |M_{ik}^*|$. We calculate the derivative

of Ψ with respect to M using the chain rule

$$\begin{aligned}\frac{\partial \Psi}{\partial M} = \frac{\partial \Psi}{\partial |M|}\frac{\partial |M|}{\partial M_{ik}} &= |M|^{-1}\frac{\partial |M|}{\partial M_{ik}} \\ &= |M|^{-1}\sum_{i=1}^{p}(-1)^{i+k}|M^*_{ik}| \\ &= |M|^{-1}M^{-1}|M| \\ &= M^{-1}\end{aligned}$$

and so the directional derivative in (6.9) for the D-optimal criterion is

$$\phi_\theta(\xi', \xi_j) = \frac{1}{\sigma^2}g(z,\theta)^T M^{-1}(\xi', \theta)g(z,\theta) - p.$$

As p is fixed we maximise $\phi_\theta(\xi', \xi_j)$ by maximising the first part of the directional derivative equation known as the sensitivity function

$$d(z_j, \xi, \theta) = \frac{1}{\sigma^2}g(z_j,\theta)^T M^{-1}(\xi, \theta)g(z_j,\theta). \tag{6.11}$$

For the D-optimal design the sensitivity function $d(z_j, \xi, \theta)$ is the variance of the predicted response at dose z_j. Maximising the sensitivity function is therefore equivalent to placing weight at the dose where the variance of the predicted response is greatest, or alternatively, the dose where there is the least information.

6.3.2 Constructing exact designs

Unlike a continuous design where the weights can take any values, an exact design is constrained so the weights relate to the number of subjects allocated to a dose. Let N be the total number of subjects to be allocated, we denote the exact design by ξ_N. The optimal exact design is the design out of all the designs with form (6.1) which for a given θ maximises $\Psi\{M(\xi_N, \theta)\}$ and is denoted ξ^*_N. The optimal exact design can be constructed using a number of methods, but we focus on the following two approaches.

1. Use the optimal continuous design ξ^*, where w_j denotes the weight that ξ^* assigns to dose z_j. We then round each w_j N to an integer n_j in such a way that $\sum_{j=0}^{J} n_j = N$ and assign n_j subjects to dose z_j.

2. Use a sequential algorithm to produce an exact design at or near the optimum design. Several algorithms have been proposed by Atkinson & Donev (1992, p. 171): forward selection, backwards elimination or the exchange algorithm.

Using the first approach there are cases where the optimal continuous design coincides with the optimal exact design of size N. In other cases, $w_j N$ does not result in an integer and so then we round $w_j N$ in such a way to ensure all the subjects are allocated to doses.

Take for example, an emax model

$$\eta(z_j, \theta) = \theta_1 + (\theta_2 - \theta_1)\frac{z_j}{\theta_3 + z_j}$$

which is non-linear in the unknown model parameters $\theta = (\theta_1, \theta_2, \theta_3)^T$. For the case with 9 doses $z_0, \ldots, z_8 = (0\text{mgs}, \ldots, 8\text{mgs})$ and $\theta = (0, 1.81, 0.79)$ the continuous D-optimal design ξ^* is

$$\xi^* = \begin{Bmatrix} z_0 & z_1 & z_2 & z_3 & z_4 & z_5 & z_6 & z_7 & z_8 \\ 1/3 & 1/3 & 0 & 0 & 0 & 0 & 0 & 0 & 1/3 \end{Bmatrix}. \tag{6.12}$$

The second row of the matrix represents the proportion of subjects to be assigned to each of the doses. If N is not a multiple of 3 then after rounding $w_j N$ we will still have subjects that need to be allocated to doses. The optimal exact design can then be found by searching over the designs where the remaining subjects are allocated to doses.

The second approach is to use a sequential algorithm to find the optimal exact design based on an iterative, one subject at a time approach. We consider three sequential algorithms: forward selection, backwards elimination and an exchange algorithm. We use these sequential methods to allocate 'theoretical' subjects and find the optimal subject allocation before the randomisation process begins. We can then randomise groups of subjects based on the optimal design. Once a subject has been randomised to a dose, they cannot be removed from this dose, and so when we use a sequential algorithm at an interim analysis, the algorithms are constrained to take into account the subjects already randomised.

We are going to focus on the D-optimal design, where the aim is to maximise the log determinant of the information matrix $\Psi\{M(\xi, \theta)\} = \log|M(\xi, \theta)|$. In D-optimality, we maximise the change in Ψ at ξ by increasing the weight at the dose z_j which maximises the sensitivity function,

$$d(z_j, \xi, \theta) = \frac{1}{\sigma^2} g(z_j, \theta)^T M^{-1}(\xi, \theta) g(z_j, \theta),$$

alternatively we can remove weight from the dose z_j which minimises the sensitivity function.

Forward selection

In forward selection an initial design n^* is chosen with $n^* < N$. Subjects are allocated to doses sequentially in a forward manner in order to maximise the optimality criteria. If there are currently n subject randomised, then for a D-optimal design the next subject is assigned to the dose where the predicted variance is greatest. A subject is added to dose z_j if

$$z_j = \underset{z \in \{z_0, \ldots, z_J\}}{\operatorname{argmax}} \{d(z, \xi_n, \theta)\}.$$

This forward selection is continued until all N subjects have been assigned to doses. The final design is dependent on the initial design n_0.

Backwards elimination

In backward elimination an initial design n^* is chosen with $n^* > N$ and subjects are removed from doses sequentially in such a way to maximises the criteria. As we are decreasing the weight at a dose (i.e. $\alpha < 0$ in (6.8)), we remove the subject from the dose which results in the smallest change in Ψ. A subject is removed from dose z_j if

$$z_j = \underset{z \in \{z_0, \ldots, z_J\}}{\operatorname{argmin}} \{d(z, \xi_n, \theta)\}.$$

Again, the optimal design is dependent on the initial design n^*, and so n^* needs to be sufficiently large.

Exchange algorithm

In the exchange algorithm, the design begins with N subjects. At each iteration a subject is added to a dose and a subject removed from a dose in such a way to maximise the optimality criterion. We add the subject to the dose z_j which has the largest change in the optimality criterion

$$z_j = \underset{z \in \{z_0, \ldots, z_J\}}{\operatorname{argmax}} \{d(z, \xi_N, \theta)\},$$

and removed a subject from the dose with the smallest change in the optimality criterion

$$z_j = \underset{z \in \{z_0,\ldots,z_J\}}{\operatorname{argmin}} \{d(z, \xi_N, \theta)\}.$$

Relative efficiency

For a model $\eta(z_j, \theta)$ with p model parameters $\theta = (\theta_1, \ldots, \theta_p)^T$, it is possible to compare two designs in terms of the optimality criterion and so find the relative efficiency of one design compared to another. The efficiency of a design ξ compared to the optimal design ξ^* is calculated as

$$\text{Eff} = \left(\frac{\Psi\{M(\xi^*, \theta)\}}{\Psi\{M(\xi, \theta)\}} \right)^{1/p}$$

where p is the number of parameters in the model. The efficiency is calculated using $1/p$ so that it is proportional to the sample size, regardless of the number of parameters in the model (Atkinson & Donev, 1992, p. 116). We write our efficiency this way so that we can discuss the increase in sample size needed in order for ξ to have the same degree of accuracy as ξ^*. For example, if Eff=1.5 then the design ξ needs 50% more subjects than the ξ^* to achieve the same level of precision. As the efficiency refers to sample size, this allows comparison of efficiencies across different models with differing numbers of parameters.

6.3.3 Adaptive D-optimal designs

For non-linear models, the D-optimal design relies on the unknown model parameters, θ. It is known that designs constructed using the 'best guess' of θ are sensitive to mis-specifications in the initial estimates (Pronzato & Walter, 1985). One way of dealing with the dependence on the parameter estimates is to use adaptive designs. The adaptive D-optimal design uses available information from subjects who have completed the trial to estimate the unknown parameters and then optimises the next randomisation scheme based on the parameter estimates.

The adaptive D-optimal design is constructed using the following steps:

1. An initial cohort of subjects is randomised equally across all the doses. Let the size of this initial cohort be denoted n_1.

2. The data from the n_1 subjects are used to fit the model $\eta(z_j, \theta)$ and estimate the model parameters θ using the MLE $\hat{\theta}$.

3. Under the constraint that n_1 subjects have already been allocated, the exact D-optimal design given $\hat{\theta}$ for the next cohort of n_2 subjects is found using forward selection and denoted $\xi_{(n_1+n_2)}$. This is equivalent to using ξ_{n_1} as the initial design for the forward selection algorithm.

4. The next cohort of n_2 subjects are then randomised using the exact D-optimal design and their data collected. Using the cumulative data the model parameters are re-estimated and the optimum exact D-optimal design for the next cohort of subjects is found.

5. This process is repeated until all N subjects have been randomised.

Informally, according to asymptotic theory as N increases, $\hat{\theta}$ will be close to θ, and so we would expect the optimal allocation from the adaptive design to tend towards the optimal design. Pronzato & Walter (1985) cite results by other authors where for some cases the model parameters 'have been shown to converge to their mean among the population'.

6.3.4 Quasi-adaptive D-optimal designs

The adaptive D-optimal design aims to optimise subject allocation at each interim analysis based on the parameter estimates $\hat{\theta}$. For a non-linear model, if the parameter estimates are reasonably close to θ, then this leads to a near optimal allocation for the next cohort of subjects. If however, the parameter estimates are far from the true θ, then the resulting locally optimal allocation for $\hat{\theta}$ may be far from optimal for the true θ. We propose a quasi-adaptive method, that only applies the optimal allocation for the next cohort of subjects if the proposed optimal design is robust to the variance in the parameter estimates. If the variance in the parameter estimates suggests adaptation may lead to suboptimal designs, then we continue with equal allocation. In this way we do not adapt automatically, but only when there is evidence to suggest that the adaptation is beneficial to the design.

To assess the variability in the model parameters at an interim analysis we use bootstrapping. The premise of bootstrapping is that the bootstrap samples $\hat{\theta}^*$ are displaced from $\hat{\theta}$ with the same distribution that $\hat{\theta}$ is displaced from θ, and so the bootstrap samples $\hat{\theta}^*$ are contenders for the true θ. For a detailed description on the bootstrap methodology see Efron & Tibshirani (1993).

To bootstrap the model parameters, let us suppose we have a dataset consisting of n

subjects, with n_j $(j = 0, \ldots, J)$ subjects allocated to dose z_j such that $\sum n_j = n$. Let the response of the i^{th} subject on dose z_j be denoted y_{ij}, hence $y_j = (y_{1j}, \ldots, y_{n_j j})^T$ is the vector of responses on dose z_j and $y = (y_0, \ldots, y_J)^T$ is the vector of responses in the current dataset. For each z_j we generate B bootstrap samples y_j^{*b} $(b = 1, \ldots, B)$, each consisting of n_j samples drawn with replacement from y_j. Then $\hat{\theta}^{*b}$ is the bootstrapped MLE of the unknown model parameters from fitting the dose response model to the data $y^{*b} = (y_0^{*b}, \ldots, y_J^{*b})^T$. Efron & Tibshirani (1993, p. 14) suggests that bootstrap samples of between 50 and 200 usually result in a good standard error estimator.

At the interim analysis we want to assess how robust the optimal design for the next cohort of subjects is to parameter mis-specification. To do this we compare the efficiency of the optimal design ξ^* found using $\hat{\theta}$ versus the equal allocation design ξ^{eq}, for each of the bootstrap samples $\hat{\theta}^{*b}$. For each $\hat{\theta}^{*b}$ $(b = 1, \ldots, B)$ the relative efficiency of a design with p unknown model parameters is calculated as

$$\text{Eff}^{*b} = \left(\frac{|M(\xi^*, \hat{\theta}^{*b})|}{|M(\xi^{\text{eq}}, \hat{\theta}^{*b})|} \right)^{\frac{1}{p}}. \tag{6.13}$$

Efficiencies greater than 1 suggest that for a given $\hat{\theta}^{*b}$ the optimal design is more efficient than the equal design. If some pre-specified proportion (e.g. 80%) of the bootstrapped efficiencies are greater than 1, then there is evidence that the optimal design is robust to parameter mis-specification and should be used to allocate the next cohort of subjects. The higher the proportion of bootstrap samples that have an efficiency greater than 1, then the stronger the evidence of robustness. The quasi-adaptive designs are constructed in the same way as the fully adaptive designs, except at each interim analysis the optimal design is tested for robustness. If the design is found not be robust to parameter mis-specifications then the next cohort is randomised equally across all doses.

Figure 6-1 is an example of a dataset where, at the interim analysis there are data available from 125 subjects allocated equally across the placebo dose and 8 active doses $(z = z_0, \ldots, z_8)$ and 125 subjects still to randomise. A four parameter sigmoid emax model,

$$\eta(z_j, \theta) = \theta_1 + (\theta_2 - \theta_1) \frac{z_j^{\theta_4}}{\theta_3^{\theta_4} + z_j^{\theta_4}},$$

has been used to model the data and 100 bootstrap samples $\hat{\theta}^{*b}$ $(b = 1, \ldots, 100)$ generated. The top left plot shows the observed means and the fitted model using

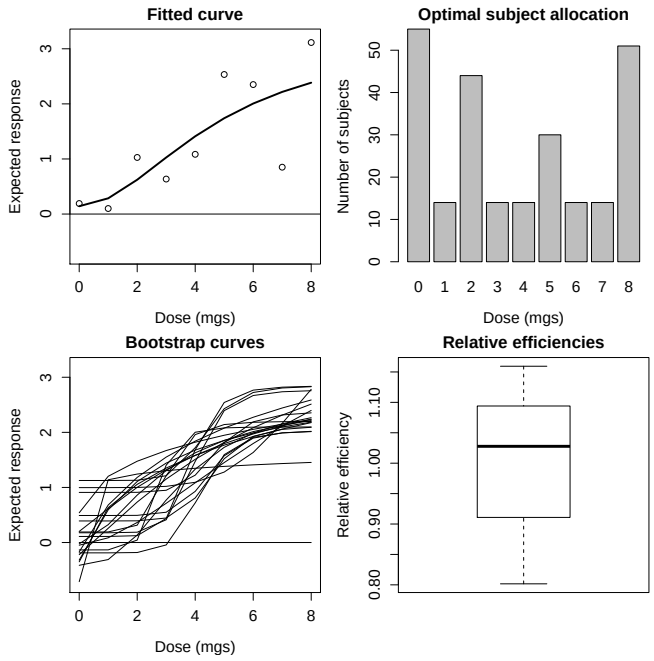

Figure 6-1: Fitted curve using $\hat{\theta}$, locally D-optimal subject allocation, fitted curves from 20 bootstrapped estimators and relative efficiencies of equal allocation versus locally D-optimal design.

the MLE $\hat{\theta}$. The top right plot is the D-optimal design for the 250 subjects, where the first 125 subjects were equally allocated across the doses. The bottom left plot shows 20 dose response curves fitted using the bootstrap estimates and the bottom right plot is a box plot of the efficiencies arising from the bootstrap estimates.

For the example dataset in Figure 6-1, the decision on whether to adapt or not depends on the level of confidence required in the adaptation. We can see the fitted models from bootstrap estimates take a range of shapes, suggesting that there is a fair amount of variability in the parameter estimates. Out of the 100 bootstrap estimates, the design has an efficiency greater than 1 in 52 cases. The mean efficiency was 0.99, suggesting that there is little or nothing to be gained from adapting in this case. We explore later how different criteria for adapting affect the results.

6.3.5 Bayesian D-optimal designs

A limitation of locally optimal designs for non-linear models is that they rely on estimates of the unknown model parameters. An alternative approach to this is to use Bayesian optimal design, where priors are placed on the model parameters. The

Bayesian optimal design takes into account the variability in the prior and so is optimal for the prior distribution rather than a single point estimate.

In Bayesian optimality we aim to maximise the criterion $\Phi\{M(\xi)\}$ which is the expectation of the criterion $\Psi\{M(\xi,\theta)\}$, averaged over the prior distribution for θ which has density $\pi(\theta)$ (Dette & Neugebauer, 1996),

$$\Phi\{M(\xi)\} = E[\Psi\{M(\xi,\theta)\}|Y=y] = \int_\theta \Psi\{M(\xi,\theta)\}\pi(\theta)d\theta.$$

The Bayesian optimality criterion Φ is a concave function. Take two designs ξ' and $\tilde{\xi}$ from the set of possible designs $\mathscr{H}$ and $\alpha \in [0,1]$, then the definition of concavity holds, as

$$\begin{aligned}\Phi\{M((1-\alpha)\xi' + \alpha\tilde{\xi})\} &= E_\theta[\Psi\{M((1-\alpha)\xi' + \alpha\tilde{\xi},\theta)\}] \\ &\geq (1-\alpha)E_\theta[\Psi\{M(\xi',\theta)\}] + \alpha E_\theta[\Psi\{M(\tilde{\xi},\theta)\}] \\ &= (1-\alpha)\Phi\{M(\xi')\} + \alpha\Phi\{M(\tilde{\xi})\}.\end{aligned}$$

Following on from the notation used in Section 6.3.1, the directional derivative of Φ at ξ' in the direction $\tilde{\xi}$ is

$$\begin{aligned}\phi(\xi',\tilde{\xi}) &= \lim_{\alpha\to 0}\frac{1}{\alpha}[\Phi\{(1-\alpha)M(\xi') + \alpha M(\tilde{\xi})\} - \Phi\{M(\xi')\}] \\ &= \lim_{\alpha\to 0}\frac{1}{\alpha}\left[\int \Psi\{(1-\alpha)M(\xi',\theta) + \alpha M(\tilde{\xi},\theta)\} - \Psi\{M(\xi',\theta)\}\pi(\theta)d\theta\right] \\ &= \int \phi_\theta(\xi',\tilde{\xi})\pi(\theta)d\theta.\end{aligned}$$

From (6.9) the directional derivative at ξ' in the direction ξ_j, where ξ_j places unit mass at dose z_j, for a given θ is

$$\phi_\theta(\xi',\xi_j) = \frac{1}{\sigma^2}g(z_j,\theta)^T\frac{d\Psi}{dM}g(z_j,\theta) - trM\frac{d\Psi}{dM}$$

and

$$\phi(\xi',\xi_j) = E[\phi_\theta(\xi',\xi_j)].$$

Following the same approach as local optimality, we maximise the change in Φ at ξ' by increasing the weight at the dose z_j which maximises $\phi(\xi',\xi_j)$.

Chaloner & Larntz (1989) extended the general equivalence theorem (Theorem 6.3.1) to show that the results of the theorem hold for the criterion Φ using the directional

derivative ϕ. There are a number of definitions of Bayesian D-optimality. We examine two criteria listed by Atkinson & Donev (1992, p. 214) which can be used to construct Bayesian D-optimal designs, these are criterion I and IV.

1. Criterion I: $\Phi\{M(\theta)\} = E[\log|M(\xi', \theta)|]$
   For this criterion the directional derivative is written

$$\begin{aligned}\phi(\xi', \xi_j) &= E[\frac{1}{\sigma^2} g(z_j, \theta)^T M^{-1}(\xi', \theta) g(z_j, \theta) - p] \\ &= E[\frac{1}{\sigma^2} g(z_j, \theta)^T M^{-1}(\xi', \theta) g(z_j, \theta)] - p \\ &= E[d(z_j, \xi', \theta)] - p.\end{aligned}$$

   We can maximise the directional derivative by maximising the expectation of the sensitivity function.

2. Criterion IV: $\Phi\{M(\theta)\} = \log E[|M(\xi', \theta)|]$
   For this criterion the directional derivative is written

$$\begin{aligned}\phi(\xi', \xi_j) &= \frac{E[|M(\xi', \theta)|\{\frac{1}{\sigma^2} g(z_j, \theta)^T M^{-1}(\xi', \theta) g(z_j, \theta) - p\}]}{E[|M(\xi', \theta)|]} \\ &= \frac{E[|M(\xi', \theta)| \frac{1}{\sigma^2} g(z_j, \theta)^T M^{-1}(\xi, \theta) g(z_j, \theta)]}{E[|M(\xi', \theta)|]} - p \\ &= \frac{E[|M(\xi', \theta)|\ d(z_j, \xi, \theta)]}{E[|M(\xi', \theta)|]} - p.\end{aligned}$$

   We can maximise the directional derivative by maximising the weighted expectation of the sensitivity function.

Bayesian optimal designs can be constructed using the same iterative algorithms as the locally optimal designs. The expectation of the sensitivity function and the weighted expectation of the sensitivity function cannot be found analytically and so we calculate them using a sample average. Let us generate T samples from the prior distribution with density $\pi(\theta)$, we denote these samples θ^t $(t = 1, \ldots, T)$. We estimate the expected sensitivity function as

$$d(z_j, \xi') = E[d(z_j, \xi', \theta)] \approx \frac{1}{T} \sum_{t=1}^{T} d(z_j, \xi', \theta^t)$$

and the expected weighted sensitivity function as

$$w(z_j, \xi') = \frac{E[|M(\xi', \theta)|\ d(z_j, \xi', \theta)]}{E[|M(\xi', \theta)|]} \approx \frac{\sum_{t=1}^{T} |M(\xi', \theta^t)| d(z_j, \xi', \theta^t)}{\sum_{t=1}^{T} |M(\xi', \theta^t)|}.$$

For the continuous design we use the Federov algorithm described in Section 6.3.1. For the two criteria the optimal dose where the algorithm places weight at the k^{th} iteration is

$$\text{for Criterion I: } z^{k-1} = \underset{z\in\{z_0,\ldots,z_J\}}{\text{argmax}}\ d(z,\xi')$$

$$\text{for Criterion IV: } z^{k-1} = \underset{z\in\{z_0,\ldots,z_J\}}{\text{argmax}}\ w(z,\xi').$$

For the exact optimal design with N subjects the optimal dose for the next subject using the forward selection algorithm is

$$\text{for Criterion I: } z_j = \underset{z\in\{z_0,\ldots,z_J\}}{\text{argmax}}\ d(z,\xi')$$

$$\text{for Criterion IV: } z_j = \underset{z\in\{z_0,\ldots,z_J\}}{\text{argmax}}\ w(z,\xi').$$

As with the locally optimal designs, it is also possible to use the Bayesian optimal designs in an adaptive manner. Rather than using the MLEs to find the optimal design at the interim analysis, the adaptive Bayesian optimal designs use the posterior distribution for $\theta|y$ to find the design that maximises the criterion,

$$\Phi\{M(\xi)\} = E[\Psi\{M(\xi,\theta)\}|Y=y] = \int \Psi\{M(\xi,\theta)\}\pi(\theta|y)d\theta.$$

6.4 Model specification

In this section we explore how robust the locally D-optimal designs are to model mis-specifications, and how robust the Bayesian D-optimal designs are to mis-specifications of the prior distribution placed on the model parameters θ.

6.4.1 Locally D-optimal designs

In local optimal design theory, the choice of model and the number of unknown parameters dictates the number of doses allocated to and the number of subjects on each dose. Figure 6-2 presents the continuous locally D-optimal designs for the dose response profiles listed in Section 2.3, using the true values of θ. The continuous D-optimal designs were constructed using the algorithm suggested by Fedorov (1972), as detailed in Section 6.3.1. For linear models the locally D-optimal design generally allocates to the same number of doses as there are model parameters. There is no such bound for non-linear models.

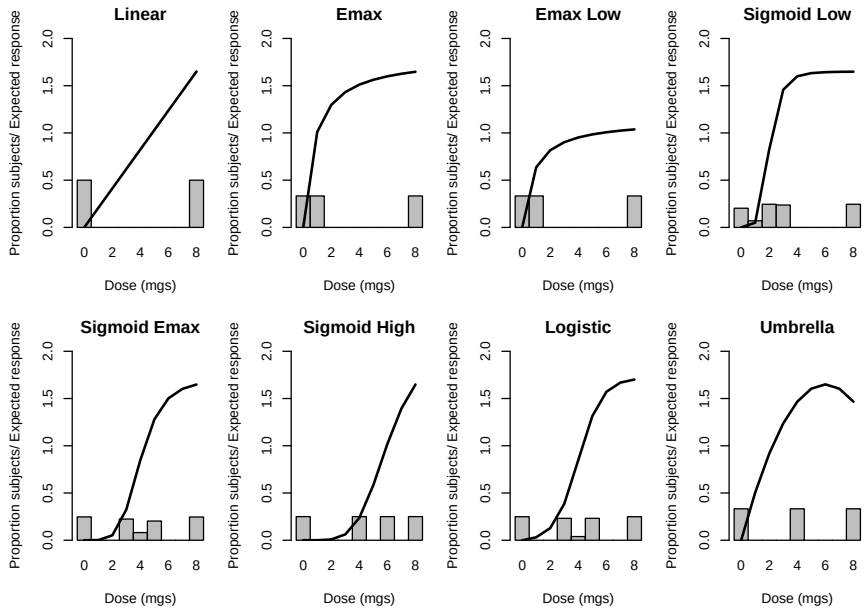

Figure 6-2: Continuous locally D-optimal designs for the true dose response profiles.

In practice, when designing a clinical trial we do not know the true shape of the dose response profile and so we are interested in fitting a model that is relatively robust to model mis-specification. That is, even if we choose the wrong model, it is flexible enough to perform adequately for all the dose response profiles we are interested in. Ideally, we want our chosen model to perform well in terms of model estimation and also to produce a D-optimal design which is relatively efficient in comparison to the continuous D-optimal design, when the correct model and model parameters are known.

We identify three candidate models which we use to model the data and find the D-optimal design;

- a quadratic model:
$$\eta(z_j, \theta) = \theta_1 + \theta_2 z_j + \theta_3 z_j^2$$
- a three parameter emax model:
$$\eta(z_j, \theta) = \theta_1 + (\theta_2 - \theta_1)\frac{z_j}{\theta_3 + z_j}$$

- a four parameter sigmoid emax model:

$$\eta(z_j, \theta) = \theta_1 + (\theta_2 - \theta_1)\frac{z_j^{\theta_4}}{\theta_3^{\theta_4} + z_j^{\theta_4}}.$$

When fitting the candidate models to the dose response profiles, we find $\hat{\theta}$ which minimises the sums of squares, and use $\hat{\theta}$ to find the D-optimal designs. The D-optimal designs found using the quadratic, emax and sigmoid emax models are denoted ξ^m $(m = 1, 2, 3)$ respectively. The continuous optimum D-optimal design for the true dose response profile with θ known is denoted ξ^*. Let ξ^{eq} denote the equal allocation design, where subjects are allocated equally across all of the doses.

To explore which of the candidate models is the most robust under a variety of dose response curves, we compare the relative efficiency of ξ^m versus the optimal continuous design for each of the dose response profiles specified in Section 2.3. The Flat and Explicit profiles are not included, as neither relate to a parametric model. The relative efficiency is the inflation in sample size needed to have the same information as the optimal continuous design. The relative efficiency of the D-optimal design found using candidate model m when the true dose response model has p parameters, is

$$\text{Eff}_m = \left(\frac{|M(\xi^*, \theta)|}{|M(\xi^m, \theta)|}\right)^{\frac{1}{p}}, \tag{6.14}$$

where θ are the true parameter values from the dose response profile. The efficiency of the equal allocation design, ξ^{eq}, relative to the optimal continuous design, ξ^*, is calculated as

$$\text{Eff}_{\text{eq}} = \left(\frac{|M(\xi^*, \theta)|}{|M(\xi^{\text{eq}}, \theta)|}\right)^{\frac{1}{p}}. \tag{6.15}$$

Figure 6-3 shows the optimal designs derived from the candidate models for a selection of the true dose response profiles, along with the model fitted by each of the candidate models. As the quadratic model is linear in θ, it constructs the same optimal design regardless of the dose response profile.

The relative efficiencies of the D-optimal designs for the candidate models compared with the optimal designs, ξ^*, for the different dose response profiles are presented in Table 6.2. When the dose response profile and the candidate model take the same form, then $\xi^m = \xi^*$ and $\text{Eff}_m = 1$. If the candidate model is not from the same family of models as the dose response profile, then the optimal design derived from the candidate

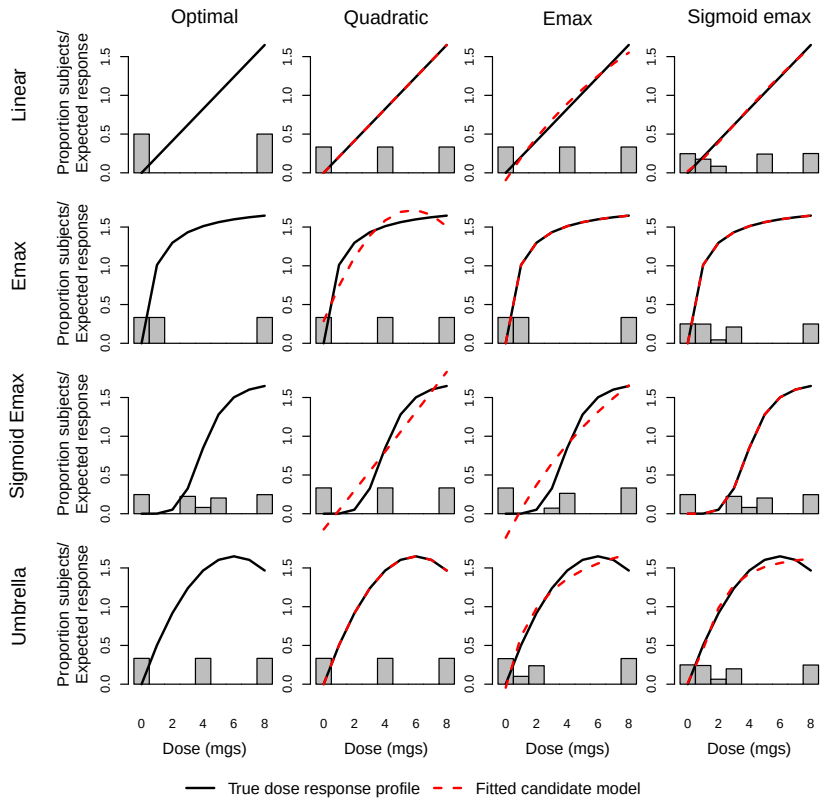

Figure 6-3: Continuous locally D-optimal designs for the true dose response profiles and for the fitted dose response curves from the candidate models.

model is unlikely to be as efficient as if we had known the true dose response profile. When fitting the quadratic and emax candidate models, some cells in the table have been left blank as the information matrix for the four parameter model cannot be calculated with only three support points.

As expected, the optimal design is always more efficient that using a equal allocation design. When there are fewer parameters in the dose response profile, the D-optimal design allocates to fewer doses and so there is more to gained over the equal allocation design. From Table 6.2 we conclude that for the dose response profiles we are interested in, the sigmoid emax model is flexible enough to produce reasonable fit. The D-optimal designs from this model are also relatively efficient compared to the optimal designs from the true dose response profiles.

In Sections 6.6, 6.7 and 6.8 we explore the impact of using adaptive, quasi-adaptive D-optimal and Bayesian D-optimal designs on the operational characteristics for each

Dose Response Profile	Eff_1	Eff_2	Eff_3	Eff_{eq}
Linear	1.23	1.23	1.27	1.55
Emax	2.14	1.00	1.14	1.56
Emax Low	2.14	1.00	1.14	1.56
Sigmoid Emax Low			1.00	1.28
Sigmoid Emax		1.29	1.00	1.16
Sigmoid Emax High			1.00	1.18
Logistic		1.34	1.00	1.17
Umbrella	1.00	1.28	1.23	1.38

Table 6.2: Relative efficiencies of the D-optimal designs for different candidate models compared with the D-optimal design for the true dose response model, ξ^*.

of the dose response profiles. For the reasons above, we model the data in these sections using the four parameter sigmoid emax model.

6.4.2 Bayesian D-optimal designs

For Bayesian D-optimal designs we average the optimality criterion for the locally optimal design over the prior distribution for the model parameters θ. We assume that the dose response curve is a four parameter sigmoid emax model,

$$\eta(z_j, \theta) = \theta_1 + (\theta_2 - \theta_1)\frac{z_j^{\theta_4}}{\theta_3^{\theta_4} + z_j^{\theta_4}},$$

and define 3 sets of prior distributions for the four unknown parameters. In Section 2 we list the densities of the distributions placed on the model parameters.

	θ_1	θ_2	θ_3	θ_4
Prior 1	$N(0,\ 1)$	$N(2,\ 1)$	$G(4,\ 4)$	$G(4,\ 4)$
Prior 2	$N(0,\ 4)$	$N(2,\ 9)$	$G(1,\ 0.25)$	$G(1,\ 0.5)$
Prior 3	$N(0,\ 25)$	$N(2,\ 25)$	$G(2,\ 0.25)$	$G(1,\ 0.25)$

In Section 6.3.5 we mention that we use two criteria for constructing the Bayesian D-optimal designs, these criteria are as listed in (Atkinson & Donev, 1992, p. 214) , and are

- Criterion I: $\Phi\{M(\theta)\} = E[\log|M(\xi, \theta)|]$
- Criterion IV: $\Phi\{M(\theta)\} = \log E[|M(\xi, \theta)|]$.

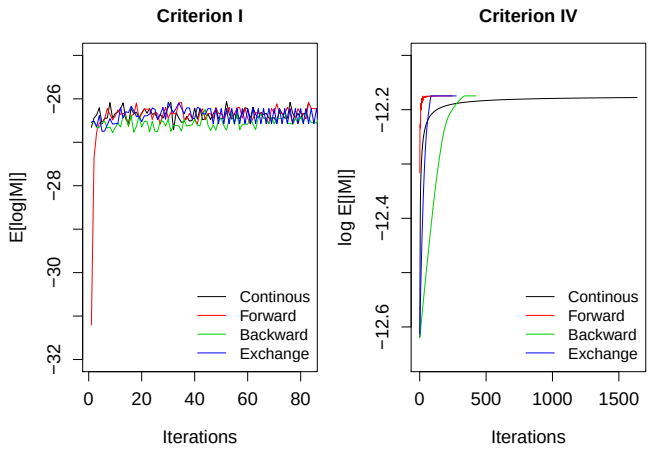

Figure 6-4: Convergence of Bayesian optimality criteria.

The Bayesian D-optimal continuous designs are constructed using the algorithm proposed by Fedorov (1972) described in Section 6.3.1 and the exact designs using the sequential algorithms described in Section 6.3.2. To find the Bayesian optimal continuous designs, 1000 samples are generated from the prior distributions for θ, these samples are denoted θ^t $(t = 1, \ldots, T)$. The optimal design is then found by maximising Φ. For the exact design found using the sequential algorithms we find the ξ_N^* design where N=250. For the forward algorithm the initial design has one subject on the placebo dose and the maximum dose, for the backwards algorithm we begin with 75 subjects on each of the 9 doses.

For criterion I, it was found that as the prior distributions became more vague the process failed to converge to the maximum of Φ. Figure 6-4 shows value of the criterion we are aiming to maximise for the continuous iterative and the sequential algorithms. Investigation into the cause of the non-convergence revealed that for some θ^t, $M(\xi, \theta^t)$ was computationally singular. Criterion IV still manages convergence as it weights the sensitivity function by $|M(\xi, \theta^t)|$ and so the samples where $M(\xi, \theta^t)$ is singular are given a weight of 0 in the computation.

As we can not ensure the convergence of criterion I, from now on we only consider Bayesian D-optimal designs constructed using criterion IV. The optimal designs for criterion IV for the three sets of prior distributions are given in Figure 6-5. The designs constructed using criterion IV for the set of prior distributions 1, 2, and 3 are denoted ξ^{p1}, ξ^{p2} and ξ^{p3} respectively. From Figure 6-5 we can see that as the prior distributions become more vague, the number of support points increases. This is in agreement with

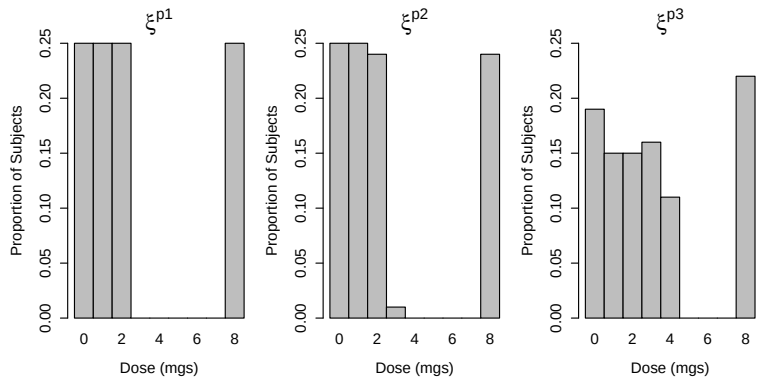

Figure 6-5: Subject allocations for Bayesian D-optimal designs using criterion IV.

results reported by Chaloner & Larntz (1989). Although, even with relatively vague prior distributions placed on the model parameters, the subject allocation is focused on the lower doses.

The prior distributions placed on the parameters in Priors 1 have small variances and are centred around the true parameter values for the Emax profile. This results in a Bayesian optimal design which is similar to the locally optimal design when a sigmoid emax model is fitted to the data. In contrast when the true dose response profile is Sigmoid Emax then the support points from ξ^{p1} do not cover the same doses as the locally optimal design. Therefore we would not expect the design ξ^{p1} to be particularly efficient for all dose response profiles.

We compare the efficiencies of the Bayesian D-optimal designs with the locally optimal designs ξ^*, when we know the true dose response profile and model parameters. The efficiency of the Bayesian designs relative to the locally optimal design is calculated for $s \in \{p1, p2, p3\}$ as

$$\text{Eff}_s = \left(\frac{|M(\xi^*, \theta)|}{|M(\xi^s, \theta)|} \right)^{\frac{1}{p}}.$$

Table 6.3 shows the efficiencies of the Bayesian designs for the different prior distributions. For completeness, we have also included in the table the efficiency of the fitted locally optimal design when a sigmoid emax model is used to model the data Eff_3 (6.14) and the equal allocation design Eff_{eq} (6.15).

Given we are assuming we know the best estimates of $\hat{\theta}$ for the fitted locally optimal designs, it is not surprising that these have the smallest relative efficiencies (i.e. the

Dose Response Model	Eff_3	Eff_{p1}	Eff_{p2}	Eff_{p3}	Eff_{eq}
Linear	1.27	1.29	1.29	1.40	1.55
Emax	1.14	1.13	1.13	1.29	1.56
Emax Low	1.14	1.13	1.13	1.29	1.56
Sigmoid Emax Low	1.00	1.41	1.35	1.09	1.28
Sigmoid Emax	1.00	4.44	3.45	1.29	1.16
Sigmoid Emax High	1.00	7.03	5.18	2.36	1.18
Logistic	1.00	3.70	3.01	1.36	1.17
Umbrella	1.23	1.39	1.38	1.20	1.38

Table 6.3: Efficiencies of the Bayesian D-optimal designs versus the locally optimal designs for different prior distributions.

Data Generated From	Eff_{p1}	Eff_{p2}	Eff_{p3}	Eff_{eq}
Priors 1	1.00	1.01	1.11	1.36
Priors 2	1.01	1.00	1.10	1.31
Priors 3	1.16	1.14	1.00	1.13

Table 6.4: Efficiencies of the Bayesian D-optimal designs for different prior distributions.

smallest inflation of sample size is needed to have the same information as the optimal design). We can see from Table 6.3 that using Priors 1 and 2 results in efficient designs for some models, whilst producing an inefficient design for others. As the prior distributions become more vague the Bayesian D-optimal design becomes more dispersed and the relative efficiency tends towards that of using the equal allocation design. Using Priors 3 produces a design which is a compromise between using the locally optimal design and the equal allocation.

Finally we look at the efficiencies of the Bayesian D-optimal designs taking into account the variance of the parameters. Let the densities for Priors 1, 2 and 3 be denoted $\pi_{p1}(\theta)$, $\pi_{p2}(\theta)$ and $\pi_{p3}(\theta)$ respectively. Let $s' \in \{p1, p2, p3\}$ and $s \in \{p1, p2, p3, \text{eq}\}$. We generate T samples of θ from the prior distributions with density $\pi_{s'}(\theta)$, denoted θ^t $(t = 1, \ldots, T)$. The expected efficiencies are calculated as follows,

$$\text{Eff}_s = \left(\frac{\int |M(\xi^{s'}, \theta)| \pi_{s'}(\theta) d\theta}{\int |M(\xi^{s}, \theta)| \pi_{s'}(\theta) d\theta} \right)^{\frac{1}{p}} \approx \left(\frac{\sum_{t=1}^{T} |M(\xi^{s'}, \theta^t)|}{\sum_{t=1}^{T} |M(\xi^{s}, \theta^t)|} \right)^{\frac{1}{p}}.$$

As we can see in Figure 6-5 the subject allocations from ξ^{p1} and ξ^{p2} are very similar, and so these two models have similar efficiencies (Table 6.4). When data are generated from the distributions for Priors 1 or 2, ξ^{p3} offers a compromise between the designs generated from the correct prior distributions and using an equal allocation design.

When Prior 3 is used generate the data, then the equal allocation is slightly more efficient than ξ^{p1} and π^{p2}, suggesting that when our prior beliefs are vague there is not so much to be lost from using a conservative design.

In Section 6.8 we see what impact the choice of prior distributions has on the operational characteristics for each of the dose response profiles.

6.5 Convergence problems in maximum likelihood estimation

The ultimate aim of using an optimal design is to be able to fit a chosen model to the data and make inferences about the dose response curve. In order to fit the model to the data, we must be able to estimate the unknown model parameters. Generally for non-linear models within a frequentist framework, we estimate the model parameters using the maximum likelihood estimators (MLEs) denoted $\hat{\theta}$. The MLE can rarely be found analytically and so we use an iterative process to find $\hat{\theta}$ (Seber & Wild, 2003, p. 91). Problems with the model fitting arise when the iterative process fails to converge. Non-convergence can occur when there are multiple parameters that need to be estimated and a lack of information in the data to estimate all the parameters (Kirby et al., 2011). In the clinical setting this is true when the doses are not high enough to provide data on the maximum response, and so within the observed range of doses there is insufficient information on the location of the asymptote.

Although there are ad-hoc methods for dealing with non-convergence, we focus on two methods that offer a practical solution to non-convergence. These methods can be specified in advance, eliminating any potential biases that can come from ad-hoc analyses. These methods are:

- Step down: If the parameters for the chosen model do not converge, a simplified model with fewer parameters is fitted. The number of parameters in the model is reduced until convergence is reached. Different approaches to model selection for the step down procedures has been explored by Kirby et al. (2011).
- Constrained convergence: A box is placed around the parameter values such that the parameters are constrained to converge within the bounds of the box. Dragalin et al. (2007) uses such a box to constrain the parameters to be $\pm 80\%$ of the true values used to generate the dose response curves in simulation studies.

These solutions to non-convergence come with their own limitations. The step down method seems the most applicable from a frequentist point of view as it always produces a model for which the MLEs converge. However the biological plausibility of fitting a linear model when the belief is that the dose response curve is sigmoid emax could bring the fitted model into question. By restricting the parameter estimates using constrained convergence, we may bias the MLEs. This is a problem if the constrained MLEs influence the dose response curve and so the inferences made.

We explore through simulation, the impact of these different approaches on the properties of the fitted dose response curves. In the simulation study, we aim to fit the four parameter sigmoid emax model to the data. The four parameter sigmoid emax model is written

$$\eta(z_j, \theta) = \theta_1 + (\theta_2 - \theta_1)\frac{z_j^{\theta_4}}{\theta_3^{\theta_4} + z_j^{\theta_4}}. \tag{6.16}$$

For this model, non-convergence arises when there is little information about the upper asymptote, making θ_2 and θ_3 hard to estimate. We use the following methods to deal with non-convergence of the model parameters.

1. Step down

   - If the algorithm used to find the parameter estimates for the sigmoid emax model given in (6.16) fail to converge, we set $\theta_4 = 1$ and reduce the model to a three parameter emax model,

   $$\eta(z_j, \theta) = \theta_1 + (\theta_2 - \theta_1)\frac{z_j}{\theta_3 + z_j}.$$

   - If the algorithm used to find the parameter estimates for the emax model fail to converge we reduce the model to a linear model with two parameters,

   $$\eta(z_j, \theta) = \theta_1 + (\theta_2 - \theta_1)z_j.$$

2. Constrained convergence
   We fit the sigmoid emax model (6.16) and define three boxes within which the model parameters, $\theta = (\theta_1, \ldots, \theta_4)^T$ are forced to converge.

	Lower bounds	Upper bounds
Box 1	(−1,0,0.01,0.01)	(1,2,2,2)
Box 2	(−2,−1,0.01,0.01)	(2,5,16,8)
Box 3	(−10,−10,0.01,0.01)	(10,10,32,16)

These boxes represent over constraining (Box 1), such that for some of the dose response profiles the true θ lies outside the range of the box; informative constraining (Box 2), based on biological plausibility about range of the parameter values; and vague constraining (Box 3), where the bounds of the box are large compared to the assumptions about the parameter values. It should be noted, that if the box is too large, situations may arise where the model fails to converge within the box.

According to large sample asymptotic theory, when the true dose response is from the same family as the fitted model, the probability of convergence increases as the sample size increases, and so in our simulation study we explore three sample sizes: N=100, 250 and 500. We use a placebo dose (0mgs) and 8 active doses (1mg, ..., 8mgs), with subjects randomised equally across these doses. Data are generated from three of the dose response profiles introduced in Section 2.3:

1. Linear: $\nu_j = \frac{1.65}{8} z_j$
2. Emax: $\nu_j = 1.81 \frac{z}{0.79+z_j}$
3. Sigmoid Emax: $\nu_j = 1.70 \frac{z_j^5}{4^5+z_j^5}$.

The response distribution of the i^{th} subject on dose z_j is

$$Y_{ij} \sim N(v_j, \sigma^2)$$

and $\sigma^2 = 4.5$. For the simulation study 1000 datasets were generated using the three sample sizes, for each of the dose response profiles. For each dataset we attempted to fit a model to the data using the two methods described for dealing with non-convergence. To find the MLE the package nlminb was used in R (Team, 2008), with the initial values for the optimisation set at (0,1,1,1). The maximum number of iterations and evaluations allowed was set to 1000, in order to increase our chances of convergence.

We compare the fitted dose response curves of the three approaches in terms of:

- The mean coverage of the 95% confidence intervals. The 95% confidence interval at a dose z_j for the fitted curve with MLE estimates $\hat{\theta}$ is constructed as

$$\eta(z_j, \hat{\theta}) \pm 1.96 \sqrt{\text{var}(\eta(z_j, \hat{\theta}))},$$

Dose response profile	N=100	N=250	N=500
Linear	28.2	32.4	37.0
Emax	23.5	30.5	29.8
Sigmoid Emax	18.31	10.2	3.5

Table 6.5: Percentage of simulations where the iterative algorithm failed to converge to the MLE when attempting to fit a sigmoid emax model.

where $\text{var}(\eta(z_j, \hat{\theta}))$ is calculated using the delta method. The coverage at a single dose is defined as the percentage of times the 95% confidence intervals for the fitted models contain the true dose response, ν_j. We then average the coverage across the range of available doses to get the mean coverage. The minimum coverage at a single dose is also presented.

- The mean absolute bias in the fitted model. The mean absolute bias is calculated as
$$\frac{1}{J+1}\sum_{j=0}^{J}|E_Y[\eta(z_j, \hat{\theta}) - \nu_j]|,$$
where $\eta(z_j, \hat{\theta})$ is the fitted model and ν_j is the true dose response profiles. The maximum absolute bias at a single dose is also presented.

- The bias in the parameter estimates. As the step down method fits different models with differing numbers of parameters, exploring the bias in the parameter estimates is not easily done. Therefore, we only calculate the bias in the parameter estimates for the constrained convergence, when the dose response profile is Emax (with $\theta_4 = 1$) and Sigmoid Emax, as for these models the number of parameters is the same as for the fitted model. We calculate the bias in the model parameters as
$$E_Y[\hat{\theta}] - \theta.$$

Table 6.5 gives the percentage of simulated datasets where the iterative algorithm failed to converge when we fit a sigmoid emax model. As expected, increasing N when the dose response profile is Sigmoid Emax and we are fitting a sigmoid emax model increases the frequency of convergence. When the dose response profile is Linear, as N increases we have more information that the correct model is not sigmoid emax and so the MLEs converge less often.

Applying the step down method, Table 6.6 gives the percentage of simulated datasets when each of the different models were fitted when N=250. As we attempt to fit

	Fitted model		
Dose response profile	linear	emax	sigmoid emax
Linear	17.0	15.4	67.6
Emax	1.0	29.5	69.5
Sigmoid Emax	5.1	5.1	89.8

Table 6.6: Percentage of simulations where each candidate model was fitted to the data for the step down method, N=250.

Method		Dose response profile		
		Linear	Emax	Sigmoid Emax
Stepdown		91.0 (87.4)	95.2 (92.1)	93.0 (87.2)
Constrained convergence	Box 1	92.6 (80.1)	98.5 (95.8)	78.0 (30.3)
	Box 2	93.1 (88.2)	96.1 (92.8)	95.2 (92.1)
	Box 3	92.2 (86.8)	95.9 (92.4)	94.2 (90.3)

Table 6.7: Mean (minimum) percentage coverage of 95% confidence intervals for the fitted dose response when applying the step down and contrained convergence approaches, N=250.

the sigmoid emax model first, this model is fitted most often. As N increases, the percentage of simulations fitting the model with the same form as the dose response profile increases.

The mean and minimum percentage coverage of the 95% confidence intervals for the different methods, when N=250 are presented in Table 6.7. The coverage of the constrained convergence when using Boxes 2 and 3, are generally closer to the target 95% across the different models than when using the step down approach. When using Box 1, the coverage for the Sigmoid Emax profile is very poor. This is because the true parameter values for the Sigmoid Emax profile are not contained within Box 1, hence the model is forced to fit curves that often do not agree with the data. The mean model fits for the different methods are illustrated in Figure 6-6. Increasing N the results are similar to those in Table 6.7. When N=500, the variance in the model fit is lower and so when we use Box 1 to force convergence of the model parameters and the true dose response profile is Sigmoid Emax, the minimum coverage decreases to 2.4%.

The mean absolute biases when N=250 are presented in Table 6.8. Again Boxes 2 and 3 perform well in terms of the bias compared to the step down approach. As with the coverage, applying Box 1 results in a poor model fits for the Linear and Sigmoid Emax profiles, and so there is large biases in the fitted model. As N increases, the parameter

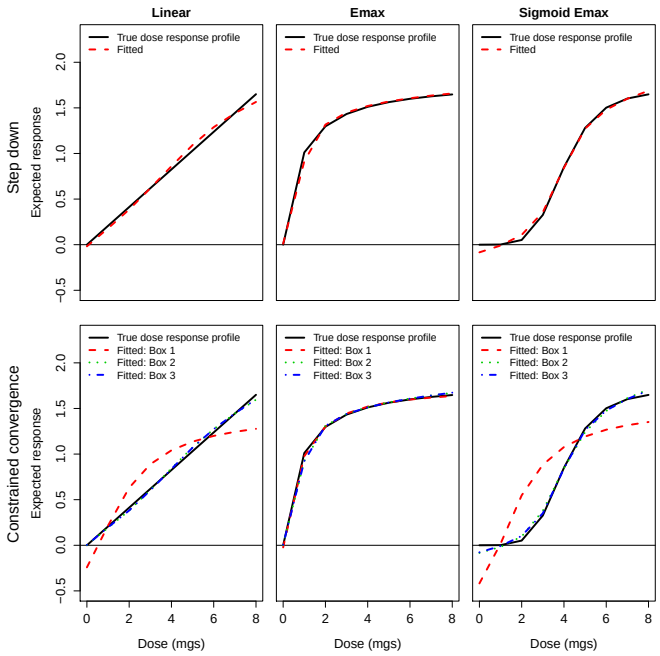

Figure 6-6: Mean fitted dose response curve for the step down and constrained approaches, N=250.

estimates tend towards their true values and so the bias decreases.

The bias in the parameter estimates from using constrained convergence, when the data are generated from the Emax and Sigmoid Emax profiles are presented in Table 6.9. As the bounds for Box 1 are relatively tight around the true parameter values for the Emax profile, the bias in the parameters is small. Increasing the bounds of the box used to constrain the convergence of the parameters, results in an increased bias provided the true parameter values are contained within the box. This is because if the iterative process fails to converge within the box, it is forced to converge at the edge of the box, and so results in a $\hat{\theta}$ which is far from θ. As the bounds of the box

Method		Dose response profile		
		Linear	Emax	Sigmoid Emax
Stepdown		0.03 (0.09)	0.02 (0.10)	0.03 (0.08)
Constrained convergence	Box 1	0.19 (0.37)	0.01 (0.03)	0.29 (0.56)
	Box 2	0.02 (0.05)	0.02 (0.09)	0.04 (0.08)
	Box 3	0.02 (0.05)	0.02 (0.09)	0.03 (0.08)

Table 6.8: Mean (maximum) absolute bias in the fitted dose response when applying the step down and constrained convergence approaches, N=250.

Dose response profile		Model parameters			
		θ_1	θ_2	θ_3	θ_4
Emax	Box 1	−0.02	−0.02	0.18	0.44
	Box 2	0.00	0.69	5.03	2.04
	Box 3	0.01	0.97	10.18	3.80
Sigmoid Emax	Box 1	−0.42	−0.19	−2.01	−3.18
	Box 2	−0.08	0.62	1.21	0.37
	Box 3	−0.08	1.17	2.89	2.84

Table 6.9: Mean bias in the model parameters for the constrained convergence approach, N=250.

become larger the iterative process can converge at larger values of $\hat{\theta}$ (Figures 6-7 and 6-8). If the box is not large enough and does not contain the true parameter values, as in the case of Box 1 and the Sigmoid Emax profile, then this also results in a bias in the model parameters.

Based on the results of the coverage and bias, when fitting the four parameter sigmoid emax model within a frequentist setting we apply Box 2 to ensure convergence of the MLEs. Although we acknowledge that using a box does bias the parameter estimates, the results show that provided the box used is large enough to contain the true θ, it does not overly bias the fitted dose response curve within the dose range of interest. This is consistent with the results observed by Dutta et al. (1996), who did not use a box to force convergence but found that even when the parameters are poorly estimated, the model fit was good within the range of the data. We note for all the scenarios we are interested in Box 2 contains the true parameter values. In reality the best we can do is to chose the bounds of the box based on prior reasoning and biological plausibility.

The step down approach performs well in terms of good coverage and small bias, however it may result in fitting models that are not biologically plausible. As we are interested in model fitting in the context of adaptive optimal designs, using the step down approach could result in fitting an over simplified model at an interim analysis which would result in a design which are far from optimal for the true dose response profile. We would also face the decision as to whether we would allow different models to be fitted at the interim and final analysis.

For completeness we note that when the cause of the non-convergence is limited available data, an alternative approach is to incorporate prior information about the model parameters and use a Bayesian analysis (Thomas, 2006).

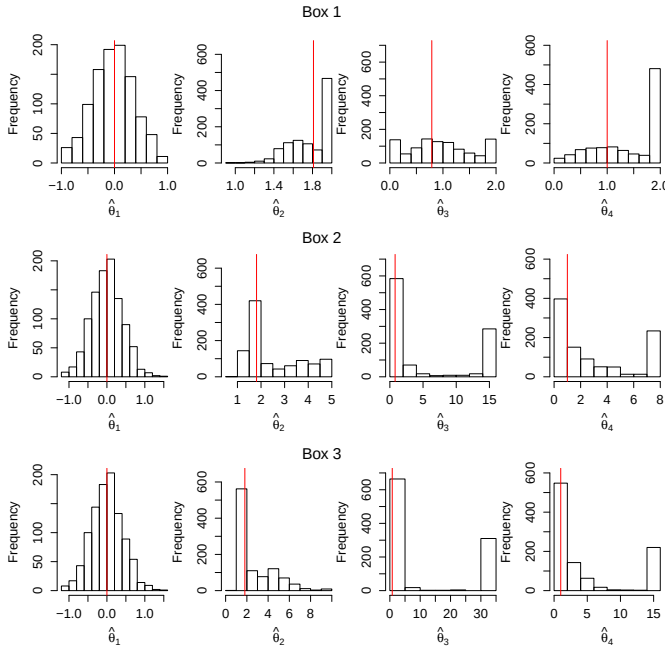

Figure 6-7: Histograms of $\hat{\theta}$ using constrained convergence when data are generated from the Emax profile. True parameter values indicated by the red line.

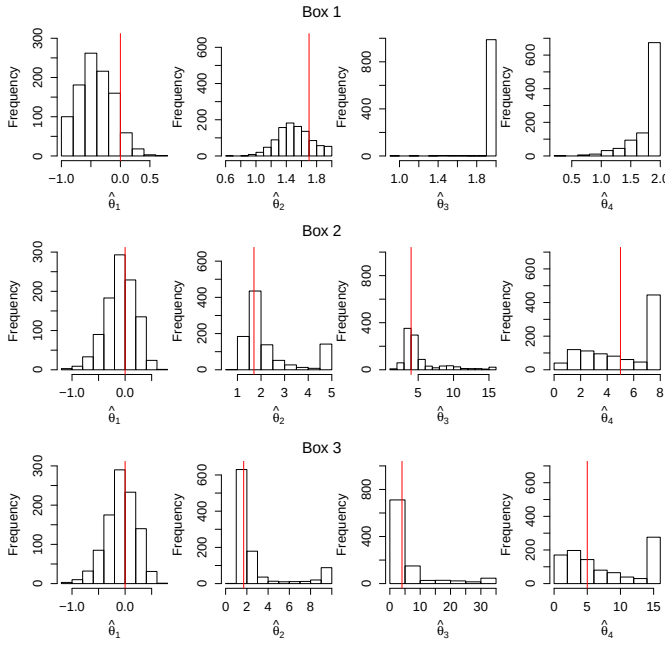

Figure 6-8: Histograms of $\hat{\theta}$ using constrained convergence when data are generated from the Sigmoid Emax profile. True parameter values indicated by the red line.

6.6 Results - adaptive D-optimal designs

To assess how well the adaptive D-optimal design performs, we carry out a simulation study. We use the scenario described in Chapter 2 and generate data from the dose response profiles in Section 2.3. For each of the dose response profiles we generate 10,000 datasets. Each simulated dataset consists of a total of N=250 subjects allocated across the placebo dose and 8 active doses (1mg,...,8mgs). The between subject variance $\sigma^2 = 4.5$ is assumed to be fixed and known. We fit the data using a four parameter sigmoid emax model,

$$\eta(z_j, \theta) = \theta_1 + (\theta_2 - \theta_1)\frac{z_j^{\theta_4}}{\theta_3^{\theta_4} + z_j^{\theta_4}}.$$

As we have shown in Section 6.4, this model is flexible enough to fit all the dose response profile reasonably well. The ANOVA method (Section 2.5) which randomises subjects equally to all doses and uses pairwise testing with placebo, has been included in the results as a control method.

Before the adaptive allocation described in Section 6.3.3 is utilised, we allocate the first cohort of subjects equally across all the doses. At the interim analysis, data from the first cohort are used to estimate $\hat{\theta}$ and the next cohort is allocated in such a way to maximise $\Psi\{M(\xi, \hat{\theta})\}$=log$|M(\xi, \hat{\theta})|$. The exact locally D-optimal design at $\hat{\theta}$ for the next cohort is found using the sequential forward selection algorithm. At each subsequent interim analysis all the available data are incorporated into the updated estimate of $\hat{\theta}$ and the D-optimal design at the updated $\hat{\theta}$ is found. This is continued until all the subjects have been randomised. We use 0 (equal allocation), 1, 2, 3, 4 and 9 interim analyses (IA) where the interim analyses are equally spaced throughout the course of the simulated study. For example, in the case of 2 interim analyses these would occur after 33% and 66% of subjects have completed the trial.

We constrain the parameter estimates to lie within a box. We constrain the upper and lower bounds of the $\theta = (\theta_1, \theta_2, \theta_3, \theta_4)^T$ parameters to be $(2, 5, 16, 8)^T$ and $(-2, -1, 0.01, 0.01)^T$ respectively. The impact of using a box to force convergence was explored in Section 6.5, and the bounds we use here correspond to Box 2 from this section. Constraining the parameter estimates is especially relevant for the adaptive D-optimal designs, as with up to 9 interim analyses we have responses from as few as 25 subjects at the first interim analysis. With such sparse data available to estimate the four parameters of the sigmoid emax model, it is likely that without using a box we would encounter non-convergence.

We use the metrics laid out in Section 2.3 to compare the methods.

Subject allocation

The percentage subject allocations for the adaptive D-optimal allocation are presented in Figure 6-9. From this figure, we can see that there is a fair amount of variability in the subject allocations. There is a substantial change in the subject allocations from using 1 to 2 interim analyses. With more than 2 interim analyses there is little change in the general trend of the subject allocations.

The aim of a D-optimal design is to allocate subjects to doses in such a way as to reduce the variance in the model parameters and not necessarily to allocate subjects to the dose that would be taken through to phase III. The result of this is that for some of the dose response profiles (e.g. the Linear and Sigmoid Emax), only a small proportion of the subjects are allocated to the target doses which are indicated in red Figure 6-9. This could be a potential concern for project teams looking to choose a dose to take forward into phase III.

Detecting dose response

The one-sided type I error rate under the Flat dose response profile is maintained at 5% for the number of interim analyses used in the adaptive D-optimal allocation. For the ANOVA method the one-sided type I error rate was controlled at 5% using a Dunnett adjustment of 2.38.

The left hand plot of Figure 6-10 shows the probability of detecting a dose response for the active dose response curves. For the Emax and Explicit dose response profiles there is an increase in the probability of detecting a dose response when an adaptive D-optimal design is used at the interim, compared with the non-adaptive equal allocation design with 0 interim analyses. For the other dose response profiles there is no room for improvement from using an adaptive design. For all of the dose response profiles, there is a benefit in modelling the data using the sigmoid emax model rather than using the adjusted pairwise testing of the ANOVA method.

The probability of detecting a dose response for the Emax Low profile is 64% for the ANOVA method, 69% when 0 interim analyses are used and approximately 81%

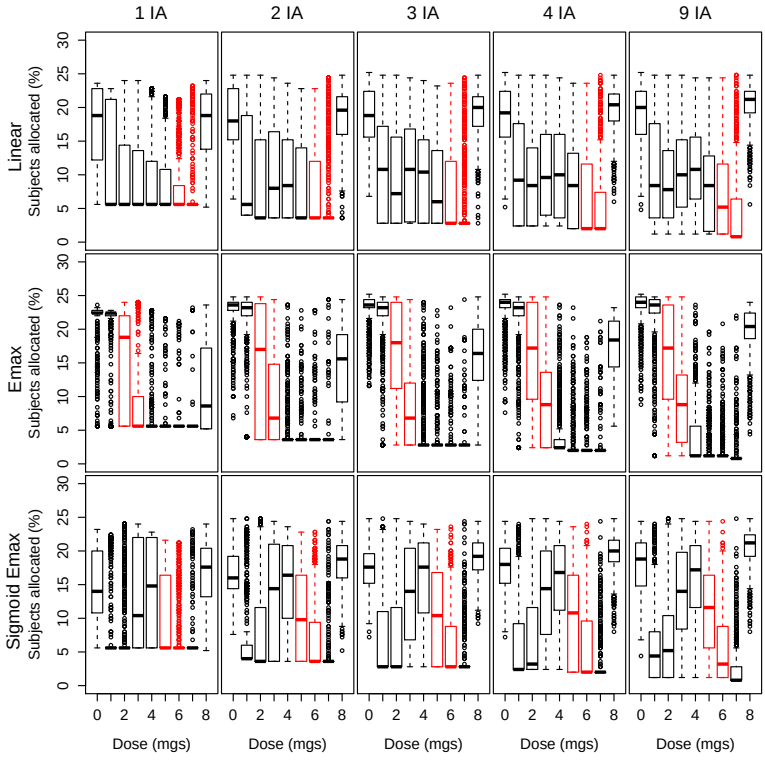

Figure 6-9: Box plots of subject dose allocations for the adaptive D-optimal allocation with increasing numbers of interim analyses (IA). Target dose intervals are given in red.

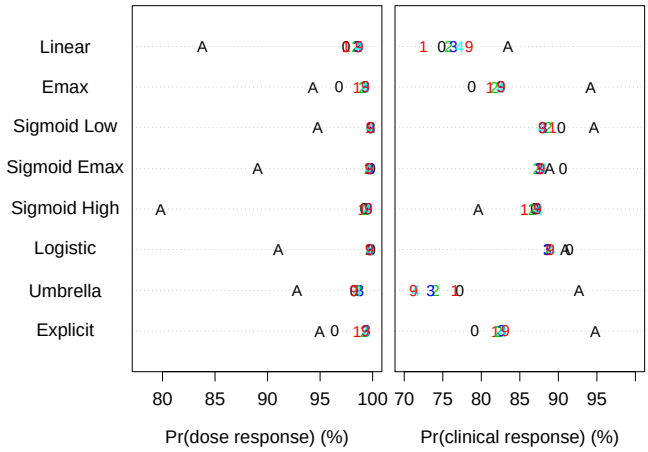

Figure 6-10: Operational characteristics for the adaptive D-optimal allocation and ANOVA methods: probability of detecting a dose response and a clinical response. The number indicates the number of interim analyses, and `A` represents the results from the ANOVA method.

for the adaptive D-optimal methods regardless of the number of interim analyses.

Detecting a clinical response

The right hand plot of Figure 6-10 shows the probability of detecting a clinical response. There is no clear and consistent improvement from using the adaptive D-optimal allocation over the equal allocation with 0 interim analyses. The ANOVA method tends to detect a clinical response more often than when a sigmoid emax model is used to model the data, with the exceptions of when the data comes from the Sigmoid High profiles. The ANOVA method has the greatest improvement over the D-optimal method when there is a plateau in the dose response curve (e.g. the Emax and Explicit profiles). When there is a plateau in the dose response profile there are multiple doses which have a clinical response and so this increases the probability of the ANOVA detecting a clinical response.

Although the ANOVA method tends to be better at detecting a clinical response for the active dose response profiles, it also has a larger probability of incorrectlyf detecting a clinical response for the Emax Low profile, which does not reach the threshold for clinical relevance. The probability of identifying a clinical response for the Emax Low profile was 64% for the ANOVA method, 29% with 0 interim analyses and approximately 24% when the adaptive D-optimal allocation was used.

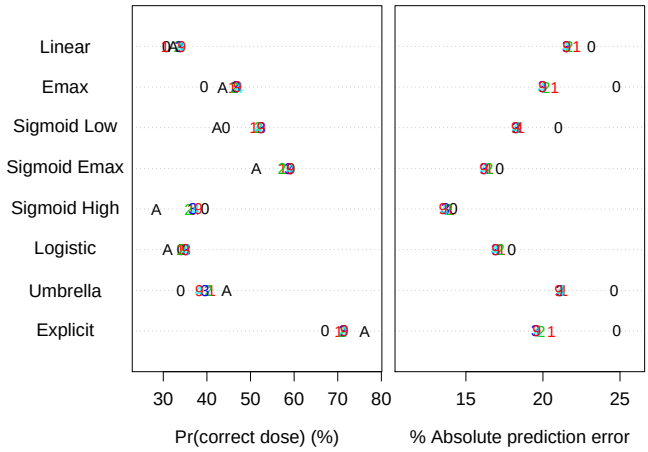

Figure 6-11: Operational characteristics for the adaptive D-optimal allocation and ANOVA methods: probability of selecting a dose in the target interval and the percentage absolute prediction error. The number indicates the number of interim analyses, and `A` represents the results from the ANOVA method.

Correctly selecting a dose in the target dose interval

Figure 6-11 gives the probability of correctly selecting a dose within the target dose interval. When the data come from an Emax, Sigmoid Low, Umbrella and Explicit profile, using an adaptive D-optimal design improves the probability of correctly identifying the target dose over the equal allocation with 0 interims. When one or more interim analyses are used there is little to distinguish between the probability of correctly identifying the target dose. For the remaining models, there is little impact from using an adaptive D-optimal design, and for the Sigmoid High profile the adaptation has had a detrimental effect on the results.

Although the ANOVA method detects a clinical response in a higher proportion of the simulations, modelling the data using the sigmoid emax model generally results in a higher probability of correctly identifying a dose in the target interval. The exceptions to this are the Umbrella and Explicit models, which are both models that the sigmoid emax model struggles to fit.

Prediction error

The D-optimal design is aimed at reducing the variance in the model parameters. Figure 6-11 illustrates that using an adaptive D-optimal design does decrease the prediction error as intended. There is a small decrease in the prediction error from

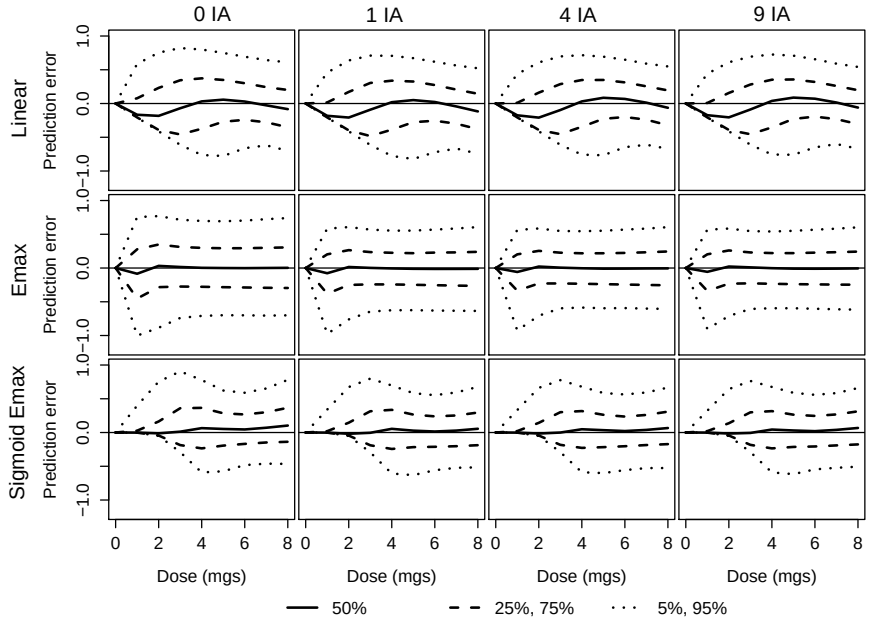

Figure 6-12: Median prediction error and prediction error quantiles for the adaptive D-optimal allocation with increasing numbers of interim analyses.

using 0 to 1 interim analysis, but then there is virtually no change from using more interim analyses.

The prediction error quantiles for the Linear, Emax and Sigmoid Emax dose response profiles for are given in Figure 6-12. The prediction error for the Linear profile reflects the fact that the sigmoid emax model is not the best choice of model for this data. We can see from the prediction error that, as expected, the sigmoid emax model fits the data for the Emax and Sigmoid Emax scenarios well. There is little to distinguish between the plots when one or more interim analyses are used.

Conclusion

Dragalin et al. (2010) carried out a simulation study using an adaptive D then c-optimal design where they also fitted a sigmoid emax model and generated data from a subset of the dose response profiles presented here. The results presented in Dragalin et al. (2010), showed little to no benefit from using an adaptive optimal design, and for some of the dose response profiles studied, the adaptive optimal design was detrimental to the operational characteristics. The results we present here show that for the Emax, Sigmoid Low, Umbrella and Explicit dose response profiles there is a benefit from using

an adaptive D-optimal allocation in terms of correctly selecting a dose in the target dose interval, compared to the equal allocation with 0 interim analyses. Where we observed a benefit from using adaptive D-optimal allocation over the equal allocation, there was little improvement in the operational characteristics from using more than one interim analysis. For the Sigmoid High profile the adaptive D-optimal design resulted in a slight reduction in the ability to correctly identify a dose in the target dose interval. For the remaining dose response profiles, the adaptive D-optimal allocation resulted in similar operational characteristics to the equal allocation. These results are fairly consistent with the relative efficiencies of the equal allocation compared with the locally optimal designs presented in Table 6.2.

In the analysis carried out in the Dragalin et al. (2010) paper, if a dose response was observed, then the model was used to estimate if there was a clinical response and to select a dose for phase III. If a clinically meaningful difference was not detected then a Bonferonni adjusted t-test was used to test if there was a dose with a clinically meaningful difference over placebo. This additional testing increased their chances of detecting a clinical response and so correctly selecting a dose in the target dose interval. When we applied this additional test to our datasets it did not change our conclusions above.

There are two differences between the design by Dragalin et al. (2010) and the design used here. This first is that in the design used by Dragalin et al. (2010), they switched from using a D to a c-optimal design half way through the trial, whereas we use an adaptive D-optimal design. The second difference is that the initial cohort in the Dragalin et al. (2010) paper were randomised to only the placebo dose and the 2, 4, 6, and 8 mg doses, whereas here the initial cohort was randomised equally to all doses. When we applied the additional testing mentioned in the previous paragraph, our results for 1 or more interim analyses were very similar to those presented in Dragalin et al. (2010). However, our results differ from those presented in Dragalin et al. (2010) for the equal allocation case, as we have used a different initial allocations. This difference in initial randomisation has lead to our results showing gains from using D-optimal allocation, whilst Dragalin et al. (2010) saw little improvement from the adaptation. This suggests starting off with a good design can negate the need to adapt. It also shows that if we start with a sub-optimal design then adaptation can be of benefit.

6.7 Results - quasi-adaptive D-optimal designs

In Section 6.6 we observed that there were scenarios where the adaptive D-optimal design improved the operational characteristics and some scenarios where adapting was detrimental. Without knowing the true dose response profile when designing a study, we do not know whether we should adapt or not. The quasi-adaptive method uses the variability in the estimates of model parameters at an interim analyses to evaluate whether adapting is efficient to parameter estimate mis-specifications. See Section 6.3.4 for more details.

We compare the cases when we never adapt (equal allocation) and when we always adapt using a D-optimal design with two versions of the quasi-adaptive method. For the two quasi-adaptive approaches, the second cohort of subjects are randomised using the D-optimal design for $\hat{\theta}$ based on the following criteria

- criterion 1: the 50^{th} percentile of the bootstrapped efficiencies (given in (6.13)) is greater than 1,
- criterion 2: the 80^{th} percentile of the bootstrapped efficiencies is greater than 1.

To test the robustness of the adaptation we generate 100 bootstrap samples. If the relevant criterion is not met, then the second cohort of subjects are allocated equally across all the doses.

As before, we aim to fit a sigmoid emax model (6.16) to the data. For simplicity we assume that there is only one interim analysis. We explore three timings for this interim analysis: after 25%, 50% and 75% subjects have completed the trial. We use the same scenarios as in Section 6.6, but only generate 1000 datasets for the quasi-adaptive approaches, due to the extra computational intensity of assessing the robustness of the adaptation at the interim. For the equal allocation and adaptive D-optimal approach we generate 10000 simulated datasets. The total sample size of each generated dataset is N=250 subjects and a between subject variance of $\sigma^2 = 4.5$.

The metrics used to assess the performance of the methods are those described in Chapter 2.

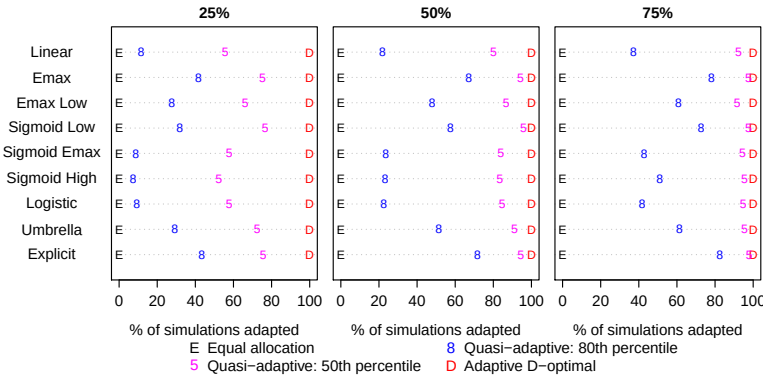

Figure 6-13: Percentage of simulated datasets where adaptation occurred at the interim analysis using the quasi-adaptive D-optimal approach.

Frequency of adaptation

The percentage of simulated datasets where the quasi-adaptive methods chose to adapt are presented in Figure 6-13. As expected, when we have the interim analysis after only 25% of subjects have completed the study, there is more variation in the model parameters and so the quasi-adaptive methods adapts less often than when the interim takes place after 75% of subjects have completed. The method adapts more often for those dose response profiles where we have previously seen benefits from using an adaptive D-optimal design (the Emax, Sigmoid Low, Umbrella and Explicit), as for these profiles there is more to gain from using an adaptive D-optimal design than continuing with the equal allocation.

Subject allocation

As the quasi-adaptive method only adapts when there is evidence the D-optimal design is efficient, the remainder of the simulated datasets receive equal allocation. From Figure 6-13 we can see with the interim analysis after 50% of subjects have completed, using criterion 2 for the Linear profile, adaptation only occurs approximately 25% of the time. The result is that the majority of the simulated datasets receive equal allocation. When we use criterion 1 to adapt, more adaptation takes place and so the subject allocations tend more towards the allocations when we always adapt, this is reflected in in the box plots of the subject allocations in Figure 6-14.

For the Linear and Sigmoid Emax profiles (Figure 6-14), where the target doses are not in the range of doses that the locally D-optimal design would generally allocate

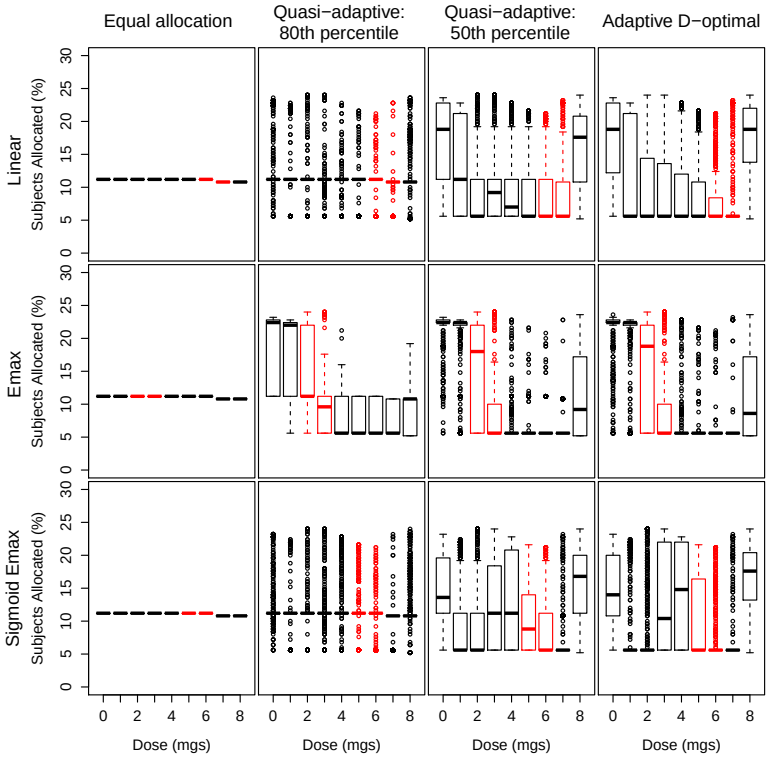

Figure 6-14: Box plot of subject dose allocations for the equal allocation, quasi-adaptive and adaptive D-optimal methods with one interim analysis performed after 50% of the subjects have completed the study. Target dose intervals are given in red.

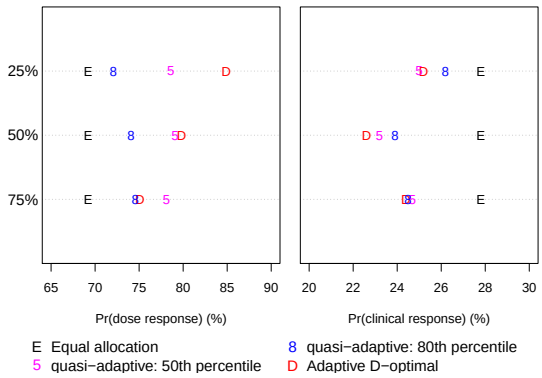

Figure 6-15: Operational characteristics for the Emax Low profile using equal allocation, quasi-adaptive and adaptive D-optimal methods by timing of interim analysis.

to, using the quasi-adaptive approach results in more subjects being allocated to the target doses than when adaptation always takes place. The potential benefit of this is that after the phase II trial, when the data are being examined as part of a bigger development process, there will be more information about the target doses and in particular more safety data.

Detecting dose response

As before, we maintain a one-sided type I error under the Flat dose response profile of 5% for each of the methods applied. For all the active dose response profiles except the Emax Low, the probability of detecting a dose response is near 1, and so there is little to distinguish between the allocation methods and timing of the interim analysis. For the Emax Low model the probability of detecting a dose response (Figure 6-15) is increased when adaptive allocation is used. When the interim analysis is early, there is more benefit from using the adaptive D-optimal allocation.

Detecting a clinical response

Adapting after only 25% of subjects have completed the study, means that although there is more variability in the model parameters, there are also more subjects to allocate. This results in adapting early being more beneficial for some scenarios (e.g. the Explicit profile), but more damaging for other scenarios (e.g. the Umbrella profile).

The quasi-adaptive methods adapt less often when the interim analysis is after 25%

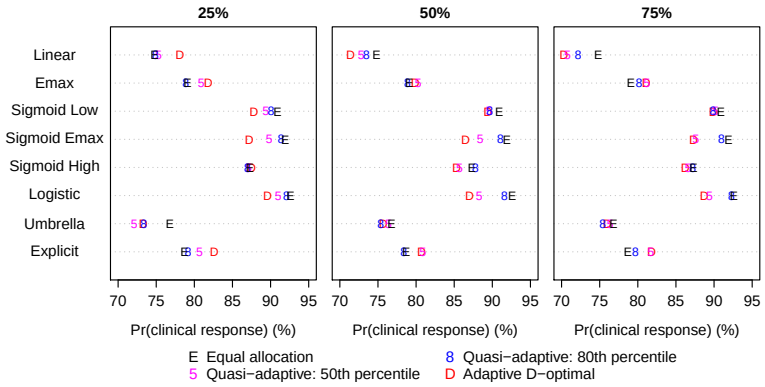

Figure 6-16: Probability of detecting a clinical response using equal allocation, quasi-adaptive and adaptive D-optimal methods by timing of the interim analysis.

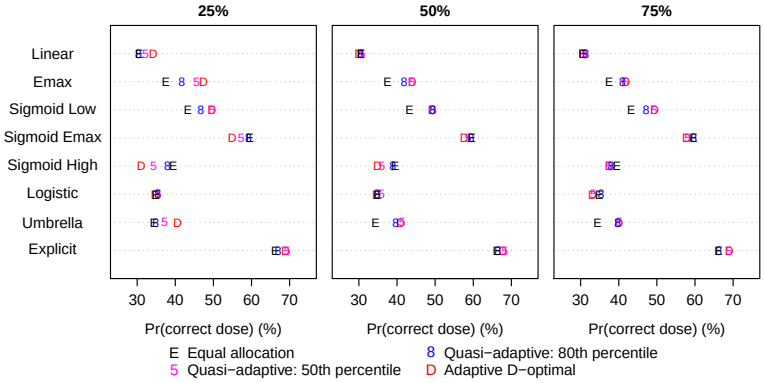

Figure 6-17: Probability of selecting a dose in the target dose interval using equal allocation, quasi-adaptive and adaptive D-optimal methods by timing of the interim analysis.

of subjects have completed, hence the probability of detecting a clinical response for the quasi-adaptive methods are closer to that of the equal allocation than the adaptive allocation. As the interim analysis is carried out later in the study, the quasi-adaptive methods adapt more often and so tend more towards the operational characteristics of the adaptive D-optimal allocation.

Correctly selecting a dose in the target dose interval

As it is linked with detecting a clinical response, the timing of the interim analysis also impacts the probability of correctly identifying a dose in the target interval (Figure 6-17), with the early adaptation benefiting some dose response profiles but not others.

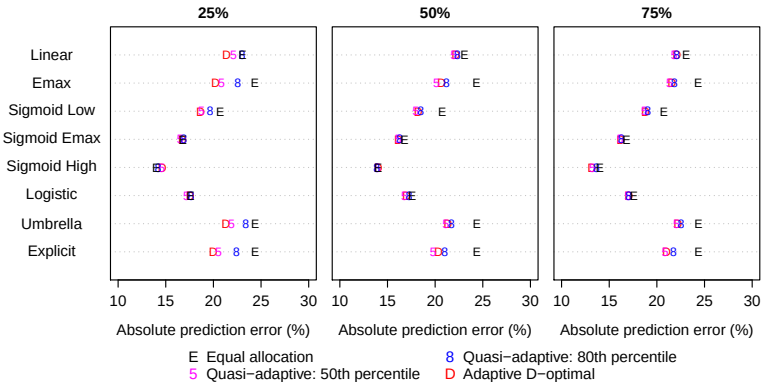

Figure 6-18: Absolute prediction error using equal allocation, quasi-adaptive and adaptive D-optimal methods by timing of the interim analysis.

The quasi-adaptive methods offer a compromise between using an adaptive design and equal allocation. When the interim analysis takes place after 50% of the subjects have completed the trial, using the quasi-adaptive method based on the 80^{th} percentile results in most of the gains from adapting. This can be seen for the Emax, Sigmoid Low and Umbrella profiles where the quasi-adaptive method gives similar results to the adaptive D-optimal design and has clear gains over equal allocation. When adaptation is detrimental to the operational characteristics, the quasi-method gives results close to if we had used equal allocation (e.g. the Sigmoid Emax and Sigmoid High profiles).

The quasi-adaptive method based on the 50^{th} percentile adapts more often than when the 80^{th} percentile is used and so although it is still a compromise between always adapting and equal allocation, it gives operational characteristics which are more comparable to the adaptive D-optimal design.

Prediction Error

In terms of the prediction error (Figure 6-18), the adaptive methods have a smaller prediction error than the equal allocation design. When the interim analysis takes place after 25% of the subjects have completed the study, the adaptive D-optimal methods generally have the smallest prediction error followed by the quasi-adaptive methods and then the equal allocation. The later the interim analysis is performed, the closer the prediction errors between the quasi-adaptive and adaptive method become.

Conclusion

In this section we have examined two aspects of the adaptive D-optimal design. We have considered the timing of the interim analysis and the operational characteristics from using a quasi-adaptive method.

The timing of the interim analysis is an important consideration when planning an adaptive design. If the interim analysis is carried out too early then there will be a lot of variability in the data and so the adaptation based on the parameter estimate may be far from optimal. If the interim analysis is carried out too late, then the number of subjects to be allocated adaptively is reduced and so any adaptation may have limited impact.

We have observed that the timing of the interim analysis does have an impact on the operational characteristics. When the interim analysis is carried out after 25% of subjects have completed the study, the potential gains and losses of using the adaptive or quasi-adaptive methods are greater than when the interim analysis is carried out later on. Therefore an early interim analysis should only be used if we are confident about the shape of the dose response profile, and that an adaptation is beneficial.

Using the quasi-adaptive method results in a compromise between the adaptive and non-adaptive allocations. When the interim analysis is carried out after 50% of subjects have completed the study, using the 80^{th} percentile to dictate adaptation results in most of the gains of the adaptive method without the losses when adaptation is detrimental. When the criterion suggest we should not adapt the quasi-adaptive method allocates subjects equally to all the doses. This could be an advantage over wrongly adapting to a few doses as it would provide a study team with efficacy and safety data for all the doses, allowing for more informed decision making about all the doses.

6.8 Results - Bayesian adaptive D-optimal designs

In the previous section we used the quasi-adaptive method to assess the variability in the model parameters at the interim analysis and so determine if the proposed D-optimal design was robust to parameter mis-specification. The Bayesian D-optimal adaptive design is a more formal methodology for dealing with variability in the model parameters, as the Bayesian D-optimal design proposed at the interim analysis is D-optimal for the posterior distribution.

In order to assess the performance of the Bayesian D-optimal designs we carry out a simulation study. For the simulation study we use the neuropathic pain scenario described in Chapter 2 and generate data from the true dose response profiles described in Section 2.3. As for the previous simulations studies, we assume the total sample size is N=250 and there are 9 available doses (0mgs, . . . ,8mgs). The between subject variance is $\sigma^2 = 4.5$. Due to the additional computation needed at each interim analysis to generate the Bayesian D-optimal design for the next cohort of subjects, we limit our simulation study to 1000 replicated datasets for each scenario and use one interim analysis carried out after 50% of subjects have completed the study.

As before we aim to fit the sigmoid emax model (6.16) which has four model parameters. To construct the Bayesian D-optimal design, we allocate the first cohort of subjects equally across all the available doses. At the interim analysis the Bayesian D-optimal design for the next cohort of subjects is found by maximising the criterion

$$\Phi\{M(\xi)\} = \log E[|M(\xi, \theta)|].$$

As the posterior distribution and so the Bayesian D-optimal design depends on the prior distributions placed on the model parameters, we use three prior joint distributions which assume independence between the model parameters.

	θ_1	θ_2	θ_3	θ_4
Prior 1	$N(0,\ 1)$	$N(2,\ 1)$	$G(4,\ 4)$	$G(4,\ 4)$
Prior 2	$N(0,\ 4)$	$N(2,\ 9)$	$G(1,\ 0.25)$	$G(1,\ 0.5)$
Prior 3	$N(0{,}25)$	$N(2,\ 25)$	$G(2,\ 0.25)$	$G(1,\ 0.25)$

To assess whether it is the Bayesian adaptivity at the interim analysis or the final inferences that have an impact on the results, we carry out the following analyses:

1. Use a Bayesian D-optimal design at the interim, but make the final inferences using a frequentist approach via the MLE $\hat{\theta}$.

2. Use a Bayesian D-optimal design at the interim and make the final inference based on the posterior distribution.

We compare the results from these two analyses with an equal allocation design and an adaptive locally D-optimal design with one interim analysis. For the frequentist analysis we use a box to constrain the convergence of the MLE. The upper and lower limits

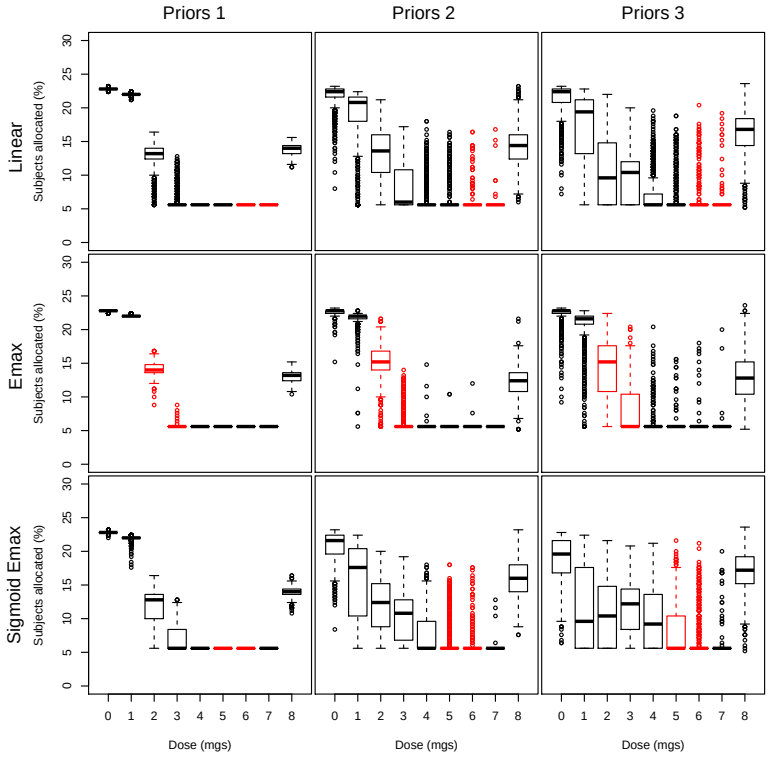

Figure 6-19: Box plot of subject dose allocations for the Bayesian adaptive D-optimal design with one interim analysis performed after 50% of the subjects have completed the study. Target dose intervals are given in red.

of the box for $\theta = (\theta_1, \theta_2, \theta_3, \theta_4)$ are $(-2,-1,0.01,0.01)$ and $(2,5,16,8)$ respectively. For more details on the use of a box to constrain the convergence of the parameter estimates see Section 6.5.

Subject allocation

The subject allocations when the dose response profiles are the Linear, Emax and Sigmoid Emax, are very similar for Prior 1 (Figure 6-19) as the prior distribution dominates the data. As the prior distribution becomes more vague, the subject allocations depend more on the data and so there are differences between the subject allocations for the different dose response profiles. Although the data play more of a role in the subject allocation as the prior distribution becomes more vague, even with Prior 3 a large proportion of subjects are allocated to the early doses. This is most like the locally D-optimal design for the Emax model (Figure 6-2) and least like the locally D-optimal design for the Sigmoid High and Umbrella models.

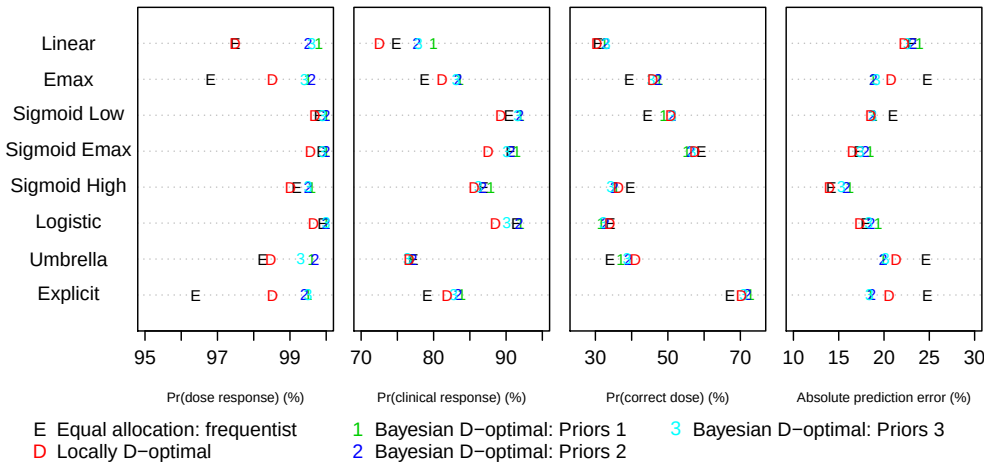

Figure 6-20: Operational characteristics using a Bayesian adaptive D-optimal design at the interim analysis and a frequentist final analysis.

Frequentist analysis

When the final analysis is frequentist, the one-sided type I error under the Flat dose response profile is maintained at 5% for each of the prior distributions. Using a Bayesian D-optimal adaptation at the interim analysis and a frequentist final analysis, generally improves the probability of detecting a dose response and a clinical response (Figure 6-20). However, this increase in the ability to detect a clinical response does not translate to an ability to correctly identify a dose in the target dose interval. Regardless of the prior distribution placed on the model parameters, the probability of correctly identifying a dose in the target dose interval is very close to that of the locally adaptive D-optimal design. Despite the different prior distributions resulting in different subject allocations, there is little to distinguish between them in terms of the overall operational characteristics.

Bayesian analysis

Although we are working within a Bayesian framework, we still maintain the frequentist one-sided type I error at 5% under the Flat profile to allow for a fair comparison across methods. When a Bayesian analysis was used as the method of inference, after using an adaptive Bayesian D-optimal design at the interim analysis, the operational characteristics are highly dependent on the choice of prior distribution placed on the parameters. As this sensitivity to the prior distributions was not observed when the analysis was frequentist, we can conclude it is not the adaptation at the interim analysis

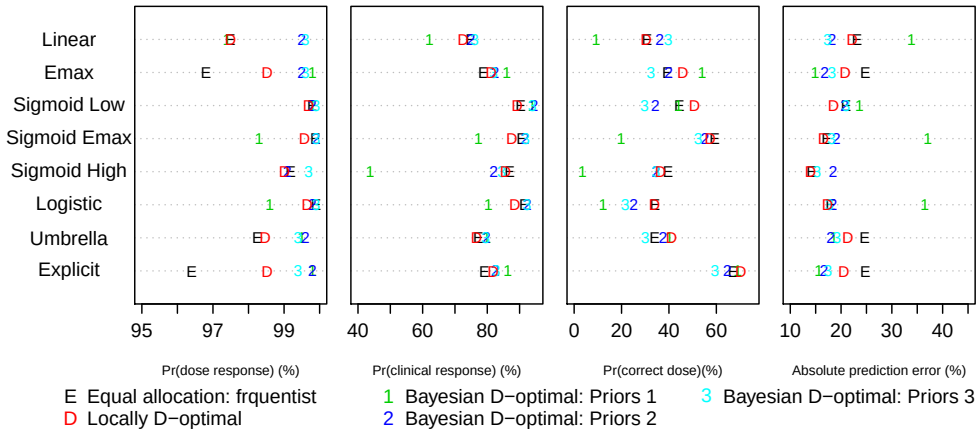

Figure 6-21: Operational characteristic of using a Bayesian adaptive D-optimal design at the interim analysis and a Bayesian final analysis.

which is impacting the operational characteristics but the final analysis. Comparing the operational characteristics of an equal allocation design with a Bayesian final inference (not presented here), we found that although the Bayesian adaptive D-optimal design led to an increase in the ability to select a dose in the target dose interval for some dose response profiles, the adaptation was detrimental to other dose response profiles. This result is consistent with the locally adaptive D-optimal designs, which also failed to show gains over the equal allocation design for all the dose response profiles.

For the Emax profile, Prior 1 outperforms the other prior distributions. This is because the prior distributions used for Prior 1 are informative about the model parameters of the Emax profile. However for some of the other dose response profiles, using Prior 1 results in poor operational characteristics as the prior distributions disagree with the true parameter values in the underlying dose response profiles. It can be seen in the prediction error that Priors 1 produces a poor fit for many of the dose response profiles. Although Priors 2 and 3 are more vague, they still perform poorly in terms of correctly identifying a dose in the target dose interval, compared to the equal allocation and locally D-optimal designs for many of the dose response profiles.

Conclusion

In this section we have shown that it is possible to apply an adaptive Bayesian D-optimal design as a formal approach for dealing with the variability in the parameter

estimates at an interim analysis. Using a Bayesian D-optimal design at the interim analysis with a frequentist inference, lead to gains in terms of detecting a dose response and a clinical relevant response when compared to the equal allocation. In terms of correctly identifying a dose in the target dose interval, using a Bayesian adaptation at the interim analysis gave very similar results to using a locally D-optimal design. These conclusions do not depend on the choice of prior distribution placed on the model parameters.

The performance of the Bayesian D-optimal design when the final analysis is Bayesian, depends on the choice of prior distribution placed on the model parameters. As we observed from Figure 6-21, there is no one choice of prior distributions which are robustly efficient. If we have strong prior information about the model parameters which is correct, then as we observed with the Emax profile, there are gains that can be made in terms of correctly identifying the target dose. The converse is also true, if the prior distribution is strong but is incorrect for the true dose response profile, then incorporating this information proves to be detrimental. Using a the less informative prior distributions, offered gains over the equal allocation in terms of detecting a dose response, but added little in terms of correctly identifying a dose in the target dose interval.

6.9 Discussion

In this chapter we have explored a number of aspects of implementing adaptive D-optimal designs. We have found that for some of the scenarios explored, there are gains to be made from using an adaptive D-optimal design at an interim analysis compared with using an equal allocation design. These gains were not present for all the dose response profiles, and for the Sigmoid High profile the adaptation was detrimental to the probability of identifying a dose in the target dose interval compared with the equal allocation. Therefore, the benefit of the adaptation is dependent on the shape of the underlying dose response profile, which is often unknown when designing a clinical trial.

We propose the use of a quasi-adaptive method which only adapts if the D-optimal design at the interim analysis is robust to the variability in the parameter estimates. The operational characteristics for the quasi-adaptive method showed that it produced most of the gain that could be achieved from adaptation over equal allocation, whilst minimising the losses when adaptation was detrimental. When designing a clinical trial we do not know the shape of the true dose response profile, and so this method provides

a safeguard against using adaptation when it is not appropriate.

Finally we explored the use of Bayesian D-optimal design as a formal way of incorporating the uncertainty in the model parameters at the interim analysis. We found that the performance of the Bayesian D-optimal design depends on the prior distributions placed on the model parameters, with no one set of prior distributions performing well for all the scenarios.

In the next chapter, we bring together all the adaptive methods we have explored so far to allow for a direct comparison. We also compare the methods in terms of the probability of success in phase III.

Chapter 7

Designing Phase II Based on Expected Gain of Programme

7.1 Introduction

So far in this thesis we have considered the phase II study as a single, stand alone trial. In reality a phase II dose-finding study is one part of a much larger development process. In this chapter we consider making decisions in phase II based on the likelihood of success in phase III using a decision theoretic approach. Decision theory is concerned with quantifying the decision making process, based on our preferences concerning consequences and our beliefs about the 'state of the world' (Schlaifer & Raiffa, 1961, p. 3). Once we have quantified the value of each decision, it is possible to order the decisions in terms of their expected returns and so optimise the decision making process. An early example of a Bayesian decision theoretic approach was carried out by Schlaifer & Raiffa (1961). Standard texts on this topic also include Berger (1985) and Lindley (1985).

Decision theoretical approaches are appealing as they take into account uncertainty in the data and the preferences of the decision maker (Sylvester, 1988). In a pharmaceutical setting, this is important as there are limited resources available and so portfolio prioritisation needs to take place (Senn, 1996). That is, the development of compounds with more potential may be expedited whilst the development of other compounds delayed or abandoned. By assigning a utility to the decision process in terms of monetary gains, it also allows for companies to distinguish between two compounds. Decision theory can also be used to compare trial designs, for example,

Julious & Swank (2005) use decision theory to compare three development plans. In their paper they find the development plan which maximises the expected 'net present value', taking into account time to product launch.

In the pharmaceutical industry decision theory can also be used to optimise a number of aspects of the clinical trial process. For example, the sample size of clinical trials has been studied by a number of authors (Brunier & Whitehead, 1994; Gittins & Pezeshk, 2000a,b, 2002; Lindley, 1997; Pezeshk & Gittins, 2002; Stallard, 1998; Sylvester, 1988). Pezeshk (2003) provides a review of Bayesian methods used for determining sample size. Another area which has been studied is the number of treatment arms that should be included in phase II, based on a fixed sample size (Whitehead, 1985) and when there is a trade off between phase II and phase III resources (Whitehead, 1986). Stallard et al. (2009) investigated the optimal choice of treatments to take into phase III to minimise the total sample size.

The decision theory set up gives us a framework for making an optimal decision as to whether to continue into phase III, and if we do choose to continue, which dose to take forward. In this chapter we use decision theory to compare the methods previously explored in terms of their potential monetary gain from a phase III success. We set up three decision rules for selecting a dose in phase II to be taken forward into phase III. These decision rules are

- decision rule 1: we select the minimum dose estimated to have a 1.3 change from placebo
- decision rule 2: we select the dose that maximises the probability of success in phase III based on a point estimate of the dose response curve
- decision rule 3: is a Bayesian decision rule, where we select the dose that maximises the posterior probability of success in phase III.

For each of these decision rules, there is also the option to stop the development process after phase II if none of the doses are deemed suitable for phase III.

7.2 Recap on methods explored in previous chapters

In the previous chapters we have explored a number of response adaptive designs for phase II dose-finding studies. For these methods we have assumed that there is a

placebo dose, z_0, and J active doses denoted $z_1, \ldots, z_J$ and we denote the number of subjects allocated to dose z_j by the end of phase II as n_j. We model the response at dose z_j using $\eta(z_j, \theta)$, where θ is the vector of unknown model parameters. We assume the response of the i^{th} subject ($i = 1, \ldots, n_j$) on dose z_j is

$$Y_{ij} \sim N(\eta(z_j, \theta), \sigma^2),$$

where σ^2 is the between subject variation. In Table 7.1 we present a summary of some of the main methods considered in this chapter.

In the previous chapters we have modelled the subject response data in three ways:

1. ANOVA: we include the ANOVA method (Section 2.5) as a control comparison with the other methods. This is a frequentist approach which uses pairwise testing with placebo and a Dunnett (1955) adjustment for multiplicity. For this analysis $\theta = (\theta_0, \ldots, \theta_J)^T$ and
$$\eta(z_j, \theta) = \theta_j.$$
We estimate θ_j using
$$\hat{\theta}_j = \frac{\sum_{i=1}^{n_j} y_{ij}}{n_j}.$$
That is, the fitted model assumes independence between doses and follows the empirical means at each dose.

2. Normal dynamic linear model (NDLM): in Chapters 4 and 5 we use a Bayesian framework where the data are modelled using an NDLM. For this model $\theta = (\theta_0, \ldots, \theta_J)^T$ and
$$\eta(z_j, \theta) = \theta_j,$$
where θ_j is the mean of the response distribution at dose z_j. In the NDLM the dependence between the response at the doses is built into the prior distribution for θ,
$$\theta \sim N(\mu, w\mathbf{\Delta}),$$
where μ and Δ are the prior mean and variance covariance matrix respectively, as defined by the system equations (4.1). We assume a discrete uniform prior distribution for W.

3. Parametric methods: in Chapters 3 and 6 we explore modelling the data using a parametric model within both frequentist and Bayesian frameworks. We model

the data using a four parameter sigmoid emax model with $\theta = (\theta_1, \ldots, \theta_4)^T$ written

$$\eta(z_j, \theta) = \theta_1 + (\theta_2 - \theta_1)\frac{z_j^{\theta_4}}{\theta_3^{\theta_4} + z_j^{\theta_4}}.$$

For the frequentist methods we find the maximum likelihood estimates (MLEs) denoted $\hat{\theta}$ for the model parameters θ. When we use a Bayesian framework, we place prior distributions on the model parameters θ and then, for a given dataset $Y = y$, sample from the posterior distribution with density $\pi(\theta|y)$ to make inferences about the dose response curve.

7.3 Decision theory notation

We follow the general notation used by Berger (1985) to construct a utility function, however we have adapted the notation to fit within the clinical trial setting. In decision theory we are concerned with making decisions based on the true state of nature, which in our case is one of the dose response profiles listed in Chapter 2. We denote the true mean response at dose z_j as ν_j and write $\nu = (\nu_0, \ldots, \nu_J)^T$ as the vector or responses. The observed data are denoted by the random variable Y, which has density $p(y|\nu)$. Particular realisations of data are denoted by y.

For each decision an action is taken, denoted a, where $\mathscr{A}$ is the set of all possible actions. As we are interested in choosing a dose to take forward into phase III we define our set of actions to be

$$a = \begin{cases} 0 & \text{stop after phase II} \\ j & \text{take dose } z_j \text{ into phase III } (j = 1, \ldots, J). \end{cases} \tag{7.1}$$

For each $\nu \in \mathscr{N}$ and action $a \in \mathscr{A}$ there is an associated reward, known as the utility function. We denote this utility function as $u(\nu, a)$. The decision rule δ is a function $\delta : Y \mapsto \mathscr{A}$. Hence if $Y = y$ is the observed data from phase II, then $\delta(y)$ is the action that is taken, and so the utility in this case is $u(\nu, \delta(y))$.

We take the expectation of the utility function over the possible values for Y to get the ***expected gain*** for a decision rule δ. For a given ν, the expected gain is,

$$G(\nu, \delta) = E[u(\nu, \delta(Y))] = \int u(\nu, \delta(y))p(y|\nu)dy. \tag{7.2}$$

Name of Method	Adaptation	Analysis	Abbreviation	No. Simulations
ANOVA	None - equal allocation to all doses	Frequentist: pairwise testing of doses with placebo using a Dunnett adjustment for multiplicity	A	10000
Equal (NDLM)	None - equal allocation to all doses	Bayesian: modelled using a Normal Dynamic Linear Model (NDLM)	N	10000
Cohort (NDLM)	Adaptation at 1 interim analysis based on posterior probabilities of being the target dose	Bayesian: modelled using a NDLM	C	10000
GADA (NDLM)	Fully adaptive, one subject at a time aimed at minimising the posterior variance at the target dose	Bayesian: modelled using a NDLM	G	5000
Equal (parametric)	None - equal allocation to all doses	Frequentist: four parameter sigmoid emax model fitted by maximum likelihood estimation	P	10000
Quasi-Adaptive D-optimal: 80th percentile (parametric)	Adaptation at 1 interim analysis based on the locally optimal design if the 80th percentile of the bootstrapped efficiencies is greater than 1	Frequentist: four parameter sigmoid emax model fitted by maximum likelihood estimation	8	1000
Local D-optimal (parametric)	Adaptation at 1 interim analysis based on the locally D-optimal design	Frequentist: four parameter sigmoid emax model fitted by maximum likelihood estimation	D	10000

Table 7.1: Summary of methods used to randomise and analyse simulated datasets.

We can also consider ν within a Bayesian framework where we place a prior distribution on ν with prior density $\pi(\nu)$. The ***Bayes gain*** of a decision rule δ is then

$$g(\delta) = \int \int u(\nu, \delta(y)) p(y|\nu) \pi(\nu) \, dy \, d\nu. \tag{7.3}$$

This can be re-written in terms of the posterior distribution $\pi(\nu|y)$ as

$$g(\delta) = \int \int u(\nu, \delta(y)) \pi(\nu|y) \, d\nu \, dy.$$

The inner integral is known as the ***expected posterior gain*** and is written

$$\rho(\pi(\nu|y), \delta(y)) = E[u(\nu, \delta(y))|Y = y] = \int u(\nu, \delta(y)) \pi(\nu|y) d\nu. \tag{7.4}$$

7.4 Determining the utility

In order to construct a utility function, we must first define what we mean by phase III success. To claim success in phase III we need to observe two things:

1. Two phase III trials with a statistically significant difference from placebo
2. A reasonable safety profile.

We use a two arm parallel group design for each of the two phase III trials, with an active dose identified during phase II versus the placebo dose. Each arm consists of n_3 subjects, chosen to given appropriate power of detecting a clinically meaningful difference from placebo. The final inference in phase III is frequentist, and consists of a pairwise comparison between the active dose z_j and the placebo dose z_0. We assume that the expected responses in phase III are normally distributed with between subject variance $\tilde{\sigma}^2$. Let $\tilde{Y}_j$ denote the response at dose z_j in a phase III trial, which is normally distributed as

$$\tilde{Y}_j \sim N\left(\nu_j, \frac{\tilde{\sigma}^2}{n_3}\right),$$

and $\tilde{Y}_0$ the placebo response,

$$\tilde{Y}_0 \sim N\left(\nu_0, \frac{\tilde{\sigma}^2}{n_3}\right).$$

We control the type I error in each phase III trial at the two sided 5% level. We conclude that there is a statistically significant difference from placebo and hence a dose response, if the lower bound of the two-sided 95% confidence interval for the

difference from placebo is greater than 0. The probability of detecting a treatment effect in one phase III trial is

$$\text{PDR}(\nu_j,\, \nu_0) = 1 - \Phi\left(-1.96 + \frac{\nu_j - \nu_0}{\sqrt{2\tilde{\sigma}^2/n_3}}\right). \tag{7.5}$$

As it is possible for a drug to be efficacious but fail to make it to market because of safety concerns, we include a term for safety in our criteria for overall success. We use a quadratic function for the probability of the drug failing due to safety

$$\text{PSF}(j) = 0.2\left(\frac{z_j}{z_J}\right)^2, \tag{7.6}$$

which does not depend on ν_j. This function for safety assumes that the maximum probability of phase III failing due to safety is 0.2. A quadratic function is used so that at higher doses the increase in safety from one dose to the next is greater than at lower doses. When fed into the utility function, incorporating a term for safety aims to balance the gain in efficacy from increasing a dose level with the increased risk in the safety profile. Without a term for safety, the highest utility would always occur for the dose with the largest difference in mean efficacy response from placebo, which for the monotonic dose response profiles is the top dose.

As we need success in both of the two phase III trials and an acceptable safety profile in order to get to market, the probability of success in phase III for dose z_j is

$$f(\nu_j, \nu_0) = \text{PDR}(\nu_j, \nu_0)^2(1 - \text{PSF}(j)). \tag{7.7}$$

The utility function is in terms of monetary gain and takes into account the cost of running the phase II and phase III trials, as well as the probability of success in phase III. The total sample size of the phase II dose-finding trial is denoted N_2. In order for a drug to get to market we need two successful phase III trials. As each phase III trial has two arms, with n_3 subjects on each arm, the total sample size of each of the phase III trials is denoted N_3=$2n_3$. Let c_2 and c_3 denote the cost per subject in the phase II and phase III trials respectively, and R denote the potential profit or reward for the company if the drug makes it to market. If the development process is stopped after phase II because the probability of success in phase III is low, then the utility for this

dose is the cost of the failed phase II trial. The utility function we use is written

$$u(\nu, a) = \begin{cases} -c_2 N_2 & \text{if } a{=}0 \\ f(\nu_j, \nu_0)R - c_2 N_2 - 2c_3 N_3 & \text{if } a = j \ (j = 1, \ldots, J). \end{cases} \tag{7.8}$$

7.5 Decision rules

We are interested in making decisions in phase II which maximise the potential gain over the whole of the phase II and phase III process. In practice we do not know the true state of nature ν, therefore we make our decisions based on the observed data $Y = y$.

7.5.1 Decision rule 1

For our first decision rule, we select the minimum dose with a clinically meaningful difference (CMD) from placebo to be taken into phase III. This rule for selecting a dose in phase II is the same as described in Chapter 2, and has been used throughout Chapters 4 to 6 as the method for selecting a dose. For the frequentist methods we obtain the MLE $\hat{\theta}$ of θ and choose z_a, where

$$z_a = \min_j \{z_j : \eta(z_j, \hat{\theta}) - \eta(z_0, \hat{\theta}) \geq \text{CMD}\}.$$

For the Bayesian methods we consider the posterior distribution of θ given the phase II data Y and choose dose

$$z_a = \min_j \{z_j : \Pr(\eta(z_j, \theta) - \eta(z_0, \theta) \geq \text{CMD} | Y = y) > 0.5\}.$$

In both these cases, the decision rule is then written,

$$\delta_1(y) = \begin{cases} 0 & \text{if no dose has a CMD from placebo} \\ j & \text{if } z_j = z_a \ (j = 1, \ldots, J). \end{cases} \tag{7.9}$$

7.5.2 Decision rule 2

For our second decision rule, we select the dose that maximises the probability of success in phase III based on the fitted dose response curve. We impose an additional condition that, in order to continue to phase III, the probability of success in phase III must be greater than a prespecified threshold x. The value of x is chosen, so that we

only continue to phase III if we have a reasonable chance of success. For the frequentist methods, for a dataset $Y = y$, we estimate ν_j at dose z_j as

$$\hat{\nu}_j(y) = \eta(z_j, \hat{\theta}),$$

where $\hat{\theta}$ is the estimate of the model parameter θ. For the Bayesian methods we shall estimate ν_j as

$$\hat{\nu}_j(y) = E[\eta(z_j, \theta)|Y = y].$$

The decision rule is written

$$\delta_2(y) = \begin{cases} 0 & \text{if } \max\limits_j(f(\hat{\nu}_j(y), \hat{\nu}_0(y))) < x \\ j & \text{where } j = \underset{k\in\{1,\ldots,J\}}{\operatorname{argmax}} (f(\hat{\nu}_k(y), \hat{\nu}_0(y))) \text{ if } \max\limits_j(f(\hat{\nu}_j(y), \hat{\nu}_0(y))) \geq x. \end{cases} \tag{7.10}$$

7.5.3 Decision rule 3

Our third and final decision rule is a Bayesian decision rule, where we choose the dose that maximises the posterior probability of success. Again, we impose an additional condition that, in order to continue to phase III, the posterior probability of success in phase III is greater than a prespecified threshold x. Within the Bayes framework we place a prior distribution on the model parameters and then make the decisions based on the posterior distribution for each ν_j, given the phase II data $Y = y$. We denote the posterior probability as

$$\text{PPS}_j = E[f(\nu_j, \nu_0)|Y = y] = \int f(\nu_j, \nu_0)\pi(\nu|y)d\nu. \tag{7.11}$$

In this Bayes framework we have $\nu_j = \eta(z_j, \theta)$ and so rather than specify a prior distribution for ν we specify a prior distribution for the parameter vector θ. We can then express (7.11) as

$$\text{PPS}_j = E[f(\eta(z_j, \theta), \eta(z_0, \theta))|Y = y] = \int f(\eta(z_j, \theta), \eta(z_0, \theta))\pi(\theta|y)d\theta.$$

The decision rule is then written

$$\delta_3(y) = \begin{cases} 0 & \text{if } \max\limits_j(\text{PPS}_j) < x \\ j & \text{where } j = \underset{k\in\{1,\ldots,J\}}{\operatorname{argmax}} (\text{PPS}_k) \text{ if } \max\limits_j(\text{PPS}_j) \geq x. \end{cases} \tag{7.12}$$

We estimate the integral for the posterior probability of success by simulation, using T samples generated from the posterior distribution $\pi(\theta|y)$ which are denoted θ^t $(t = 1, \ldots, T)$,

$$\text{PPS}_j \approx \frac{1}{T} \sum_{t=1}^{T} f(\eta(z_j, \theta^t), \eta(z_0, \theta^t)).$$

7.6 Phase III set up

For the phase III trial design, we use a two arm parallel study design to compare the placebo dose with the dose identified in phase II. For each phase III trial, we use a sample size of $n_3 = 86$ subjects on each dose, which gives us 90% power to detect a difference of 1.3 with a between subject variance $\tilde{\sigma}^2 = 6.75$. The between subject variance for the phase III design is 50% bigger than that used in the phase II design to account for the potential additional variability that may be in the phase III population.

We assume the cost of a subject in phase II is the same as a subject in phase III and assign $c_2 = c_3 = 1$, where this represents 1 unit of some larger monetary value. We assign a reward for successfully getting the drug to market of R=12000. Hence the return for getting a compound to market is 12000 times the cost of a phase II or phase III subject. For decision rules 2 and 3 we use a threshold of 0.25 to determine if we continue to phase III. This was chosen as it is equivalent to having at least a 50% chance of success in each of the two phase III trials, including the possibility of failure due to safety reasons.

7.7 Target dose

Previously we have defined the target dose to be the minimum dose with a 1.3 change from placebo, and the target dose interval to include the doses with ±10% of the 1.3 clinically meaningful difference from placebo, with some rounding of the doses as discussed in Section 2.3.3. Table 7.2 presents the target dose and target dose intervals based on this previous definition, for each of the dose response profiles. We also include the probability of success at the target dose as defined by (7.7), with j equal to the index of the target dose, using the phase III trial design described in Section 7.6.

We now define our target dose to be the dose that maximises the probability of success in phase III, $f(\nu_j, \nu_0)$. We include doses in the target dose interval that have a

Dose Response Profile	Target Dose			Target Dose interval		
	Dose	Response	Pr(success)	Doses	Response	
					min	max
Linear	6	1.23	0.68	{6,7}	1.23	1.44
Emax	2	1.30	0.81	{2,3}	1.30	1.43
Sigmoid Low	3	1.46	0.89	{3}	1.46	1.46
Sigmoid Emax	5	1.29	0.75	{5,6}	1.29	1.51
Sigmoid High	7	1.39	0.75	{7}	1.39	1.39
Logistic	5	1.31	0.77	{5}	1.31	1.31
Umbrella	3	1.24	0.75	{3,4}	1.24	1.47
Explicit	1	1.29	0.81	{1,2,3}	1.29	1.42

Table 7.2: Target dose and target dose intervals based on the minimum dose with a 1.3 clinically meaningful difference from placebo.

probability of success in phase III of greater than or equal to

$$0.975 \times \max_j f(\nu_j, \nu_0).$$

Table 7.3 presents the new target dose and target dose intervals for each of the dose response profiles under this new definition. We note that the Emax Low profile is now considered to have a target dose, but that the mean response and probability of success in phase III is relatively low compared to the other dose response profiles. Under the previous definition, the Emax Low profile does not have a target dose, as no dose meets the 1.3 clinically meaningful difference from placebo. Figure 7-1 illustrates how the overall probability of success depends on the probability of detecting a dose response and the probability of a safety concern for the Linear, Emax and Sigmoid Emax profiles.

The doses identified as the target doses using the probability of success (Table 7.3) are higher than when the target dose was defined as the minimum dose with a CMD of 1.3 from placebo (Table 7.2). This is because the probability of detecting a dose response is still increasing at the CMD, and so although we penalise choosing a higher dose due to safety concerns, the penalty for safety does not outweigh the gains in terms of efficacy, hence higher doses are chosen.

Dose Response Profile	Target Dose			Target Dose interval		
	Dose	Response	Pr(success)	Doses	Response	
					min	max
Linear	8	1.65	0.78	{7,8}	1.44	1.65
Emax	4	1.51	0.89	{3,4,5}	1.43	1.56
Emax Low	6	1.01	0.46	{5,6,7}	0.98	1.01
Sigmoid Low	4	1.60	0.91	{4,5}	1.60	1.63
Sigmoid Emax	6	1.51	0.83	{6,7}	1.51	1.61
Sigmoid High	8	1.65	0.77	{8}	1.65	1.65
Logistic	6	1.57	0.85	{6}	1.57	1.57
Umbrella	5	1.60	0.89	{4,5}	1.47	1.60
Explicit	5	1.60	0.89	{3,4,5}	1.42	1.60

Table 7.3: Target doses and target dose intervals based on probability of success in phase III.

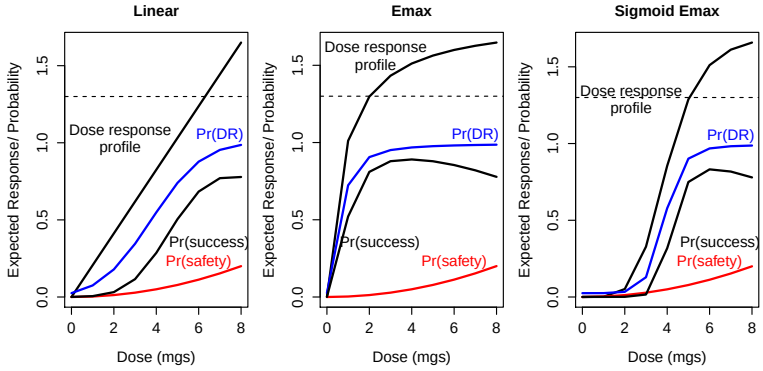

Figure 7-1: Probabilities of detecting a dose response, observing a safety concern and success in phase III based on true dose response profiles. Dashed line represents clinically meaningful difference from placebo.

7.8 Metrics

In the previous chapters we have compared the methods in terms of the metrics described in Chapter 2. As our aim is now to maximise the probability of success in phase III, we define new metrics to measure how well each method does in meeting this new objective. Where expectations are estimated using the sample average, we use M simulated datasets y^m $(m = 1, \ldots, M)$ which have density $p(y^m|\nu)$.

Correct dose For each dataset we select a dose to be taken through to phase III using the decision rules described in Section 7.5. We measure the performance of the methods, by calculating the percentage of datasets where the selected dose is contained in the target dose intervals given in Table 7.3.

Expected gain The expected gain is as defined in (7.2). We estimate the expected gain via simulation as

$$G(\nu, \delta) \approx \frac{1}{M} \sum_{m=1}^{M} u(\nu, \delta(y^m)). \tag{7.13}$$

Expected gain bias The expected gain bias, is the bias in the predicted gain based on the observed data compared to the true gain.

For decision rules 1 and 2, we estimate the true state of nature using the observed data $Y = y$. For the frequentist methods we estimate ν_j at dose z_j as

$$\hat{\nu}_j(y) = \eta(z_j, \hat{\theta}),$$

where $\hat{\theta}$ is the estimate of the model parameter θ. For the Bayesian methods we shall estimate ν_j as

$$\hat{\nu}_j(y) = E[\eta(z_j, \theta)|Y = y].$$

The utility of a decision rule δ based on the observed data y is then $u(\hat{\nu}(y), \delta(y))$. This is the utility that may then be reported by study team prior to embarking on a phase III trial. The expected value of the 'predicted gain' is

$$E[u(\hat{\nu}(Y), \delta(Y)]$$

and the value of the true expected gain is $G(\nu, \delta)$, which is estimated by (7.13). We calculate the percentage bias as

$$100 \times \frac{E[u(\hat{\nu}(Y), \delta(Y)] - G(\nu, \delta)}{G(\nu, \delta)}. \tag{7.14}$$

For decision rule 3 we use a Bayesian framework. We model ν_j using $\eta(z_j, \theta)$ and denote the true state of nature for a given θ as $\nu(\theta)$, we then place prior distributions on the model parameters θ. The 'predicted gain' from continuing to phase III after observing data $Y = y$ is the expected posterior gain,

$$\rho(\pi(\theta|y), \delta(y)) = \int u(\nu(\theta), \delta(y))\pi(\theta|y)d\theta,$$

which is estimated by generating T samples from the posterior distribution with density $\pi(\theta|y)$. We denote these samples as θ^t $(t = 1, \ldots, T)$ and so $\nu(\theta^t) = \eta(z_j, \theta^t)$. Taking

the sample average, the expected posterior gain is

$$\rho(\pi(\theta|y), \delta(y)) \approx \frac{1}{T} \sum u(\nu(\theta^t), \delta(y)).$$

On average the predicted gain is

$$E[\rho(\pi(\theta|Y), \delta(Y))] \approx \frac{1}{M} \rho(\pi(\theta|y^m), \delta(y^m)).$$

The expected gain bias is the bias in the predicted gain compared to the true gain, and is calculated as

$$100 \times \frac{E[\rho(\pi(\theta|Y), \delta(Y))] - G(\nu, \delta)}{G(\nu, \delta)}. \tag{7.15}$$

7.9 Results

7.9.1 Decision rule 1

Figure 7-2 illustrates the doses selected by each method using decision rule 1, when the true dose response profile are Linear, Emax and Sigmoid Emax. These are the doses that were selected in previous chapters, but for the first time we can see all the methods compared directly. The target dose interval indicated in red are based on the new definition where we aim to maximise the probability of success in phase III (Table 7.3). Datasets where the action was to stop after the phase II trial are represented as having selected the placebo dose.

It can be seen that the Bayesian methods which model the data using a NDLM tend to choose higher doses than the other methods. As seen in Chapters 4 and 5, modelling the data with an NDLM resulted in a tendency to underestimate the response at the early doses, resulting in higher doses being selected for phase III. The frequentist methods have a larger proportion of studies where a clinically relevant difference was not detected. These methods also tend to choose lower doses than the methods that use the Bayesian NDLM to model the data. For both the frequentist parametric and Bayesian NDLM methods, there is little difference between the doses chosen for the adaptive and non-adaptive subject allocations.

Figure 7-3 displays the operational characteristics based on the metrics in Section 2.3, for the different methods listed in Table 7.1. The one-sided type I error rate under the Flat dose response profile has been maintained at the one-sided 5% level for each of the methods. For the active dose response profiles, the methods which use a parametric

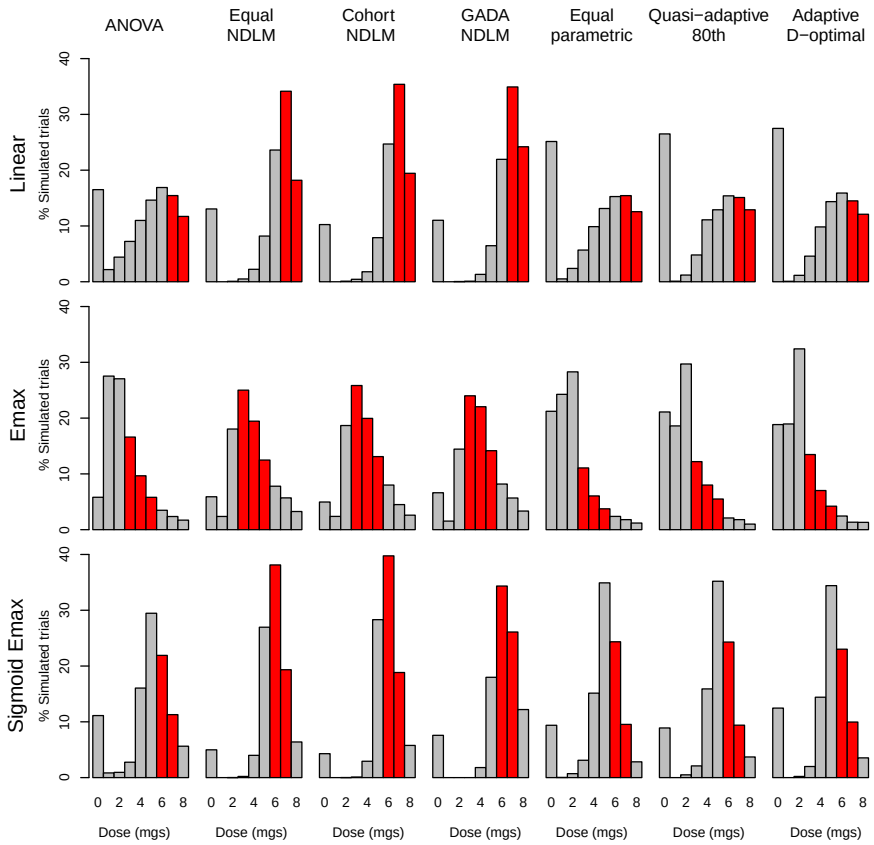

Figure 7-2: Histogram of doses selected in phase II for all methods, based on the clinically meaningful difference from placebo (decision rule 1). Target dose intervals are indicated in red.

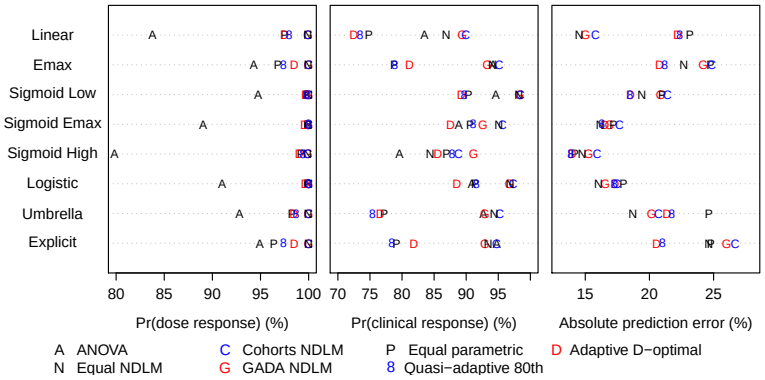

Figure 7-3: Operational characteristics for all methods listed in Table 7.1, based on the metrics in Chapter 2.

sigmoid emax model or the NDLM detect a dose response approximately 100% of the time. The ANOVA method detects a dose response with a similar frequency with which it detects a clinical response. As we can see from Figure 7-3, the methods which use the Bayesian NDLM tend to have the highest probability of detecting a clinical response.

From Figure 7-3 the absolute prediction error for all the methods are similar, with the exception of the Linear, Emax, Umbrella and Explicit profiles. For the Linear and Umbrella profiles, the methods which use a Bayesian NDLM have a smaller prediction error than the parametric methods which modelled the data using the four parameter sigmoid emax model. This is because the NDLM, unlike the sigmoid emax model, makes no assumptions about the underlying shape of the dose response curve and so is better able to fit the Linear and Umbrella dose response profiles. On the other hand the parametric sigmoid emax model is more capable of fitting the Emax and Explicit profiles than the NDLM, as the change in efficacy at the early doses is too steep for the NDLM to fit well.

Figure 7-4 illustrates the probability of correctly selecting a dose in the target dose interval, based on the old and new definitions of the target dose interval (Tables 7.2 and 7.3 respectively). We can see that when using the old definition of the target dose interval, the performance of the different allocations and analysis methods depends on the shape of the true dose response profile. Using the new definition, the performance of the methods which model the data using an NDLM have improved while the performance of the parametric methods has deteriorated. As the new target dose interval tends to favour higher doses, the methods which model the data using an NDLM now perform consistently better than the other methods. The adaptive

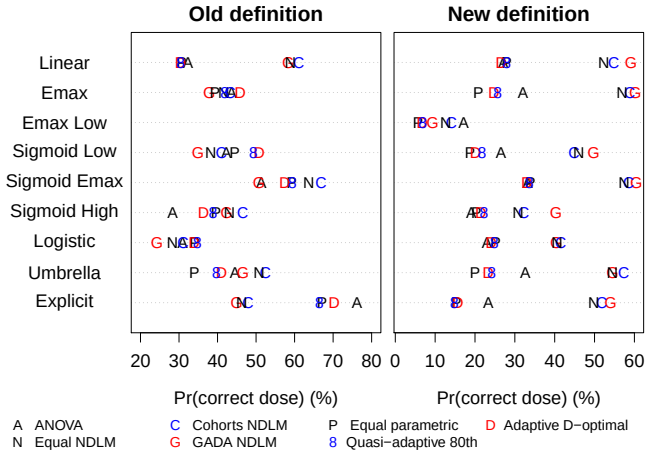

Figure 7-4: Probability of choosing a dose in the target dose interval using decision rule 1, based on old and new definitions of the target dose interval.

methods tend to perform better than the non-adaptive methods under this new metric.

The expected gains of different methods are presented in Figure 7-5. From Figure 7-5 we see that the methods which model the data using a Bayesian NDLM have a consistently larger gain than the other methods. This is consistent with the results presented in Antonijevic et al. (2010), who attributes this success to the adaptive nature of the GADA method. However, we observe that using an equal allocation design with an NDLM analysis also does equally well. Our explanation of the success of the NDLM methods is that they tend to choose higher doses. For the majority of the dose response profiles, choosing a higher dose increases the power in phase III. Although this also increases probability of failing due to safety concerns, in our formulation the increase in power often outweighs the additional safety risk. This results in higher doses having a larger probability of success in phase III and therefore a larger utility.

The expected gain bias in Figure 7-5 suggests that the ANOVA and frequentist parametric methods tend to overestimate the response at the target dose identified in phase II. The methods which model the data using an NDLM have a consistently smaller gain bias. The box plots in Figure 7-6 illustrates the difference between the fitted curve and the true dose response profile at the selected dose, excluding the cases where there was no clinical meaningful difference from placebo. We can see that for the methods which model the dose response using an NDLM, the response at the selected dose is close to that of the true response. Despite the aim of the GADA and cohort methods to focus the subject allocations on the target dose, there is little to distinguish

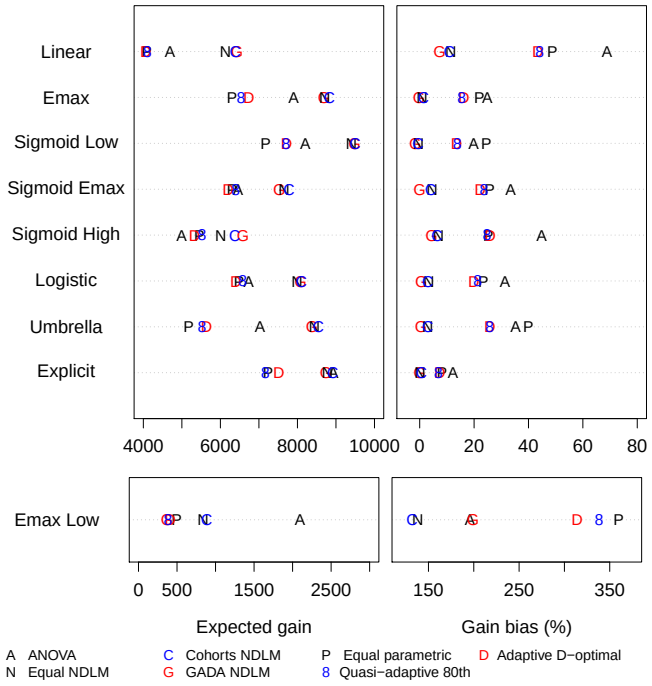

Figure 7-5: Expected gain and the expected gain bias. Dose selected using the clinically meaningful difference from placebo (decision rule 1).

between the adaptive and non-adaptive subject allocations. As predicted from the gain bias, the ANOVA and parametric methods overestimate the response at the selected dose.

7.9.2 Decision rule 2

Using decision rule 2, we first decide if there is a dose response and then proceed directly to selecting the dose to take forward into phase III. We no longer check if there is a clinically meaningful difference from placebo, as this does not drive our choice of dose. Figure 7-7 shows the histogram of doses chosen for some of the true dose response curves, with the correct target dose interval based on our new definition highlighted in red. As before, the methods which model the data using an NDLM tend to chose higher doses than the other methods. Due to the monotonicity of the parametric methods, if an asymptote is observed, then at the asymptote there is little to gain in power from choosing a higher dose and more to lose in terms of a higher safety risk. Therefore these methods tend to choose lower doses. As the NDLM methods underestimate the dose response at the early doses, if there is an asymptote in the data, it is reached later in the dose range and so these methods tend to choose higher doses. As the target

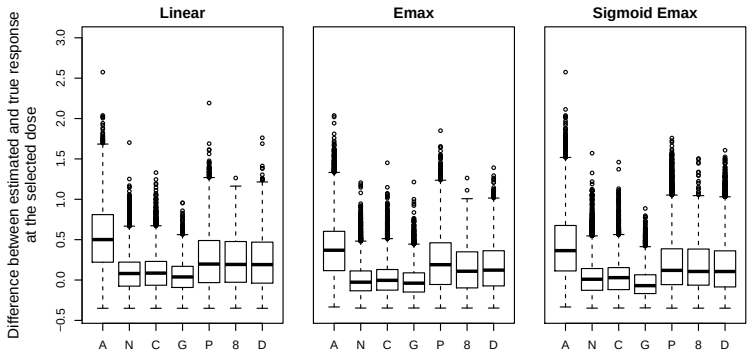

Figure 7-6: Box plots of the difference between the estimated response and the true response at the dose selected using the clinically meaningful difference from placebo (decision rule 1). Cases where there was no clinically meaningful difference from placebo are omitted.

dose intervals now include higher doses, this results in the NDLM methods correctly identify a dose in the target dose interval more often than the other methods (Figure 7-8).

The probabilities of correctly selecting a dose in the target dose interval, using decision rules 1 and 2 are presented in Figure 7-8, for each of the dose response profiles. For all the methods the probability of correctly identifying the target dose either remains unchanged or is improved by using decision rule 2 over decision rule 1. This is to be expected, as decision rule 2 chooses the dose that maximises the expected gain and so is in line with the new metric. The decrease in the ability of the all methods to correctly identify that the Emax Low model should be stopped after phase II is due to removing the step where a clinically relevant response is established before the target dose is found. For simulations where a difference less than the CMD are observed, using decision rule 2 a dose for phase III is still selected. If this was of concern to the project team, then the frequency with which we continued to phase III when the data were generated from the Emax Low profile could be reduced by increasing the threshold x in decision rule 2.

When we select the dose that maximises the probability of success in phase III, we can see that the expected gain in Figure 7-9 is larger than when we chose the minimum dose with a clinically meaningful difference (Figure 7-5). This increase in the expected gain is partly due to choosing higher doses, and partly because we stop less often at the end of phase II. The expected gain bias is lower than when decision 1 was used,

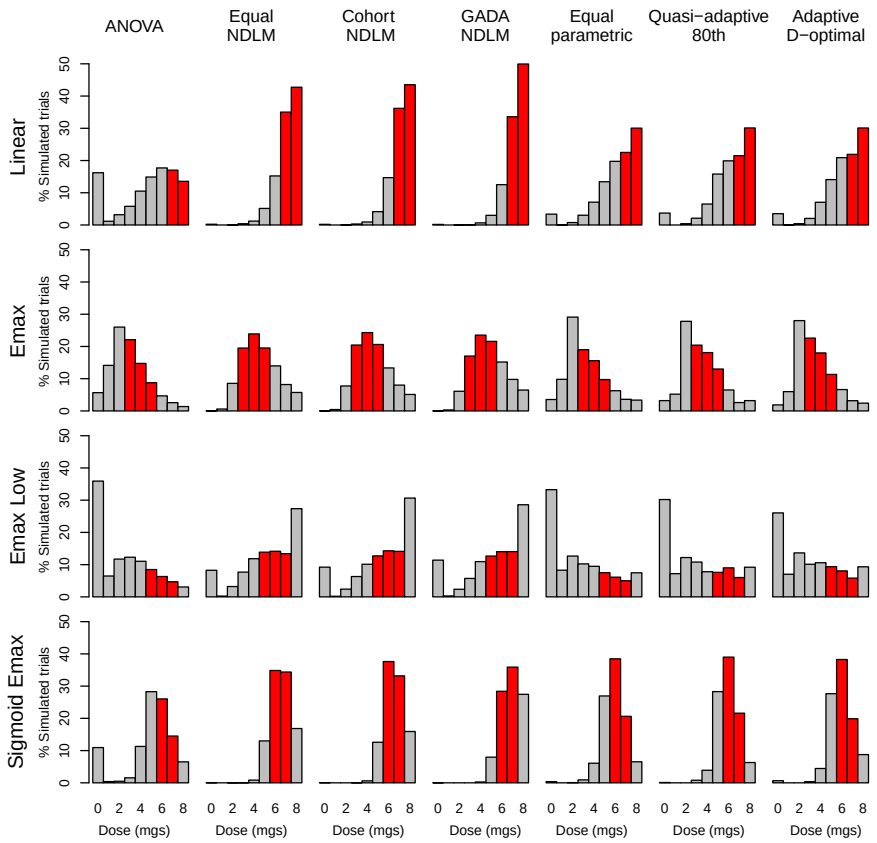

Figure 7-7: Histogram of doses selected in phase II for all methods, based on the probability of success in phase III (decision rule 2). Target dose intervals are indicated in red.

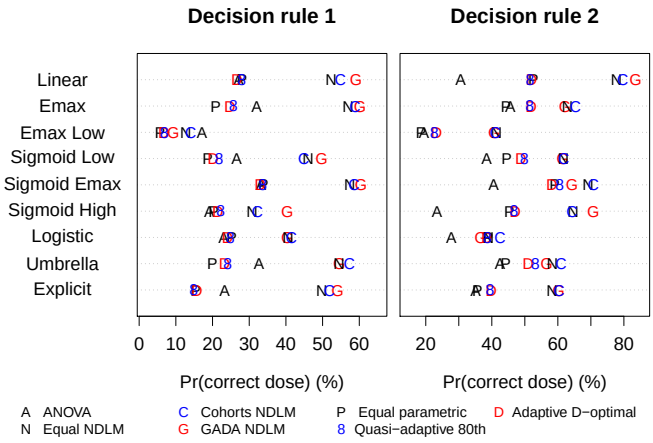

Figure 7-8: Probability of selecting a dose within the target dose interval using decision rules 1 and 2.

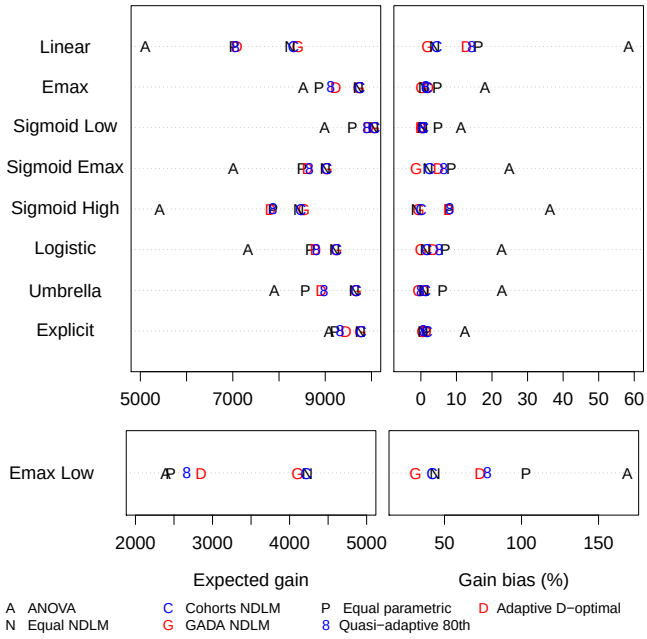

Figure 7-9: Expected gain and the expected gain bias. Dose selected using the probability of success in phase III (decision rule 2).

although the general trends are similar. The ANOVA method has the largest bias due to overestimating the response at the target dose (Figure 7-10). As we can see from Figure 7-10, the difference between the estimated response and the true response at the dose selected is smaller for the parametric methods than when decision rule 1 was used (Figure 7-6), and hence this leads to a smaller expected gain bias. The methods which model the data using an NDLM, have the smallest expected gain bias as the observed responses are close to the true responses at the dose selected using decision rule 2.

7.9.3 Decision rule 3

For decision rule 3, we identify the target dose for phase III as the dose that maximises the posterior probability of success. We therefore only consider Bayesian methods. We consider the three allocation methods that were modelled using an NDLM; the equal, cohort and GADA allocation methods. We also include the scenario where subjects were allocated using a Bayesian D-optimal design at the interim analysis after 50% of subjects had completed the study, and the data modelled using a sigmoid emax model

$$\eta(z_j, \theta) = \theta_1 + (\theta_2 - \theta_1)\frac{z_j^{\theta_4}}{\theta_3^{\theta_4} + z_j^{\theta_4}},$$

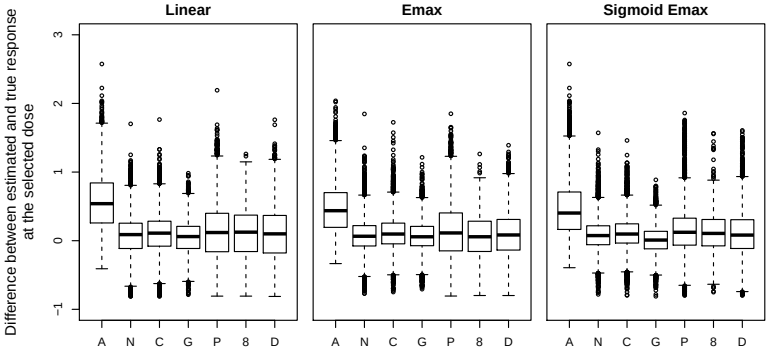

Figure 7-10: Box plots of the difference between the estimated response and the true response at the dose selected using the probability of success in phase III (decision rule 2). Cases where there the probability of success in phase III was less than 0.25 are omitted.

with three sets of prior distributions placed on the model parameters.

	θ_1	θ_2	θ_3	θ_4
Prior 1	$N(0,\ 1)$	$N(2,\ 1)$	$G(4,\ 4)$	$G(4,\ 4)$
Prior 2	$N(0,\ 4)$	$N(2,\ 9)$	$G(1,\ 0.25)$	$G(1,\ 0.5)$
Prior 3	$N(0,\ 25)$	$N(2,\ 25)$	$G(2,\ 0.25)$	$G(1,\ 0.25)$

To keep our results consistent with those presented in Section 6.8, we use a Bayesian adaptive D-optimal with one interim analysis after 50% of subjects had completed the trial. The Bayesian adaptive D-optimal designs were based on the same sets of prior distributions listed above. We generate samples from the posterior distribution for the sigmoid emax model using the HARIS method detailed in Chapter 3.

Figure 7-11 is a histogram of the doses selected after phase II based on decision rule 3, for a selection of the dose response profiles. For the three methods which model the data using an NDLM, similar doses are chosen to when the decision rule 2 was used process was (Figure 7-7). The dose chosen by the Bayesian parametric methods depends on the choice of prior used. Prior 1 is strongly informative and so the prior distribution dominates the data causing the same range of doses to be chosen regardless of the dose response profile. Priors 2 and 3 are less informative and so the choice of dose depends more on the data, hence they are more able to correctly identify a dose in the target dose interval, with the histograms for Prior 3 taking a similar shape as to when an NDLM is used to fit the data.

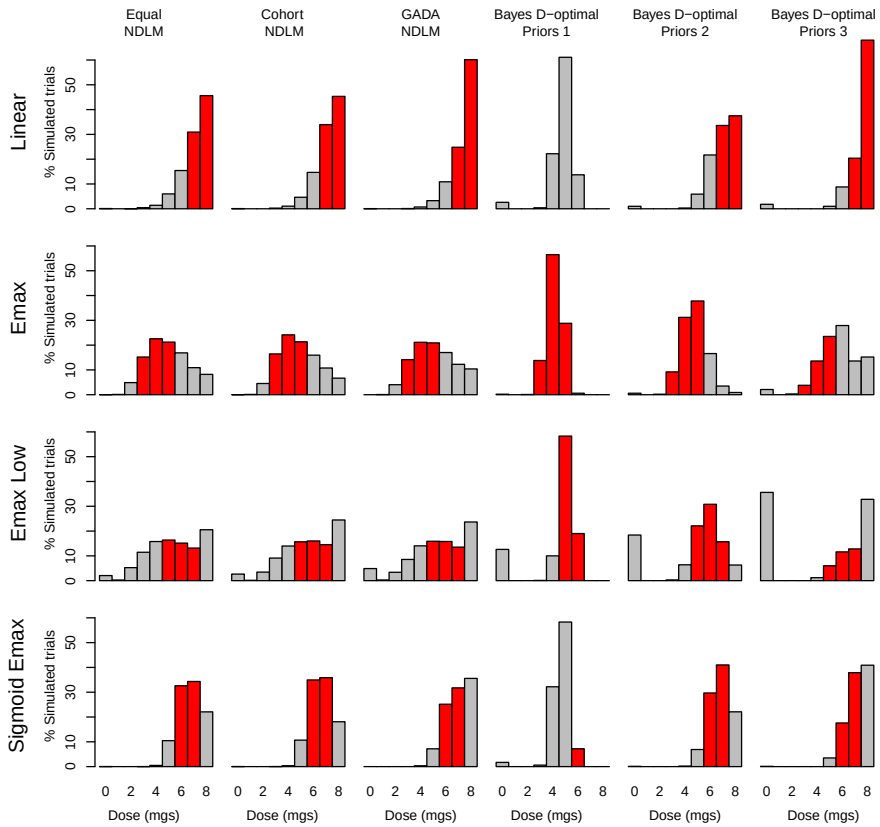

Figure 7-11: Histogram of doses selected in phase II for all Bayesian methods, based on the posterior probability of success in phase III (decision rule 3). Target dose intervals are indicated in red.

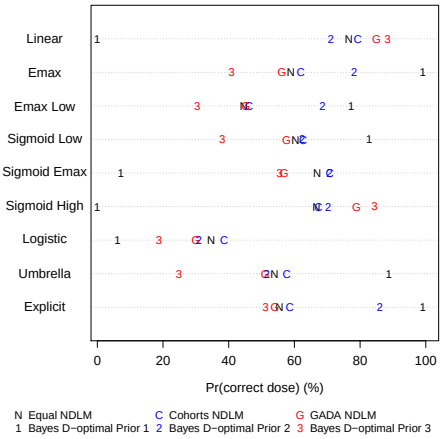

Figure 7-12: Probability of identifying a target dose within the target dose interval using the decision rule 3.

The sensitivity of the results to the prior distribution placed on the parameters of the sigmoid emax model can be seen in Figure 7-12, which is a plot of the probability of selecting a dose in the target interval. Prior 1 has a high probability of selecting a dose in the target dose interval for some of the dose response profiles, but performs poorly for other dose response profiles. Prior 2 does reasonably well in identifying a dose in the target interval for all the dose response profiles, whilst Prior 3 tends to flatten the dose response curve and so choose higher doses. This does well for the Linear and Sigmoid Emax profiles, but not so well for the other dose response profiles.

The probabilities of choosing a dose in the target interval for the methods which used an NDLM to model the data, are very similar to when decision rule 2 is used. Using the posterior probability of success to identify the target dose, has resulted in the GADA allocation being better at identifying the target dose than the cohort and equal allocations methods when the dose response is Linear, Emax Low or Sigmoid High. However, for the other dose response profiles, the cohort and equal allocation have better operational characteristics than the GADA approach.

As the doses chosen using the posterior probability of success in phase III for the NDLM methods are similar to those chosen using the probability of success, this results in a similar expected gain (Figure 7-12). For the parametric methods, the doses chosen and so the expected gain are sensitive to the choice of prior distribution. The bias in the expected gain are generally negative. This is because the probability of success is not linear in θ, and so samples of θ which result in a efficacious responses have less to gain

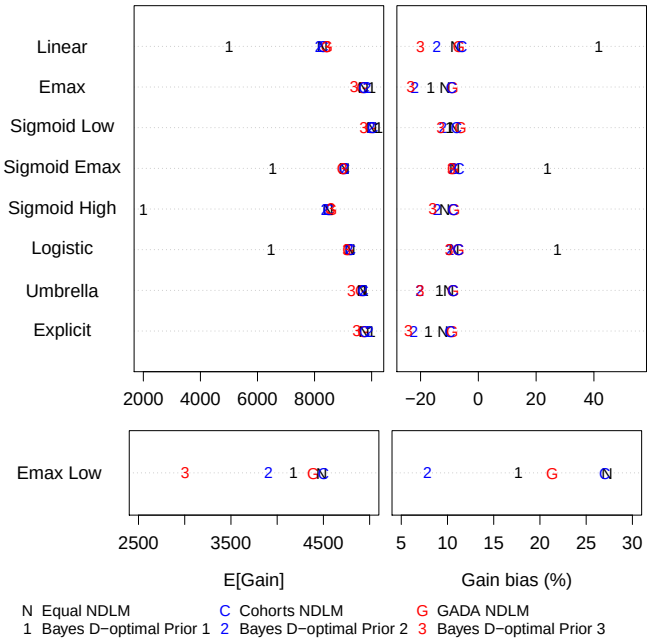

Figure 7-13: Expected gain and the expected gain bias. Dose selected using the posterior probability of success in phase III (decision rule 3).

in terms of probability of success than samples with ineffective responses have to lose. Hence, when we average over the posterior distribution we tend to underestimate the utility. The expected gain bias for the methods which use the NDLM tend to be closer to 0, this suggests that there is less variability in the dose response curve at the selected dose, than the Bayesian parametric methods.

7.10 Discussion

It is widely accepted that selecting the correct dose for phase III is a considerably harder task than detecting a dose response or a clinical response (Bornkamp et al., 2007). In this chapter we have explored different decision rules for selecting the dose in phase II to take into phase III.

We redefined the target dose interval to be the set of doses with at least 97.5% of the maximum probability of success in phase III. Under this new definition, higher doses were in the target dose interval which favours the NDLM methods when using decision rule 1, as the NDLM methods tend to choose higher doses than the parametric methods. The probability of correctly selecting a dose in the target interval was the

same or higher when using decision rule 2 over decision rule 1, with the NDLM methods consistently outperforming the parametric methods. Using decision rule 2 also improves the expected gain and reduces the gain bias compared with decision rule 1. For decision rule 3, we incorporated the variability in the dose response model by maximising the posterior probability of success in phase III. For the NDLM methods, there was little improvement in the expected gain over decision rule 2, but when using decision 3 there was a negative gain bias suggesting we are more conservative about the predicted gain when we take the variability in the dose response curve into account. Using decision 3, the expected gain of the parametric methods were sensitive to the choice of prior distribution placed on the parameters.

Decision rules 2 and 3 have the advantage that they attempt to take into account possible safety problems that may arise in phase III. If the risk of safety problems were increased, then the expected gains for all the decision rules would be reduced, but where decision rules 2 and 3 would tend to identify lower doses, decision rule 1 would not be impacted. We have shown that based on our knowledge of the dose response curve in phase II and our beliefs about the possible safety concerns in phase III, it is possible to optimise the decision making process.

We have found that regardless of the decision rule used, the methods which model the data using an NDLM tend to have a higher expected gain and a lower gain bias. This was because the NDLM methods tend to estimate the dose response better at the selected dose, whereas the parametric methods and the ANOVA method tend to overestimate the response. We observed that for all three decision rules, there were some gains to be made in terms of correctly selecting a dose in the target interval, when adaptive designs were used compared to the non-adaptive design.

We acknowledge that choosing a dose to take into phase III is a complicated procedure, taking account of a number of sources of information such as pharmacokinetic and pharmcodynamic data and not made solely using phase II. However, the way in which we use the phase II data should still, where possible, be optimised. Choosing a dose to be taken into phase III is one of the main aims of a phase II trial, and so the rule for identifying this should be ascertained in the design stage. Like any design option, the characteristics of such a rule can then be evaluated through simulation studies.

A limitation of using decision theory methods is the problem of specifying a realistic utility function (Stallard et al., 2009; Chen & Smith, 2009). Realistic costings

and projection of profits also need to be provided, which involves multidisciplinary involvement (Julious & Swank, 2005). However the advantages are that they allow project teams to consider clinical trials in the context of a larger development program, and make decisions between competing trial designs or compounds. Burman et al. (2006) suggests that Bayesian decision theoretic approaches could be used for making in-house company decisions, whilst frequentist results are communicated to regulators.

Chapter 8

Discussion

In this thesis we have explored how the use of adaptive designs can impact the operational characteristics of phase II dose-finding studies, with the aim of identifying when adaptive designs are beneficial. This thesis was motivated by the work of Bornkamp et al. (2007) which explored a number of adaptive and non-adaptive allocation methods. One of the conclusions of this paper was that 'adaptive dose-ranging designs and methods clearly lead to gains in power to detect dose response and in precision to select target dose(s) and to estimate the dose response.' This paper was then followed up by Dragalin et al. (2010) who explored further adaptive methods and came to the same conclusions. We have followed in the general footsteps of these two papers however, we have taken the methodology further with the aim of explaining whether it is the adaptation or the analysis which affects the operational characteristics.

The conclusions of this thesis are not as straightforward as those made by Bornkamp et al. (2007). We have observed improvements in the probability of detecting a clinical response and selecting a dose in the target interval from some of the adaptive designs, but these gains were dependent on the choice of adaptation and the underlying dose response profile. Our results suggest that there are gains to be made when we are cautious in our adaptation, either using the cohort method (Chapter 5) to allocate to a range of doses around the minimally effective dose, or using the quasi-adaptive D-optimal design (Chapter 6), which tests the proposed adaptive designs is efficient for parameter mis-specifications before adapting. Both these methods have the capability to adapt when there is a clear signal in the data, but if there is a lot of variability in the data, then the methods are conservative and tend towards using equal allocation. In this way, the methods are more robust against being mis-led by interim data.

When the adaptation methods are more focussed on allocating to a few doses, the conclusions are less clear. For the GADA method (Chapter 4), we found some gains in the probability of detecting a clinical response but the adaptation was detrimental to the ability of the method to select a dose in the target dose interval when compared to using equal allocation with the same final analysis. For the adaptive D-optimal design (Chapter 6) the results were varied. For some of the dose response profiles, the adaptive D-optimal design leads to gains in the probability of identifying a dose in the target dose interval over the equal allocation design, whilst for other dose response profiles the adaptation was detrimental.

Adaptation is often proposed to compensate for the lack of knowledge about the expected dose response profile. If this is the case, then it seems sensible to be more cautious in our adaptation. If there is reasonable experience with a compound, then it is generally possible to propose a good design at the outset and so adaptation has little to offer.

Another conclusion of the Bornkamp et al. (2007) paper was that 'detecting dose response is considerably easier than estimating it, or identifying the target dose to bring into the confirmatory phase.' Our results agree with this conclusion. In Chapter 7 we look at optimising the selection of the target dose for phase III. Our results show, with suitable model assumptions, that selecting the dose that maximises the probability of success in phase III we can increase our expected gain compared with using the estimated minimally effective dose. When the expected gain was used to compare methods, there was a clear distinction between the Bayesian methods which model the data using the normal dynamic linear model (NDLM) and the frequentist methods, with the Bayesian methods having a consistently higher gain and lower gain bias. The expected gain bias was high for the frequentist methods as they tend to overestimate the response at the dose selected for phase III.

In order to assess the validity of a design, suitable simulations studies need to be carried out to identify which aspect of the design or analysis impacts the operational characteristics. The control in the Bornkamp et al. (2007) paper was a non-adaptive equal allocation design with frequentist analysis using pairwise testing with a Dunnett (1955) adjustment for multiplicity. This differs from the adaptive method explored in this thesis in terms of the adaptation and the final analysis, therefore it is unsurprising there are differences between the operational characteristics. In order to claim the benefit of an adaptive method we first need to understand how the same analysis performs

when a non-adaptive allocation is used. This is consistent with the comments of Cheng & Chow (2010) who emphasise the importance of investigators comparing adaptive and non-adaptive designs when choosing the best design for the study objectives.

An element of adaptation which is often explored but has been excluded from this thesis, is the possibility to stop a trial at an interim analysis for either efficacy or futility, and in doing so, reduce the average sample size, saving both time and resources. The option to stop at an interim analysis was not considered here as it would add an extra dimension to differentiate between the methods. In addition to this, as all but one of the active dose response profiles that are considered here have a clinically meaningful difference, stopping for futility was not particularly relevant for these examples.

Throughout this thesis we have used simulation studies to evaluate the performance of the methods. These simulations studies have made a number of assumptions that would not hold true in real clinical trials. For example, we assume that subject responses are available immediately and so when adapting we can use these data to find the randomisation scheme for the next cohort of subjects. In reality there would be a delay in obtaining the subject responses, hence at an interim analysis only partial data would be available for some subjects. A method for dealing with partial data at interim analyses would need to be incorporated into the design and so should also be incorporated into any simulation studies carried out. This could take the form of excluding subjects with partial data from the interim analysis or using a longitudinal model to predict final responses. In either case, having partial rather than complete responses available at an interim analysis would increase the variability in the data. It is our conjecture that the extra variability would have a detrimental effect on the results for the GADA and adaptive D-optimal methods, as both methods are sensitive to the variability in the interim data. We would expect the additional variability to result in the cohort method dropping fewer doses at the interim analysis, and the quasi-adaptive D-optimal approach opting more often for equal allocation. Therefore, we anticipate that the results of the cohort and quasi-adaptive methods would tend towards the results for using an equal allocation design.

The scenarios we have explored in this thesis have been chosen to make the results as comparable as possible with the Bornkamp et al. (2007) and Dragalin et al. (2010) papers. In these papers two dose schemes were explored; 5 even doses, and all 9 available doses. We chose to run our simulation studies with only one dosing scheme for equal allocation, using all 9 available doses. We acknowledge that this is a large num-

ber of doses to be included in a dose response study, but as Antonijevic et al. (2010) observes for the adaptive GADA design; 'the performance of designs with 9 doses is frequently better than that of the design with 5 doses.' If we had chosen to use 5 doses, then the placement of the 5 doses may have had an impact on the results.

We began this thesis by proposing an efficient method for sampling from the posterior distribution for a non-linear dose response model. One area for further work would be to improve the efficiency of this method by re-using rather than discarding the initial grid points. There is also the potential to generalise this method to other non-linear models which can be re-written as a linear model with a non-linear term.

In Chapter 7 we explored different decision rules to select the target dose for phase III. Another avenue of further work would be to incorporate these decision rules into the adaptation process. For example, rather than dropping doses based on the probability of a clinically meaningful difference from placebo, we could explore dropping doses based on the probability of success in phase III with the option of incorporating up to date safety data.

Finally, an opportunity to further explore the gains of response adaptive designs would be to consider dose-extension trials. In a dose-extension trial we begin with a few low doses, but then can extend the dose range at an interim analysis as the data deems necessary. An example of such a trial design is Berry et al. (2010).

Bibliography

Abdelbasit, K. & Plackett, R. (1983). Experimental design for binary data. *Journal of the American Statistical Association* **78**, 90–98.

Adams, C. & Brantner, V. (2006). Estimating the cost of new drug development: is it really $802 million? *Health Affairs* **25**, 420–428.

Antonijevic, Z., Pinheiro, J., Fardipour, P. & Lewis, R. (2010). Impact of dose selection strategies used in phase II on the probability of success in phase III. *Statistics in Biopharmaceutical Research* **2**, 469–486.

Atkinson, A. (1982). Developments in the design of experiments, correspondent paper. *International Statistical Review/Revue Internationale de Statistique* **50**, 161–177.

Atkinson, A. (1988). Recent developments in the methods of optimum and related experimental designs. *International Statistical Review/Revue Internationale de Statistique* **56**, 99–115.

Atkinson, A. C. & Donev, A. (1992). *Optimum Experimental Designs*. Clarendon press.

Bauer, P. & Kohne, K. (1994). Evaluation of experiments with adaptive interim analyses. *Biometrics* **50**, 1029–1041.

Berger, J. (1985). *Statistical decision theory and Bayesian analysis*. Springer.

Berry, D., Mueller, P., Grieve, A., Smith, M., Parke, T., Blasek, R., Mitchard, N. & Krams, M. (2001). *Case Studies in Bayesian Statistics*, chap. Adaptive Bayesian Designs for Dose-Ranging Drug trials. New York: Springer-Verlag, pp. 99–167.

Berry, S. M., Spinelli, W., Littman, G. S., Liang, J. Z., Fardipour, P., Berry, D. A., Lewis, R. J. & Krams, M. (2010). A Bayesian dose-finding

trial with adaptive dose expansion to flexibly assess efficacy and safety of and investigational drug. *Clinical Trials* **7**, 121–135.

Bornkamp, B., Bretz, F., Dmitrienko, A., Enas, G., Gaydos, B., Hsu, C.-H., Knig, F., Krams, M., Liu, Q., Neuenschwander, B., Parke, T., Pinheiro, J., Roy, A., Sax, R. & Shen, F. (2007). Innovative approaches for designing and analyzing adaptive dose-ranging trials. *Journal of Biopharmaceutical Statistics* **17**, 965–995.

Box, G. & Lucas, H. (1959). Design of experiments in non-linear situations. *Biometrika* **46**, 77–90.

Brunier, H. & Whitehead, J. (1994). Sample sizes for phase II clinical trials derived from Bayesian decision theory. *Statistics in medicine* **13**, 2493–2502.

Burman, C., Grieve, A. & Senn, S. (2006). Decision analysis in drug development. *Pharmaceutical Statistics Using SAS: A Practical Guide* , 385–428.

Chaloner, K. & Larntz, K. (1989). Optimal Bayesian design applied to logistic regression experiments. *Journal of Statistical Planning and Inference* **21**, 191–208.

Chaloner, K. & Verdinelli, I. (1995). Bayesian experimental design: A review. *Statistical Science* **10**, 273–304.

Chen, Y. (2005). Another look at rejection sampling through importance sampling. *Statistics & probability letters* **72**, 277–283.

Chen, Y. & Smith, B. (2009). Adaptive group sequential design for phase II clinical trials: A Bayesian decision theoretic approach. *Statistics in medicine* **28**, 3347–3362.

Cheng, B. & Chow, S. (2010). On flexibility of adaptive designs and criteria for choosing a good one: A discussion of FDA draft guidance. *Journal of Biopharmaceutical Statistics* **20**, 1171–1177.

Chernoff, H. (1953). Locally optimal designs for estimating parameters. *The Annals of Mathematical Statistics* **24**, 586–602.

Chib, S. & Greenberg, E. (1995). Understanding the metropolis-hastings algorithm. *American Statistician* **49**, 327–335.

Dette, H., Bretz, F., Pepelyshev, A. & Pinheiro, J. (2008). Optimal designs for dose-finding studies. *Journal of the American Statistical Association* **103**, 1225 – 1237.

Dette, H., Kiss, C. & Bevander, M. (2010). Optimal designs for the emax, log-linear and exponential models. *Biometrika* **97**, 513–518.

Dette, H. & Neugebauer, H. (1996). Bayesian optimal one point designs for one parameter nonlinear models. *Journal of statistical planning and inference* **52**, 17–31.

DiMasi, J. A., Hansen, R. W. & Grabowski, H. G. (2003). The price of innovation: new estimates of drug development costs. *Journal of Health Economics* **22**, 151 – 185.

Dragalin, V. (2006). Adaptive designs: terminology and classification. *Drug information journal* **40**, 425–435.

Dragalin, V., Bornkamp, B., Bretz, F., Miller, F., Padmanabhan, S., Patel, N., Perevozskaya, I., Pinheiro, J. & Smith, J. (2010). A Simulation Study to Compare New Adaptive Dose–Ranging Designs. *Statistics in Biopharmaceutical Research* **2**, 487–512.

Dragalin, V., Hsuan, F. & Padmanabhan, S. (2007). Adaptive designs for dose-finding studies based on sigmoid emax model. *Journal of Biopharmaceutical Statistics* **17**, 1051–1070.

Dunnett, C. W. (1955). The multiple comparison procedure for comparing several treatments with a control. *Journal of the American Statistical Association* **50**, 1096 – 1121.

Dutta, S., Matsumoto, Y. & Ebling, W. (1996). Is it possible to estimate the parameters of the sigmoid emax model with truncated data typical of clinical studies? *Journal of pharmaceutical sciences* **85**, 232–239.

Efron, B. & Tibshirani, R. (1993). *An introduction to the bootstrap*. Chapman & Hall/CRC.

Evans, I. (1965). Bayesian estimation of parameters of a multivariate normal distribution. *Journal of the Royal Statistical Society. Series B (Methodological)* **27**, 279–283.

Fedorov, V. V. (1972). *Theory of Optimal Experiments*. Academic Press, New York.

Food and Drug Administration (2010). Draft guidance for industry: Adaptive design clinical trials for drugs and biologics .

Ford, I., Titterington, D. & Kitsos, C. (1989). Recent advances in nonlinear experimental design. *Technometrics* **31**, 49–60.

Friede, T. & Kieser, M. (2001). A comparison of methods for adaptive sample size adjustment. *Statistics in medicine* **20**, 3861–3873.

Friede, T. & Kieser, M. (2006). Sample size recalculation in internal pilot study designs: a review. *Biometrical Journal* **48**, 537–555.

Gallagher, E., Liebman, M. & Bijur, P. (2001). Prospective validation of clinically important changes in pain severity measured on a visual analog scale. *Annals of emergency medicine* **38**, 633–638.

Gallo, P., Anderson, K., Berry, D., Burnham, N., Chuang-Stein, C., Dudinak, J., Fardipour, P., Givens, S., Lewis, R., Maca, J., Pinherio, J., Prichett, Y. & Krams, M. (2009). Good practices for adaptive clinical trials in pharmaceutical product development. *Drug Information Journal* **43**, 539–556.

Gelman, A., Carlin, J., Stern, H. & Rubin, D. (2004). *Bayesian data analysis*. CRC press.

Geman, S. & Geman, D. (1984). Stochastic relaxation, Gibbs distributions, and the Bayesian restoration of images. *Pattern Analysis and Machine Intelligence, IEEE Transactions on* **6**, 721–741.

Geyer, C. (1992). Practical Markov chain Monte Carlo. *Statistical Science* **7**, 473–483.

Gittins, J. & Pezeshk, H. (2000a). A behavioural bayes method for determining the size of a clinical trial. *Drug Information Journal* **34**, 355–363.

Gittins, J. & Pezeshk, H. (2000b). How large should a clinical trial be? *Journal of the Royal Statistical Society: Series D (The Statistician)* **49**, 177–187.

Gittins, J. & Pezeshk, H. (2002). A decision theoretic approach to sample size determination in clinical trials. *Journal of biopharmaceutical statistics* **12**, 535–551.

Gordian, M., Singh, N., Zemmel, R. & Elias, T. (2006). Why products fail in phase III. *IN VIVO* **24**, 49–54.

Grieve, A. P. (2007). Discussion of the 'white paper of the phrma working group on adaptive dose-ranging designs'. *Journal of Biopharmaceutical Statistics* **17**, 997–1004.

Grieve, A. P. & Krams, M. (2005). Astin: a Bayesian adaptive dose-response trial in acute stoke. *Clinical Trials* **2**, 340–351.

Haario, H., Saksman, E. & Tamminen, J. (2001). An adaptive metropolis algorithm. *Bernoulli* **7**, 223–242.

Han, C. & Chaloner, K. (2003). D-and c-optimal designs for exponential regression models used in viral dynamics and other applications. *Journal of Statistical Planning and Inference* **115**, 585–601.

Hastings, W. K. (1970). Monte Carlo sampling methods using Markov chains and their applications. *Biometrika : a journal for the statistical study of biological problems* **57**, 97–109.

Hung, H. M. J., Wang, S.-J. & O'Neill, R. T. (2006). Methodological issues with adaptation of clinical trial design. *Pharmaceutical Statistics* **5**, 99–107.

Jennison, C. & Turnbull, B. (2000). *Group sequential methods with applications to clinical trials*. CRC Press.

Julious, S. & Swank, D. (2005). Moving statistics beyond the individual clinical trial: applying decision science to optimize a clinical development plan. *Pharmaceutical Statistics* **4**, 37–46.

Katz, D., Schumitzky, A. & Azen, S. (1982). Reduction of dimensionality in Bayesian nonlinear regression with a pharmacokinetic application. *Mathematical Biosciences* **59**, 47–56.

Kiefer, J. (1974). General equivalence theory for optimum designs (approximate theory). *The Annals of Statistics* **2**, 849–879.

Kiefer, J. & Wolfowitz, J. (1960). The equivalence of two extremum problems. *Canadian Journal of Mathematics* **12**, 234.

Kirby, S., Brain, P. & Jones, B. (2011). Fitting emax models to clinical trial dose–response data. *Pharmaceutical Statistics* **10**, 143–149.

Kola, I. & Landis, J. (2004). Can the pharmaceutical industry reduce attrition rates. *Nature Reviews Drug Discovery* **3**, 711–715.

Krams, M., Lees, K., Hacke, W., Grieve, A., Orgogozo, J.-M. & Ford, G. (2003). Acute stroke therapy by inhibition of neutrophils (astin): An adaptive dose-response study of uk-279,276 in acute ischemic stroke. *Stroke (1970)* **34**, 2543–2548.

Lachin, J. (2005). A review of methods for futility stopping based on conditional power. *Statistics in medicine* **24**, 2747–2764.

Lindley, D. (1985). *Making decisions*. Wiley.

Lindley, D. (1997). The choice of sample size. *Journal of the Royal Statistical Society: Series D (The Statistician)* **46**, 129–138.

Liu, J. (2001). *Monte Carlo strategies in scientific computing*. Springer Verlag.

Liu, J., Chen, R. & Wong, W. (1998). Rejection control and sequential importance sampling. *Journal of the American Statistical Association* **93**, 1022–1031.

Lunn, D., Thomas, A., Best, N. & Spiegelhalter, D. (2000). Winbugs – a Bayesian modelling framework: concepts, structure, and extensibility. statistics and computing. *Statistics and computing* **10**, 325–337.

Meeker, W. (1984). A comparison of accelerated life test plans for weibull and lognormal distributions and type I censoring. *Technometrics* **26**, 157–171.

Metropolis, N., Rosenbluth, A., Rosenbluth, M., Teller, A. & Teller, E. (1953). Equation of state calculations by fast computing machines. *The journal of chemical physics* **21**, 1087–1092.

Morgan, B. (1984). *Elements of simulation*, vol. 194. Chapman & Hall/CRC.

Neal, R. (1997). Markov chain Monte Carlo methods based onslicing'the density function. *Preprint* .

Neal, R. (2003). Slice sampling. *Annals of Statistics* **31**, 705–741.

Ogungbenro, K., Dokoumetzidis, A. & Aarons, L. (2009). Application of optimal design methodologies in clinical pharmacology experiments. *Pharmaceutical statistics* **8**, 239–252.

Orloff, J., Douglas, F., Pinheiro, J., Levinson, S., Branson, M., Chaturvedi, P., Ette, E., Gallo, P., Hirsch, G., Mehta, C. et al. (2009). The future of drug development: advancing clinical trial design. *Nature Reviews Drug Discovery* **8**, 949–957.

Padmanabhan, S., Berry, S., Dragalin, V. & Krams, M. (2012). A Bayesian dose-finding design adapting to efficacy and tolerability response. *Journal of Biopharmaceutical Statistics* **22**, 276–293.

Pezeshk, H. (2003). Bayesian techniques for sample size determination in clinical trials: a short review. *Statistical methods in medical research* **12**, 489–504.

Pezeshk, H. & Gittins, J. (2002). A fully Bayesian approach to calculating sample sizes for clinical trials with binary responses. *Drug information journal* **36**, 143–150.

Pinheiro, J., Bretz, F. & Branson, M. (2006). *Analysis of Dose–Response Studies-Modeling Approaches*. Springer, pp. 146–171.

Pronzato, L. & Walter, É. (1985). Robust experiment design via stochastic approximation. *Mathematical Biosciences* **75**, 103–120.

Quinlan, J., Gaydos, B., Maca, J. & Krams, M. (2010). Barriers and opportunities for implementation of adaptive designs in pharmaceutical product development. *Clinical Trials* **7**, 167–173.

Rao, C. R. (1965). *Linear Statistical Inference and Its Applications*. Wiley.

Reilly, P. (1976). The numerical computation of posterior distributions in Bayesian statistical inference. *Applied Statistics* **25**, 201–209.

Ripley, B. (1987). *Stochastic simulation*. Wiley Online Library.

Schlaifer, R. & Raiffa, H. (1961). *Applied statistical decision theory*. Harvard University.

Seber, G. & Wild, C. (2003). *Nonlinear regression*. LibreDigital.

Senn, S. (1996). Some statistical issues in project prioritization in the pharmaceutical industry. *Statistics in medicine* **15**, 2689–2702.

Shen, J., Preskorn, S., Dragalin, V., Slomkowski, M., Padmanabhan, S., Fardipour, P., Sharma, A. & Krams, M. (2011). How adaptive trial designs can increase efficiency in psychiatric drug development: A case study. *Innovations in Clinical Neuroscience* **8**, 26–24.

Smith, K. (1918). On the standard deviations of adjusted and interpolated values of an observed polynomial function and its constants and the guidance they give towards a proper choice of the distribution of observations. *Biometrika* **12**, 1–85.

Smith, M. K., Jones, I., Morris, M. F., Grieve, A. P. & Tan, K. (2006). Implementation of a Bayesian adaptive design in a proof of concept study. *Pharmaceutical Statistics* **5**, 39–50.

Snapinn, S., Chen, M., Jiang, Q. & Koutsoukos, T. (2006). Assessment of futility in clinical trials. *Pharmaceutical Statistics* **5**, 273–281.

Stallard, N. (1998). Sample size determination for phase II clinical trials based on Bayesian decision theory. *Biometrics* **54**, 279–294.

Stallard, N., Posch, M., Friede, T., Koenig, F. & Brannath, W. (2009). Optimal choice of the number of treatments to be included in a clinical trial. *Statistics in medicine* **28**, 1321–1338.

Sturtz, S., Ligges, U. & Gelman, A. (2005). R2winbugs: A package for running winbugs from r. *Journal of Statistical Software* **12**, 1–16.

Sylvester, R. (1988). A Bayesian approach to the design of phase II clinical trials. *Biometrics* **44**, 823–836.

Team, R. D. C. (2008). *R: A Language and Environment for Statistical Computing*. R Foundation for Statistical Computing, Vienna, Austria. ISBN 3-900051-07-0.

Thomas, A., OHara, B., Ligges, U. & Sturtz, S. (2006). Making bugs open. *R news* **6**, 12–17.

Thomas, N. (2006). Hypothesis testing and Bayesian estimation using a sigmoid Emax model applied to sparse dose-response designs. *Journal of biopharmaceutical statistics* **16**, 657–677.

Weir, C. J., Spiegelhalter, D. J. & Grieve, A. P. (2007). Flexible design and efficient implementation of adaptive dose-finding studies. *Journal of Biopharmaceutical Statistics* **17**, 1033–1050.

West, M. & Harrison, J. (1997). *Bayesian forecasting and dynamic models*. Springer Verlag.

White, L. (1973). An extension of the general equivalence theorem to nonlinear models. *Biometrika* **60**, 345–348.

Whitehead, J. (1985). Designing phase II studies in the context of a programme of clinical research. *Biometrics* **41**, 373–383.

Whitehead, J. (1986). Sample sizes for phase II and phase III clinical trials: an integrated approach. *Statistics in Medicine* **5**, 459–464.

Whittle, P. (1973). Some general points in the theory of optimal experimental design. *Journal of the Royal Statistical Society. Series B (Methodological)* **35**, 123–130.